Maynooth University
National University of Ireland Maynooth

Identification and generation of new germplasms in barley with increased tolerance to waterlogging

Alexandra Miricescu, M.Sc.

This thesis is submitted to the National University of Ireland Maynooth for the degree of Doctor of Philosophy

February 2019

Head of School: Prof. Paul Moynagh
Supervisor: Dr. Emmanuelle Graciet

Table of contents

Declaration of Authorship

This thesis has not been submitted in whole or in part to this or any other university for any degree, and is original work of the author except where otherwise stated.

Signed:

Date:

Abstract

The ability to maintain high yields for barley production in Ireland is crucial for the indigenous brewing industry. However, high yields are threatened by global climate change, as Ireland is predicted to have increased flooding events. In consequence, the identification and development of barley varieties that are more tolerant to waterlogging has become an important research focus. The N-end rule protein degradation pathway has been shown to play an important role in the response of plants to flooding in *Arabidopsis thaliana*. Based on sequence similarities, N-end rule components were identified in barley and used as targets to develop new cultivars with increased waterlogging tolerance. Also, barley varieties that are part of AGOUEB population were tested for their waterlogging tolerance. Gene expression together with physiological parameters such as plant height, tiller number, chlorophyll content and root architecture were assessed in order to select varieties that are more tolerant to waterlogging

Acknowledgments

I want to say that completion of this thesis would have not been possible without the support of many, many people that played an important role in my life and had a major impact to my growth and development as a person and as a scientist.

First of all, I want to thanks to my parents and my family for their love, support and encouragement. They always believed in me even when I didn't. I can't express in words how much I appreciate you!

I would like to express my sincere appreciation to my supervisor, Dr. Emmanuelle Graciet. She knew how to direct my steps during my PhD and how to motivate me to go the extra mile when things didn't work as smooth as I expected. I really think that all the conversations that we had, all the time and energy that she offered were really beneficial for my development as a scientist. From her I learned that discipline, commitment and perseverance are three major skills so important in research and in life, in general. I want to thank her for opening so many doors for me and giving me the chance to work with wonderful people, both in Maynooth and in Carlow (Oak Park).

I would like to thank to Dr. Jackie Nugent and Dr. Ozgur Bayram for serving as my committee members.

I have to say that I am really happy and lucky that I got to work in a brilliant team in Maynooth -Brian Mooney, Dr. Kevin Goslin, Dr. Maud Sorel, Remi de Marchi, Tara O'Connor. Cheers for all the good memories, for the help and support and for the fun times as well. You are amazing colleagues!

I want to thank to all the staff from National University of Maynooth for all their help in the last 4 years. They are very well prepared and also lovely people, ready to help in any situation. I want to show my appreciation to Patricia Colton, that was in charge with organizing the laboratory practicals. Due to her, my time as a demonstrator was really enjoyable.

I want to thank to my students, especially Patrick Langan and Rhiona Burke that helped me in the lab with the tissue preparation for microscopy.

I would like to thank to the team from Oak Park, supervised by Dr. Ewen Mullins. In his lab, I was extremely lucky to work with Dr. Dheeraj Sing Rathore that trained me to do the embryo-transformation technique in barley. I want to

show my gratitude to Dr. Evelin Zuniga, Ashok Govindan, Dr. Manuel Lopez Vernaza and Brendan Burke. They received me in their lab with open arms and helped me a lot.

I want to thank to our collaborators from Teagasc: Dr. Susanne Barth, John Spink, Lena Forster and Tomas Byrne and Petra KockAppelgren and from Trinity College Dublin: Professor Dr. Frank Welmer and Dr. Bennett Thomson.

Many thanks for all the people that I have met since I moved in Maynooth: Dr. Gratiela Parcalabioru, Dr. Aoife Joyce, Dr. Sinead Murphy, Dr. Thuy Do, Sarah Delaney, Dr. Johana Isaza Corea, Ciara Tyrell, Aidan O'Flaherty, Nicholas Irani, Noel Gavin, Dr. Nezira Delagic, Dr. Simone Georgi, Lacramioara Neagu, Marina Dvorski, Oana, Ema and Mircea Musat, Dr. Mevlut Ulas, Dr. Andrei Palade for their support. Thank you all for great moments!

I want to thank to my housemate, Gwen McIntyre who received me with open arms in her house. I am happy that I met such a nice and understanding housemate, that became a good friend.

I want to thank to my special friends that I met here, in Maynooth, Claudia, Sabin and Steven Toderic that are my second family and made me feel loved and appreciated and taught me wonderful things. You made my life better!

I want to thank to all my dear friends from Romania, Magda Cazan, Cosmina Ionita, Liviana and Adrian Huzuna, Alina, Doru and Luca Pantelimon, Dr. Ioana Druga, Ana Seciu, Oana Popa, Dr. Iulia Florescu, Dr.Alexandru Burcea, Cristina and Oana Vasilica, Viorica Dinescu, Ramona Ionescu for being part of my life.

I really want to show my appreciation to Professor Margareta Vasilescu, my first biology teacher that made me love this discipline. I want to thank to, Dr. Margareta Costache, Dr. Sorina Dinescu, Dr. Mihaela Diaconu and Angelica Constantinescu for guiding my first steps in science.

I want to say a big thank you to my very special man, Diarmaid Diviney. He is the one that brings joy, love and peace in my life.

This thesis is dedicated to my family, especially to the loving memory of my grandmother, Lucretia Ionescu, that teached me to love the nature and to see the best in everything.

1. Introduction

Plants in the wild need to continuously respond and adapt to a wide range of environmental cues, as well as stresses. Understanding how they sense and mount a response to a particular stress, or to simultaneous stresses, is key for our ability to maintain crop production in the future. This need is further exacerbated by the effects of global climate change, which result in more variable and extreme weather conditions. In Europe, countries of the Northern hemisphere are predicted to have increased precipitation and flooding events, which have the potential to decrease crop production. This is however a broader problem worldwide (Bailey-Serres *et al*., 2012). My PhD thesis is largely focused on waterlogging stress.

1.1. Plants and the excess of water

1.1.1. Effects of waterlogging and submergence on crop yield

Waterlogging and submergence are associated with an excess of water, mostly due to increased precipitations, increased moisture and poor soil drainage. The term '*waterlogging*' is typically used in situations in which only the roots are in contact with the excess of water in the soil. The other term that is sometimes used in the literature is 'soil flooding'. In contrast, '*submergence*' is a more severe case, which occurs when the entire plant (i.e. including aerial organs) is covered by water. Intermediate situations are typically termed 'partial submergence' and correspond to cases in which roots and part of the shoot are under water (Sasidharan *et al*., 2017).

In the last years, waterlogging alone was registered as one of the main stresses that affected crop yield (FIGURE 1.1) (Bailey-Serres *et al*., 2012). Plant survival in waterlogging conditions is greatly influenced by the duration of treatment, the level of submergence (i.e. whether the plant is completely or partially submerged) (Vervuren, 2003) and the actual energy requirements of the plant at the time at which waterlogging occurs (Setter, 2003). The type of soil also plays a very important role (Zeng *et al*., 2013). It is expected that plants are particularly sensitive to waterlogging

during the early stages of development, when they require increased levels of cellular energy to grow, as well as during late stages, when plants produce flowers and set seeds. Studies in wheat showed that this crop is more sensitive to waterlogging during early stages of development (Yavas *et al*., 2012). Similar results were obtained with barley that was exposed to waterlogging at the leaf 1 developmental stage (Zeng *et al.*, 2013; Celedonio *et al*., 2015). Additional experiments with barley and rapeseed also indicated that these crops were also severely affected by waterlogging at a later developmental stage (Celedonio *et al*., 2015; Ploschuk *et al*., 2018).

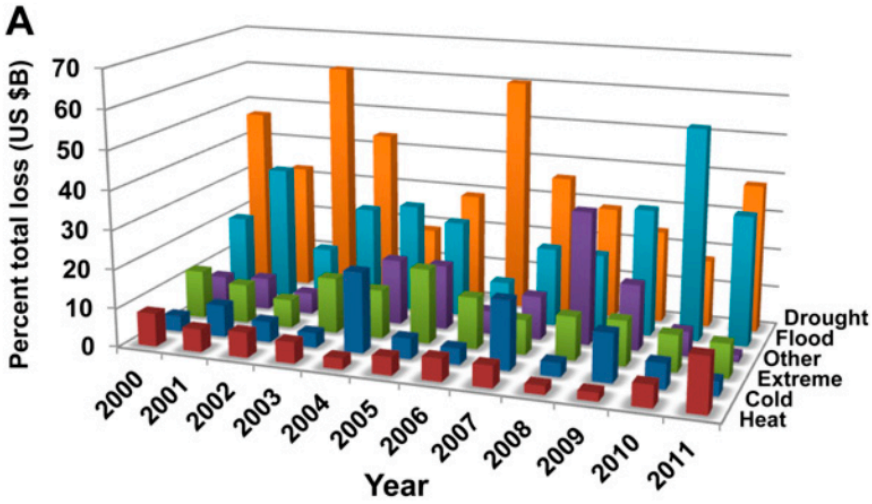

FIGURE 1.1. Analysis of total crop losses based on insurance fees paid to farmers in the United States between 2000 and 2011. Different types of factors that affect the crop yield were assessed: drought, flood due to increased precipitation, cold, heat, and others such as fire, insects and diseases and extremes like hurricanes, cyclones, frosts, freeze and hot winds (Bailey-Serres *et al*., 2012).

1.1.2. Plant responses to waterlogging and submergence

Gas exchange, especially for oxygen (O_2) and carbon dioxide (CO_2), is crucial for two essential metabolic pathways in plants. Through photosynthesis, CO_2 is fixed into carbohydrates, using energy provided by the light, while respiration uses O_2 as the final electron acceptor in the mitochondrial oxidative phosphorylation (Gupta *et al*., 2009) that will provide energy necessary for plant growth and development (Sasidharan and Voesenek, 2013).

The main negative effect of waterlogging and submergence on plants is the reduced availability of O_2. This is due to the fact that gas diffusion in water is 10,000 times lower than in air (Armstrong, 1979; Armstrong, 2002). This affects both the gas diffusion from the atmosphere into the cells (inwards) and from the living cells towards the outside (outwards). Under waterlogging or submergence conditions, the inward diffusion of O_2 and CO_2 is limited, leading to decreases in O_2 and CO_2 levels inside the cells, which affect both photosynthesis and cellular respiration. In contrast the outward diffusion of gaseous phytohormones such as ethylene, which plays an essential role in plant responses to waterlogging and submergence, is reduced. This results in the accumulation of ethylene inside the cells (Sasidharan and Voesenek, 2013). In the case of submergence, another factor that is reduced is light, due to water turbidity, which results in reduced photosynthesis (Vervuren *et al*., 2003). Decreased photosynthesis and respiration activities in turn negatively affect energy and carbohydrate levels (Voesenek and Bailey-Serres, 2015). As a result, ATP production is based mainly on glycolysis and other pathways, such as ethanol fermentation and alanine (Ala) production, which play an important role to regenerate nicotinamide adenine dinucleotide (NAD^+) (Ismond *et al*., 2003; Ricoult *et al*., 2006).

In addition to the energy-related problems associated with flooding and/or submergence, in barley , it was shown that waterlogging leads to changes in micronutrients (e.g. manganese and iron) concentration and redox potential in the soil which results in the increased intracellular accumulation of elements that can be toxic for the plant (Zeng *et al*., 2013). Another side effect caused by waterlogging is a general reduction of amino acid and protein synthesis that can be explained by lower levels of nitrogen, due to inhibited nitrogen fixation (Geigenberger, 2000; Rocha *et al*., 2010b).

1.1.2.1. Molecular and physiological changes

Molecular and metabolic changes occur very rapidly in response to waterlogging. In particular, genes coding for proteins that promote plant survival are induced, while genes encoding proteins involved in processes that require a lot of energy are down-regulated (Mustroph *et al*.2009; Bailey-Serres and Voesenek, 2010; Arora *et al*., 2017). All the molecular changes that occur are tightly regulated and have a great impact on plant physiology. Due to their strong interconnection,

molecular and physiological changes that occur under low O_2 conditions, are discussed together (Bailey-Serres and Voesenek, 2010).

In order to maintain cell homeostasis during waterlogging, several anaerobic pathways such as starch catabolism, glycolysis, ethanolic fermentation and bifurcated tricarboxilic acid (TCA) cycle are activated. It was proposed that there are 2 types of TCA cycles: a conventional cyclic flux mode that requires pyruvate as substrate and a non-cyclic flux that is activated in response to changes in the ATP requirements and might increase the metabolic flexibility (Steuer *et al*., 2007; Poolman *et al*., 2009; Sweetlove *et al*.,2010). Together, these pathways will provide the ATP required for many processes, especially for synthesis of proteins involved in metabolite transport that will allow a better mobilization and utilization of nutrients reserves (Hong *et al*., 2012) , reactive oxygen species (ROS) protection and chaperone activity (Bailey-Serres *et al*., 2012; Bailey-Serres and Voesenek, 2008, 2010). On the other hand, processes related to growth – e.g. cell division, DNA replication, protein synthesis, and cell wall synthesis are kept to a minimum during waterlogging, because energy resources are limited (Christianson *et al*., 2010; Lee *et al*., 2011; Mustroph and Bailey-Serres, 2010; Nanjo *et al.*, 2011; Narsai *et al*., 2009; Sasidharan *et al*., 2013; Tamang *et al*., 2014; van Veen, 2013).

In the next paragraphs, I will detail the role of specific metabolic enzymes (i.e. lactate dehydrogenase (LDH), alcohol dehydrogenase (ADH) and pyruvate decarboxylase (PDC)) that play an important role in the switch from aerobic to anaerobic metabolism. In general, low O_2 conditions that accompany waterlogging and submergence are characterized by an increased glycolytic flux (Magneschi and Perata, 2009; Narsai *et al*., 2009). Fermentative pathways that use the pyruvate produced through the reactions of glycolysis are also rapidly activated, as they provide oxidized NAD^+, which is needed for glycolysis and ATP production (Kennedy *et al*., 1992; Ricard, 1994).

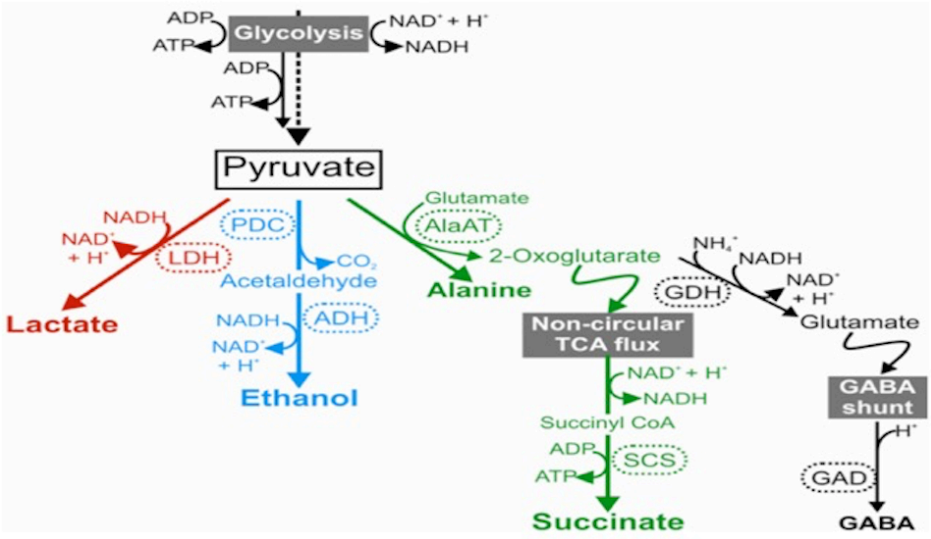

(Banti *et al*., 2013)

FIGURE 1.2. Fermentation pathways activated in response to low O_2 conditions. In hypoxia conditions, plants switch to fermentative metabolism to maintain ATP production. Using pyruvate as a substrate, there are three active pathways (indicated in red, blue and green) that lead to the production of lactate, ethanol, succinate and glutamate to γ-aminobutiric acid (GABA), while allowing for the production of NAD^+ which is important to main glycolysis and ATP production (Banti *et al*., 2013). Lactate dehydrogenase (LDH) in involved in pyruvate metabolism to lactate. Pyruvate dehydrogenase (PDC) and alcohol dehydrogenase (ADH) are key enzymes for converting pyruvate to ethanol. Alanine aminotransferase (AlaAT) is involved in transferring one amino group from glutamate to pyruvate leading to alanine (Ala) and 2-oxoglutarate (2-OG). Succinyl CoA ligase (SCS) is converting 2-OG to succinate and glutamate dehydrogenase is catalysing 2-OG oxidation to glutamate. Glutamate decarboxylase (GAD) is converting glutamate to GABA (Aurisano, 1995; Banti *et al*., 2013).

- **<u>Role of lactate dehydrogenase</u>**

Lactate is produced by the enzyme lactate dehydrogenase (LDH) during hypoxia (FIGURE 1.2), but only for a short period of time due to lactate's negative effect on cytoplasmic pH. After the first hours of low O_2 conditions, the lactate produced is rapidly exported from the cells to avoid the pH acidification (Licausi *et*

al., 2009). There are contradictory data regarding the importance of lactate for fermentative metabolism for plant tolerance to hypoxia (and hence also waterlogging and submergence).

Experiments conducted in maize (*Zea mays*) exposed to low O_2 conditions showed an increase in ZmLDH activity compared to untreated plants (Christopher and Good, 1996), suggesting a role of ZmLDH in the early stages of low O_2 stress response. Similarly, in barley, Hv*LDH* expression is induced, and is maintained for several days (up to 14 d after hypoxia) (Hondred, 1990; Hoffman *et al*., 1986), suggesting that Hv*LDH* might play a role during both early and late stages of hypoxia treatment. Notably though, experiments in tomato that overexpressed the barley Hv*LDH* under the control of 35S promoter (Rivoal and Hanson, 1994) indicated that increasing LDH activity by a factor 50 did not necessarily correlate with an increased rate of fermentation and higher lactate accumulation in response to low O_2 conditions (Rivoal and Hanson, 1994).

- **Role of ethanolic fermentation**

It has been proposed that after a short period during which pyruvate is converted to lactate, pyruvate metabolism could be switched to ethanol production (FIGURE 1.2). It was shown that overexpression of At*LDH* in *Arabidopsis* roots increased the root tolerance to hypoxia and also correlated with a higher AtPDC activity, suggesting a link between the lactic and ethanolic pathways (Dolferus *et al*., 2008). Other studies suggested that the pH acidification due to the short-term lactate accumulation also positively regulated PDC activity and ethanol fermentation (Felle *et al*., 2005; Roberts *et al*., 1984), providing another link between these 2 fermentative pathways.

Ethanol is produced by the action of two enzymes pyruvate decarboxylase (PDC) and alcohol dehydrogenase (ADH) (Dolferus *et al*., 1997). Several studies in barley (Mendiondo *et al*., 2016), *Medicago truncatula* (Ricoult *et al*., 2006), rice, lotus (*Nelumbo nucifera*) (Rocha *et al*., 2010a; Matsumura *et al*., 1998) demonstrated that *ADH* and *PDC* are induced in response to low O_2 stress and play a role in plant survival. In *Arabidopsis thaliana,* there are 4 *PDC* genes (At*PDC1,* At*PDC2,* At*PDC3* and At*PDC4*) encoded in the genome *(Kursteiner et al*., 2003). Some studies showed that both At*PDC1* and At*PDC2*, are induced in response to low O_2 stress (Mithran *et al*., 2014), whereas other studies suggest that actually only At*PDC1* and

not At*PDC2* is induced by low O_2 (Kursteiner *et al*., 2003). The explanation of these differences in the gene induction might be related to the plant developmental stage at which the plants were subjected to low O_2 treatment (Loreti *et al*., 2005). Experiments in *Arabidopsis* seedlings also suggested that AtPDC function might be tissue specific, with AtPDC1 playing a role in roots, whereas AtPDC2 appears to be specific for leaves (Mithran *et al*., 2014). Notably, *pdc1* and *pdc2 Arabidopsis* mutants displayed a lower survival rate after submergence, thus highlighting the important roles of PDC enzymes in plant tolerance and survival to low O_2 stress (Mithran *et al*., 2014).

As mentioned above, the other important enzyme in ethanolic fermentation is ADH. In rice, *adh* mutants display reduced coleoptile elongation compared to the wild type under submergence. Despite the reduced coleoptile length, the *adh* mutant seedlings were able to grow during low O_2 conditions. This suggests that while OsADH might play a role in seed germination under submergence, it is not essential for plant growth under low O_2 condition (Matsumura *et al*., 1995). In *Arabidopsis*, *adh* null mutants showed reduced tolerance to hypoxic treatment compared to the wild type. This effect was specific for roots, as shoots of *adh* mutants showed the same level of tolerance as the wild type (Ellis *et al*., 1999). These results suggest that AtADH is also important for hypoxia tolerance.

- **<u>Alanine-dependent pathways</u>**

Other products of anaerobic metabolism are alanine (Ala), GABA and succinate (de Sousa *et al*., 2003; Rocha *et al.*, 2010) (FIGURE 1.2). One amino group is transferred from glutamate to pyruvate leading to Ala and 2-oxoglutarate (2-OG) (Branco-Price *et al*., 2008). The reaction is catalysed by Ala aminotransferase (AlaAT) (Ricoult *et al*., 2006). 2-OG can then be oxidized by glutamate dehydrogenase (GDH) producing glutamate (Bailey-Serres *et al*., 2012) and NAD^+. Glutamate is converted to GABA, by glutamate decarboxylase (GAD). GABA is metabolized to succinic semialdehyde, that might play a role in cytolosic pH alcalinization (Aurisano *et al*., 1995; Banti *et al*., 2013). 2-OG can be metabolized into succinate, by succinyl CoA ligase (SCS) (Rocha *et al*., 2010). A recent study in lotus linked glycolysis with the TCA cycle through Ala (Rocha *et al*., 2010). Ala accumulation might also play a role in avoiding pyruvate accumulation, leading to

continuous glycolysis during waterlogging (Rocha *et al*., 2010). Another study in *Medicago truncatula* embryos indicated that *AlaAT* is induced in response to anoxia and correlated with Ala, GABA and glutamine accumulation (Ricoult *et al*., 2006)

- **Roles of non-symbiotic hemoglobin**

Another protein that plays an important role in plants in response to hypoxia is hemoglobin. The latter has been shown to accumulate during low O_2 stress (Bailey-Serres and Voesenek, 2008). There are 3 different classes of hemoglobins in plants: 1- leghemoglobins or symbiotic hemoglobins that play a role in O_2 diffusion to nitrogen-fixing bacteria found in plant nodules; 2- non-symbiotic hemoglobins and 3- truncated hemoglobins. The non-symbiotic haemoglobin is divided in 2 groups: group 1 and group 2. Group 1 HAEMOGLOBIN1 (HB1) is characterized by a higher O_2 affinity and is induced under low O_2 conditions (Dordas *et al*., 2003).

Overexpression of *HB1* was correlated with reduced ethanolic fermentation and increased ATP levels under hypoxia, due to a maintained respiration (Bailey-Serres and Voesenek, 2008). In order to study the role of *Arabidopsis* At*HB1* during low O_2 stress, overexpressing At*HB1* seeds were generated and subjected to low O_2 conditions. Seeds that overexpressed At*HB1* showed enhanced respiration rate, increased seed weight and decreased NO accumulation during hypoxia, compared to wild-type seeds. This suggests that At*HB1* plays a role in plant tolerance to low O_2 stress (Thiel *et al*., 2011). A detailed transcriptomics analysis of *Arabidopsis* plants overexpressing At*HB1* revealed that genes encoding receptor-like kinases, mitogen activated kinase (MAP), WRKY and APETALA2/ETHYLENE-RESPONSIVE ELEMENT BINDING PROTEIN (AP2/EREBP) transcription factors were induced. Genes coding for components related to ROS metabolism (Thiel *et al*., 2011) were also expressed at higher levels, suggesting a role of At*HB1* in the regulation of gene expression changes. Under normal O_2 conditions (normoxia), overexpression of At*HB1* plants resulted in the repression of *NITRATE REDUCTASE 2* (At*NIA2*) and *NITRITE REDUCTASE 1* (At*NiR1*) genes. The repression of the above mentioned genes might negatively regulate the nitrate assimilation (Thiel *et al.*, 2011). Importantly, AtNIA2 plays a role in converting nitrite to nitric oxide (NO) (Yamasaki and Sakihama, 2000), an important signalling molecule especially under hypoxic

conditions (see also Section 1.2.1.3, below). In At*HB1* overexpressing plants, NO production is reduced and this correlates with increased respiration rate during hypoxia (Thiel *et al*., 2011). In addition, transcripts of At*HB1*-overexpressing plants subjected to hypoxia were characterized by up-regulation of At*MnSOD1* and At*GLUTATIONE-S-TRANSFERASE*, which play a role in the regulation of ROS metabolism compared with the wild-type hypoxic plants (Thiel *et al*., 2011).

1.1.2.2. Anatomical and morphological changes in response to waterlogging

During waterlogging, the root is the first organ affected by hypoxia. Root acclimation to reduced O_2 due to waterlogging plays an important role in plant survival.

- **Aerenchyma formation**

One of the main changes observed in waterlogged plants is the formation of aerenchyma or intercellular lacunae in the root cortex (FIGURE 1.3 A in blue). Aerenchyma increases the tissue porosity and enhances gas diffusion.

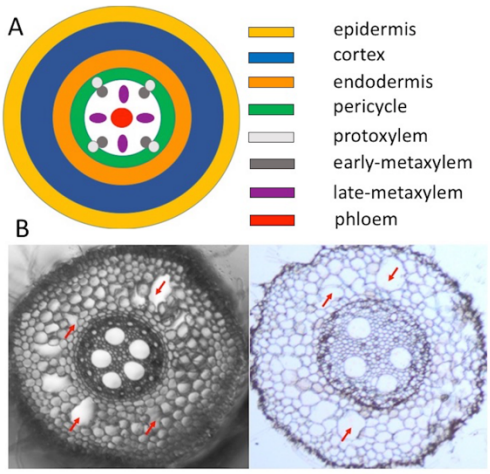

FIGURE 1.3 Aerenchyma formation in barley in response to waterlogging. A. Anatomy of a barley root (transverse section; modified from Knipfer and Fricke, 2014). **B.** Cross section of the barley roots exposed to waterlogging were visualized under the microscope. On the left side tissue was

hand sectioned and on the right side the tissue was sectioned using the microtome. The presence of aerenchyma is indicated by red arrows.

Aerenchyma positively affects the inward diffusion of O_2 in roots (Colmer *et al*., 2003; Laanbroek *et al*., 2010), leading to increased O_2 concentration in roots, enhanced oxidative phosphorylation and ATP production (Drew *et al*., 1985). Aerenchyma also plays an important role in the outward diffusion of ethylene (Colmer *et al*., 2003; Laanbroek *et al*., 2010), leading to reduced ethylene levels inside the cells.

Aerenchyma can be constitutively present in plants that are growing in wet lands or induced in response to waterlogging, mechanical impedance or nutrients deficiencies (Voesenek and Bailey-Serres, 2015; Abiko and Obara, 2014; Bouranis *et al*., 2003; He *et al*., 1994). Aerenchyma is observed in roots and shoots, in secondary tissues and in newly formed organs (e.g. adventitious roots) (Voesenek and Bailey-Serres, 2015). Based on the processes involved in aerenchyma formation, it can be classified as:

- lysigenous aerenchyma formed by programmed cell death (PCD) in the root cortex (Joshi and Kumar, 2012)
- schizogenous aerenchyma, which is formed as a result of cell separation
- expansigenous aerenchyma, which is the result of cell division and expansion (Colmer *et al*., 2003; Evans *et al*., 2003; Seago *et al*., 2005; Steffens *et al*., 2011).

The development of lysigenous aerenchyma in waterlogged roots is triggered by ethylene signalling (He *et al*., 1996; Rajhi *et al*., 2011; Shiono *et al*., 2008; Yamauchi *et al*., 2014) and involves Ca^{2+} and ROS signalling as well (Drew *et al*., 2000; Evans *et al*., 2003). In wheat, ROS production and downstream aerenchyma formation depends on the up-regulation of the *RESPIRATORY BURST OXIDASE HOMOLOGS* (*RBOH)* transcript (Yamauchi *et al*., 2014). The up-regulation of *RBOH*, a Ca^{2+}-dependent plasma membrane-localized respiratory burst oxidase that enhances ROS production, has also been shown to depend on ethylene signalling in wheat (Yamauchi *et al*., 2014). In addition, transcriptomics data from maize waterlogged root cortex showed an increased expression of genes encoding superoxide dismutase (SOD) and cell wall-loosening enzymes, that might also play a role in aerenchyma formation.

Additional experiments in barley demonstrated that aerenchyma formation was important for increased tolerance to waterlogging (Zhang *et al*., 2016). For example, Yerong (FIGURE 1.4 F), a waterlogging-tolerant barley variety is characterized by increased aerenchyma formation and changes in root porosity. In contrast, Franklin (FIGURE 1.4 G), a waterlogging-sensitive barley variety, does not form aerenchyma to the same extent. This indicates a positive role of aerenchyma formation for plant survival to waterlogging (Zhang *et al*., 2016).

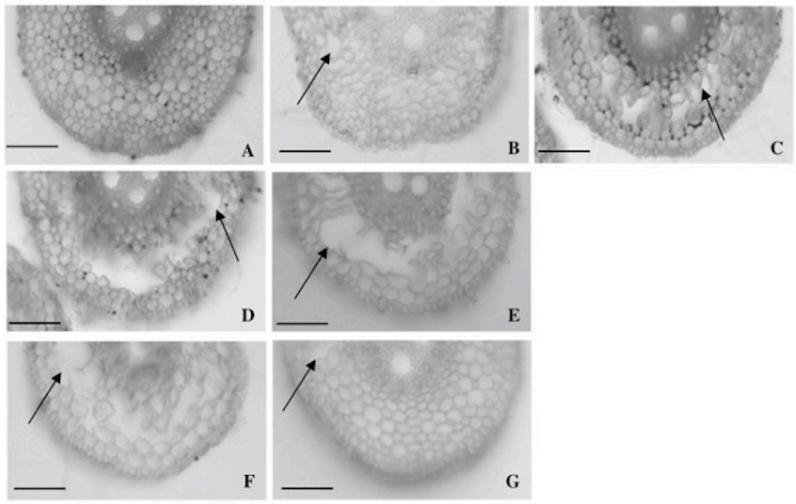

Light micrographs of cross section of adventitious roots. After 7 days waterlogging, aerenchyma formation from 0 (no aerenchyma) to 4 (well-formed aerenchyma), respectively from **a** to **e**. Yerong (**f**) had a larger proportion of aerenchyma than Franklin (**g**). *Bar* = 100 µm

FIGURE 1.4 Overview of aerechyma formation in seminal roots and associated scores. (Zhang *et al*., 2016)

- **<u>Apoplastic barrier development</u>**

Another trait observed in barley roots affected by waterlogging was the formation of an apoplastic barrier (Zhang *et al.*, 2016), which is formed at the outer layers of the roots (FIGURE 1.5) and functions to reduce radial oxygen losses (Colmer, 2003). Another function of the apoplastic barrier is to prevent the entry of toxic compounds from the soil inside the cells (Armstrong, 2006). Indeed, during waterlogging, decreased O_2 availability enhances the growth of anaerobic microorganisms, which release toxic metabolites (Conrad and Klose, 1999). The exact chemical composition of the apoplastic barrier is not known and seems to differ between plant species. Nevertheless, suberin (a natural polymer present in cell wall)

accumulation was observed at the exodermal and hypodermal root layers that were waterlogged (De Simone *et al*., 2003; Garthwaite *et al.*, 2008; Soukup *et al*., 2007).

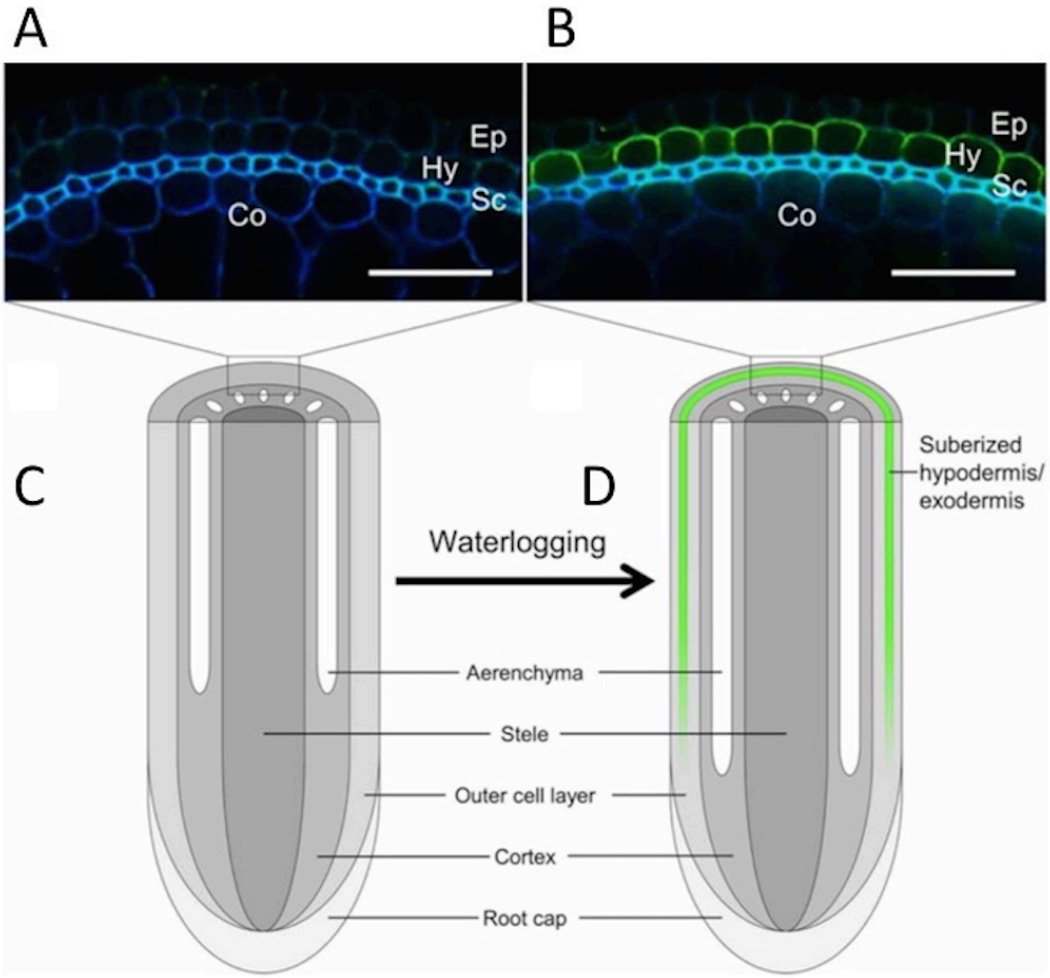

FIGURE 1.5 Apoplastic barrier in rice roots. A. Root section of rice plants grown in aerated conditions (Watanabe *et al*., 2013). **B.** Root section of rice plants grown in deoxygenated solution (Watanabe *et al*., 2013). **C.** Schematic diagram of a longitudinal view of rice root in aerated conditions (Watanabe *et al*., 2013). **D.** Schematic diagram of a longitudinal view of rice root in anaerobic conditions (Watanabe *et al*., 2013). In A and B cortex (Co), hypodermis/ exodermis (Hy), sclerenchyma (Sc) and epidermis (Ep) can be observed.

- **<u>Adventitious root formation</u>**

Another known response to waterlogging is the formation of adventitious roots (ARs). Adventitious roots form from leaf explants, stems and nodes, and from other roots (Steffens and Rasmussen, 2015). During waterlogging, the ARs can

replace the damaged primary root, positively affecting the plant survival. ARs formed in response to waterlogging also have a higher porosity compared to the primary root *(Laan et al.*, 1989), a trait that influences inwards O_2 diffusion. Importantly too, ARs grow closer to the surface layers of the soil (FIGURE 1.6), where more O_2 is available (Dawood *et al*., 2014).

AR formation involves ethylene signalling. Indeed, studies in cucumber (*Cucumis sativus*) indicate that pre-treatment with an ethylene precursor, 1-aminocyclopropane-1-carboxylic acid (ACC) prior to waterlogging treatment resulted in plants with an increased number of ARs compared with non-ACC treated plants. In contrast, treatment with an ethylene inhibitor 1-MCP, reduced the number of ARs (Qi *et al*., 2018). Auxin also appears to play a role in the formation of ARs in response to waterlogging. For example, in cucumber, treatment with synthetic auxin 1-naphthaleneacetic acid (NAA) increased the number of ARs, whereas N-1-naphthylphthalamic acid (NPA), an auxin transport inhibitor, reduced the AR formation, suggesting that auxin also positively regulates AR development (Qi *et al*., 2018). In addition, similarly to the mechanisms leading to aerenchyma formation, ROS accumulation and the activation of *RBOH* genes plays a role in AR formation (Steffens *et al*., 2012; Qi *et al*., 2018).

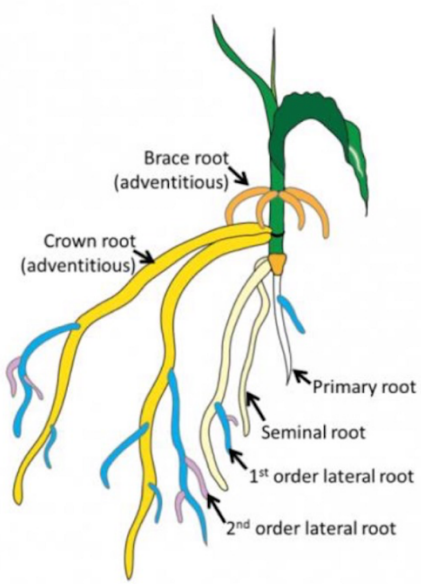

FIGURE 1.6. Schematic representation of different root types. White - primary root; Cream - seminal roots; Blue - first order lateral root; Pink - second order lateral root; Yellow - crown roots; Orange - Brace roots. Both crown roots and brace roots are adventitious roots.

1.1.3. Plant strategies to survive in waterlogged conditions

In order to survive in waterlogged conditions, plants have evolved two very different strategies, escape and quiescence (Bailey-Serres and Voesenek, 2008, 2010; Fukao *et al*., 2006; Hattori *et al*., 2009; Voesenek and Bailey-Serres, 2015).

1.1.3.1. Escape strategy

The escape strategy relies on consuming the small amount of energy left during waterlogging in order to reach an O_2 rich environment that will provide more energy (Bailey-Serres and Voesenek, 2008). In other words, plants that survive waterlogging through the escape strategy tend to promote growth of their aerial organs, so that they may remain out of the water, in contact with the atmosphere (FIGURE 1.7.).

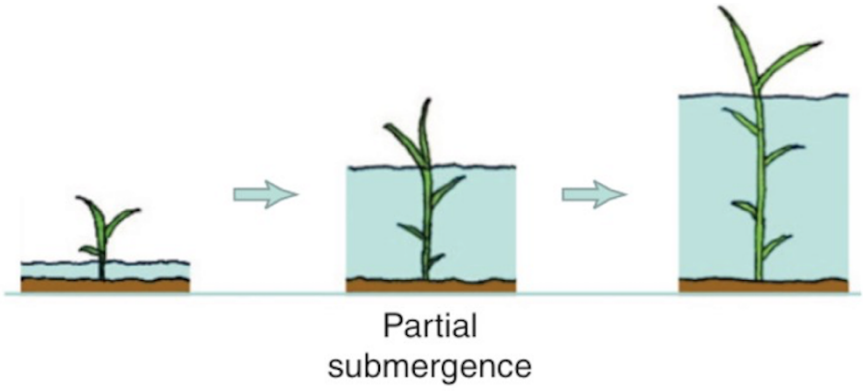

FIGURE 1.7. Schematic representation of the escape strategy. In response to partial submergence, plants elongate their stem to reach the air, which is richer in O_2. Figure from (Bailey-Serres *et al*, 2011).

The molecular mechanism that underlies the escape strategy was first characterized in rice varieties that are grown in deep water. More specifically, it involves SNORKEL1 (SK1) and SK2, two ethylene response factor (ERF) transcription factors (Hattori *et al*., 2009), which together with other regulators activate the expression of *GIBBERELIN20* (GA20) oxidase, a key enzyme involved in gibberellin (GA) biosynthesis (Ashikari *et al*., 2002; Kaneko *et al*., 2003). GA

accumulation then leads to enhanced internode elongation in plants growing in low O_2 conditions (Raskin and Kende, 1984; Hattori *et al*., 2009), which allows their aerial organs to grow out of the water. It was shown that in response to GA, both cell division and cell elongation at the internode region are enhanced (Raskin *et al*., 1984). Also, it was shown that the presence of light represses internode elongation (Raskin *et al.*, 1984), and hence suggests that the dark conditions experienced during submergence may contribute to shoot elongation.

The escape strategy is specific to plants that are submerged. As it was described before (Sasidharan *et al*., 2017) submergence is more severe than waterlogging, due to the fact that shoots and leaves are covered by water. In consequence, phenotypes related to low O_2 stress can be observed in leaves and shoots, not only in roots, as is the case for waterlogged plants (Bailey-Serres *et al*., 2012). Experiments in *Rumex palustris*, a model plant used to study the response to submergence, described leaf-related phenotypes. It was shown that the leaf area was reduced compared with the leaves of untreated plants and this also correlated with a reduced starch accumulation. The submerged leaves also had more stomata and their chloroplasts localized towards epidermis.

1.1.3.2. Quiescence strategy

The quiescence strategy is based on energy conservation and growth limitation during waterlogging (Bailey-Serres and Voesenek, 2008; Fukao *et al*., 2006). It was first described in rice and is specific to varieties grown in lowland areas (Bailey-Serres and Voesenek, 2008). A major quantitative locus, found on chromosome 9 and named *SUBMERGENCE1 (SUB1)* (Xu *et al*., 1996) correlated with a quiescence strategy (Bailey-Serres and Voesenek, 2008; Fukao *et al*., 2006). The *SUB1* locus contains 3 genes that code for ERF domain transcription factors, noted *SUB1A*, *SUB1B* and *SUB1C*, as well as 10 genes that are unrelated to ERF transcription factors (Xu *et al*., 2006). It was shown that *SUB1B* and *SUB1C* are present in most rice cultivars, whereas *SUB1A* is found in only some of the varieties (Xu *et al*., 2006). More detailed studies revealed the presence of two different *SUB1A* alleles, *SUB1A-1* that correlates with a submergence tolerant phenotype and *SUB1A-2* which correlates with a submergence intolerant phenotype (Xu *et al*., 2006). *SUB1A-1* allele is strongly induced in response to submergence compared to *SUB1A-*

2, that is barely induced (Xu *et al*., 2006). On the other hand, *SUB1C* induction in response to submergence was observed in intolerant cultivars (Xu *et al*., 2006). *SUB1B* gene expression was slightly induced in response to submergence in both tolerant and intolerant cultivars (Xu *et al*., 2006). These results suggest that *SUB1A-1* and *SUB1C* might have opposite roles in regulating rice tolerance to waterlogging (Xu *et al*., 2006). Ectopic expression of *SUB1A-1* in a submergence intolerant rice cultivar led to increased survival rate, demonstrating the important role of *SUB1A* in plant survival during submergence (Fukao *et al*., 2006; Xu *et al*., 2006). Plants that expressed *SUB1A-1* were characterized by low induction of *SUB1C* in response to submergence, result that is in agreement with the theory that *SUB1A* and *SUB1C* might play opposite roles in rice response to submergence (Xu *et al*., 2006). Overexpression of Os*SUB1A* leads to Os*ADH* induction and the down-regulation of *SUCROSE SYNTHASE* (*SUS*) genes, which play a role in carbohydrate metabolism. As a result, ethanol fermentation is enhanced and carbohydrate mobilization is attenuated (Fukao *et al*., 2006). Also, SUB1A induces the expression of *SLENDER RICE1* (*SLR1*) and *SLR2*, which act as negative regulators of GA signalling (Fukao *et al*., 2009), resulting in the inhibition of cell expansion and shoot elongation (Fukao *et al*., 2009). Using this strategy (FIGURE 1.8.), processes considered as unimportant and that are energy-consuming are shut-down (Perata *et al*., 2007).

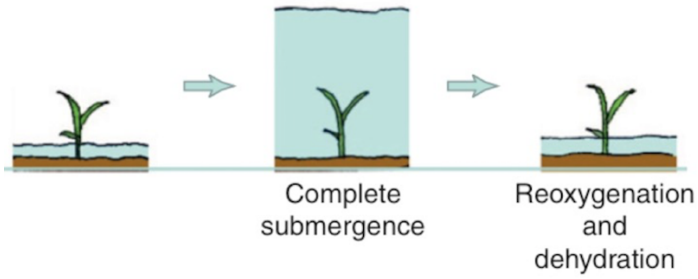

FIGURE 1.8. Visual summary of the quiescence strategy. In response to complete submergence, plants undergo a dormant period, during which growth is stopped. Figure from (Bailey-Serres *et al*, 2011).

1.2. Hypoxia sensing in plants

The molecular mechanisms that allow a plant to detect or sense hypoxic conditions which occur as a consequence of waterlogging or submergence rely on a ubiquitin-dependent protein degradation pathway, the N-end rule pathway.

1.2.1 The N-end rule pathway in *Arabidopsis thaliana*

The ubiquitin-proteasome system plays an important role in protein degradation *via* the conjugation of the small protein ubiquitin (Ub) to substrate proteins that need to be targeted for degradation (Varshavsky, 2006). Ub is a small protein that is present in all eukaryotes (Callis *et al*., 1995). Ub conjugation to substrate proteins is an ATP-dependent process that involves the action of three enzymes: E1, E2 and E3 (Ciechanover *et al*, 1982, Hershko *et al*., 1983, Hershko *et al*., 2000). First, an E1 or Ub-activating enzyme catalyses the formation of an acyl phosphoanhydride bond between the adenosine monophosphate (AMP) of ATP and the C-terminal carboxyl group of Ub, leading to Ub activation (Sadanandom, 2012). Upon activation, Ub binds to a cysteine residue present in the E1 *via* a thioester bond (Sadanandom, 2012). The activated Ub is transferred from E1 to E2 (also known as Ub-conjugating enzyme) by trans-esterification. Ub can then be conjugated to a substrate after recognition of the substrate by an E3 or Ub ligase and formation of a substrate/E3/E2 complex (Sadanandom, 2012). Once the first Ub is attached to the substrate via an isopeptide bond between the ε-amino group of a substrate's lysine residue and the carboxyl group of Ub, more Ub molecules can be conjugated using the lysine residue of another Ub, leading to the formation of a poly-Ub chain. Importantly, Ub contains 7 conserved lysine residues (K6, K11, K27, K29, K31, K48 and K63), which are important for the formation of different types of poly-Ub chains on a substrate protein (Sadanandom, 2012). Attachment of poly-Ub chain involving Ub's K48 is an important signal for degradation by the 26S proteasome (Pickart and Fushman, 2004).

Protein degradation mediated by the N-end rule pathway depends on the identity of a substrate's N-terminal amino acid residue, or some of its modifications (Bachmair *et al*., 1986; Varshavsky *et al*., 2005). Although different N-end rule pathways have now emerged in yeast and mammals (Baker and Varshavsky, 1995;

Grigoryev *et al*., 1996; Kwon *et al*., 2000; Kwon *et al*., 2002; Lee *et al*., 2005; Varshavsky, 2011) here, I will focus on one particular branch, which relies on the activity of an E3 ubiquitin ligase termed PROTEOLYSIS6 (PRT6). E3 ligases of the N-end rule pathway (also termed N-recognins) have the ability to recognize so-called destabilizing N-terminal residues of a substrate protein. In addition to the presence of this destabilizing residue, an N-end rule substrate is expected to have an internal lysine residue (the site of ubiquitylation) and a flexible region close to the N-terminus (Bachmair and Varshavsky, 1989).

Based on the identity of the residue present at their N-terminus, proteins can be stabilized or quickly degraded. In *Arabidopsis,* the stabilizing residues that result in long-lived proteins are Met, Gly, Val, Thr, Ser and Ala (Graciet *et al*., 2010) (FIGURE 1.9). In contrast, the N-terminal destabilizing residues Gln, Asn, Cys, Glu, Asp, Arg, Lys, His, Leu, Ile, Phe, Trp and Tyr can be sufficient to target a protein for degradation through the N-end rule pathway (Bachmair *et al*., 1986; Huang *et al*., 1987; Gonda *et al*., 1989; Graciet *et al*., 2010, Varshavsky, 2011; Tasaki *et al*., 2012; Gibbs *et al*., 2014), if they are made N-terminal. Depending on the number of modifications that they require before the protein is targeted for degradation by an N-recognin, the destabilizing residues can be classified as tertiary (Asn, Gln, Cys), secondary (Asp, Glu, oxidized Cys) or primary destabilizing residues (Arg, Lys, His, Leu Phe, Trp, Tyr and Ile) (Bachmair *et al*., 1993; Worley *et al*., 1998. Stary *et al*., 2003; Garzon *et al*., 2007; Tasaki, *et al*., 2009; Graciet *et al*., 2010;).

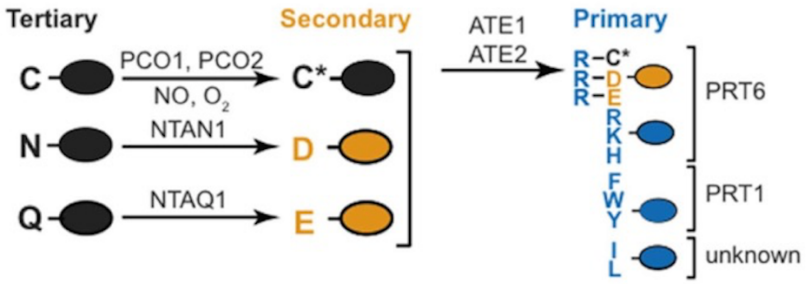

FIGURE 1.9. Hierarchical organization of the N-end rule pathway in plants, including enzymatic components. Ovals denote protein substrates. N-terminal residues are indicated using single letter abbreviations. C* corresponds to oxidized cysteine, which is obtained through the enzymatic activity of PLANT CYSTEINE OXIDASE (PCO) enzymes (Weits *et al*., 2014; White *et al*., 2017; White *et al*., 2018). AtNTAN1 (N-TERMINAL ASPARAGINE AMIDASE) and AtNTAQ1 (N-TERMINAL GLUTAMINE AMIDASE) code for 2 amidases that deamidate Asn and

Gln into Asp and Glu, respectively (Kwon *et al*., 2000; Wang *et al*., 2009; Graciet *et al*., 2010). AtATE1/2 are 2 functionally redundant Arg-transferases (Yoshida *et al*., 2002) that conjugate Arg, a primary destabilizing residue, to the N-terminus of proteins starting with Asp, Glu or oxidized Cys (Hu *et al*., 2005; Lee *et al*., 2005; Graciet *et al*., 2010).Finally, primary destabilizing residues are directly bound by N-recognins, of which 2 have been identified in Arabidopsis: PRT6 and PRT1 (Garzon *et al*., 2007; Potushak *et al*., 1998; Graciet *et al*., 2010; Gibbs *et al*., 2014). Figure from (de Marchi *et al*, 2016).

1.2.1.1 Enzymatic components of the N-end rule pathway that are relevant to O_2 sensing

- **Plant cysteine oxidases**

Cys, a tertiary destabilizing residue (Hu *et al*., 2005; Lee *et al*., 2005; Graciet *et al*., 2010), is oxidized by PCOs, in the presence of O_2 and NO, leading to Cys-sulfinic acid, a secondary destabilizing residue (Gibbs *et al*., 2014; Weits *et al*., 2014; White *et al*., 2017). PCOs are key enzymes required to target substrate proteins bearing Cys at their N-terminus for degradation through the N-end rule pathway (Weits *et al*., 2014). It is known that RELATED TO APETALA2.12 (AtRAP 2.12) (see Section 1.2.1.2) induces the expression of At*PCO1* and At*PCO2*, suggesting that the existence of a positive feedback loop mechanism that regulates the abundance of these proteins in plant cells (Weits *et al*., 2014). Also, the fact that At*PCO1* and At*PCO2* are induced by hypoxia further supports the role of the N-end rule pathway in O_2 sensing (Gibbs *et al*., 2014; Weits *et al*., 2014; White *et al*., 2017) (FIGURE 1.10.).

- **Arginine transferases**

Secondary destabilizing residues (Asp, Glu and oxidized Cys) are arginylated by arginyl-tRNA-protein transferases, AtATE1 and AtATE2, leading to a primary destabilizing residue (Arg) at the N-terminus of the substrate protein (Ciechanover *et al*., 1988; Balzi *et al*., 1990; Kwon *et al*., 1999; Yoshida *et al*., 2002). It was shown that At*ATE1* and At*ATE2* play a role in leaf senescence (Yoshida *et al*.,2002), shoot

and leaf development and internode elongation (Graciet *et al*., 2009). It was also shown that *ate1 ate2* double mutants constitutively express genes involved in hypoxic response, demonstrating the relevance of the N-end rule pathway in this process (Gibbs *et al*., 2011; Licausi *et al*., 2011; Mendiondo *et al*., 2016; Mustroph *et al*., 2009) (FIGURE 1.10.).

- **PRT6**

Primary destabilizing residues (Arg, Lys, His, Leu Phe, Trp, Tyr and Ile) are recognized by N-recognins, ubiquitylated and degraded by the 26S proteasome. In *Arabidopsis*, there are two N-recognins, PRT1 and PRT6 (Bachmair *et al*., 1993; Potuschak *et al*., 1998; Stary *et al*., 2003; Garzon *et al*., 2007). PRT6, in particular, shares sequence similarities with yeast and mammalian UBR1 (Varshavsky *et al*., 1996) and contains the characteristic UBR domain (Garzon *et al*., 2007) (Tasaki *et al*., 2005). The latter was shown to be necessary to bind basic N-terminal destabilizing residues such as Arg, Lys and His. Notably, PRT6 acts downstream of the Arg transferases (FIGURE 1.10.).

1.2.1.2 N-end rule substrates and their role in O_2 sensing

The genome of *Arabidopsis* codes for 5 different ERF-VII transcription factors: RELATED TO APETALA2.2 (RAP2.2), RAP2.3, RAP2.12, HYPOXIA RESPONSE ELEMENT1 (HRE1) and HRE2 (Licausi *et al*., 2010). Experiments in *Arabidopsis*, demonstrated that At*HRE1*, At*HRE2* (Nakano *et al*., 2006), At*RAP2.2* and At*RAP2.12*, but not At*RAP2.3* were induced by hypoxia (Licausi *et al*., 2010). Also, At*HRE1* and At*HRE2*, seemed predominantly expressed in roots (Licausi *et al*., 2010). In order to determine the function of At*HRE1* and At*HRE2* in tolerance to hypoxia, mutant lines for these two transcription factors (i.e. *hre1*, *hre2*, *hre1 hre2* lines), as well as At*HRE1* and At*HRE2* overexpression lines were used. Following a 10-hr anoxia treatment, the survival rate of the different plants was compared. While the survival rate was approximately 10% for wild-type plants, as well as *hre1* and *hre2* single mutant plants, *hre1 hre2* double mutant plants were more sensitive to anoxia. This indicated that (i) these 2 transcription factors are important for anoxia tolerance; and (ii) At*HRE1* and At*HRE2* might have at least partially redundant roles in mediating plant response to anoxia (Licausi *et al*., 2010). In contrast, At*HRE1*

overexpression lines, but not At*HRE2* overexpressing lines, showed enhanced survival rates after anoxia treatment (Licausi *et al*., 2010). The increased tolerance observed in At*HRE1* overexpression lines correlated with a higher induction of At*ADH1* and At*PDC1* (Licausi *et al*., 2010), as well as reduced expression of genes coding for ROS protective enzymes, suggesting that these plants may produce less ROS during anoxia (Licausi *et al*., 2010).

Notably, the 5 above-mentioned ERF-VII transcription factors start with the sequence Met-Cys at their N-terminus (Licausi *et al*., 2010). It was hypothesized that the initial Met residue could be removed by the action of methionine aminopeptidases, resulting in the exposure of a Cys residue at the N-terminus of these transcription factors. If this N-terminal Cys residue could be oxidized (e.g. in the presence of O_2), the ERF-VII transcription factors could constitute a set of N-end rule substrates. In order to test if AtHRE1 and AtHRE2 were N-end rule substrates, *in vivo* assays were performed with plants expressing HA-tagged At*HRE1-HA*, At*HRE2-HA* or HA-tagged mutant versions of the transcription factors, in which the second Cys residue was mutated into Ala (mutants noted C2A). In this case, action of methionine aminopeptidases would expose Ala (a stabilizing residue) at the N-terminus of the ERF-VII transcription factors, which should result in their stabilization, if they are N-end rule substrates. In agreement with an N-end rule-mediated degradation of AtHRE1/2, only the C2A mutated versions of the transcription factors could be detected in wild-type plants (Gibbs *et al*., 2011). In addition, HA-tagged AtHRE2 also accumulated in *prt6* mutant plants, thus confirming a role of PRT6 and the N-end rule pathway in the regulation of HRE2 protein levels (Gibbs *et al*., 2011).

In order to check the effect of oxygen concentration on the transcription factors stability, the accumulation of AtHRE1-HA, AtHRE2-HA, AtHRE1(C2A)-HA, AtHRE2(C2A)-HA was checked during normoxia and hypoxia (Gibbs *et al*., 2011). AtHRE2-HA, but not AtHRE1-HA accumulated after 2 hrs of hypoxia. AtHRE2-HA accumulation was diminished when plants were returned to normoxia, suggesting an O_2-dependent stabilization of the ERF-VII transcription factor (Gibbs et al., 2011). Interestingly, seedlings overexpressing the mutated versions of At*HRE1* and At*HRE2* (C2A), were more tolerant to hypoxia, suggesting the importance of AtHRE1 and AtHRE2 stabilization for plant tolerance to waterlogging or flooding (Gibbs *et al*., 2011).

In addition, *Arabidopsis* plants overexpressing At*RAP2.12* under the control of the constitutive 35S promoter were more tolerant to submergence. The increased tolerance could be explained by the stronger up-regulation of hypoxia-response genes such as At*PDC1*, At*HB1*, At*ADH1*, At*SUS4* and At*SUS1* (Licausi *et al*., 2011). In order to test if RAP2.12 was an N-end rule substrate, accumulation of transiently expressed AtRAP2.12-GFP was tested in *ate1ate2* and *prt6* mutant plants, as well as in the wild type (Licausi *et al*., 2011). AtRAP2.12-GFP accumulated in the nucleus of *ate1ate2* and *prt6* plants, even under normoxic conditions, indicating that its stability relates to the N-end rule pathway (Licausi *et al*., 2011). In order to check that the stabilization of At*RAP2.12* was O_2 dependent, the N-terminal region of AtRAP2.12 was fused to a luciferase (LUC) reporter. Upon hypoxia treatment, LUC activity was enhanced, while upon re-oxygenation, LUC activity decreased, thus linking AtRAP2.12 degradation with the oxidation of its N-terminal Cys residue as well (Licausi *et al*., 2011).

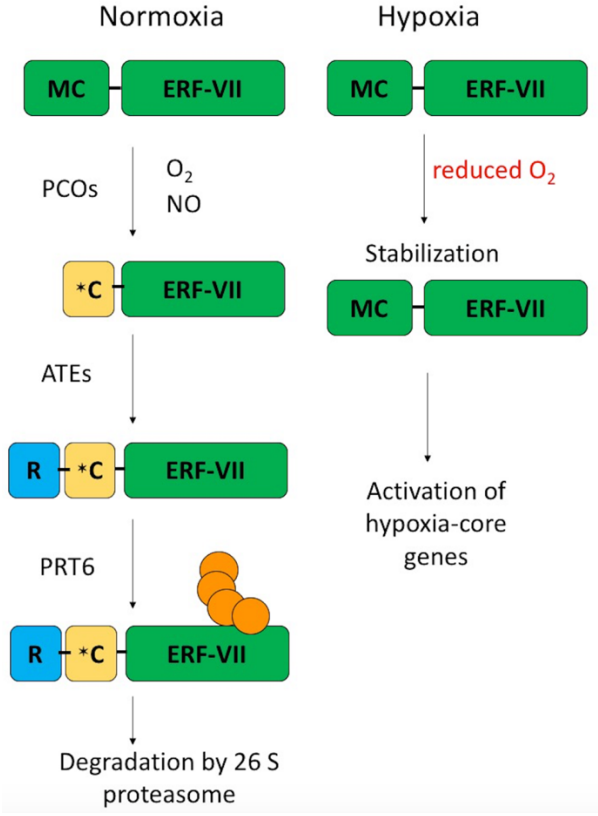

FIGURE 1.10. N-end rule pathway and its role in oxygen sensing. During normoxia, ERF-VII transcription factors bearing MC at their N-terminus are degraded through the N-end rule pathway. First, Met is removed by methionine aminopeptidases (MetAPs) (Bradshaw *et al*., 1998; Huang *et al*., 1987), exposing

Cys at the N-terminus. Cys, in the presence of oxygen, nitric oxide and by the action of PCOs is oxidized, leading to oxidized Cys (*C) (Weits *et al*., 2014; Gibbs *et al*., 2011; Licausi *et al*., 2011; Gibbs *et al*., 2014, White *et al*., 2016, White *et al*., 2018), a secondary destabilizing residue. The oxidized cysteine is then arginylated by ATEs, exposing Arg at the N-terminus of the protein. Arg, a primary destabilizing residue is recognized by PRT6, ubiquitylated (orange circles) and degraded by the 26S proteasome (Garzon *et al*., 2007; Graciet *et al*.,2009). On the other hand, during hypoxia, the ERF-VII transcription factors are stabilized due to the absence of Cys oxidation, triggering the activation of hypoxia-core genes (Licausi *et al*., 2010; Gibbs *et al*., 2011; Licausi *et al*., 2011).

1.2.1.3. The N-end rule pathway and nitric oxide signalling

As indicated above, NO is an essential signalling molecule that plays an important role in plant responses to waterlogging or submergence. Importantly, the oxidation of N-terminal Cys in mammals was shown to be also dependent on NO. Hence, the mechanisms uncovered for ERF-VII degradation could also serve as a link for NO signalling. In mammals, NO is produced by nitric oxide synthases (NOSs) (Crane *et al*., 1998). In plants, however, there are no NOS homologs. Instead, NO synthesis relies on the activity of NIAs and NITRIC OXIDE-ASSOCIATED PROTEIN1 (AtNOA-1) (Besson-Bard *et al*., 2008). In order to assess if the N-end rule dependent degradation of the ERF-VII transcription factors is regulated by NO, N-end rule reporters were used. The reporters consisted of MC- or MA-GUS or a ubiquitin-Cys-GUS fusion protein. The first 2 reporters are expected to be modified by methionine aminopeptidase, thus resulting in the exposure of a GUS reporter with either N-terminal Cys or N-terminal Ala. The second reporter, is typically cleaved after the last residue of ubiquitin by deubiquitylating enzymes, thus releasing a Cys-GUS reporter. Seedlings containing the different reporter constructs were treated with a NO scavenger - 2-(4-carboxyphenyl)-4,4,5,5-tetramethylimidazoline-1-oxyl-3-oxide (cPTIO) - or NO donors, S-nitroso-N- acetyl-DL-penicillamine (SNAP) or sodium nitroprusside (SNP). MC-GUS stability was increased by cPTIO and reduced

by SNAP and SNP treatment. cPTIO did not enhance the stability of the MA-GUS reporter. Also, MC-GUS activity was not increased in *prt6* and *ate1ate2* N-end rule mutants, suggesting that NO is regulating the stability of N-end rule substrates that bear Cys at their N-terminus (Gibbs *et al*., 2014). To confirm that this is the case for ERF-VII TFs, similar assays were done in seedlings expressing MC-At*RAP2.3*-HA and MC-At*HRE2*-HA. Treatment with cPTIO led to the accumulation of MC-AtRAP2.3-HA and MC-AtHRE2-HA in wild type seedlings, confirming the role of NO in their degradation. MC-HRE2-HA accumulated in a *prt6* mutant, linking AtHRE2 stability to the N-end rule and NO (Gibbs *et al*., 2014). To further confirm the link between the N-end rule pathway-mediated degradation of the ERF-VII transcription factors and NO availability, a *nia1 nia2* double mutant that is characterized by very low NO levels (Desikan *et al*., 2002; Lozano-Juste and Leon, 2010; Rockel *et al*., 2002) was used. More specifically, the *nia1 nia2* mutant was crossed with a plant encoding the 35S:MC-At*HRE2*-HA transgene. The stability of MC-AtHRE2-HA was increased in *nia1 nia2* background and was reduced when seedlings were treated with NO donors, confirming again the role of NO in the regulation of AtHRE2 stability (Gibbs *et al*., 2014).

1.2.2 The N-end rule pathway and hypoxia response in barley

Studies in barley demonstrated the role of the N-end rule protein degradation pathway in waterlogging tolerance in this monocot crop (Mendiondo *et al*., 2016). Barley Hv*PRT6* RNAi lines, characterized by reduced Hv*PRT6* mRNA, were isolated and their response to waterlogging was assessed (Mendiondo *et al*., 2016). Compared with-type barley plants, Hv*PRT6* RNAi lines were more tolerant to waterlogging based on increased biomass and yield, enhanced expression of hypoxia-core genes and their ability to maintain chlorophyll content even during low O_2 conditions (Mendiondo *et al*., 2016). Hv*PRT6* RNAi lines were also able to retain their chlorophyll content during darkness, a trait that can be important during submergence, when light is reduced (Mendiondo *et al*., 2016). In addition to the RNAi lines, plants with point mutations in Hv*PRT6* were also isolated and characterized. They behaved similarly to lines expressing an RNAi for Hv*PRT6* (Mendiondo *et al*., 2016).

Altogether, these results indicate that the role of the N-end rule pathway in the regulation of waterlogging response in conserved in barley.

In barley, there are 13 APETALA2 (AP2) proteins that poses MC at their N-terminus, but only 7 of them share enhanced similarity with the MCGGAI(I/L) N-terminal conserved motif, which is specific for ERF-VII transcription factors (Mendiondo *et al*., 2016). So far, two barley ERF-VII transcription factors have been described: Hv*RAF* (Jung *et al*., 2007) and Hv*BERF1* (Osnato *et al*., 2010), which is closely related to At*RAP2.12* (Licausi *et al*., 2011). Importantly, HvBERF1 also bears the Met-Cys sequence at its N-terminus, and was shown to be an N-end rule substrate in barley as well (Mendiondo *et al*., 2016).

Additional experiments with GUS reporter constructs introduced in barley indicated that O_2-dependent N-terminal Cys oxidation was both possible and important in barley (Mendiondo *et al*., 2016). This indicated that, in barley, the N-terminal Cys residue that is conserved in several ERF-VII transcription factors could sense low O_2 conditions (Mendiondo *et al*., 2016) and that this mechanism is conserved across flowering plants (Gibbs *et al*., 2011; Gibbs *et al*., 2014).

Other similarities between *Arabidopsis* and barley, include (i) the fact that NO is also sensed through the N-end rule pathway (Gibbs et al., 2014); (ii) the constitutive expression of hypoxia-core genes, especially *ADH1*, *HB* and *PDC1* (Gibbs *et al*., 2011; Licausi *et al*., 2011; Mendiondo *et al*., 2016; Mustroph *et al*., 2009); and (iii) increased tolerance to waterlogging.

1.3. Aims

1.3.1. Characterization of waterlogging response in barley using the AGOUEB population

The main objective of this work was to characterize the responses of different commercial barley cultivars to waterlogging with the aim of identifying varieties that are more tolerant to this abiotic stress. This project was done in collaboration with Teagasc. The work focused on winter barley varieties that are part of Association Genetics Of UK Elite Barley (AGOUEB) population, which consists of barley

varieties that have been commercialized on the UK National and Recommended List trials between 1988 and 2006 (www.cereals.ahdb.orh.uk), and involved field waterlogging experiments, as well as experiments in controlled conditions.

Another aim of this work was to understand the molecular mechanisms underlying the waterlogging tolerance or sensitivity of the different varieties of the AGOUEB population. For this purpose, I established a waterlogging protocol in controlled conditions and identified the parameters that could be monitored to reliably assess the response of the different barley cultivars. I complemented this approach with transcriptomics approaches in order to monitor genome-wide gene expression changes, and determine if specific pathways were either activated or repressed in tolerant or sensitive varieties.

1.3.2. Generation of barley plants mutant for Arg-transferase

Another aim of my PhD project was to generate barley plants that are affected for the activity of the Arg-transferase Hv*ATE1*, and to characterize their response to waterlogging. Previous studies in *Arabidopsis thaliana* indicated that *ate1 ate2* double mutant plants for the Arg-transferases were more tolerant to hypoxia compared to wild-type plants, as a result of the ERF-VII transcription factors stabilization (Gibbs *et al*., 2011; Licausi *et al*., 2011). We had hence hypothesized that barley plants with decreased Arg-transferase activity would likely have improved waterlogging tolerance. This possibility was confirmed by Mendiondo *et al*. after I started my PhD project (Mendiondo *et al*., 2016), although the component that was targeted in this paper was the N-recognin PRT6 that acts downstream of the Arg-transferases.

1.3.3. Investigating the role of BIG in Arabidopsis

A last aim of my PhD, was to characterize a potential role of the *Arabidopsis* protein BIG in the N-end rule pathway. It was speculated that BIG might act as an E3 ligase of the N-end rule pathway (Tasaki *et al*., 2005), based on its sequence similarities with the mammalian N-recognin UBR4 (Tasaki *et al*., 2005). As the N-recognin that targets proteins bearing Leu and Ile at their N-terminus has thus far not been identified, BIG could be a possible candidate. As part of my PhD, I aimed at

testing a role of BIG as an N-recognin and also studied a potential link between BIG and PRT6.

2. Materials and methods

2.1 Materials

2.1.1 Barley lines

For barley-related experiments, the following commercial cultivars were used:
Arma, Isa, Louise, Retriever, Dura, Masquerade, Passport, Regina, Madrigal, Pilastro, Vesuvius, Tapir, Cosmos, Infinity, Maeva, Siberia, Breeze, Cavalier, Mahogany and Tamaris, all of which are part of the AGOUEB population (Xu et al., 2018). Other commercial barley varieties used include Golden promise, Barke, Tesla, Sanette.

Targeting Induced Local Lesion IN Genome (TILLING) lines carrying mutations in Hv*ATE1* (Table 2.1) were kindly provided by Dr. Nils Stein (Leibniz-Institut für Pflanzengenetik und Kulturpflanzenforschung (IPK), Gatersleben, Germany).

Table 2.1: TILLING lines carrying mutations in Hv*ATE1*. The number in the upper part of the gene represents the position from ATG in CDS.

Line	Background	Reference
TILLING *4 (HvATE1$^{664G/A}$)*	Barke	Dr Nils Stein
TILLING 5 *(HvATE1$^{725C/T}$)*	Barke	Dr Nils Stein
TILLING 6 *(HvATE1$^{748G/A}$)*	Barke	Dr Nils Stein
TILLING 9 *(HvATE1$^{1091G/A}$)*	Barke	Dr Nils Stein
TILLING 10 *(HvATE1$^{1199G/A}$)*	Barke	Dr Nils Stein

2.1.2 *Arabidopsis thaliana* lines

For all experiments, *A. thaliana* accession Columbia-0 (Col-0) was used, as indicated in Table 2.2 below.

Table 2.2: *Arabidopsis thaliana* lines used in this study.

Line	Accession	Reference
big (SALK_045560)	Col-0	(Ivanova *et al*., 2014)
prt6-5 (SALK_051088)	Col-0	*(*Graciet *et al*., 2009*)*
big prt6-5	Col-0	(Walter, 2010)

2.1.3 Bacterial strains and plasmids

The following bacterial strains have been used:

- *E. coli* stbl2^{TM}: *F-, mcrA, Δ(mcrBC-hsdRMS-mrr), recA1, endA1, gyrA96, thi-1, supE44, relA1, λ-, Δ(lac-proAB)*

- *E. coli* TP611: *thi thr leuB6 lacY1 tonA21 supE44 hsdR hsdM recBC lop-11 cya-610 pcnB80 zad:Tn10* (Glaser *et al*., 1993)

- *A. tumefaciens* AGL1 (Matthews *et al*., 2001)

Plasmids used are listed in Table 2.3 below.

Table 2.3: Plasmids used in this study.

Plasmid	**Details**	**Reference**
pJET1.2/blunt	pJET1.2/blunt	
pICSL90003	Plasmid coding for the wheat U6 promoter	Addgene #68262; (Lawrenson *et al*., 2015)
pICH47751	Level 1, position 3 acceptor	Addgene #48002; (Lawreson *et al*., 2015)

pICH86966	Plasmid coding for sgRNA template	Addgene #46966; (Lawreson *et al*., 2015)
pICSL11059	Plasmid coding for barley plant selection cassette	Addgene #68263; (Lawreson *et al*., 2015)
pICSL11056	Plasmid coding for barley Cas9 cassette	Addgene #68258; (Lawreson *et al*., 2015)
pICH50892	Plasmid coding for position 3 end linker	Addgene #48046; (Lawreson *et al*., 2015)
pAGM8031	Binary Vector Backbone; Level M acceptor	Addgene #48037; (Lawreson *et al*., 2015)
pJET1.2 $T7_{pro}$: Hv*ATE1*$^{398\text{-}1630}$ (pAM16)	Plasmid coding for Hv*ATE1*$^{398\text{-}1630}$	This study
pICH47751 $U6_{pro}$: sgRNA expression cassette targeting Hv*ATE1v1* (pAM17)	Plasmid coding for sgRNA targeting Hv*ATE1v1*	This study
pICH47751 $U6_{pro}$: sgRNA expression cassette targeting Hv*ATE1v2* (pAM18)	Plasmid coding for sgRNA targeting Hv*ATE1v2*	This study
pAGM8031 $U6_{pro}$: sgRNA expression cassette targeting Hv*ATE1v1*, $CaMV35S_{pro}$: *HptII*, $ZmUbi_{pro}$: *Cas9*, position 3 end linker (pAM19)	Plasmid coding for sgRNA targeting Hv*ATE1v1, Cas9* and *HptII*	This study

pAGM8031 U6$_{pro}$: sgRNA expression cassette targeting Hv*ATE1v2*, CaMV35S$_{pro}$: *HptII*, ZmUbi$_{pro}$: *Cas9*, position 3 end linker (pAM20)	Plasmid coding for sgRNA targeting Hv*ATE1v2, Cas9* and *HptII*	This study

2.1.4 Oligonucleotides

Oligonucleotides used to generate plasmids, to genotype plants and to monitor gene expression are listed in Table 2.4.

Table 2.4. List of oligonucleotides used in this study

Name	**Sequence 5'-3'**
AM8_up	TGGTCATTACACCATTGGCAAGGAGA
AM9_lo	GTGTATGTTGGGCGCTCAATGTCA
AM_20 up	cgctGT CGA C ATG GAG ACC AAC TCT TCT CTT TTT G
AM_21	cactGT CGA CTT AAT GTA AGA CGG CTC CAA TTG TG
AM_35	tgtggtctca CTTG CATATACCATACGTCTGAA ***gttttagagctagaaatagcaag***
AM_36	tgtggtctca AGCG ***taatgccaactttgtac***
AM_37	tgtggtctca CTTG GAGAGCTTGACCCACAGGT ***gttttagagctagaaatagcaag***
AM_38	tgtggtctca CTTG TCCAATGAGTTCTTCTCTC ***gttttagagctagaaatagcaag***
AM_39	tgtggtctca CTTG GTTCCAGAAGAGCACCTGC ***gttttagagctagaaatagcaag***
AM_40	tgtggtctca CTTG TAGAAGAAAACAAGACAGA ***gttttagagctagaaatagcaag***
AM_45	GCA AGT GGT CGT ACT ACT GGT ATC GTT C

AM_46	GGATCTTCATAAGGGAGTCCGTGAGAT
AM_47	CCACCATCCCAACCATCGGTTT
AM_48	CCTGCGTATTCTGGAAGTAGTGCCT
AM_49	GCT CAC TTG AAG GGT GGT GCC
AM_50	TGATGGCATGAACAGTGGTCATCAGAC
AM_51	CGGGAAGGAAGCCATGTCTGC
AM_52	TCTGCCTCGCCGACGG
AM_53	CCGCCTACGAGAACTACAAGAGGATC
AM_54	TTCATACCCGCAGCCCTCG
AM_55	tataCCCGGGATGGCAGATGACTTG
AM_56	ttttGTCGACgctTTCTCCAAGCTGATCTGC
AM_59	agagGAATTCTGACACGGATCTTTTGCAGC
AM_60	gagaGGATCCATATCTCCTAACAAAAGCCGTATGA
AM_67	TCTGACAGTTCTGGTGCTCAACA
AM_82	TGGTTTTGCAGTGAAcGCTTGTAATGGagAT
AM_83	TGG TAC AAA GCA tAC TCC TCA GGG TCA
AM_84	AAAAGAAAGTAGGAGAAGCAGCACAAGAAttAtA
AM_85	TGAATAGAAGTTCAGATGaCCATTACAAGCT
AM_86	AAAGAAAGTAGGAGAAGCAGCACAAGAAATCTAG
AM_87	ATTACAAGaTaTCACTGCAAAACCAGCT
AM_88	AGCACAAGAAAAGAAGGGAGGAACAGTTCTA
AM_89	TAGAAGTTCAGATGaCCATTACAAGaTTTC
AM_91	CTGTCTaCAGTAACTAAGCGT GCAAAGC
AM_92	ATCAATGCTAGTATGGTTCTGAATTGCCTGAAT
AM_93	TACGGACGAGTACAAGGTGCCG
AM_94	GCTTGGTGATCTGGCGTGTCTCA
AM_95 up	TCCGACCTGATGCAGCTCTCG
AM_96 lo	TCTACACAGCCATCGGTCCAGAC
AM_97	GCA TTG CCT GAA GAA AAA CGT GCA GTT ATA
AM_98	AGTCTTGCATCATTTTTGTTCAGTGAGCT

AM_99	AGTTCATAAGGAGAAGACAGTCACAGAgA
AM_100	TCCAAGAGATAGGAAAGCAAGGTCAGG
AM_101	GCG GTT TTG GTT CAT TCC ATC AGC ATT ATA
AM_102	GGTAATAGTGCTCAAGGCTAGGGCAA
AM_103 up	AGCCTGAGATGGAACGGACATGC
AM_104 lo	GAGAAGTTCTGATGGTCGATATGCAGCTT
AM_107	TTCTAATACGACTCACTATAGCATATACCATACGTCTGAAGT TTTAGAGCTAGA
AM_108	TTCTAATACGACTCACTATAGGAGAGCTTGACCCACAGGTG TTTTAGAGCTAA
AM_109	TTCTAATACGACTCACTATAGTGTACTTAAAAGGATGCAAG TTTTAGAGCTAGA
AM_110	TTCTAATACGACTCACTATAGTAGGTACGTGCTTCCAAGGGT TTTAGAGCTAGA
AM_134 lo	GACCTGATGCAGCTCTCGGA
AM_135 up	GCA TCA CAA TCA TGG AGC GAT CAA G
AM_136 lo	CTG TCT CCA CCG AGC TGA GAG
HvADH 1 F	CACTGACCTGCCCAATGTC
HvADH 1 R	GCACGCTGTGTGTGATGAA
HSP 70 F	GCTCAACATGGACCTCTTCAGG
HSP 70 R	CCGACAAGGACAACATCATGG
At104_ up	**Ttgagagccccagtcccgt**

At105_lo	**Gtcaccttgaccactccaag**
At120_up	AAAATTGATCCTTTCCATGCC
At121_lo	CAACATAAGAATCTGCGGGAG
LB2	CCAAACTGGAACAACACTCAACCCTATCTC
PADH1_up	ACCAAGCATACAATCAACTCCAA

2.2 Methods

2.2.1 Bacteria-related methods

2.2.1.1 Preparation of chemically competent *E. coli* stbl2

Chemically competent *E. coli* cells were prepared as described in (Inoue, et al. 1990). stbl2 cells were streaked on a lysogeny broth (LB) plate (Appendix 1) and incubated overnight at 37°C. Next, a 2 mL LB culture (Appendix 1) was inoculated and grown overnight at 37°C with shaking. The next day, 200 µL of the initial culture were used to inoculate 250 mL super optimal broth (SOB) medium (Appendix 1). The culture was grown with shaking (200-250 rpm) at 18-25°C. until an OD_{600} of 0.6 was reached. The cells were cooled on ice for 10 min and centrifuged at 4,000xg for 10 min at 4°C. The supernatant was discarded and the pellet was resuspended in 80 mL ice-cold tris borate (TB) buffer (Appendix 1). The cells were spun at 4,000xg for 10 min at 4°C. The bacterial pellet was resuspended in 20 mL ice-cold TB buffer. Next, dimethyl sulfoxide (DMSO) was added until a final concentration of 7% (v/v) was reached. Cells were incubated on ice for 10 min and aliquoted. Aliquots were immediately frozen in liquid nitrogen and stored at -80°C.

2.2.1.2 *E. coli* transformation

For every transformation, 100 µL of competent cells were used. The *E. coli* cells were thawed on ice. Plasmid DNA or an aliquot of a ligation reaction was added while keeping the cells on ice. Immediately after adding the plasmid DNA or the ligation product, the cells were transferred to 42°C for 60 sec and then back on ice for 2 min. After the heat shock, 1 mL LB was added to each transformation and suspensions were incubated at 37°C for 1 hr. An aliquot of each reaction was plated on LB agar plates containing the appropriate antibiotic selection.

2.2.1.3. *A. tumefaciens* transformation

For each transformation, 47 µL of AGL1 electro competent cells were used. The *A. tumefaciens* cells were thawed on ice for 30 min. Plasmid DNA was added while keeping the cells on ice. Immediately after adding the plasmid DNA, the cells were electroporated (2500 V, 25 µF, 400 Ω, 2 mm). After electroporation the cells

were recovered in 1 mL of super optimal broth with catabolite repression (SOC) medium. The cells were incubated for 3 hrs at 28 °C with shaking. 100 µL of transformed cells were plated on LB containing rifampicin (10 µg/mL) and spectinomycin (100 g/ml).

2.2.2 *Arabidopsis thaliana*-related methods

2.2.2.1 Growth conditions

Plants were grown on a medium containing compost, perlite and vermiculite in the following ratios 5:2:3. Also, for some of the plants that were used for phenotypical characterization, commercially purchased jiffy pots were used. The plants were kept in the dark for 3 days at 4°C before being moved in the plant rooms. The plants were grown under constant illumination at 20ºC or in short-day conditions (9 hrs light/15 hrs of dark) at 20°C.

2.2.2.2 Seed sterilization

Seeds were sterilized using hypochlorous acid, which was generated by adding 3 mL concentrated (37%) hydrochloric acid to 100 mL of bleach (Domestos). Sterilization was done in a sealed container for 3.5 hrs.

2.2.2.3 Selection of transformants

Selection for transformants carrying a kanamycin resistance gene was done by sowing sterilized seeds on 0.5xMS agar plates (Appendix 1) containing 50 µg/mL kanamycin. The plates were kept in the dark at 4°C for 3 days and transferred to short-day conditions. Plants that germinated and formed true leaves were transferred onto soil and genotyped for the presence of the transgene.

Selection for transformants encoding an ammonium-glufosinate (BASTA) resistance gene, was done by spraying the seedlings three times at 3-day intervals with

0.15% (v/v) BASTA (Bayer). Seedlings that survived after the treatment were genotyped for the presence of the transgene.

Selection for transformants carrying BASTA resistance gene was also done by sowing sterilized seeds on 0.5xMS agar plates (Appendix 1) containing 50 μg/mL phosphinothricin. The plates were kept in the dark at 4°C for 3 days and transferred to the short-day room. Plants that germinated and formed true leaves were transferred onto soil and genotyped for the presence of the transgene.

2.2.2.4 Genomic DNA isolation for genotyping

Genomic DNA was extracted using a protocol based on Edwards *et al*., 1991. Briefly, a small area of the callus was transferred to a microcentrifuge tube and 400 μL of extraction buffer (Appendix 1) was added. The tissue was ground with a pestle and then centrifuged for 1 min at full speed. 300 μL of the supernatant was transferred to a new tube and an equal volume of isopropanol was added. After vortexing, the sample was centrifuged at maximum speed (room temperature) for 5 min to pellet the DNA. The supernatant was slowly removed and the pellet was washed with 500 μL of 70% ethanol. After 3 min of centrifugation at maximum speed (room temperature), the supernatant was removed and the pellet was air-dried. The pellet was then dissolved in 75 μL of sterile water. The genomic DNA was kept at -20°C for further analyses.

2.2.2.5 Genotyping assays

In order to genotype the *big* mutant and check the presence of the T-DNA in *BIG*, a PCR-based method was used. Two pairs of oligonucleotides were used: At104/At105 to amplify the wild-type allele and At104/LB2 to test for the presence of the T-DNA (oligonucleotide sequences are described in Table 2.4.). *prt6-5* mutants were genotyped by PCR using the following pairs of primers: At120/ At121 to amplify the wild-type allele and At121/LB2 to check the presence of the T-DNA in

PRT6. The *big prt6-5* double mutant plants were genotyped by PCR using the primer combinations described above.

2.2.2.6 Phenotypic characterization

In order to characterize the phenotype of *big*, *prt6-5* and *big prt6-5* mutant plants, pictures were taken every 2 weeks. The day on which the main inflorescence was observed was noted in order to assess the transition to flowering. In addition, the cauline and rosette leaves were counted when the stem reached the 10 cm length.

2.2.3 Barley-related methods

2.2.3.1 Growth conditions

Plants were grown on John Innes No.2. The plants were kept in the dark for 10 d at 4ºC before being moved to the plant room, where they were grown under long-day conditions (16 hrs light/8 hrs dark) at 15°C. When plant height reached 85 cm, they were transferred to the greenhouse (16 hrs light/8 hrs dark, 19°C).

2.2.3.2 Seed sterilization

Immature barley seeds were collected when the embryos were 1.5-2 mm in length. The seeds were removed from the spike and the awns were detached gently without damaging the seed coat. The seeds were first treated with 70% (v/v) ethanol for 30 sec, followed by 3 washes in sterile distilled water. The seeds were then sterilized using a solution of sodium hypochlorite (1:1 dilution in sterile distilled water) for 4 min, followed by 5-6 washes with sterile distilled water as described by Harwood *et al*., 2009.

2.2.3.3 Isolation of immature embryos

The immature embryos were isolated following the protocol described by Harwood *et al*., 2009. Briefly, two pairs of fine forceps were used: one to keep the seed steady and the other one to remove the seed coat and the embryonic axis. Immediately after removing the axis, the immature embryos were plated scutellum side up on callus induction medium (Appendix 1). Each 9 cm plate contained 25 embryos, which were incubated at 23-24°C overnight in the dark.

2.2.3.4 *A. tumefaciens*-mediated immature embryo transformation

Agrobacterium strain AGL1 transformed with pAM19 or pAM20 (Table 2.1.3) was cultured overnight in 10 mL SC medium containing 100 μg/mL spectinomycin at 28 °C with mild shaking (180 rpm). The culture was centrifuged at 3,000 rpm for 30 min (SORVALL RT7 Plus). The supernatant was discarded and the pellet was resuspended in 15 mL of 1x callus induction medium (CIM), (Appendix 1). A small amount of *Agrobacterium* was dropped onto each embryo from the plate. Once all the embryos from a plate were treated with *Agrobacterium* the plate was positioned vertically to allow any excess of bacteria to run off the embryos. Each embryo was then transferred to a new CIM plate, scutellum side down and incubated at 23-24°C in the dark, for 3 days.

2.2.3.5 Selection of transformants

After 3d of co-cultivation with AGL1 *Agrobacterium* strains coding for the T-DNA of interest, the embryos were transferred to a plate with fresh CIM that contained 50 μg/mL hygromycin for selection of the transformants and 160 μg/mL timentin (antibiotic) to prevent *Agrobacterium* growth on the plates. The immature embryos were kept scutellum side down and incubated at 23-24°C in the dark. After 2 weeks, the immature embryos (and associated calli) were transferred to a plate with fresh CIM containing both hygromycin and timentin at the same concentrations as above. Two weeks later, the embryo and the derived callus were again transferred to

fresh CIM-containing plates as described above. The embryo and callus were kept for 6 weeks on the CIM. After this period, they were transferred to transition medium (Appendix1), that contained 50 µg/mL hygromycin and 160 µg/mL timentin for another 2 weeks at 24°C under low light conditions (i.e. the plates were covered with a white sheet of paper). At this stage, the transformed calli should start to produce green tissue and shoots.

2.2.3.6 DNA isolation from callus

In order to test if callus formed contained the transgene(s) of interest, genomic DNA was extracted using a protocol based on Edwards *et al*., 1991. Briefly, a small area of the callus was transferred to a micro-centrifuge tube and the protocol described in Section 2.2.3.4 was used.

- **Genotyping assays**

In order to genotype the calli and test the presence of the T-DNAs coding for Hv*ATE1* targeting constructs, a PCR method was used. Four pairs of primers were used:

- AM35/AM36 to check for the presence of the sgRNA expression cassette that targets one region of Hv*ATE1* (construct called variant 1 or v1)
- AM37/AM36 to verify the presence of the sgRNA expression cassette that targets a different region of Hv*ATE1* (construct called variant 2 or v2)
- AM135/AM136 to test for the presence of the Cas9 expression cassette
- AM133/AM134 to check for the presence of Hpt (hygromycin) selection cassette.

TILLING lines carrying point mutations in Hv*ATE1* were also genotyped using the derived cleaved amplified polymorphic sequences (dCAPS) method to check the presence of the mutations in Hv*ATE1*. For all TILLING lines, a first PCR was performed with primers AM103 and AM104 using genomic DNA of the line of interest as a template. This resulted in a product of ~1.2 kb that contained the region with the expected mutations. Depending on the line to genotype, a second PCR

reaction was carried out using this first product as a template and different sets of primers. The resulting products were then digested with different enzymes to determine the presence (or absence) of the expected point mutation.

More specifically:

- for **line 4** (Table 2.1.), the second PCR was performed using primers AM88 and AM89, which resulted in a product of 225 bp. After digestion of the PCR product with *Xba*I, a fragment of 225 bp indicated the presence of a mutant version of Hv*ATE*1, while bands at 201 bp and 24 bp indicated the presence a wild-type copy of Hv*ATE1*.
- for **line 5** (Table 2.1.), the second PCR was performed with primers AM91 and AM92, which resulted in a product of 204 bp. After digestion of the PCR product with *Hind*III a fragment of 204 bp indicated the presence of the wild type Hv*ATE1* and bands at 183 bp and 21 bp indicated the presence a mutant version of Hv*ATE*1.
- for **line 6** (Table 2.1.), primers AM97 and AM98 were used for the second PCR, resulting in a product of 254 bp. After digestion of the PCR product with *Psi*I a fragment of 254 bp indicated the presence of the wild type Hv*ATE1* and bands at 229 bp and 25 bp indicated the presence. mutant version of Hv*ATE*1.
- for **line 9** (Table 2.1.), primers AM99 and AM100 were used for the second PCR, which resulted in a product of 244 bp. After digestion of the PCR product with *Psi*I a fragment of 244 bp indicated the presence of a mutant version of Hv*ATE1* and bands at 219 bp and 25 bp indicated the presence of wild type version of Hv*ATE1*.
- for **line 10** (Table 2.1.) the second PCR was performed with primers AM101 and AM102, which resulted in a product of 213 bp. After digestion of the PCR product with *Psi*I a fragment of 213 bp indicated the presence of wild type version of Hv*ATE* and bands at 188bp and 25 bp indicated the presence of a mutant version of Hv*ATE1*.

2.2.3.7 Histological methods to observe aerenchyma

In order to observe aerenchyma formation in barley, seminal root samples

from plants subjected to 7 or 15 days of waterlogging and from control barley plants of the same age were collected. The tissue was prepared according to Muhlenbock *et al*., 2007 protocol with some modifications or it was hand sectioned as described by Zhang *et al*., 2016. More specifically, the seminal roots were washed with water and dried using an ethanol series (30%, 40% and 50% (v/v), for 30 min). After this, the tissue was fixed in formaldehyde (70% ethanol, 5% acetic acid and 1.75% formaldehyde (v/v)) for 1 hr, at room temperature. The fixed material was then washed in ethanol (70%, 80% and 90% (v/v)) for 30 min in each ethanol solution. The samples were stained in 5 % eosin Y prepared in 95% ethanol and left overnight. The next day, the stained tissue was washed with 100% ethanol to remove the excess of eosin Y. After this, the tissue was washed in a histoclear:ethanol solution (1:1) for 1 hr. Then, the tissue was transferred for 1 hr to 100% histoclear. The samples were moved to a new 1.5 mL microcentrifuge tube containing hot wax (56°C) and incubated for an hour at 60°C. The old wax was discarded and fresh wax was added, followed by incubation for another hour. The tissue was then embedded in wax and the samples were transferred to 4°C. The tissue was sectioned (18 microns) using a microtome (Leica RM2135). The sections were hydrated and stuck to the slides. Once the tissue was dry, the wax was removed by washing the slides twice (for 5 min each time) with 100% histoclear. The cross sections were visualized under a bright field light microscope (Olympus BX51l).

2.2.3.8. Chlorophyll extraction

In order to measure the chlorophyll a, b and total carotenoid concentration in barley leaves, in control and waterlogged conditions, total chlorophyll was extracted using 80% acetone as described by Sumanta *et al*., 2014. Chlorophyll a (chl a), chlorophyll b (chl b) and total carotenoid content was measured based on the absorbance at 646 nm (A_{646}), 663 nm (A_{663}) and 470 nm (A_{470}), respectively (Sumanta *et al*., 2014). The equations used to calculate the amount of chlorophyll were: chl a = 12.25 A_{663} – 2.79 A_{646}; chl b = 21.5 A_{646} – 5.1 A_{663}; total carotenoids = (1000 A_{470} – 1.82 chl a – 85.02 chl b)/198.

2.2.4 Molecular biology methods

2.2.4.1 Plasmid DNA extraction from *E. coli*

Bacterial DNA was obtained after inoculation of 5 mL LB medium with the appropriate selection. Cultures were grown overnight at 37°C at 250 rpm. The next day, the cultures were centrifuged at 3,000 rpm (Sorvall RT7 Plus) for 10 min. The supernatant was discarded and the plasmids were purified using the commercial kit for plasmid extraction - E.Z.N.A Plasmid Mini Kit (Omega).

2.2.4.2 Genomic DNA extraction using the CTAB method

This protocol was used to generate contaminant-free genomic DNA preparations from barley tissue, which were used as template in PCR reactions for genotyping barley TILLING lines. First, leaf tissue was ground in CTAB buffer (Appendix 1) and centrifuged to pellet the cellular debris. The plant material was purified by phenol-chloroform extraction with phase-lock tubes twice. The DNA was precipitated using isopropanol and left to air dry. The dry DNA pellet was then resuspended in sterile distilled water.

2.2.4.3 Total RNA extraction

In order to isolate total RNA from barley, plant tissue was ground in liquid nitrogen, using a mortar and pestle. The total RNA was purified using the commercial kit, from Sigma (Plant Total RNA Kit). When total RNA was extracted from roots, these were washed carefully with tap water and dried on hand towels before freezing and grinding in liquid nitrogen.

2.2.4.4 cDNA synthesis

1 µg of mRNA was reverse transcribed using an oligo(dT)$_{18}$ primer and the RevertAid reverse transcriptase (Fermentas) according to manufacturer's instructions. cDNA obtained from this reaction was used for PCR.

2.2.4.5 PCR based methods

- **Quantitative RT-PCR (qRT-PCR)**

Primers were designed to have a melting temperature (Tm) of 60 ± 1°C. The Oligo Analyzer software, available at the Integrated DNA Technologies website (http://eu.idtdna.com) was used to check the melting temperature and to check for secondary structures, as well as primer dimerization.

In order to quantify the relative amount of cDNA in each sample, the Lightcycler 480 (Roche)-with SYBR green master 1 (Roche) was used. Each reaction mix contained 5 µL of 2x SYBR green master 1, 1 µL cDNA, 1 µL of 10 µM primers and 3 µL of molecular biology grade water. An equivalent time of 60 sec per 1 kb was given to generate the amplicons. All the primer sequences can be found in Table 2.4. The following primer pairs were used to test expression of:

- Hv*ATE1* (MLOC_52389) - AM4/AM5
- Hv*PRT6.1* (MLOC_47469) - AM6/AM7
- Hv*PRT6.2* (MLOC_55623) - AM3/AM2
- Hv*ADH1* (HORVU4Hr1G016810) -HvADH1F/HvADH1R (Mendiondo *et al*., 2016)
- Hv*HB* (HORVU4Hr1G066200) - AM51/AM52
- Hv*PDC1* (HORVU4Hr1G056050) - AM53/AM54
- Hv*TUB-alpha2* (MLOC_7079) - AM8/AM9
- Hv*ADP* (HORVU3Hr1G079700) –AM47/AM48
- *HvACTIN* (HORVU1Hr1G002840) -AM45/AM46
- *HvGAPDH* (HORVU7Hr1G074690) -AM49/AM50

Note: For barley (*Hordeum vulgare*) primers were designed based on the DNA sequences provided by EnsemblPlants (www.plantensembl.org)

- **Colony PCR**

Colony PCR was performed in order to check the presence of relevant inserts in *E. coli* cells transformed with a ligation reaction. Single colonies were picked from the plate and resuspended in 10 µL LB. The cell suspension was vortexed and a volume of 1.5 µL was used as PCR template in a 15 µL PCR reaction mix.

2.2.4.6 *In vitro* Cas9 assay

In order to check that the Cas9 endonuclease, guided by the 2 different single guide RNAs (sgRNA) generated against Hv*ATE1*, was able to cut the target DNA, an *in vitro* Cas9 assay was performed as detailed below.

- **sgRNA synthesis (EnGen NEB#E3322S)**

First, a target specific oligo was designed based on manufacturer instructions. The designed oligo coded for the T_7 promoter sequence (in blue below), 20 nucleotides that represents the target sequence (black) and 14 nucleotides that are complementary with the *S. pyogenes* Cas9-specific Scaffold Oligo (included in the EnGen 2x sgRNA Reaction Mix).
The target specific oligo sequence is:
TTCTAATACGACTCACTATA(N)$_{20}$GTTTTAGAGCTAGA

3 µL of nuclease-free water, 10 µL of EnGen 2x sgRNA Reaction Mix, *S. pyogenes,* 5 µL of 1 µM target-specific DNA oligo and 2 µL of EnGen sgRNA Enzyme mix were mixed together and incubated at 37°C for 30 min. The reaction was transferred to ice and 30 µL of nuclease-free water were added, followed by treatment with 2 µL DNase I. The sample was incubated at 37°C for 15 min.

- **sgRNA purification**

EZNA Micro Elute RNA Clean up kit (R6247-00) was used for sgRNA purification. sgRNA was treated with 175 µL of QVL lysis buffer and mixed by vortexing. 125 µL of 100% ethanol was added to the sample and vortexed. The

solution was added to Micro Elute LE RNA Mini Column and centrifuged at 10.000 g for 15 sec. The flow-through was discarded and the collection tube was kept. 500 µL of RNA Wash Buffer II was added into the same column and centrifuged at 10.000 g for 30 sec. The flow-through was discarded. Another 500 µL of RNA Wash Buffer II was added into the column and centrifuged at 13.000 g for 2 min. The flow-through was discarded. The column was transferred to a new collection tube and centrifuged at maximum speed for 5 min. The column was transferred to a clean 1.5 mL microcentrifuge tube and 15 µL of DEPC water was added in the center of the column. The sample was centrifuged for 1 min at maximum speed and the purified sgRNA was stored at -20°C. A small aliquot of the purified sgRNA was run on a 2% agarose gel to check the integrity of the product.

- **dsDNA template synthesis**

Reverse transcription with an oligo$(dT)_{18}$ primer was used to generate cDNA from barley leaves total RNA (as described in 2.2.4.5). This cDNA was used as template to amplify the *HvATE1*$^{218\text{-}1499}$ sequence using oligonucleotides AM_103 and AM_104. The resulting PCR fragment was run on an agarose gel. The PCR product was purified using E.Z.N.A Gel extraction kit (Omega). The purified PCR product was ligated into pJET1.2/blunt vector. Ligation reactions were set up and incubated overnight at 4°C. *E coli* competent cells were transformed (described in 2.2.1.2 section) with the ligation reactions and the cells were plated on LB medium supplemented with 100 g/mL ampicillin. Colonies were cultured overnight for miniprep and the presence of the insert was checked by PCR using AM103 and AM104 primers. The plasmid generated, pJET1.2: Hv*ATE1*$^{398\text{-}1630}$ was linearized with *Dra*III restriction digest and used as template for the *in vitro* Cas9 assay.

- **Cas9 digestion of dsDNA template in the presence of sgRNA**

20 µL of nuclease-free water were mixed with 3 µL of 10x Cas9 Nuclease Reaction Buffer, 3 µL of 300 nM sgRNA and 1 µL of 1 µM Cas9 nuclease from *S. pyogenes* (MO386S) and incubated at 25°C for 10 min. After this incubation, 3 µL of 30 nM substrate DNA was added to the reaction mixture, followed by incubation at 37°C for 15 min, according to the manufacturer's instructions (NEB #E3322S). After that, 1 µL of Proteinase K was added and incubated at room temperature for 10

min, following the manufacturer's instructions (NEB #E3322S). The fragments were analyzed on agarose gel to check the efficiency of the Cas9 digestion.

2.2.4.7 Generation of plasmids to target Hv*ATE1* using CRISPR/Cas9

- **Assembly of sgRNA expression cassette**

In order to assemble the sgRNA cassette, plasmid pICH86966 AT U6:sgRNA-PDS (#46966) was used as template in a PCR reaction with oligonucleotides AM35 and AM36 (Table 2.4). Oligonucleotide AM_35 (forward oligo) had the following sequence tgtggtctca CTTG NNNN NNNNN NNNNN NNNNN ***gttttagagctagaaatagcaag,*** in which (i) the *Bsa*I recognition site is indicated in blue; (ii) the four base pair overhang produced after *Bsa*I digestion is underlined (this short sequence anneals to the last four base pairs of the AtU6-26 promoter in plasmid pICSL90002); (iii) the 20-bp target sequence is in red; (iv) the portion of the oligonucleotide that anneals to the sgRNA template is in bold italics. Oligonucleotide AM36 (reverse oligo) had the following sequence: tgtggtctca AGCG ***taatgccaactttgtac,*** in which (i) the *Bsa*I recognition site is in blue; (ii) the four base pair overhang produced by digestion with *Bsa*I is underlined (this overhang anneals to the Level 1 acceptor plasmid); (iii) the portion of the oligonucleotide that anneals to the sgRNA template is in bold italics.

To target Hv*ATE1*, two constructs were designed:

- v1, in which the target sequence was GCATATACCATACGTCTGAA
- v2, which had the following target sequence GGAGAGCTTGACCCACAGGT

The PCR reaction was performed using Phusion DNA Polymerase and the PCR amplicon (noted PCR1) had the following sequence:

tgtggtctcaA/CTTGNNNNNNNNNNNNNNNNNNGTTTTAGAGCTAGAAATA
GCAAGTTAAAATAAGGCTAGTCCGTTATCAACTTGAAAAAGTGGCACCG

AGTCGGTGCTTTTTTTCTAGACCCAGCTT
TCTTGTACAAAGTTGGCATTACGCTtgagaccaca

The PCR product was run on an agarose gel and purified using E.Z.N.A Gel extraction kit, from Omega.

- **Assembly of level 1 transcriptional units**

In order to assemble the level 1 transcriptional units, the above-mentioned PCR1 product was mixed with pICSL9003 coding for the U6 promoter from *Triticum aestivum* ($U6_{pro}$) and pICH47751 (Level I, position 3 acceptor) plasmids, as described by Lawrenson et al, 2015.

Each level 1 assembly reaction contained sgRNA amplicon and 100-200 ng of the Level 1 acceptor plasmid (pICH47751) at a 2:1 molar ratio. 10 units of *Bsa*I (NEB) were mixed with 2 µL 10x BSA, 400 units of T4 DNA ligase (NEB) and 2 µL of T4 ligase buffer. Sterile distilled water was added up to 20 µL. The reactions were incubated in a thermocycler: 26 cycles 37°C for 3 min/ 16°C for 4 min for, then at 50°C for 5 min and at 80°C for 5 min.

Competent *E. coli* cells were transformed with 2 µL of the ligation reaction. Cells were spread on LB agar medium containing 100 mg/L carbenicillin; 25 mg/L isopropyl β-D-1-thiogalactopyranoside (IPTG) and 40 mg/L 5-bromo-4-chloro-3-indolyl-β-D-galactopyranoside (X-gal) and white colonies were kept for further analysis. Single colonies were inoculated in LB medium containing the appropriate antibiotic selection and cultures were incubated overnight at 37°C. The next day, cells were spun down and the supernatant was discarded. The plasmids were extracted using the commercial kit E.Z.N.A Plasmid Mini kit (Omega). Plasmids were checked for the presence of insert using restriction digest analysis and Sanger sequencing.

- **Assembly of level M binary vectors**

The level 1 constructs assembled were used to generate the so-called level M binary vectors. To this aim, the level I construct was mixed together with pICSL11059 (codes for the hygromycin selection marker), pICSL11056 (encodes the Cas9 expression cassette), pICH50892 (position 3 end linker) plasmids and assembled in the pAGM8031 plasmid (resulting in the level M acceptor construct) as described by Lawrenson et al., 2015.

Each level M assembly reaction contained 100-200 ng of the Level M acceptor plasmid and Level 1 plasmids (level 1 construct, pICSL11059, pICSL11056, pICH50892) such that the inserts were at a 2:1 molar ratio to the acceptor pAGM803. 20 units of *Bpi*I (ThermoFisher) were mixed with 2 μL of 10xBSA, 400 units of T4 DNA ligase (NEB) and 2 μL of T4 DNA ligase buffer. Sterile distilled water was added up to 20 μL. The reactions were incubated in a thermocycler: 26 cycles 37°C for 3 min/ 16°C for 4 min for, then at 50°C for 5 min and at 80°C for 5 min.

Immediately after this, competent *E. coli* cells were transformed with 2 μL of the ligation reaction and spread on LB agar medium containing 100 mg/L spectinomycin; 25 mg/L IPTG and 40 mg/L X-gal. White colonies were used to inoculate LB medium supplemented with spectinomycin and grown overnight. Miniprep was carried out using the E.Z.N.A Plasmid Mini Kit (Omega). Plasmids were checked for the presence of sgRNA, Cas9 and Hpt cassettes by restriction digest analysis and Sanger sequencing.

2.2.5 Biochemical methods

2.2.5.1 Monitoring the stability of Ub-X-LUC reporters in *Arabidopsis thaliana*

- **Protein extraction from *Arabidopsis thaliana***

In order to check the stability of Ub-X-LUC reporters, protein extracts were prepared from 10-day-old seedlings. Whole seedlings (~10 seedlings per tube) were collected and frozen in liquid nitrogen. Samples were then ground in liquid nitrogen and the powder was resuspended in 1x CCLR buffer (Promega) supplemented with 1 mM phenylmethylsulfonyl fluoride (PMSF) and plant protease inhibitors (Sigma-Aldrich, diluted 100-fold). Samples were centrifugated for 5 min at 14,000 rpm at 4°C. The supernatants were transferred to a clean microcentrifuge tube and used for subsequent analyses.

- **Determination of protein concentration using Bradford**

In order to determine the protein concentration in different samples, the Bradford reagent (Sigma-Aldrich) was used. For generation of a standard curve, bovine serum albumine (BSA) solutions at different concentrations, ranging from 1 mg/mL to 10 mg/mL were used.

- **LUC activity assays to monitor the stability of Ub-X-LUC reporter constructs**

First, 100 µL of 1x luciferase buffer (Appendix 1) was dispensed in a white 96-well plate well. Then, 2 µL of the cell lysate was added in a well and mixed by pipetting. Luminescence was measured immediately twice for a period of 10 seconds each time, with 3 seconds in-between the 2 measurements (Biotek Omega Polastar Plate Reader). LUC activity was measured in relative light unit (RLU) per $.min^{-1}.mg^{-1}$.

- **GUS activity assays to monitor the stability of Ub-X-LUC reporter constructs**

To quantitatively measure β-glucuronidase (GUS) activity, methylumbelliferyl β-D-glucuronic acid (MUG) was used as substrate. For each reaction, 149.5 μL 1x GUS buffer (Appendix 1) was aliquoted and incubated at 37°C for 10 min. Also, for each sample, 4 tubes containing 270 μL of the stop reagent (1M Na_2CO_3) were prepared. 0.5 μL of protein extract was added to the reaction tubes containing the 1x GUS buffer, at 30 sec intervals. After exactly 10 min, 30 μL of the first reaction was transferred into the stop reagent. The following samples were transferred into the stop reagent at 30 seconds intervals. This was repeated at exactly 20, 30 and 40 min. After this, 150 μL of the stopped reactions were transferred to a black 96 well plate and the fluorescence was measured (Biotek Omega Polastar Plate Reader) using the following parameters: excitation wavelength 365 nm, emission wavelength 455 nm and filter 430 nm.

Different concentrations of 4-methylumbelliferone (4-MU) ranging from 12.5 μM to 400 μM were used to calibrate the fluorometer and to generate the standard curve. The amount of 4-MU per unit of time ($nmoles.min^{-1}.mL^{-1}$) was calculated using the standard curve. Specific activities ($nmoles.min^{-1}.mg^{-1}$) were calculated using the protein concentrations determined by the Bradford method.

3. Characterization of barley response to waterlogging

Given the expected increase in global population and also the effects of global climate change, there is a need for increased yield in arable crops that are part of human and animal diets. Barley is one of the most important cereal crops cultivated in Ireland. Both spring and winter varieties are grown, with an increased preference for winter crops due to a higher number of varieties and more scientific knowledge available (TEAGASC TECHNOLOGY FORESIGHT 2030 Irish Crop Production: Current situation, future prospects to 2030 and development needs). Barley is very important for the Irish economy, as it is used for malting, as well as fodder. However, future yields are threatened by the consequences of global climate change, which in Ireland, are likely to trigger increased precipitations and flooding events in winter. The latter are particularly negative for barley, which is considered to be a sensitive crop to either submergence or waterlogging. It is also expected that winter barley varieties may be particularly affected in the future. The main objective of this work was to characterize the responses of different commercial winter barley cultivars to waterlogging with the aim of identifying varieties that are more tolerant to this abiotic stress.

3.1 Waterlogging experiments in the field

The work I have conducted during my PhD thesis was based on the results of waterlogging/submergence field experiments conducted by collaborators at Teagasc (Dr. Susanne Barth, John Spink, Lena Forster and Tomas Byrne). I contributed to these experiments by scoring the plants of the first field trial (conducted in 2016-2017) and whose results are described below. Additional field waterlogging experiments were conducted in subsequent years (2017-2018 and 2018-2019), but these were managed and scored entirely by Tomas Byrne (Teagasc). The results of these replicates are therefore not presented in this thesis.

The starting material for this first waterlogging field experiment were 420 winter barley varieties part of the Association Genetics Of UK Elite Barley (AGOUEB) population. Seeds were sown in mini-plots in October 2016 in order to

have 3 replicates for control conditions (i.e. not submitted to waterlogging or submergence) and 3 replicates for waterlogging treatment (FIGURE 3.1). As this was the very first waterlogging field trial to be conducted in Ireland, this experiment also served to determine potential problems and limitations associated with the current infrastructure.

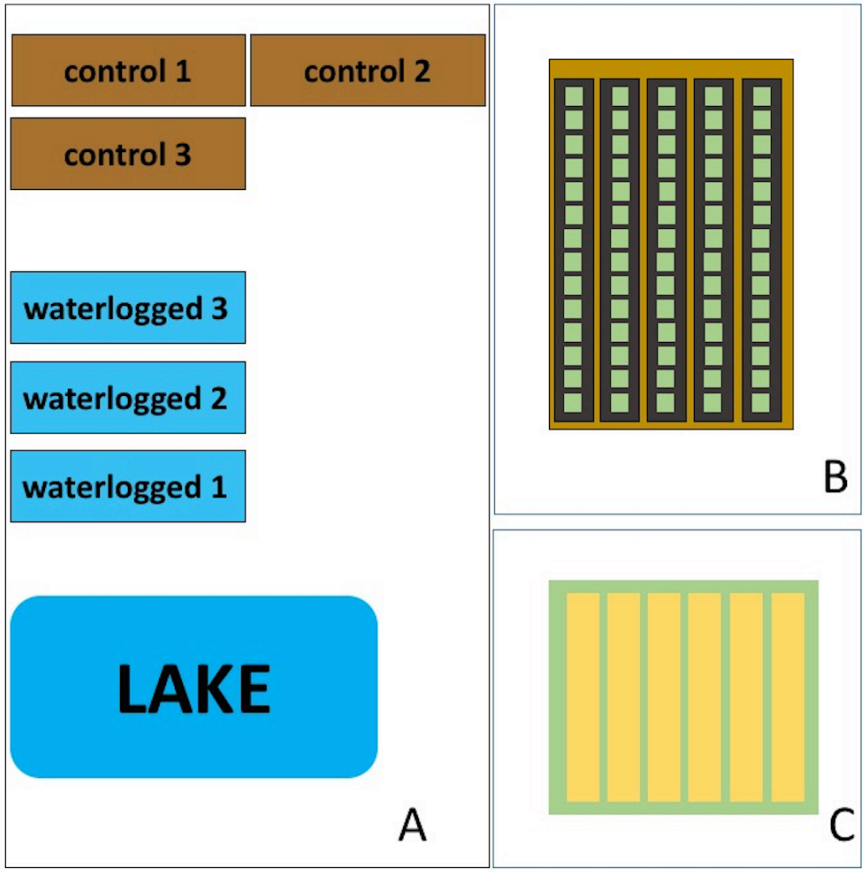

FIGURE 3.1. Plan of the field waterlogging experiment (2016-2017). Barley seeds were sown at the end of October 2016. **A.** There were 3 replicates for control conditions (represented by brown rectangles) and 3 replicates for waterlogged conditions (blue rectangles). **B.** Each replicate (e.g. control 1) contained all 420 varieties distributed in 5 rows (dark brown). In each row, there were 14 mini-plots (represented by green squares). **C.** In each mini-plot there were 6 different varieties (yellow rectangles). For each variety, there were 6-7 seeds planted in a given row of a mini-plot.

Unexpectedly, that autumn was extremely dry and seedlings were not exposed to waterlogging treatment for the first months after germination. An irrigation system that pumped the water from the lake onto the plots that were supposed to be waterlogged was set up early January 2017. However, the water simply drained back into the lake, so that the waterlogged plots were not equally affected by the treatment. In early February 2017, the level of the lake was raised and this improved the quality of the treatment. In early March, waterlogging was stopped, allowing the plants to recover.

3.1.1. Characterization of AGOUEB lines in response to waterlogging

Although irrigation and raising the level of the lake allowed for waterlogging to be applied more consistently, there were still some discrepancies in the level of the water in the different plots. For example, while some mini-plots were waterlogged, others were submerged (FIGURE 3.2). This would be expected to generate some heterogeneity in plant growth and plant responses to the stress, also affecting the scoring of the different varieties as tolerant or sensitive to the waterlogging.

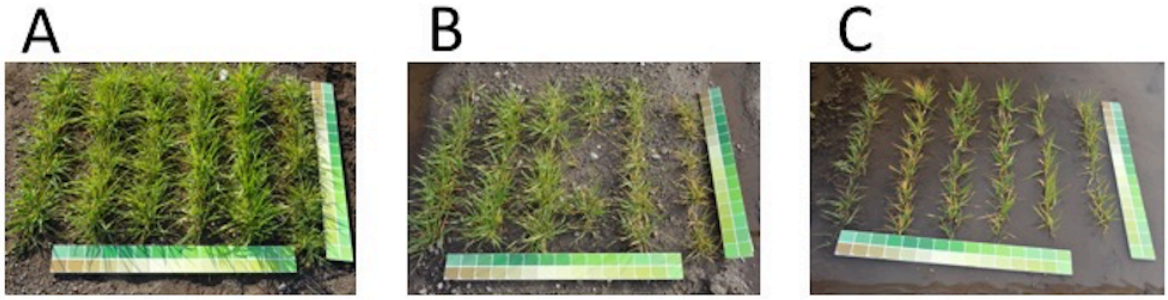

FIGURE 3.2. Example of different mini-plots of the 2016-2017 waterlogging field experiment. A. A control mini-plot. **B.** Example of a waterlogged mini-plot. **C.** Representative mini-plot experiencing submergence.

Despite these obvious limitations, we decided to score the plants potential tolerance or sensitivity to waterlogging based on pictures taken (i) in March 2017 (termed ‘set 1 pictures’) and (ii) May 2017 (noted ‘set 2 pictures’) Based on a visual analysis of the pictures with a focus on general health, height, leaf chlorosis and leaf

necrosis, all 420 barley varieties were classified as either tolerant or sensitive to waterlogging at 2 different developmental stages.

I started to analyze the first set of pictures taken in March 2017 by comparing to each other all the varieties under waterlogged conditions. Because of the heterogeneous waterlogging treatment, scoring across the 3 plots and each of their mini-plots was very difficult. The easiest cases were those where plants from the same mini-plot (i.e. plants that had experienced similar level of waterlogging or submergence) exhibited a marked phenotypic difference (e.g. FIGURE 3.3 B and C orange and white arrow). Next, for each variety, I compared the phenotype in waterlogged conditions to the phenotype under control conditions. This was important to ensure that the classification as either sensitive or tolerant was not due to the natural growth habit of a particular variety. Indeed, some plants, even in the control conditions, looked healthier (FIGURE 3.3D; blue arrow) than others (FIGURE 3.3D; red arrow). As expected, though, the control plants were in general much larger, with greener leaves and without signs of chlorosis or necrosis (FIGURE 3.3D-F).

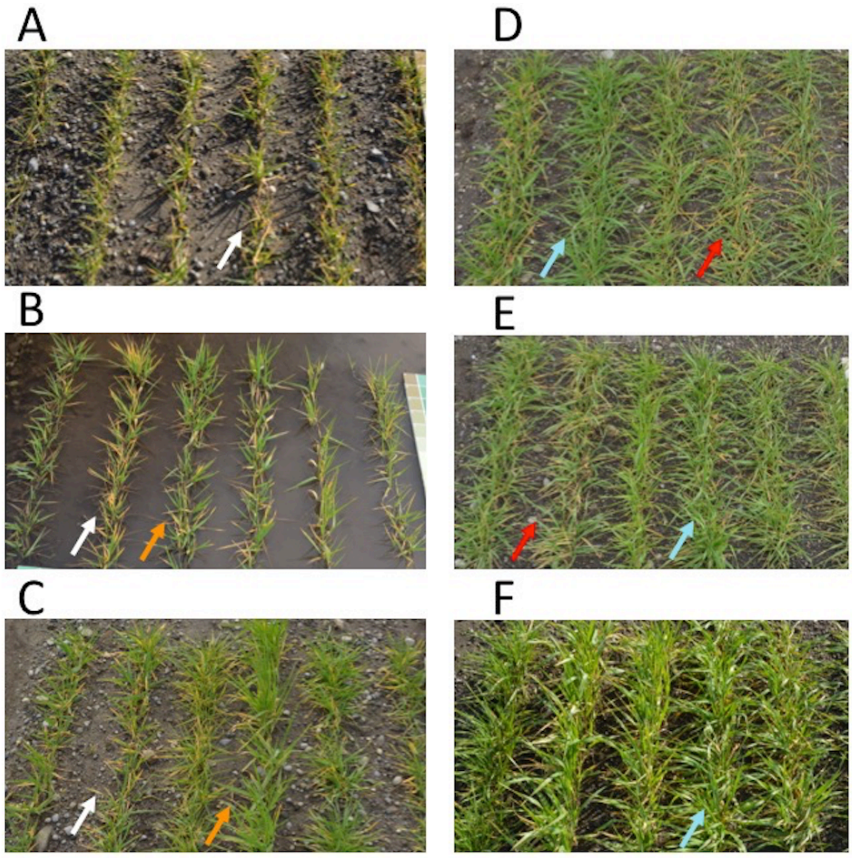

FIGURE 3.3. Examples of varieties classified as tolerant or sensitive, and of heterogeneity observed in control plots in March 2017. A-C. Pictures of mini-plots undergoing waterlogging or submergence. Based on general health, height and leaf chlorosis plants were classified as sensitive (white arrows) or tolerant to waterlogging (orange arrows). **D-F.** Pictures of different control mini-plots showing the variety of phenotypes. The blue arrow indicates a variety that has stronger growth, while the red arrow indicates a variety that tends to be smaller and shows signs of yellowing.

The same analysis was carried out for the second set of pictures (taken in May 2017). However, due to the fact that the plants were at a later developmental stage (flag leaf formation) and that a ~ 10 weeks recovery period had been applied, it was more difficult to identify sensitive varieties based on the presence of leaf chlorosis or necrosis. Instead, I analysed the plants based on the total green area visible and the general health and growth. As indicated above, the analysis was first done by comparing all the varieties in waterlogged conditions. The varieties were then compared with their respective control plants to ensure that the classification as either tolerant or sensitive was not linked to the normal growth habit of a particular variety. Even though fewer plants showed a marked phenotype in response to waterlogging, I was able to classify some varieties as either sensitive (FIGURE 3.4A-C; orange arrows) or tolerant (FIGURE 3.4A-C; white arrows) to the waterlogging treatment. Similarly, to the earlier developmental stage, varieties grown in control conditions had different phenotypes (FIGURE 3.4D-E).

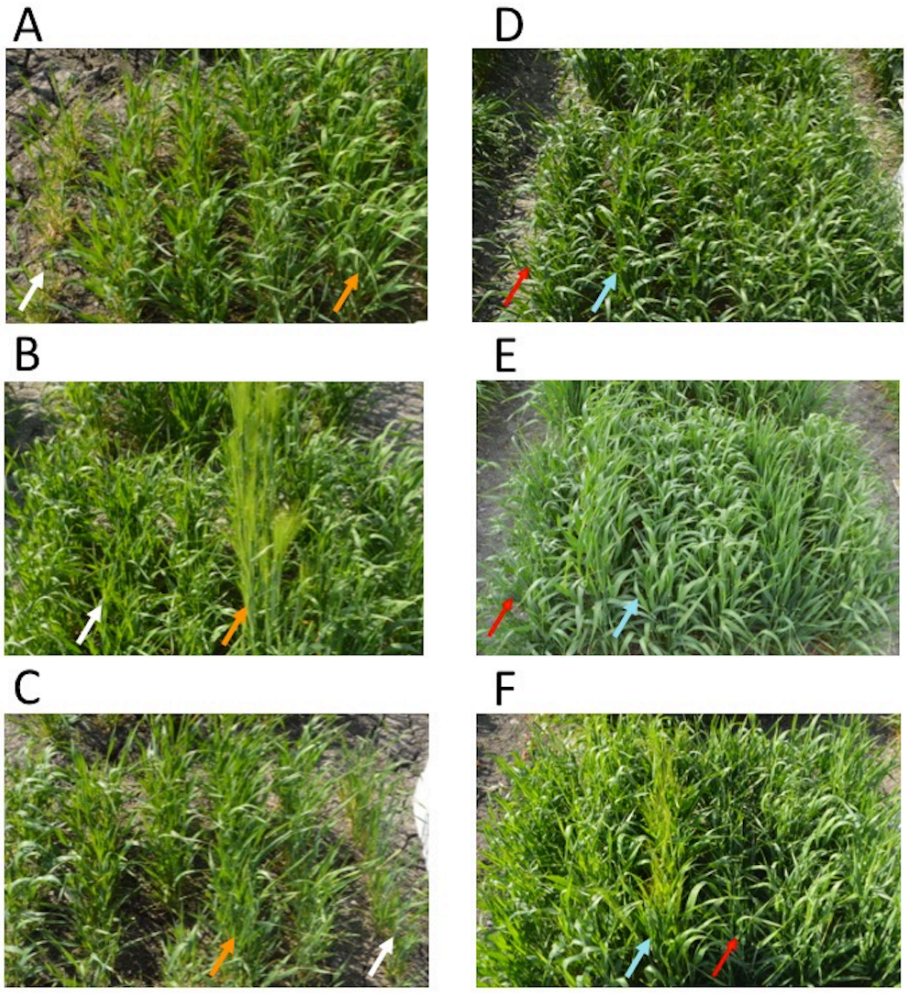

FIGURE 3.4. Examples of varieties classified as tolerant or sensitive, and of heterogeneity observed in control plots in May 2017. A-C. Pictures of mini-plots undergoing waterlogging or submergence. Based on general health, height and leaf chlorosis plants were classified as sensitive (white arrows) or tolerant to waterlogging (orange arrows). **D-F.** Pictures of different control mini-plots control showing the variety of phenotypes. The blue arrow indicates a variety that has stronger growth, while the red arrow indicates a variety that tends to be smaller and shows signs of yellowing.

3.1.2. Determination of tolerant and sensitive varieties

In order to identify sensitive and tolerant varieties, I used the picture-based classification and conducted a series of analyses to select the higher confidence tolerant and sensitive varieties. The selection was largely done by determining the overlap between the different replicates and across the two sets of pictures. For

example, I used the BioVenn software (http://www.biovenn.nl/), to identify varieties that were considered as sensitive (FIGURE 3.5A) or as tolerant (FIGURE 3.5B) in the 3 different replicates within Set 1 pictures. Based on this analysis, I found 51 sensitive varieties and 66 tolerant varieties that were common to all 3 replicates within Set 1 pictures.

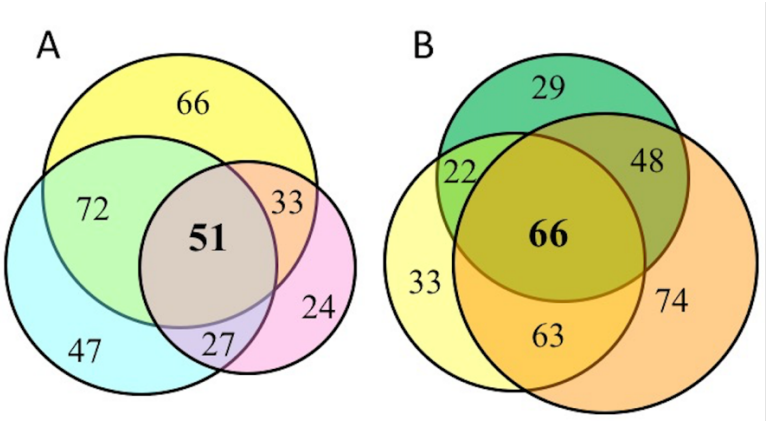

FIGURE 3.5. Overlap analysis of the different waterlogging sensitive and tolerant varieties in Set 1 pictures. **A.** Overlap between sensitive varieties found in replicate 1 (yellow), replicate 2 (blue) and replicate 3 (pink). **B.** Overlap between the tolerant varieties found in replicate 1 (green), replicate 2 (yellow) and replicate 3 (orange).

I conducted the same analysis for the second set of pictures and found 18 sensitive varieties that were common to all 3 replicates (FIGURE 3.6A), and 137 tolerant varieties that were identified in all 3 replicates (FIGURE 3.6B).

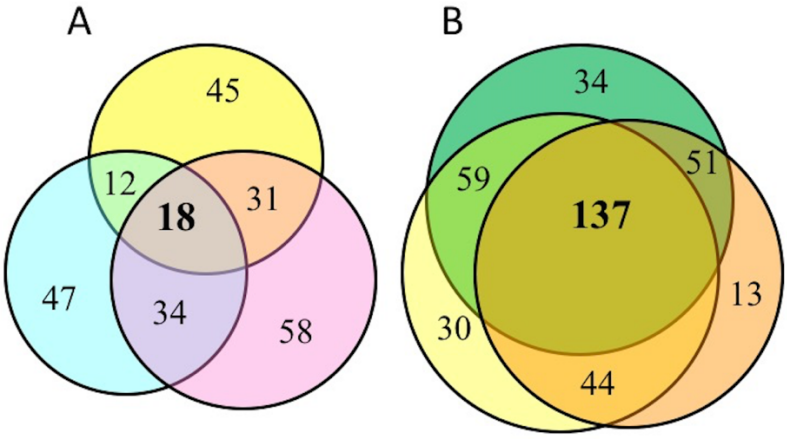

FIGURE 3.6 Overlap analysis of the different waterlogging sensitive and tolerant varieties in Set 2 pictures. **A.** Overlap between the sensitive varieties found in replicate 1 (yellow), replicate 2 (blue) and replicate 3 (pink). **B.** Overlap between the tolerant varieties identified in replicate 1 (green), replicate 2 (yellow) and replicate 3 (orange).

Finally, I compared the overlap between Set 1 and Set 2 pictures to further narrow down the list of waterlogging tolerant and sensitive varieties and increase the likelihood that the plants were not classified as either tolerant or sensitive by accident. In this analysis, the 51 waterlogging sensitive varieties that were common replicates 1-3 within Set 1 were compared with the 18 varieties that were considered as sensitive in replicates 1-3 in Set 2 pictures. Only 4 sensitive varieties were common to both Set 1 and Set 2 (FIGURE 3.7A). I performed the same analysis with the waterlogging tolerant varieties and found 32 varieties in common to both Set1 and Set 2 pictures (FIGURE 3.7B).

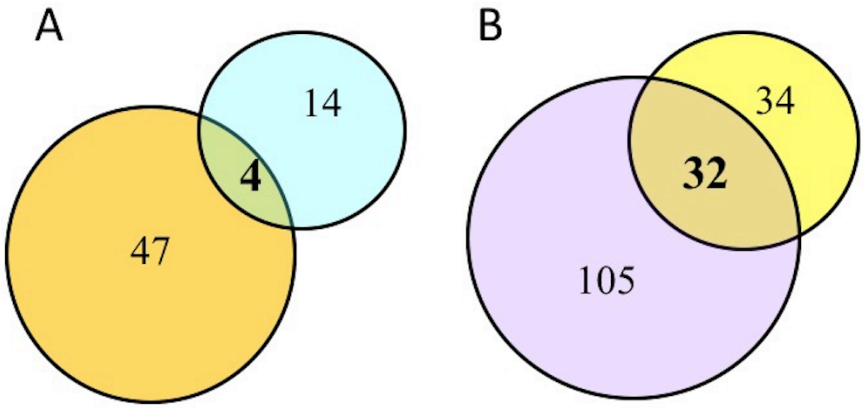

FIGURE 3.7. Overlap between the waterlogging sensitive and tolerant varieties between Set 1 and Set 2 pictures. A. The list of sensitive varieties that were common to replicates 1-3 in Set 1 pictures (orange) was compared to the list of sensitive varieties that were present in replicates 1-3 of Set 2 pictures (blue). **B.** The list of waterlogging tolerant varieties that were common to replicates 1-3 in Set 1 pictures (yellow) was compared to the list of tolerant varieties that were identified in replicates 1-3 of Set 2 pictures (purple).

Based on this analysis, I generated a list of waterlogging sensitive and tolerant varieties. Pictures of these specific varieties were revisited and for the

waterlogging tolerant varieties, I chose the best varieties based on their general health, leaf chlorosis and necrosis. In contrast, for the sensitive varieties, I chose the varieties with increased leaf chlorosis and necrosis and reduced yield. Due to the inconsistency of the waterlogging treatment across the mini-plots and the scoring method, it was challenging to identify with confidence a sufficient number of varieties that were either sensitive or tolerant across the two sets of pictures. Consequently, I chose varieties that were scored as sensitive or tolerant in both 2 sets of pictures or in only one of the sets (FIGURE 3.8). For example, Passport and Madrigal were chosen because they were classified as sensitive in both sets of pictures. Similarly, Arma, Ragusa and Vesuvius were classified as tolerant in both sets of pictures. Pilastro, Regina, Liebniz, Retriever, Masquerade, Dura and Louise were classified as sensitive based on set 1 pictures and tolerant based on set 2. In contrast, Isa was classified tolerant in set 1 and sensitive in set 2 (FIGURE 3.8).

Variety	Set 1 March 2017	Set 2 May 2017
Liebniz	**sensitive**	**tolerant**
Retriever	**sensitive**	**tolerant**
Masquerade	**sensitive**	**tolerant**
Pilastro	**sensitive**	**tolerant**
Passport	**sensitive**	**sensitive**
Madrigal	**sensitive**	**sensitive**
Arma	**tolerant**	**tolerant**
Ragusa	**tolerant**	**tolerant**
Vesuvius	**tolerant**	**tolerant**
Isa	**tolerant**	**sensitive**
Dura	**sensitive**	**tolerant**
Louise	**sensitive**	**tolerant**
Regina	**sensitive**	**tolerant**

FIGURE 3.8. List of higher confidence waterlogging sensitive and tolerant varieties selected for further characterization. In bold there are the high confidence varieties that were classified as sensitive or tolerant in both sets of pictures.

Below are some pictures of a representative higher confidence waterlogging sensitive or tolerant varieties selected. Vesuvius, one of the varieties classified as tolerant, is showing general good health in waterlogged conditions, with very little

leaf chlorosis in both Set 1 and Set 2 pictures (FIGURE 3.9). In contrast, Retriever, one of the sensitive varieties, is showing signs of leaf chlorosis especially in Set 1 (FIGURE 3.11A,B), compared to its control (FIGURE 3.11C). For Set 2 of pictures, the growth of waterlogged Retriever (FIGURE 3.11E,F) seems to be reduced compared to its control (FIGURE 3.11G,H).

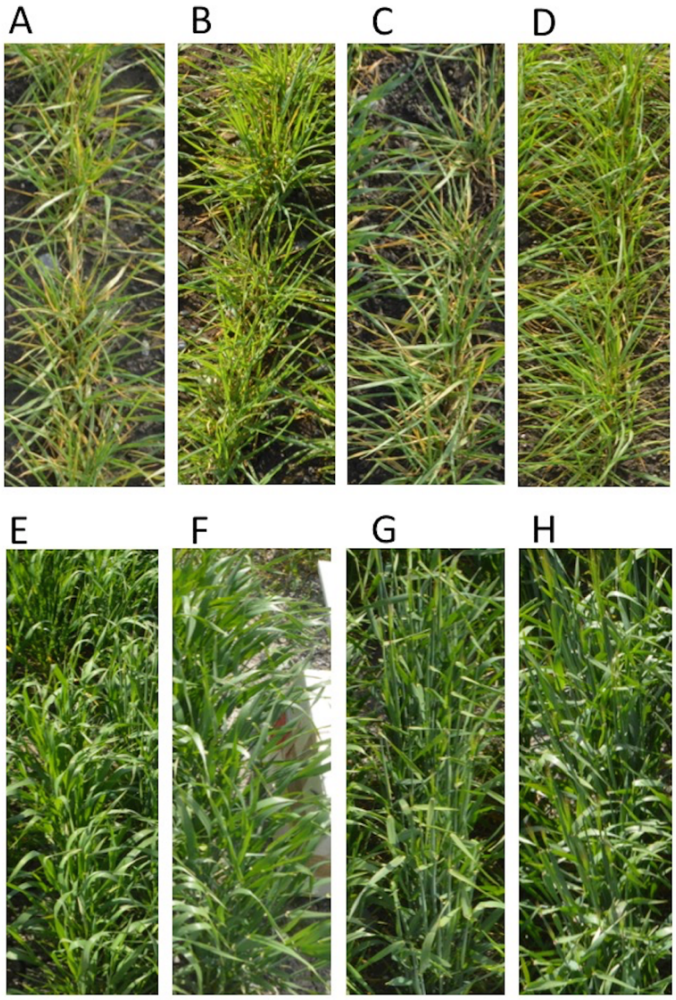

FIGURE 3.9. Pictures of Vesuvius, a representative waterlogging tolerant variety. **A and B.** Waterlogged plants from replicates 1 and 2 (pictures taken in March 2017). **C and D.** Control plants from replicates 1 and 2 (March 2017). **E and F.** Waterlogged plants from replicates 1 and 2 (May 2017). **G and H.** Control plants from replicates 1 and 2 (May 2017).

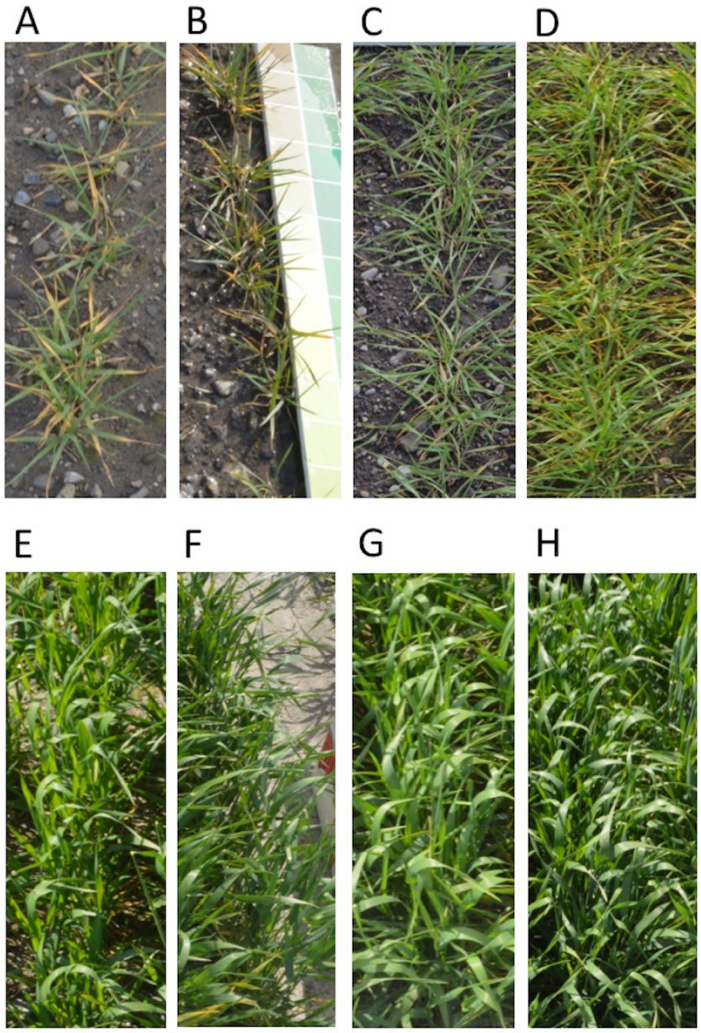

FIGURE 3.10. Pictures of Retriever, a representative waterlogging sensitive variety. **A and B.** Waterlogged plants from replicates 1 and 2 (pictures taken in March 2017); **C and D.** Control plants from replicates 1 and 2 (March 2017); **E and F.** Waterlogged plants from replicates 1 and 2 (May 2017); **G and H.** Control plants from replicates 1 and 2 (May 2017).

The results obtained in the field led to a preliminary classification of the varieties based of their general health in control and waterlogged conditions in the field (FIGURE 3.8). However, because the waterlogging treatment was not evenly applied across the different plots, the scoring may be inaccurate or inconsistent across the different replicates. While field trials were repeated, applying waterlogging under controlled conditions would help to (i) confirm (or not) the classification of the different varieties; and (ii) test the effect of waterlogging alone on the growth of these varieties. Indeed, in the field, plants were also subjected to other stresses, such as cold

and possibly drought at later developmental stages. To achieve this aim, I set up a standardized waterlogging protocol that would work reliably to characterize in more detail the response of the different varieties that are listed in FIGURE 3.8.

3.2. Optimization of experimental conditions to test waterlogging response in a controlled environment

Based on the known response of plants to waterlogging, we focused on establishing a reliable waterlogging protocol for barley in controlled conditions, which would allow us to (i) monitor the gene expression changes of known waterlogging response genes; (ii) characterize the timing of aerenchyma development in roots; and (iii) examine changes in root and shoot anatomy. Upon waterlogging (and also submergence), plant metabolism switches from aerobic to anaerobic (fermentative) pathways. Under these conditions, plants also undergo a series of anatomical and morphological changes, such as aerenchyma development, adventitious root formation and shoot elongation (see also Section 1.1.3.1), all of which are accompanied by changes in gene expression. These gene expression, metabolic, anatomical and physiological changes are all essential for plant survival under waterlogging stress (Bailey-Serres and Voesenek, 2008; Colmer *et al*., 2009; Voesenek *et al*., 2006).

3.2.1. Choice of waterlogging response genes

We decided to focus first on monitoring expression changes of known waterlogging-response genes. For this analysis, we selected the *ADH1* and *PDC1* genes because of their well-established role in fermentative metabolism, which is key to plant response to waterlogging. Our choice was based on previously published findings showing that *ADH1* is induced in response to waterlogging, flooding or hypoxia in different plant species (Bailey-Serres and Voesenek, 2010; Chung *et al*., 1999; Johnson, 1994). For example, when exposed to mild hypoxic conditions, expression of At*ADH1* is induced in the roots of *Arabidopsis thaliana* plants (Chung

et al., 1999). In addition, signal transduction from roots to shoots results in the induction of At*ADH1* expression in shoots as well (Chung *et al*., 1999). In the monocot crop *Zea mays*, it has been shown that induction of Zm*ADH1* expression in response to anoxia plays a role in maize survival (Johnson, 1994). Also, in the more tolerant rice (*Oryza sativa*) varieties, Os*ADH1* and Os*PDC1* expression is induced at a higher level compared to sensitive rice varieties (Bailey-Serres and Voesenek, 2010), suggesting that the level of expression of *ADH1* upon waterlogging could be a good indication of the plant's ability to survive waterlogging stress.

Another gene that we decided to focus on was *HEMOGLOBIN* (*HB*), which codes for a non-symbiotic hemoglobin. This protein plays an important role in modulating nitric oxide (NO) levels in different cell types, and hence is an important regulator of metabolism and cell signaling under waterlogging conditions (Hebelstrup *et al*., 2014). During hypoxia, oxy-hemoglobin is able to oxidize NO to NO_3^-, leading to increased homeostasis of cellular redox and energy status (Igamberdiev *et al*., 2005). In barley, oxidation of NO prevents the loss of nitrogen by reducing NO emission levels in leaves and roots. This is due partially to overexpression of the non-symbiotic hemoglobin Hv*HB1* (Hebelstrup *et al*., 2014; Hebelstrup *et al*., 2012). Maize Zm*HB1* expressed in tobacco was also shown to increase plant tolerance to submergence (Trevisan *et al*., 2011). In *Arabidopsis*, At*HB1* is induced during submergence and positively regulates ATP homeostasis under low oxygen conditions (Lee *et al*., 2011). In addition, (Thiel *et al*., 2011) showed that overexpression of At*HB1* in *Arabidopsis s*eeds promotes plant adaptation to hypoxia. Finally, a more recent study in 5-week old *Arabidopsis thaliana* plants showed that all selected genes (At*ADH1*, At*HB1* and At*PDC1*) were indeed induced upon hypoxia treatment (1% O_2). This induction was dependent on 2 ERF-VII transcription factors, At*RAP2.2* and At*RAP2.12,* as the double mutant *rap2.2 rap2.12* did not respond to the hypoxic treatment (Bui *et al*., 2015).

Before setting up experimental conditions to test the expression of the above-mentioned genes in response to waterlogging, I verified that the selected genes were indeed responsive to hypoxia using reverse transcription coupled to quantitative PCR (qRT-PCR). This experiment also served as a control to test the quality of the primers I had designed to monitor the expression changes of Hv*ADH1*, Hv*PDC1* and Hv*HB1*. For these preliminary experiments, I used the commercial variety Tesla because seeds for this variety were available in the lab. More specifically, 7-day old barley seedlings

grown on MS agar medium at 15°C (16 hrs light/8 hrs dark) were transferred to an anaerojar with an anaerogen sachet for 8 hrs. In these experimental conditions, O_2 levels are expected to drop below 0.1% within 2.5 hrs, thus resulting in a hypoxic environment. For the duration of the treatment, the anaerojars were kept in the dark. After treatment, whole seedlings were collected to monitor expression of the selected genes, as well as the expression of a reference gene, Hv*TUBULIN*. As a control, I monitored the expression of the same genes in 7 day-old seedlings exposed to 8 hrs of darkness, but kept in normal oxygen conditions (FIGURE 3.11). Crossing point-PCR-cycle (Cp) values were analyzed. Cp value represent the cycle at which fluorescence reaches a well-defined threshold. A lower Cp value indicates an abundance of mRNA for the gene of interest in the sample. In contrary, a high Cp value means that more cycles are needed to reach the certain threshold and this correlates with a less abundant mRNA for the gene of interest in the sample.

Analysis of the Cp values obtained for Hv*TUBULIN* were similar under both control and low oxygen conditions, thus indicating that this gene was suitable as a reference gene in these experiments (FIGURE 3.11). I then calculated the expression level of Hv*ADH1*, Hv*PDC1* and Hv*HB* relative to the level of Hv*TUBULIN* (FIGURE 3.11). As expected, all 3 hypoxia-response genes studied were induced after 8 hrs of hypoxia. Melting-curve analysis (data not shown) of the different primer pairs used further indicated that the primers designed were suitable.

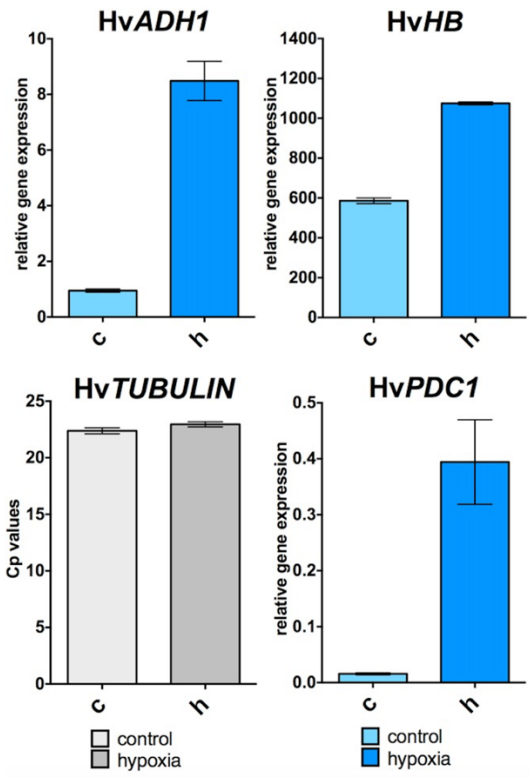

FIGURE 3.11. Overview of gene expression in 7 day-old barley (variety: Tesla) seedlings exposed to hypoxia in the dark for 8 hrs. Cp values of Hv*TUBULIN* in control (c) and hypoxia-treated (h) samples are shown. The other panels show the relative gene expression of Hv*ADH1*, Hv*HB* and Hv*PDC1* in control (c) and hypoxia-treated (h) seedlings. The expression of hypoxia-response gene was analyzed relative to that of the reference gene Hv*TUBULIN*. Data represent the average of 3 individual 7 day-old barley seedlings from one single replicate. Error bars correspond to standard deviations.

Based on these experiments, I decided to establish a protocol for waterlogging treatment under controlled conditions, using the expression of these 3 hypoxia-response genes as an indicator of waterlogging treatment and of plant responses to the treatment.

3.2.2. Optimization of a waterlogging protocol for barley at Leaf 7 developmental stage

In order to establish experimental conditions that would allow me to monitor barley response to waterlogging reliably under controlled conditions, I tested different protocols, which varied depending on the developmental stage at which the stress was applied, the duration of the stress or the type of tissue that was analyzed.

In a first preliminary experiment, I used the Tesla and Golden Promise varieties because seeds were easily accessible in the lab at the beginning of the project. Seeds were sown on John Innes No. 2, and plants were grown in long-day conditions as described in Section 2.1.3.1. At the Leaf 7 (L7) developmental stage (i.e. when the first node is seen, typically when plants were ~100 day-old), pots were transferred to a plastic tub filled with tap water, so that water level was up to 1 cm above soil level. In these conditions, ~1 cm of the stem was immersed in water, thus corresponding to a partial submergence (Sasidharan *et al*., 2017). However, because most of the aerial parts of the plant were above water level, the term 'waterlogging' will be used subsequently.

After 14 days of waterlogging treatment, the plants were kept for recovery period until the grain growth stage with a normal watering regime. In order to determine the kinetics of expression of the 3 above-mentioned hypoxia-response genes, leaf samples were collected during the waterlogging treatment (day 2, day 7, day 14 after the beginning of waterlogging treatment) for RNA extraction and qRT-PCR analysis for the above-mentioned genes. The data obtained indicate that the expression of the reference gene (Hv*TUBULIN*) varied at the different time points or developmental stages at which samples were collected. In addition, at a given time point, there were also differences in the level of gene expression between waterlogged and control samples (FIGURE 3.12). For example, at day 14, the expression level of Hv*TUBULIN* was different in control or waterlogged Golden Promise leaves, which could yield artefactual differences in hypoxia-response gene expression if this gene was used as reference. One difficulty in analyzing the data, was that it was not always possible to consistently collect the same leaf from each of the plants (e.g. leaf number 4). This problem was exacerbated at later stages of development, so that it was unclear

whether the leaves collected are of the same age and have experienced waterlogging conditions for the same length of time.

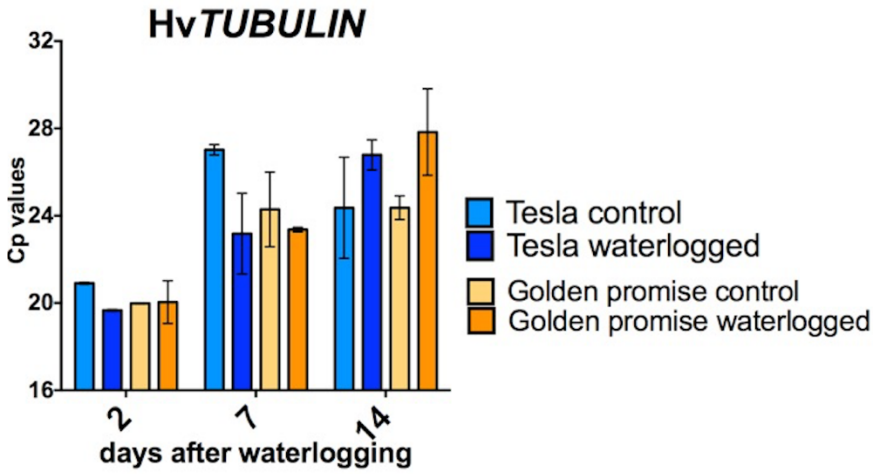

FIGURE 3.12. Overview of Cp values of Hv*TUBULIN* in Tesla and Golden Promise during waterlogging treatment. Cp values of Hv*TUBULIN* were determined using qRT-PCR on leaf samples from waterlogged and control barley plants. Leaf tissue was collected at 2, 7 and 14 days after the beginning of the waterlogging treatment, which finished at day 14. Data represent averages of Cp values obtained from 3 individual barley leaves., that were part of one single replicate. Error bars correspond to standard deviations.

The second aim of this preliminary experiment was to analyze the relative expression of Hv*ADH1*, Hv*HB* and Hv*PDC1* in response to waterlogging. Given that the Cp values of the Hv*TUBULIN* were not stable between the different time-points and varieties, I was not able to calculate the relative gene expression. Instead, I analyzed the Cp values obtained. As shown in FIGURE 3.13, based on the Cp values of Hv*ADH1*, Hv*HB* and Hv*PDC1*, I could not detect up-regulation of the 3 hypoxia-response genes, even after 2 weeks of waterlogging treatment, except for Hv*HB* in 7 days waterlogged Tesla leaves.

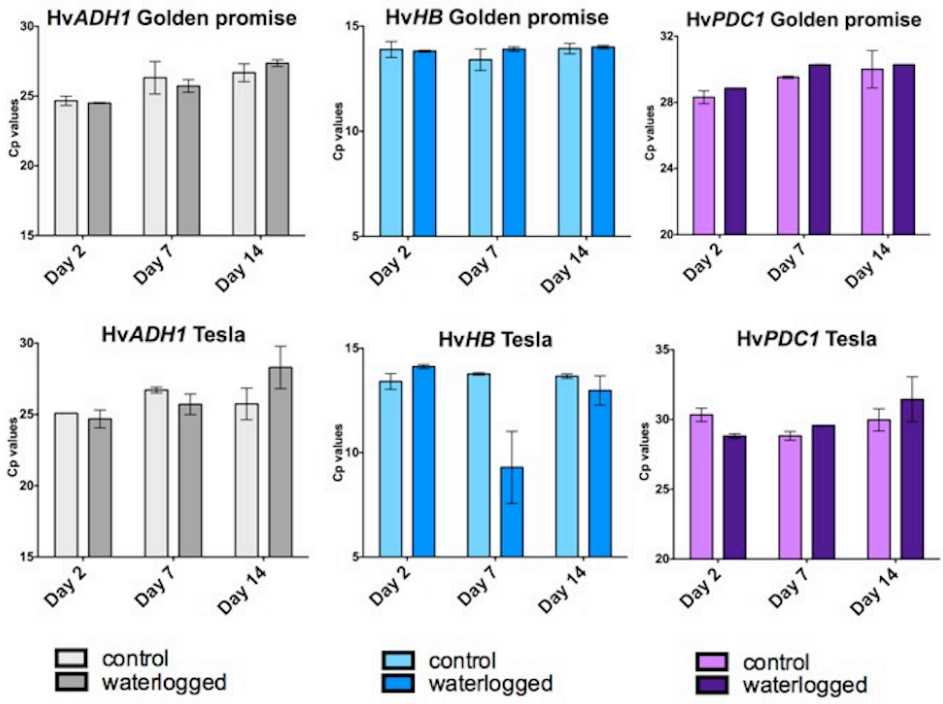

FIGURE 3.13. Expression of hypoxia-response genes in leaves of waterlogged and control barley plants. The average Cp values obtained for the Hv*ADH1*, Hv*HB* and Hv*PDC1* in waterlogged and control barley plants (Tesla and Golden promise varieties) are presented. Leaf samples were collected at 2, 7 and 14 days from the beginning of the waterlogging treatment. Data represent averages of Cp values obtained from 2 individual barley leaves within the same experiment that were part of one replicate. Error bars correspond to standard deviations.

The third aim of this preliminary experiment was to verify if the total chlorophyll content was affected in response to waterlogging. For this purpose, leaf segments (~half a leaf corresponding to the tip and the middle of the leaf) were collected and the total chlorophyll was extracted using 80% acetone as described in Section (2.1.3.8). As observed in FIGURE 3.14, the chlorophyll content did not appear to be affected by the waterlogging treatment. However, there were several limitations to this experiment: (i) it was difficult to ensure that the same leaf was collected (e.g. leaf 4); and (ii) the leaf sample was collected based on size instead of weight, so the measurements could not be normalized. It was therefore difficult to draw conclusions from these measurements.

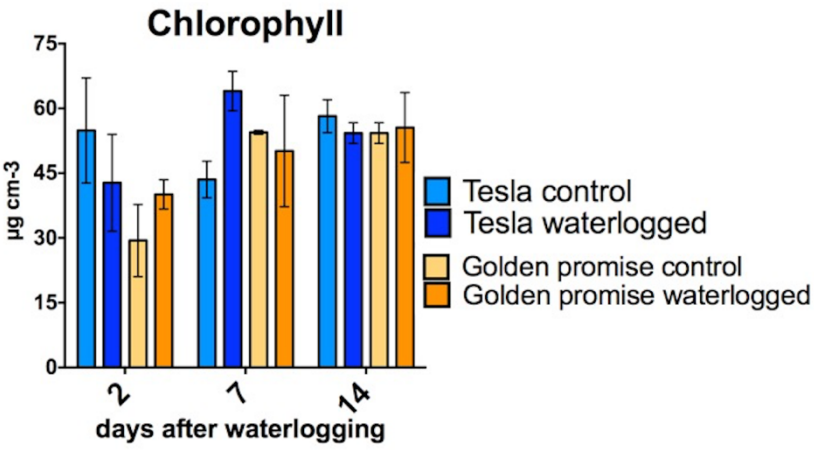

FIGURE 3.14. Chlorophyll content in leaves of Tesla and Golden Promise plants subjected to waterlogging. Chlorophyll was extracted using 80% acetone from waterlogged and control barley plants. Leaf tissue was collected at 2, 7 and 14 days after the beginning of the waterlogging treatment. Data represent averages of total chlorophyll content obtained from 3 individual barley leaves (one replicate only). Error bars correspond to standard deviations.

Altogether, the results of this preliminary experiment indicated that this first waterlogging protocol was not triggering the expected response, so that additional optimization steps were needed.

3.2.3. Optimization of a waterlogging protocol for barley at the Leaf 1 developmental stage

In order to develop a waterlogging protocol, I next decided to apply the waterlogging treatment at the Leaf 1 (L1) developmental stage, when barley plants are supposed to be more susceptible to the waterlogging (Zeng *et al.*, 2013; Celedonio *et al.*, 2015). For these preliminary experiments, I used the Tesla and Sanette varieties instead of Golden Promise (due to a lack of seeds for this variety). Seeds were sown on John Innes No. 2, and plants were grown in long-day conditions as described in Section 2.1.3.1. At the Leaf 1 (L1) developmental stage (i.e. stage 1 when 1 leaf is visible; typically when plants were ~7 day-old), pots were transferred to a plastic tub

filled with tap water, so that water level was up to 1 cm above soil level. In these conditions, ~1 cm of the stem was immersed in water, as described for the previous experiment. After 21 days of waterlogging treatment, the plants were kept for a recovery period of 14 days with a normal watering regime. In order to determine the kinetics of expression of the 3 above-mentioned hypoxia-response genes, leaf samples were collected every 7 days during the waterlogging treatment (day 7, 14 and 21 after the beginning of waterlogging treatment) and also during recovery period (day 28 and 35 after starting waterlogging treatment).

Previous studies in barley have shown that the expression of reference genes can vary greatly depending on the tissue and organ tested (Janska ́*et al*., 2013). Considering our previous data with Hv*TUBULIN* (FIGURE 3.12) and that the waterlogging treatment is performed over a long period of time, I tested the expression of 4 different 'classic' reference genes described in the literature, namely Hv*ACTIN*, Hv*ADP*, Hv*GAPDH*, Hv*TUBULIN* (Janska ́*et al*., 2013; Ferdous *et al*., 2015) and determined if their expression was indeed constant over the course of the experiment (FIGURE 3.15).

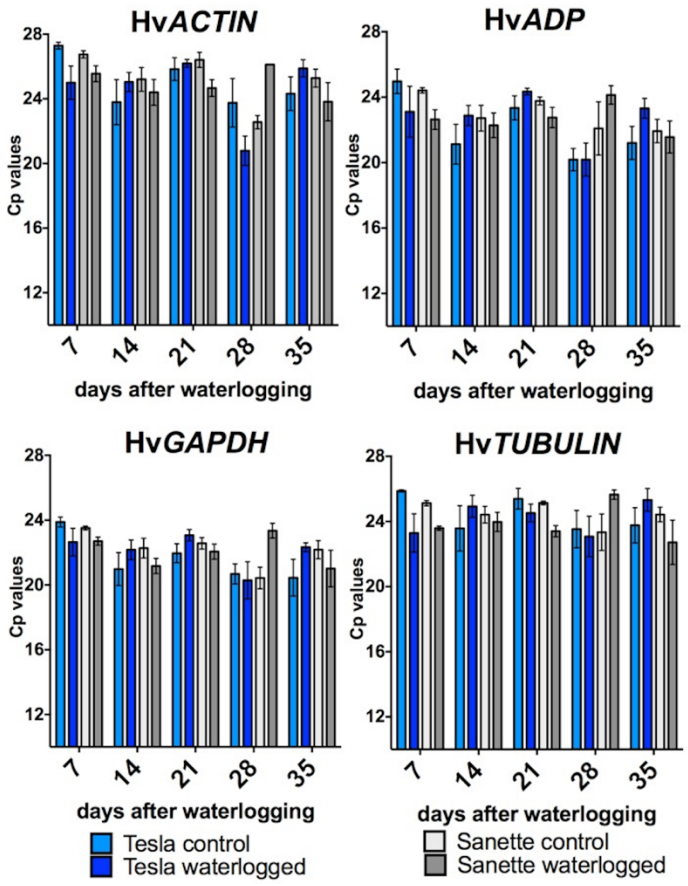

FIGURE 3.15. Expression of different reference genes during waterlogging treatment and recovery. Cp values of 4 different reference genes (Hv*ACTIN*, Hv*ADP*, Hv*GAPDH*, Hv*TUBULIN*) were determined using qRT-PCR on leaf samples from waterlogged and control barley plants. Leaf tissue was collected every 7 days after the beginning of the waterlogging treatment, which lasted 21 days. The recovery period lasted for another 14 days. Data represent averages of Cp values obtained from 4 individual barley leaves. There were 2 independent replicates, in each replicate 2 leaf segment were analyzed. Error bars correspond to standard deviations.

Again, the data obtained indicate that for a given variety (e.g. Sanette), the expression of the 4 reference genes varied at the different time points or developmental stages. In addition, at a given time point, there were also differences in the level of gene expression between waterlogged and control samples (FIGURE 3.15). For example, at day 28, the expression level of Hv*ACTIN*, Hv*TUBULIN* and Hv*GAPDH* was different in control or waterlogged Sanette leaves, which could yield artefactual differences in hypoxia-response gene expression if these genes were used as references. One difficulty in analyzing this data, however, is that it was not always possible to consistently collect the same leaf from each of the plants (e.g. leaf number 4). This problem was exacerbated at later stages of development, so that it is unclear whether the leaves collected are of the same age and have experienced waterlogging conditions for the same length of time.

I also analyzed the expression of Hv*ADH1*, Hv*HB* and Hv*PDC1* in response to waterlogging. Given that the Cp values of the 4 reference genes tested were not stable between the different time-points and varieties, I was not able to calculate the relative gene expression. Instead, I analyzed the Cp values obtained. As shown in FIGURE 3.16, based on the Cp values of Hv*ADH1*, Hv*HB* and Hv*PDC1*, I could not detect up-regulation of the 3 hypoxia-response genes, even after 3 weeks of waterlogging treatment.

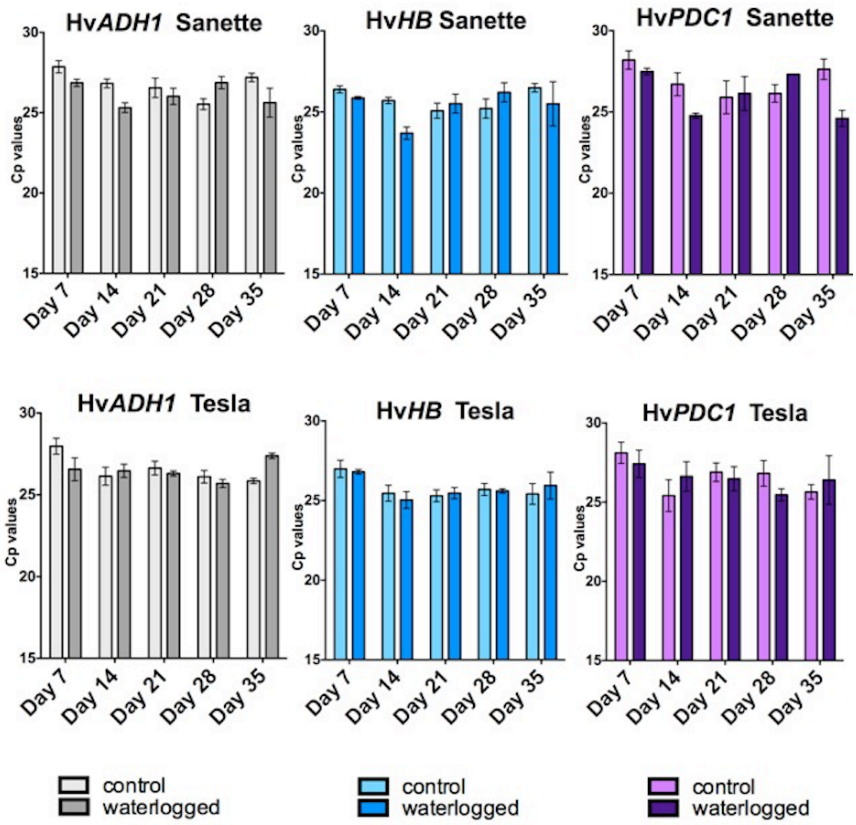

FIGURE 3.16. Expression of hypoxia-response genes in leaves of waterlogged and untreated barley plants. The average Cp values obtained for the Hv*ADH1*, Hv*HB* and Hv*PDC1* hypoxia-response genes in waterlogged and control barley plants (Tesla and Sanette varieties) are presented. Leaf samples were collected every 7 days from the beginning of the waterlogging treatment and during the recovery period, which started at Day 21. Data represent averages of Cp values obtained from 4 individual barley leaves. There were 2 independent replicates, in each replicate 2 leaf segments were analyzed. Error bars correspond to standard deviations.

Another parameter analyzed was the chlorophyll content. Having in mind the previous experiment, this time I collected and weighed the tissue before chlorophyll extraction. The results were normalized using the weight of the leaf sample collected. As observed in FIGURE 3.17, the chlorophyll content seemed to be negatively affected by the waterlogging at 14 days (for Tesla) and 28 days (for Sanette) after the beginning of the treatment. Note however, that the same leaf number was probably not collected during this experiment, making interpretation of the results difficult.

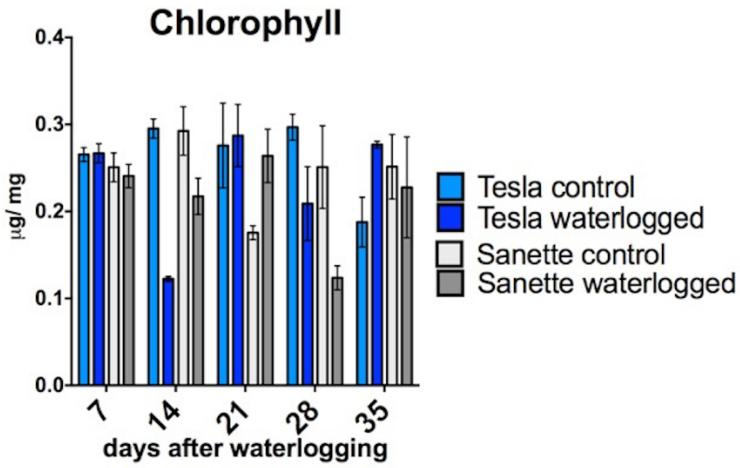

FIGURE 3.17. Chlorophyll content in the leaves of Tesla and Sanette plants. Chlorophyll was extracted using 80% acetone from leaf samples from waterlogged and control barley plants. Leaf tissue was collected at 2, 7 and 14 days after the beginning of the waterlogging treatment, which finished at day 14. Leaf tissue was also collected during the recovery period (days 28 and 35). Data represent averages of total chlorophyll content obtained from 3 individual barley leaves (3 independent replicates). Error bars correspond to standard deviations.

In sum, these preliminary experiments conducted at the L1 stage did not yield satisfying results. I hence repeated these experiments in the same conditions (i.e. waterlogging applied at the L1 stage), but this time, I collected roots to analyze the expression of the selected hypoxia-response genes. In order to have a more accurate characterization of the changes in gene expression in leaves, I also collected systematically the L1 for each time-point. This experiment was performed with the Tesla variety only. At the L1 developmental stage, pots were transferred to a plastic tub filled with tap water, so that water level was up to 1 cm above soil level. After 21 days of waterlogging treatment, the plants were kept for a recovery period of 14 days with a normal watering regime. Samples were collected every 7 days during the waterlogging treatment (day 7, 14, 21 after the beginning of waterlogging treatment) and also during recovery period (day 28 and 35 after starting waterlogging treatment). For each time-point and condition, the entire root system, as well as the L1 were collected. I then extracted total RNA and carried out qRT-PCR analysis to determine the expression level of the 4 classic reference genes and of the 3 selected hypoxia-

response genes in the two tissue types, in both waterlogged and control samples. Similarlyws to the results of the previous experiment, the Cp values of the 4 reference genes were not constant in leaves (FIGURE 3.18). In contrast with the data obtained with leaf tissue, in roots, the Cp values for Hv*ACTIN* and Hv*TUBULIN* were more stable between the treatments and between the time-points (FIGURE 3.18). Based on this, these 2 genes were chosen as reference genes when root tissue was used for analysis.

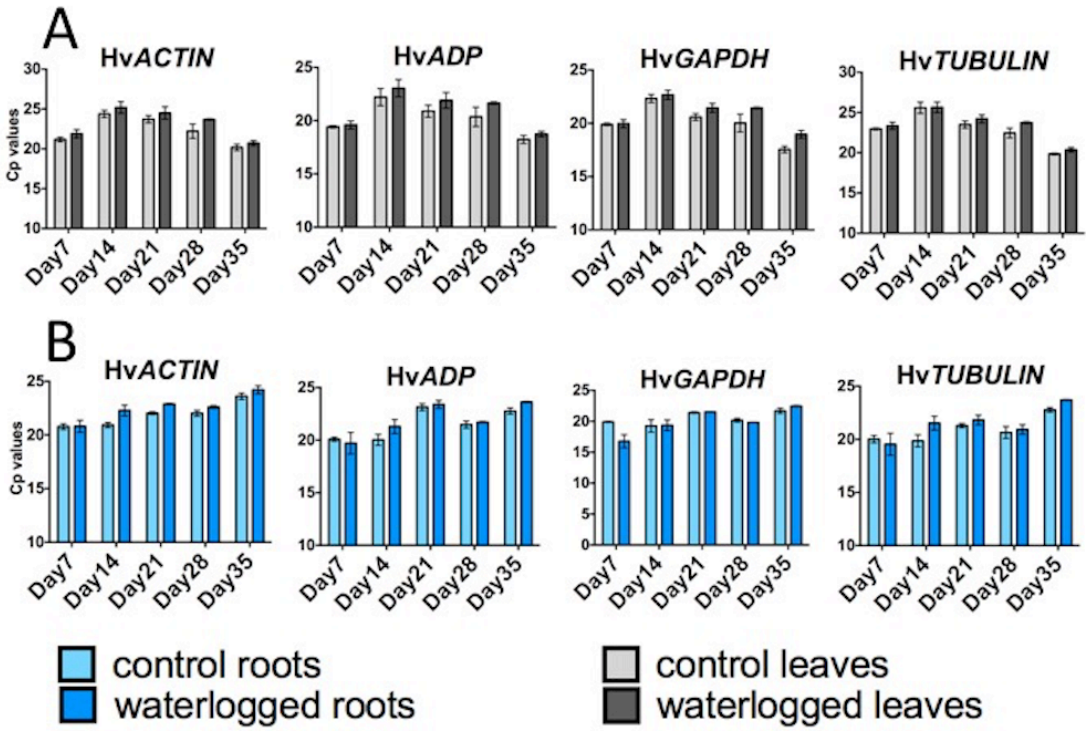

FIGURE 3.18. Characterization of reference gene expression in roots and L1 leaves of waterlogged and control barley plants (Tesla variety). Cp values obtained for the reference genes Hv*ACTIN*, Hv*ADP*, Hv*GAPDH*, Hv*TUBULIN* in waterlogged and control barley L1 leaves (A) and roots (B). Average Cp values obtained for 3 individual barley leaves and for 3 root systems from individual plants are shown. Data presented here is from one single experiment, when 3 plants were used for each time-point and condition. Error bars correspond to standard deviations.

I then analyzed the expression of the 3 hypoxia-response genes using Hv*ACTIN* as a reference gene to calculate the relative expression of these genes for root and L1 leaf samples (FIGURE 3.19). In leaves, the Cp value obtained for

Hv*ACTIN* was similar between waterlogged and control leaf samples at a given time point, so that it could be used to calculate the relative expression of the 3 hypoxia-response genes at a given time point and compare the response of the waterlogged plants to expression in untreated plants at this particular time point. However, the Cp values for Hv*ACTIN* changed across the duration of the experiment, making it difficult to compare the evolution of the expression changes from one time point to another. Considering these limitations, the data obtained (FIGURE 3.19) suggest that the expression of the 3 hypoxia-response genes in the L1 leaf was similar between waterlogged and control plants.

In roots, the Cp value of Hv*ACTIN* was quite constant between the control and waterlogged samples and also for the duration of the experiment. This allowed me to not only compare expression between control and waterlogged samples, but also the kinetic of induction/repression over the entire duration of the experiment. The results obtained indicate that the 3 hypoxia response genes are up-regulated at 7 days after the beginning of the waterlogging treatment, with a significant difference between control and waterlogged roots. At 14 days after the beginning of the waterlogging treatment, the expression of the 3 hypoxia-response genes decreased and remained lower for the rest of the experiment. From 21 days onwards, the relative expression was similar in roots of control and waterlogged plants. Based on these results, I decided to focus on the expression of the 3 hypoxia-response genes in roots for all subsequent experiments.

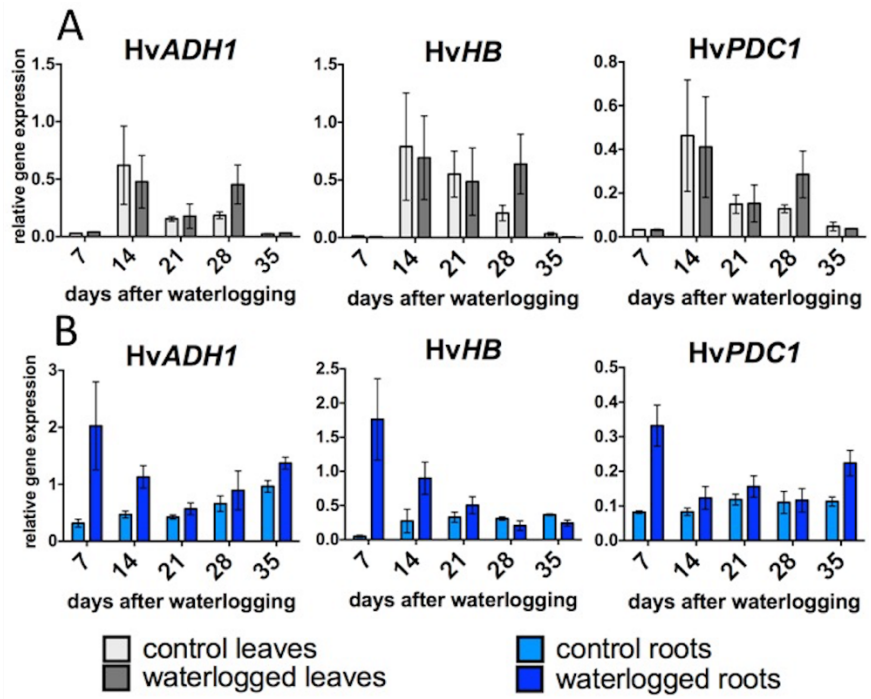

FIGURE 3.19. Comparison of the relative expression of the 3 hypoxia-response genes in L1 leaves and roots of waterlogged and control barley plants (Tesla variety). A. Relative gene expression of the Hv*ADH1*, Hv*HB*, Hv*PDC1* hypoxia-response genes in L1 leaves. **B.** Relative gene expression of the Hv*ADH1*, Hv*HB*, Hv*PDC1* hypoxia-response genes in roots. At the L1 stage, barley seedlings of the Tesla variety were subjected to waterlogging (water 1 cm above soil level). The L1 leaf and roots were collected at 7-day intervals during waterlogging treatment (days 7, 14 and 21) and during the recovery period (days 28 and 35). Average relative expression values were obtained after normalization with Hv*ACTIN*. Data presented originates from 3 individual L1 leaves or 3 root systems from individual plants, all of which were grown at the same time and were part of the same experiment. Error bars correspond to standard deviations.

For the previous preliminary experiments, I measured chlorophyll content, but no differences were observed between untreated and waterlogged plants. As indicated above, this could be due to the fact that different leaf numbers were used. To overcome this potential problem, I repeated the waterlogging treatments at the L1 stage as described above and analyzed the chlorophyll content from the same leaf (L1) for each time-point and condition. Despite using consistently the L1 leaf, no decrease in the chlorophyll content was observed in waterlogged plants compared to

the control ones, even after 21 days of waterlogging (FIGURE 3.20). In fact, there was even a small increase in the chlorophyll content in waterlogged plants compared to untreated ones at 7 and 28 days. It is however difficult to draw conclusions because of the small sample size.

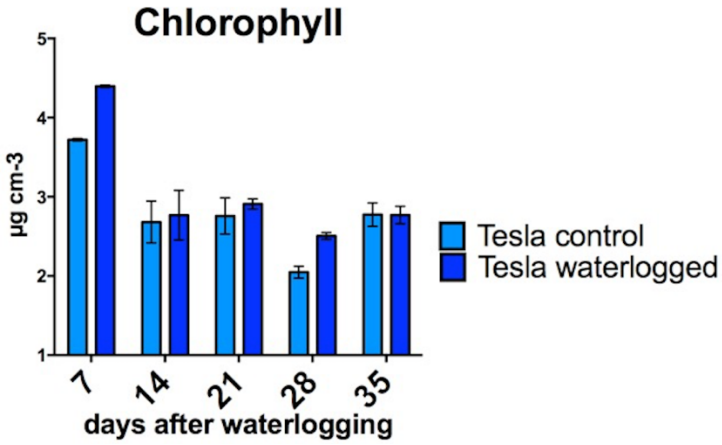

FIGURE 3.20. Chlorophyll measurements in L1 leaves of waterlogged barley plants (Tesla variety). Chlorophyll was extracted using 80% acetone from 5 leaf discs (5 mm in diameter each) from waterlogged and control barley plants. Leaf tissue was collected every 7 days from the beginning of the waterlogging treatment, which finished at day 21 and during the recovery period (days 28 and 35). Data represent averages of total chlorophyll content obtained from 3 L1 leaves (all originating from the same experiment). Error bars correspond to standard deviations.

After observing that the Hv*ADH1*, Hv*HB* and Hv*PDC1* genes were already induced in roots 7 d after starting the waterlogging treatment, I sought to determine if these genes were also induced at an earlier time point after the beginning of the treatment. In order to obtain a better resolution for the induction of the hypoxia-response gene expression, I repeated the waterlogging experiment in the same conditions as above (i.e. at the L1 stage, with water 1 cm above soil level and using the Tesla variety), but collected whole root systems at earlier time points (i.e. day 1, 2, 4, 6, 7, 9, 11 and 13). Following total RNA extraction, I carried qRT-PCR experiments and first checked if the Cp values for the Hv*ACTIN*, Hv*TUBULIN*, Hv*GAPDH* and Hv*ADP* reference genes were constant at these time-points. As expected, and similarly to the results obtained with a longer time course experiment

(FIGURE 3.18) the Cp values of Hv*ACTIN* and Hv*TUBULIN* were stable between the time-points and treatments (FIGURE 3.21) in roots. However, based on the Cp values, the expression of Hv*ADP* was more variable. In addition, the Cp values of Hv*GAPDH* were lower in waterlogged compared to untreated samples, which correlated with an induction of Hv*GAPDH* upon waterlogging treatment. The latter is not surprising, considering the role of GAPDH in glycolysis and the known metabolic changes that occur in response to waterlogging.

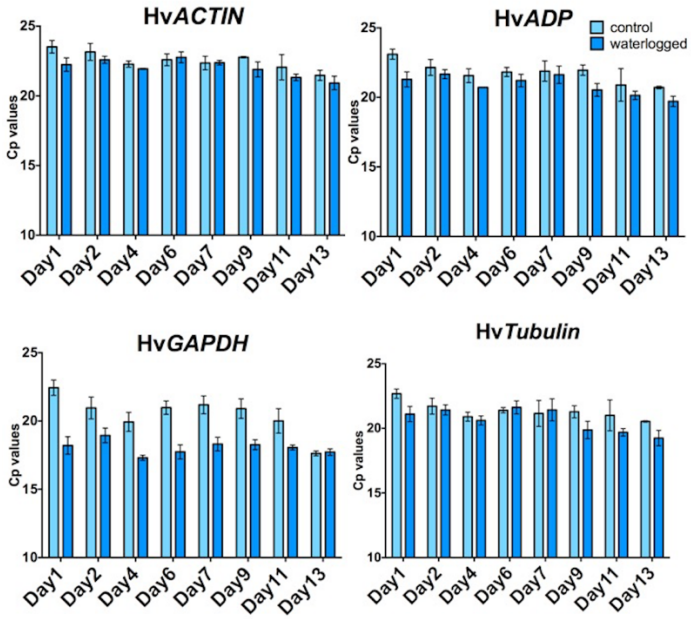

FIGURE 3.21. Comparison of different reference genes in roots of waterlogged and untreated plants (Tesla variety). Average Cp values for the Hv*ACTIN*, Hv*TUBULIN*, Hv*GAPDH*, Hv*ADP* reference genes in roots control and waterlogged barley seedlings. At the L1 stage, barley seedlings of the Tesla variety were subjected to waterlogging (water 1 cm above soil level). Roots were collected at days 1, 2, 4, 6, 7, 9, 11 and 13 after starting the waterlogging treatment. Average Cp values obtained for 2 root systems from individual plants are shown. All plants were part of one single experiment. Error bars correspond to standard deviations.

Using the same cDNA and Hv*ACTIN* as a reference gene, I examined the relative expression of the 3 hypoxia-response genes. This experiment revealed that all hypoxia genes were induced already 24 hrs after the beginning of waterlogging. The expression of these genes then decreased (days 2 and 4) and reached another peak at days 6-7 (FIGURE 3.22). Importantly, changes in the expression of the 3 hypoxia-response genes was specific to the waterlogged samples and was not observed in roots

of untreated plants. In addition, these results independently confirmed our previous data, which showed a waterlogging-specific induction of Hv*ADH1*, Hv*HB*, Hv*PDC1* expression in roots at 7 days after the onset of waterlogging (FIGURE 3.19).

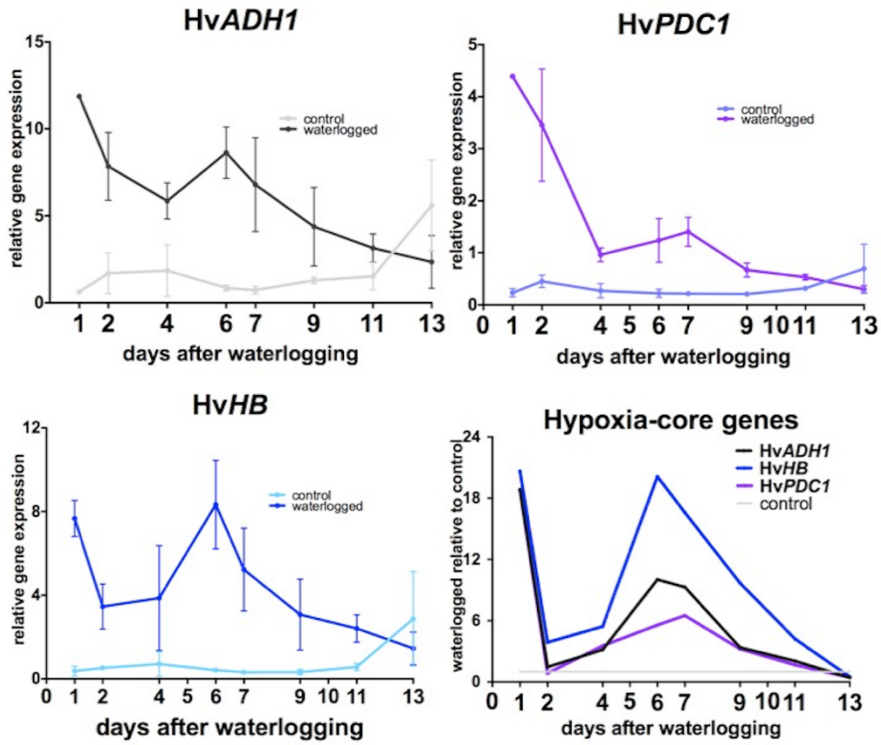

FIGURE 3.22. Characterization of the expression of hypoxia-response genes in roots of waterlogged plants. Using Hv*ACTIN* as a reference gene, the relative gene expression of the 3 hypoxia-response genes in roots of untreated and waterlogged plants was calculated. At the L1 stage, barley seedlings of the Tesla variety were subjected to waterlogging (water 1 cm above soil level). Roots were collected at days 1, 2, 4, 6, 7, 9, 11 and 13 after starting the waterlogging treatment. Average Cp values obtained for 2 root systems from individual plants are shown. The data presented are part of one single experiment. Error bars correspond to standard deviations.

In sum, these preliminary results suggest that (i) the waterlogging treatment applied at the L1 developmental stage triggers the expected gene expression changes; and (ii) root tissue is more appropriate than leaf tissue to monitor the expression of the hypoxia-response genes selected. Also, based on this experiments, chlorophyll content is not affected by the waterlogging treatment.

Next, I tested if the waterlogging-specific induction of the 3 hypoxia-response genes was also observed in other varieties than Tesla. To this aim, I repeated the same

experiment with both the Tesla and Golden Promise varieties. The latter was chosen because it was being used to generate mutant lines for this project (see Section 4.4). As expected based on the results of my experiment, with Tesla, the Hv*ADH1*, Hv*HB* and Hv*PDC1* were all induced in response to waterlogging (FIGURE 3.23). Similarly, the expression of these genes was also induced in Golden Promise plants that were waterlogged, but not in untreated plants. However, the extent of gene activation was reduced compared to Tesla. In addition, especially for Hv*HB*, there seemed to be a delay in gene induction in Golden Promise compared with Tesla.

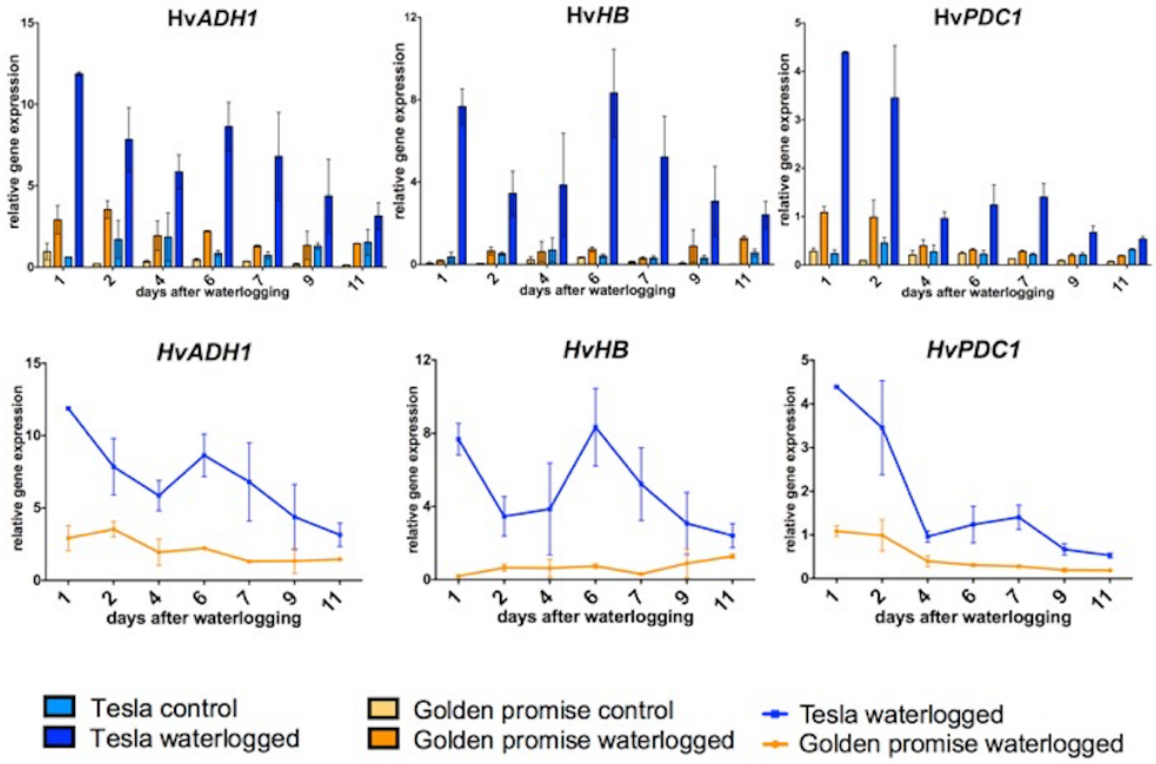

FIGURE 3.23. Comparison of the expression of hypoxia-response genes in Tesla and Golden Promise. Relative gene expression of hypoxia-response genes, Hv*ADH1*, Hv*HB* and Hv*PDC1* in barley roots of Golden Promise (orange) and Tesla (blue) plants left untreated (control) or waterlogged. At the L1 stage, barley seedlings were subjected to waterlogging (water 1 cm above soil level). Roots were collected at days 1, 2, 4, 6, 7, 9 and 11 after starting the waterlogging treatment. Average relative expression obtained for 2 root systems from individual plants are shown. The data presented originate from 2 independent replicates (i.e. 1 plant per replicate was analyzed). Error bars correspond to standard deviations.

In conclusion, root tissue is best to monitor the gene expression changes of Hv*ADH1*, Hv*HB* and Hv*PDC1* upon waterlogging. Also, these experiments allowed me to select the best reference genes for our experimental conditions (Hv*ACTIN* and Hv*TUBULIN*). Finally, we observed differences in the induction of these genes depending on the varieties used (i.e. the expression of these genes was higher in Tesla compared to Golden Promise upon waterlogging).

3.2.4. Developing the methods to combine waterlogging treatment at the L1 stage with analyses of root anatomy and morphology

Two types of roots are found in barley: embryonic roots and post-embryonic roots. Embryonic roots form first during development: they consist of the primary root (grey arrow in FIGURE 3.24) and the seminal roots (blue arrow in FIGURE 3.24). Post-embryonic roots are formed at later stages of development and are typically called crown roots (red arrow in FIGURE 3.24). Because the waterlogging treatment is applied at early stages of the development (L1 stage), before the first crown roots have formed, I decided to focus on seminal roots to analyze aerenchyma formation in control conditions, and in response to waterlogging.

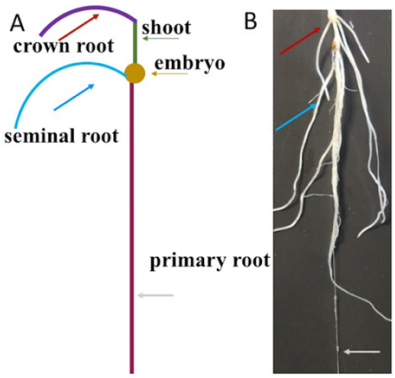

FIGURE 3.24. The different types of roots in barley. A. Schematic representation of a barley root system. **B.** Picture of the root system of 20 day-old of a waterlogged barley plant.

In a first experiment, seminal roots were collected from barley plants waterlogged for 7 days (waterlogging was applied as above: at the L1 stage, 1 cm

above soil level). In this experiment the Pilastro, Retriever and Louise varieties were used. Initially, only 3 varieties were used in order to set up the experiment. These 3 varieties has been classified as sensitive in the first set of pictures and tolerant in the second set of pictures (FIGURE 3.8.). Because aerenchyma is considered as an important response for waterlogging tolerance (Zhang *et al*., 2016), this experiment could provide valuable information to classify more reliably these varieties as either sensitive or tolerant. Seminal roots from control and waterlogged plants were collected, washed and hand sectioned as described in (Zhang *et al*., 2016). The degree of aerenchyma observed was scored from 0 (no aerenchyma) to 4 (well-developed aerenchyma) based on the scoring system described in (Zhang *et al*., 2016). Analysis of the hand-made sections suggested that all varieties used formed aerenchyma 7 days after the onset of waterlogging treatment (FIGURE 3.25). Some varieties also developed aerenchyma in control conditions (e.g. Louise). This may be of interest, as this may result in increased tolerance to waterlogging.

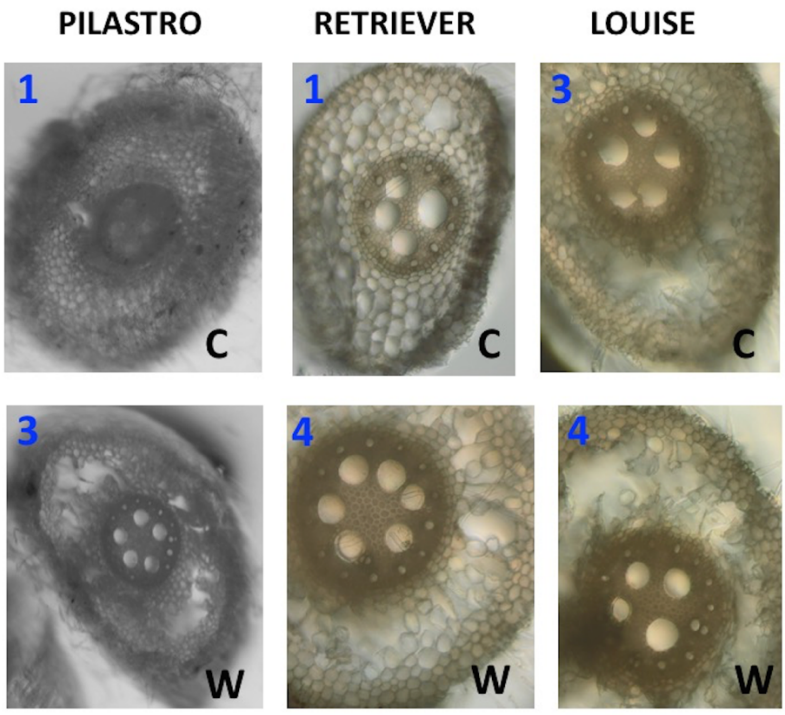

FIGURE 3.25. Aerenchyma formation in seminal roots of 3 different varieties. Pilastro, Retriever and Louise varieties were used in this experiment. L1 seedlings were waterlogged for 7 days. Seminal roots from control (**C**) and waterlogged (**W**) plants were collected. Roots were hand sectioned as described in section 2.1.3.7. The

degree of aerenchyma observed was scored (score indicated in blue in the top left corner of each picture) from 0 (no aerenchyma) to 4 (well-formed aerenchyma).

Although differences could be observed between control and waterlogged samples, the hand sectioning was extremely laborious and made it difficult to obtain a sufficient number of sections that would be suitable for scoring. To overcome this problem, I established a fixation method for microtome sectioning, and also tested if there were differences in aerenchyma formation between seminal and crown roots. To this aim, L1 seedlings (Pilastro and Louise varieties) were waterlogged for 7 days. Seminal (S) roots and crown (C) roots from control and waterlogged plants were collected. The first cm (counted from the base of the roots) was used for this analysis. Roots were cleaned with tap water, fixed with formaldehyde and sectioned with the microtome, as described in Section 2.1.3.7. As observed in FIGURE 3.26, for both varieties, seminal roots appeared to have a more developed aerenchyma compared to the crown roots. For Louise, but not Pilastro, there were visible signs of aerenchyma development in crown roots. Unfortunately, for the control plants, tissue was damaged during the sectioning (data not shown).

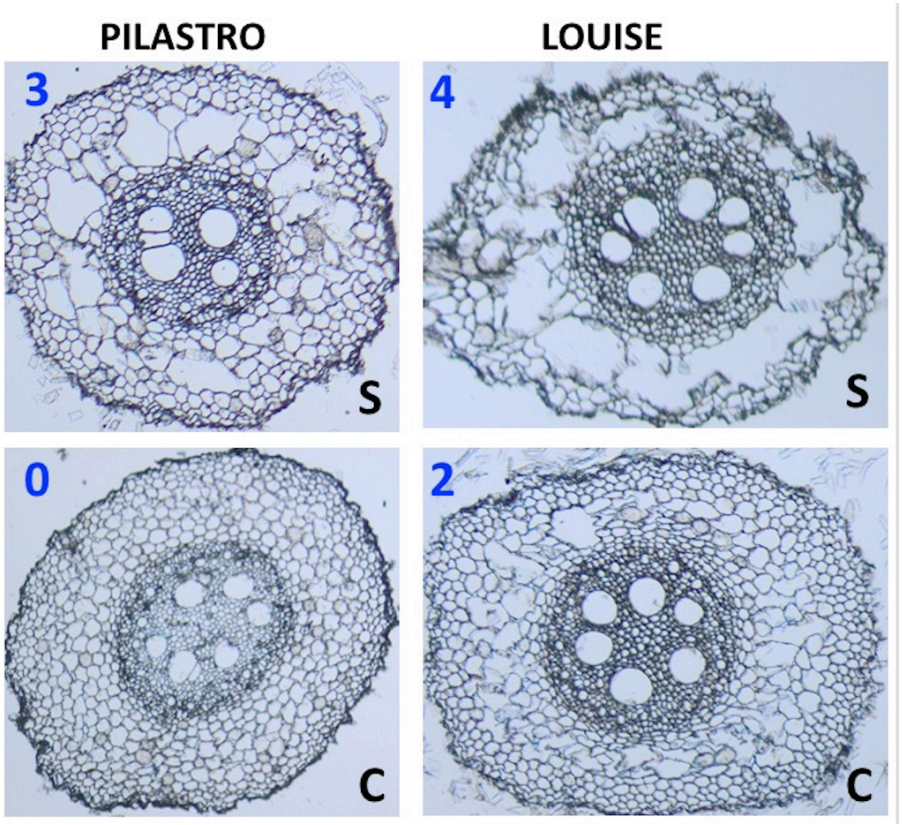

FIGURE 3.26. Aerenchyma formation in seminal and crown roots after fixation and microtome sectioning. Pilastro and Louise varieties were used in this experiment. L1 seedlings were waterlogged for 7 days. Seminal (S) roots and crown (C) roots from waterlogged and control plants were collected. They were cleaned with tap water, fixed with formaldehyde and sectioned with a microtome. The sections were 18 μm thick. Data presented is from waterlogged plants only. The degree of aerenchyma formation observed was scored (score indicated in blue in the top left corner of each picture) from 0 (no aerenchyma) to 4 (well-formed aerenchyma).

In conclusion, the waterlogging protocol I optimized, not only allowed me to monitor reliably gene expression changes in response to waterlogging, but also to observe and score aerenchyma formation. As expected, these preliminary experiments showed that aerenchyma formation was triggered upon waterlogging, although some varieties present aerenchyma even in control conditions. Based on these preliminary experiments, seminal roots appear to form more aerenchyma compared with crown roots in waterlogged conditions. This could be related to the fact that the seminal roots are formed before the crown roots and hence are exposed to waterlogging from the beginning of the treatment.

3.3. Screening for waterlogging tolerance in controlled conditions

As indicated at the beginning of this chapter, one of the aims of my PhD work was to characterize the response of different commercial winter barley cultivars to waterlogging with the aim of identifying varieties that are more tolerant to this abiotic stress. A first field waterlogging experiments allowed us to identify varieties that were potentially more tolerant or sensitive to waterlogging (FIGURE 3.8). Having developed a reliable waterlogging protocol, I now sought to characterize these varieties under controlled conditions.

3.3.1 Expression of hypoxia response genes

Before comparing the waterlogging sensitive and tolerant varieties to waterlogging, I first conducted a time-course experiment to check if the kinetics of gene expression observed for Tesla and Golden Promise was maintained in the AGOUEB varieties chosen after the first field experiment (FIGURE 3.8). The only varieties I could not include because of insufficient seed stock were Liebniz and Ragusa. Instead, I added Tapir to the list. I applied the waterlogging stress at the L1 stage, as described in Section 3.2.3. Root samples were collected just before starting and during the waterlogging treatment (8 h, day 1, day 2, day 6 day 7 after the beginning of waterlogging treatment). I then examined the relative expression of Hv*ADH1*, Hv*HB* and Hv*PDC1* using qRT-PCR. In roots of untreated samples, the expression of these genes remained low (FIGURE 3.27A). There are some differences between the varieties in control conditions, but a more detailed analysis, with more replicates is required to check if some varieties indeed express at a higher level Hv*ADH1*, Hv*HB* and Hv*PDC1* in control conditions. Similarly to the results shown in FIGURE 3.23 for Tesla and Golden Promise, I found that for most of the varieties the hypoxia-response genes tested were induced at day 1 after the beginning of waterlogging, with a few exceptions (FIGURE 3.27B):

- for Hv*ADH1*, Louise had the peak at day 2 and Madrigal at day 6.
- for Hv*HB*, Louise, Vesuvius, Arma and Isa had their peak of expression at day 2 and Madrigal at day 6.
- for Hv*PDC1*, Retriever, Louise and Madrigal reached maximum level of expression at day 2.

In conclusion, these results indicate that for most of the selected varieties, all the hypoxia genes analyzed are induced and have their peak of expression around day 1 after the beginning of waterlogging. The results obtained also indicate that some varieties are able to induce the hypoxia-response genes faster and also more strongly than others.

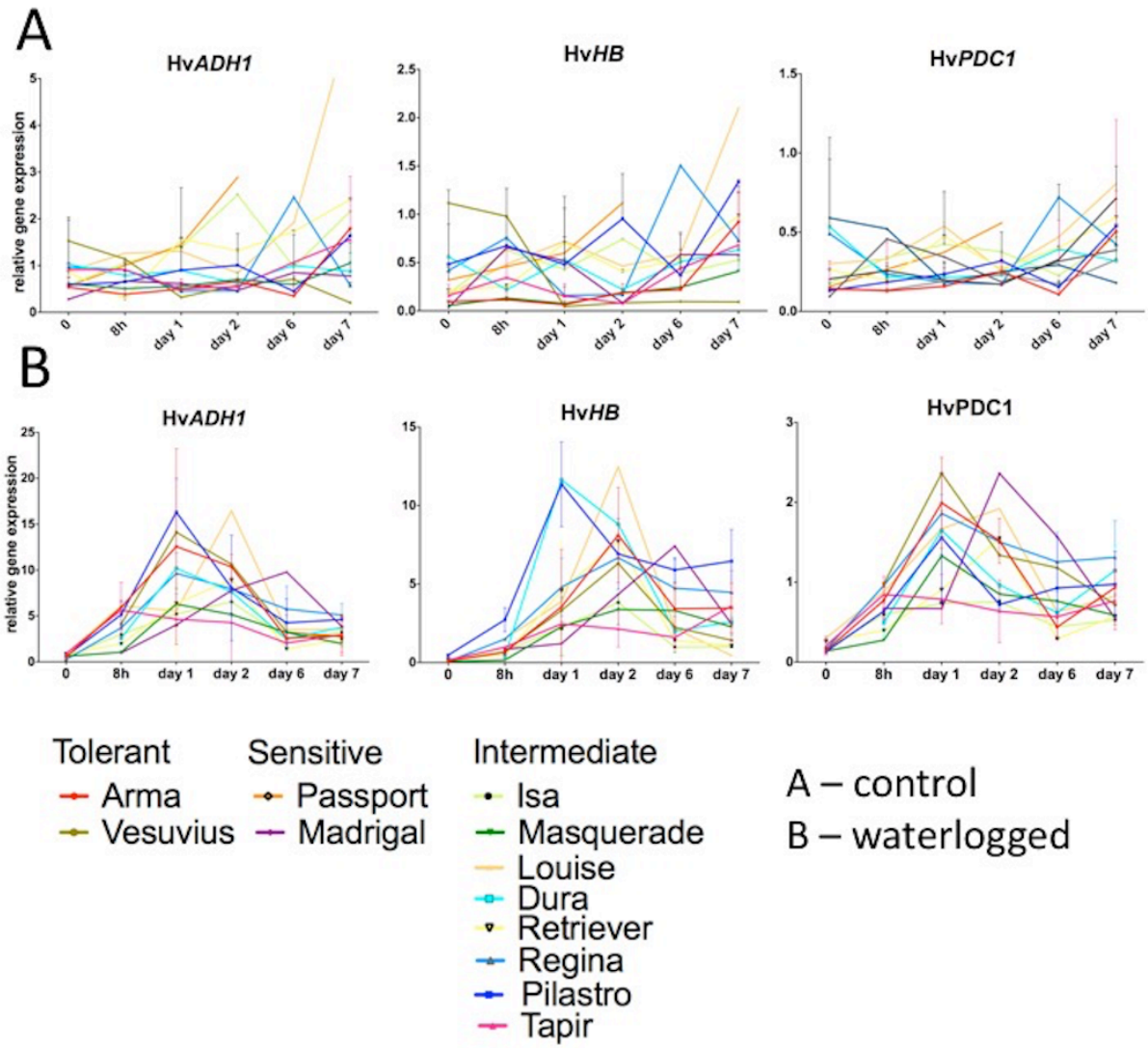

FIGURE 3.27. Expression of hypoxia-response genes in roots of different barley varieties in control conditions and upon waterlogging treatment. Using Hv*ACTIN* as a reference gene, the relative gene expression of 3 hypoxia-response genes in roots of untreated and waterlogged plants was calculated. At the L1 stage, barley seedlings of the Pilastro, Vesuvius, Dura, Regina, Madrigal, Masquerade, Arma, Tapir, Passport, Louise, Retriever, Isa varieties were subjected to waterlogging (water 1 cm above soil level). Roots were collected at 0, 8 hrs, day 1, day 2, day 6 and day 7 after starting the waterlogging treatment. Average relative gene expression obtained for 2 root systems from individual plants are shown. Each root was considered one independent replicate. Error bars correspond to standard deviations. Data presented in (A) is for control plants and in (B) is for waterlogged samples. The classification as 'tolerant', 'sensitive' or 'intermediate' was based on the picture analyses presented above.

Because of varieties reached a peak of expression 1 day after the beginning of waterlogging, and there were clear differences between varieties at this particular time point, I decided to focus on the differences observed in the amplitude of gene activation at day 1 after waterlogging in independent sets of experiments that were conducted in the same conditions as above. To improve the relevance of the results, this time, roots from 3 independent plants were pooled together and considered as one replicate. I also conducted 3 independent experiments to be able to carry out a statistical analysis. Additional varieties were added to complement other experiments that were being conducted by our collaborators at Teagasc (S. Barth and T. Byrne).

I observed that some varieties had a higher amplitude for the expression of all the hypoxia response genes. For example, Regina and Pilastro had a higher induction for Hv*ADH1*, Hv*HB* and Hv*PDC1* expression compared with Passport, Retriever and Isa (FIGURE 3.28B). Varieties such as Siberia, Dura, Vesuvius and Mahogany expressed at higher levels genes related to fermentative pathway (Hv*ADH1* and Hv*PDC1*), but not Hv*HB* (FIGURE 3.28B). Even in the untreated samples (FIGURE 3.28A), there were some differences in the level of expression between the varieties for Hv*ADH1*, Hv*HB* and Hv*PDC1*. For example, Pilastro had a higher level of expression for all 3 genes in control conditions, compared to Louise, Retriever and Passport, all of which had a lower level of expression for Hv*ADH1*, Hv*HB* and Hv*PDC1*. It is possible that some varieties have a higher level of expression for Hv*ADH1*, Hv*HB* and Hv*PDC1* before waterlogging is applied and this might play a role in their tolerance to waterlogging. A more detailed analysis will be required in order to conclude this.

In sum, the expression of hypoxia-response genes in the different barley varieties is different depending on the varieties. However, this is not sufficient to conclude if a variety is more tolerant or not to the stress, so this gene expression analysis was complemented with a more thorough phenotypic characterization of the selected varieties during waterlogging, but also during a recovery period of 6 weeks. The varieties were selected together with our collaborators (S. Barth and T. Byrne), so that our data would complement their analyses as well. For all experiments described below, I focused on the following 8 varieties: Cavalier, Dura, Golden promise, Infinity, Isa, Passport, Pilastro, Siberia.

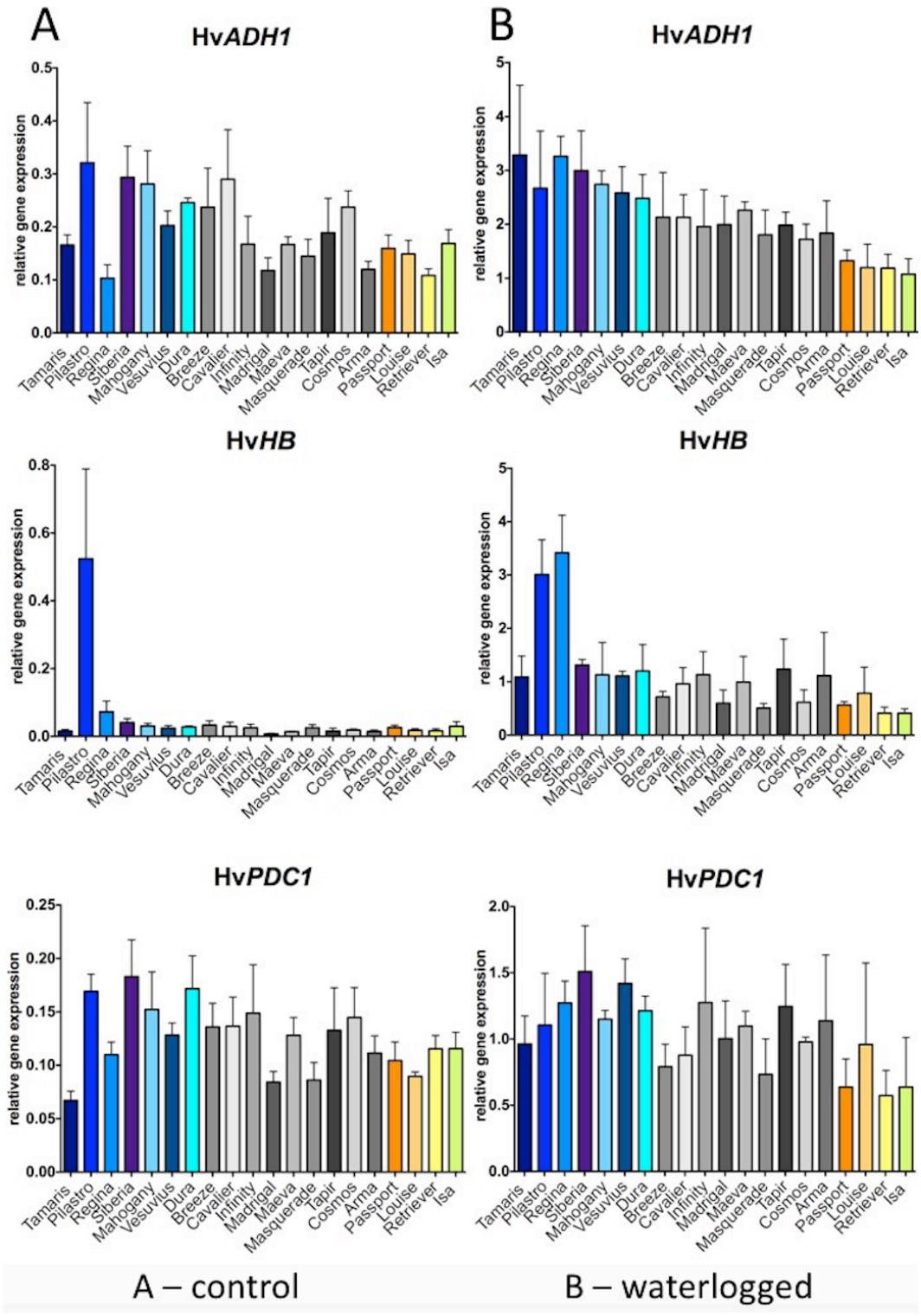

FIGURE 3.28. Differences in hypoxia-response gene expression 1 day after the beginning of waterlogging. Using Hv*ACTIN* as a reference gene, the relative gene expression of 3 hypoxia-response genes in roots of untreated and waterlogged plants was calculated. At the L1 stage, barley seedlings of the Tamaris, Pilastro, Regina, Siberia, Mahogany, Vesuvius, Dura, Breeze, Cavalier, Infinity, Madrigal, Maeva,

Masquerade, Tapir, Cosmos, Arma, Passport, Louise, Retriever, Isa varieties were subjected to waterlogging (water 1 cm above soil level). Roots were collected at day 1 after starting the waterlogging treatment. For each experiment, roots from 3 individual plants were pooled together. Average relative gene expression obtained from 3 independent experiments are shown. Error bars correspond to standard deviations. Data presented in A is for control and in B is for waterlogged samples.

3.3.2. Measurement of chlorophyll content

In order to quantify more accurately changes in chlorophyll content, I also used a SPAD chlorophyll meter, which measures the chlorophyll content and can detect and quantify small changes in plant colour before they are visible to the eye. This complements the chlorophyll measurements based on acetone extraction. At the L1 developmental stage, pots were transferred to a plastic tub filled with tap water, so that water level was up to 1 cm above soil level. The plants were waterlogged for 15 days. The SPAD parameter was measured on the L1 leaf every 5 days during the waterlogging treatment (day 0, day 5, day 10 and day 15). Given the fact that the SPAD measurements do not affect the plants, the same leaf could be assessed at each of the time points. The analysis was done on 3 independent replicates. For each replicate, the measurements were done on the L1 leaves of 4 different plants *per* variety. Although the SPAD values changed over the course of the experiment, perhaps due to developmental effects, there were no significant differences (threshold p-value: 0.05) between waterlogged and control plants for each variety (FIGURE 3.29).

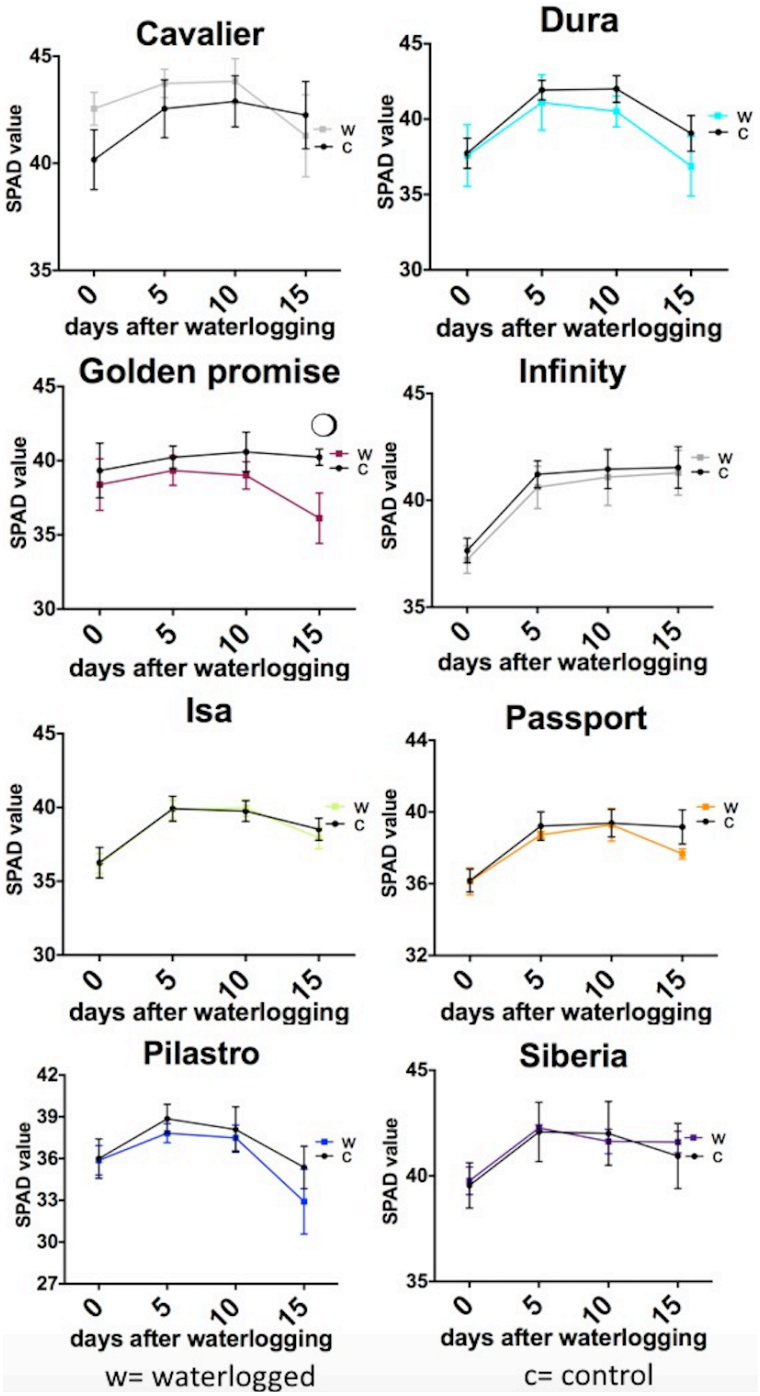

FIGURE 3.29. Results of SPAD measurements. At the L1 stage, barley seedlings were subjected to waterlogging (water 1 cm above soil level) for 15 days. The SPAD value was measured every 5 days during waterlogging (day 0, day 5, day 10, day 15). Three independent experiments were performed and for each experiment the SPAD values of the L1 leaf were measured for 4 plants/variety. The average SPAD values are presented. Error bars correspond to standard error of the mean. Note that the small difference observed between the control and waterlogged samples for Golden promise

is not statistically significant (p-value: 0.082). An open circle indicates values for which a p-value close to 0.05 was obtained, suggesting that the differences observed might be significant, but that additional replicates are required.

To complement the measurements made with the SPAD meter, and to score a potential chlorosis, I also measured the chlorophyll content of L1 leaves at day 15 of the waterlogging treatment. Importantly, the same plants on which SPAD measurements had been done were used for chlorophyll extraction. More specifically, at the end of the waterlogging (day 15), the tip of each L1 was cut and then 5 mg were weighted (the tip was taken as this is where the first signs of chlorosis typically appear). Chlorophyll a, chlorophyll b and total carotenoid content (see Section 2.1.3.8) were measured based on the absorbance at 646 nm (A_{646}), 663 nm (A_{663}) and 470 nm (A_{470}), respectively (Sumanta *et al.*, 2014). As observed in FIGURE 3.30, the chlorophyll a and total carotenoid contents were not affected by the waterlogging treatment in any of the varieties tested. For chlorophyll b, the only variety that showed a lower content at 15 days of waterlogging was Dura.

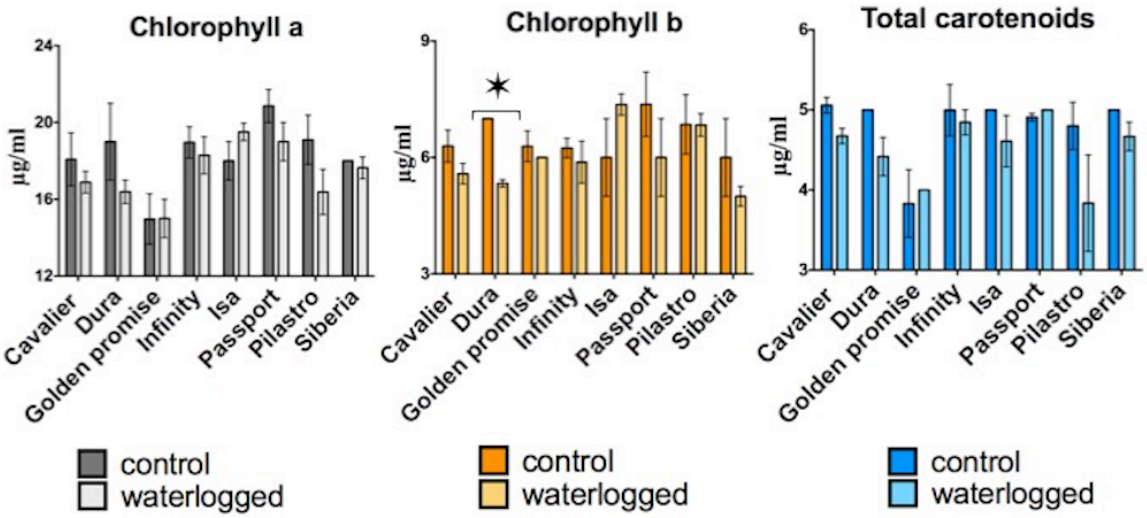

FIGURE 3.30. Measurement of photosynthetic pigments in control and waterlogged barley varieties. Plants on which SPAD values were measured were also used for photosynthetic pigment extraction in 80% acetone (v/v) from the leaf L1. Three independent experiments were performed and for each experiment 4 L1 leaves were used for pigment extraction. Error bars correspond to standard error of the mean. Student's t-test was performed to test statistical significance. Black star indicates statistically significant differences ($p < 0.05$).

3.3.3. Assessment of the vegetative organs upon waterlogging treatment

It is known that waterlogging stress affects plant growth, including height, tiller numbers and general health. Here, I measured these different parameters for the 8 selected varieties after waterlogging treatment and in control conditions. At the L1 stage, pots were transferred to a plastic tub filled with tap water, so that water level was up to 1 cm above soil level. After 15 days of waterlogging treatment, the plants were kept for a recovery period of 6 weeks with a normal watering regime.

- **Effect of waterlogging on plant height**

The total length of the plant from base of the stem to the tip of the longest leaf was measured every 3 days during the waterlogging treatment (day 0, day 3, day 6, day 9, day 12, day 15) and every 2 weeks during recovery period (day 29, day 43, day 57). During the waterlogging treatment none of the varieties showed any decrease in height, compared with their respective control plants (FIGURE 3.31). During the recovery period, Infinity, Isa and Siberia showed a significant decrease in height at day 57 (corresponding to 6 weeks of recovery) compared to the control. Interestingly, Passport was the only variety that showed differences in the height at day 43, but this was not statistically significant ($p > 0.05$). However, given the fact that the p-value is so close to the threshold ($p=0.06$), more replicates are required to check if there is really a difference or not.

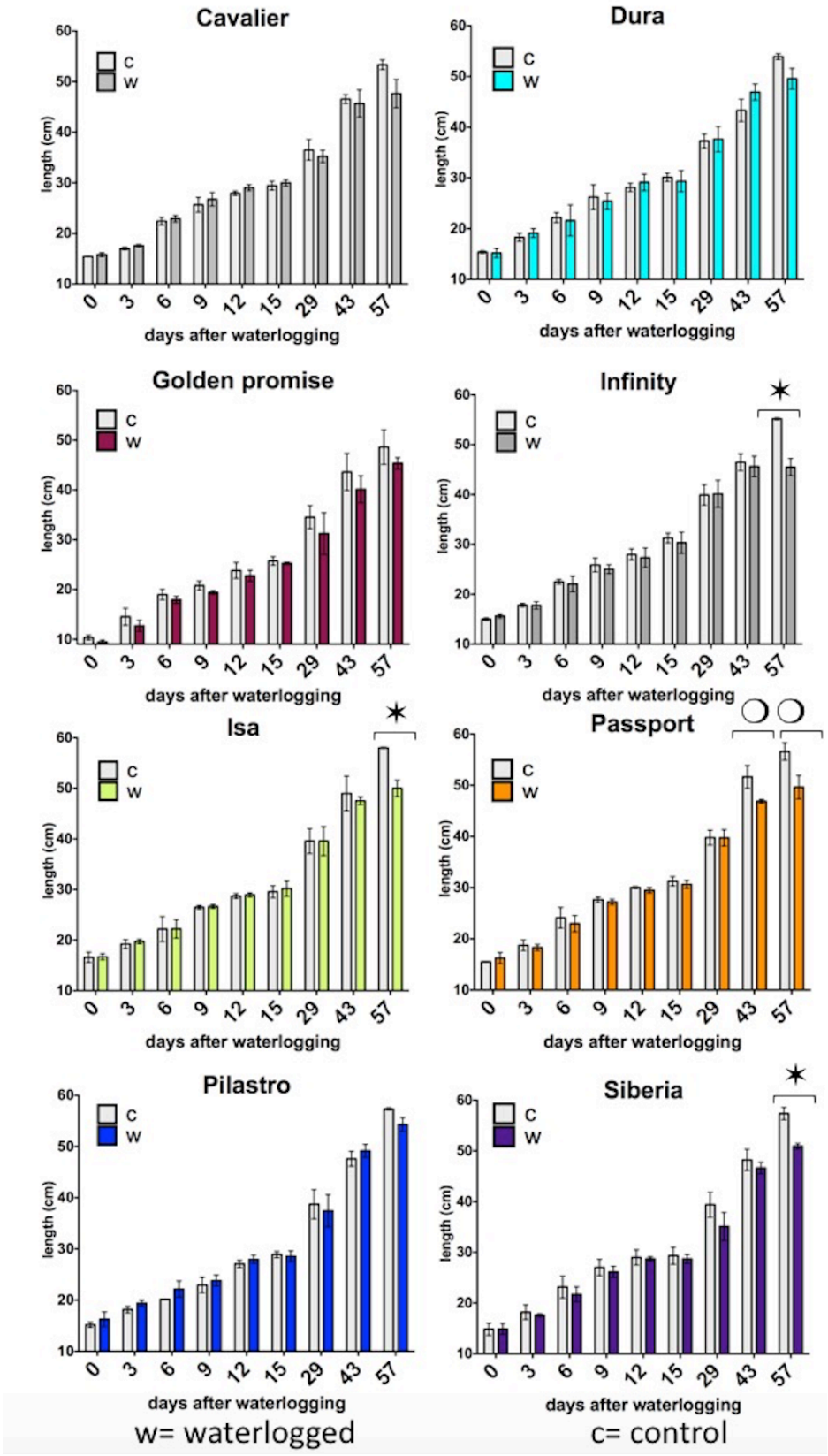

FIGURE 3.31. Height measurements during and after waterlogging. At the L1 stage, seedlings were subjected to waterlogging (water 1 cm above soil level). Height was measured every 3 days during the waterlogging (day 0, day 3, day 6, day 9, day

12, day 15) and every 2 weeks during recovery period (day 29, day 43, day 57). Three independent experiments were performed and for each experiment 4 plants per variety were scored. Error bars correspond to standard error of the mean. Note: for the statistical analysis if the calculated p-value is smaller than 0.05, this is indicated with a black star; an open circle indicates values for which a p-value close to 0.05 was obtained, suggesting that the differences observed might be significant, but that additional replicates are required.

- **Analysis of tiller numbers in waterlogged plants**

Another parameter that I was interested in analyzing in response to waterlogging was the number of tillers (FIGURE 3.32), as this is important for yield. In addition, it is known that due to a decrease in available nutrients, the number of tillers can be negatively affected by waterlogging. To measure the number of tillers, I used the same plants used to measure height. More specifically, the number of tillers was assessed every 2 weeks, starting at day 15 of the experiment, which corresponded with the beginning of the recovery period. During waterlogging treatment, this parameter was not measured because the seedlings were too young and had only one tiller.

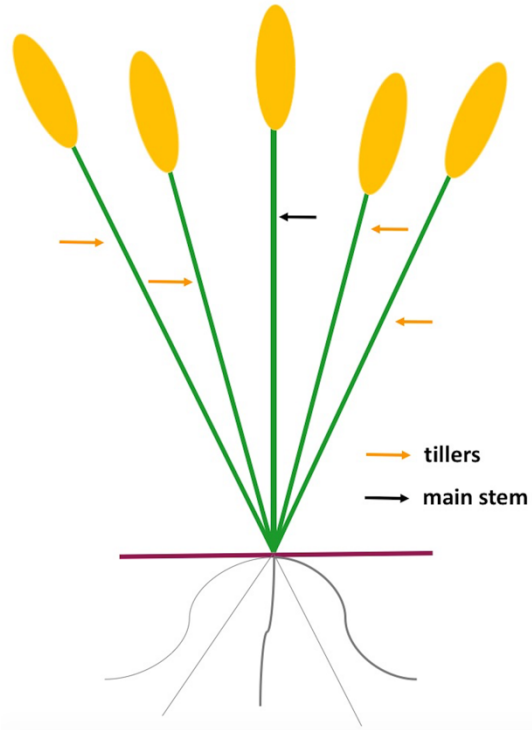

FIGURE 3.32. Schematic representation of a barley plant. Each barley plant posseses a main stem, indicated by a black arrow and several tillers that are shown using orange arrows.

Based on this experiment, differences in tiller number only appeared 6 weeks after the beginning of the recovery period. Not all varieties were affected equally though, so that Golden promise and Siberia showed a small decrease in the number of tillers at 6 weeks, which was however not statistically significant. Additional replicates are required to analyze this more carefully and check if the differences are indeed significant. For Dura, Cavalier, Infinity and Pilastro, a significant decrease in the number of tillers in response to waterlogging was observed (FIGURE 3.33).

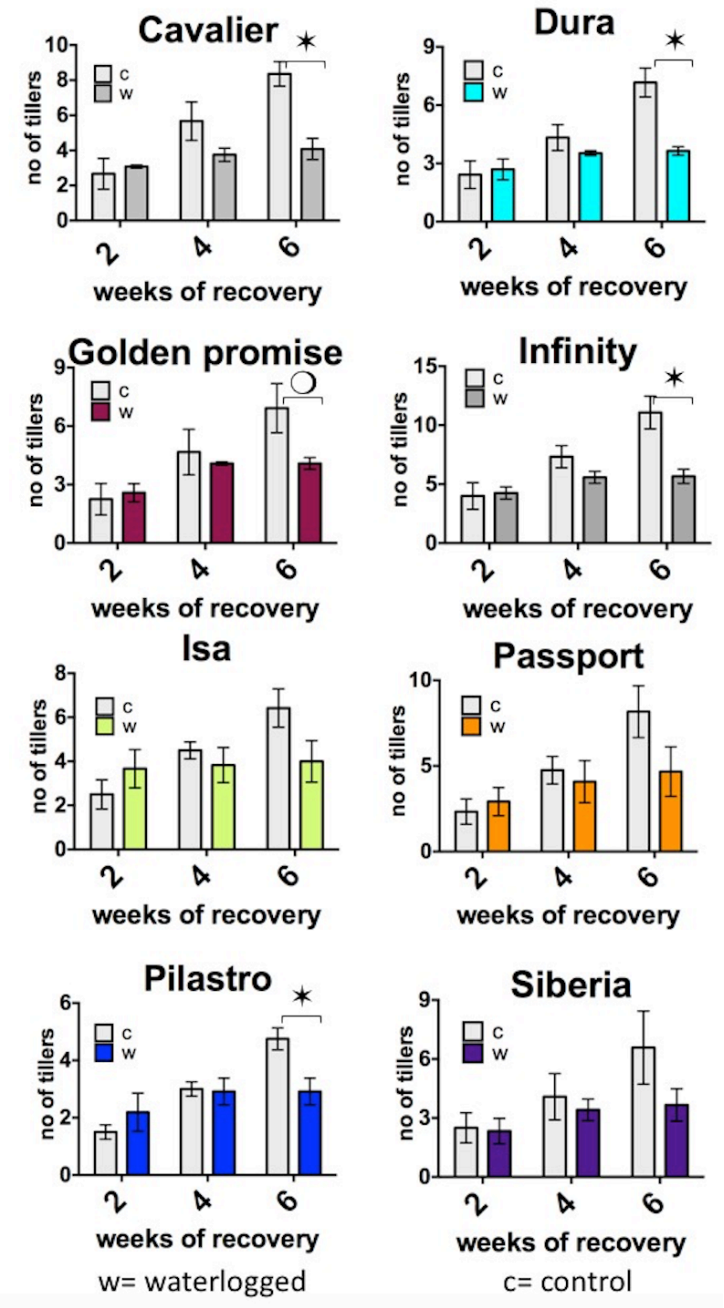

FIGURE 3.33. Tiller number measurement in control and waterlogged barley varieties. The number of tillers was counted every 2 weeks during recovery period (here, week 2 corresponds to day 29 from the beginning of the waterlogging treatment, weeks 4 and correspond to days 43 and 57). Three independent experiments were performed and for each experiment 4 plants were measured. The average number of tillers obtained from 3 independent experiments are shown. Error bars correspond to standard error of the mean. Note: for the statistical analysis if the calculated p-value is smaller than 0.05, this is indicated with a black star; an open circle indicates values for which a p-value close to 0.05 was obtained, suggesting that

the differences observed might be significant, but that additional replicates are required.

- **Overall health of the plants**

In order to complement all the parameters quantified above, pictures of control and waterlogged plants were also taken to compare the varieties. The same plants as those used for tiller counts and height measurements were used. All the symptoms were obvious at 6 weeks of recovery only (FIGURE 3.34), which is in agreement with the results presented in FIGURES 3.31 and 3.33.

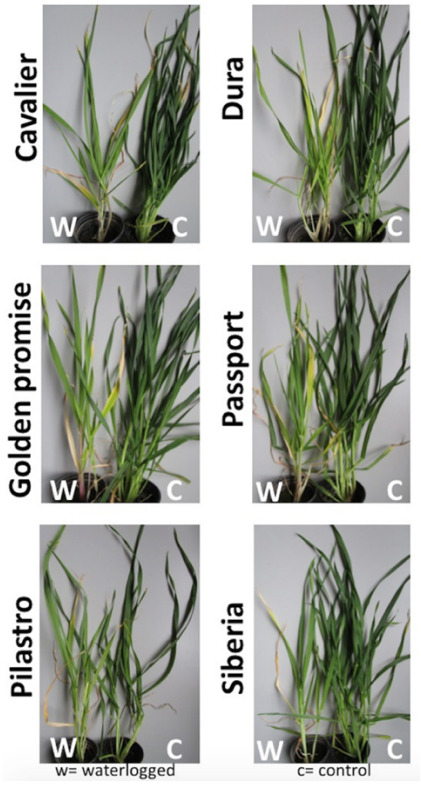

FIGURE 3.34. Pictures of representative plants after a 6-week recovery period. Pictures were taken after a 6-week recovery period after waterlogging was applied for 15 days, starting at the L1 stage. Three independent experiments were performed with similar results. Representative pictures from one replicate are shown.

Also, at this stage (i.e. after 6 weeks of recovery), leaves from plants that were waterlogged showed clear symptoms of chlorosis. In the future, I will hence also measure chlorophyll content at this time point, rather than at the end of the waterlogging treatment. Based on the pictures in FIGURE 3.34, some varieties appear to be more severely affected by waterlogging more than others, so that these pictures

may also be good general indicators of the general health (leaf chlorosis and necrosis, height, number of tillers) of the plants after a recovery period. However, it is very hard to classify the varieties based only on this information, as it is not quantitative.

- **Summary of the main results**

All the parameters characterized above, from chlorophyll content, SPAD value and general growth of vegetative organs such as height and number of tillers are indicators of general health (Huang *et al*., 2014; Ren *et al*., 2016; Wang *et al*., 2017). Except for the SPAD values and the measurement of photosynthetic pigments using acetone extraction, the varieties were affected by the waterlogging treatment in a manner that is consistent with the literature (i.e. reduced growth, up-regulation of hypoxia response genes). This suggests that it may be possible to use these different parameters (with the exception of the photosynthetic pigment measurements) to determine with sufficient accuracy, using controlled conditions, whether a variety is either tolerant or sensitive to waterlogging stress. However, a more thorough cross-comparison is needed for this, which I did not have time to conduct at this stage. This is discussed in more detail in Section 3.5.

3.3.4. Characterization of root architecture in response to waterlogging

The changes observed in the root architecture in response to waterlogging seem to play an important role for plant survival upon waterlogging stress (see Section 1.1.2.2.). When collecting root samples for RNA extraction, I observed that in the waterlogged-treated samples, for some varieties, the length of primary root was negatively affected. Also, I observed that in waterlogged conditions some varieties formed more and longer seminal roots compared to control plants. Based on these qualitative observations, I decided to quantify these different root phenotypes to determine if there was a correlation between the elongation of the primary root and the development of seminal roots. Indeed, based on my initial observations, waterlogged plants seemed to allocate resources into developing seminal roots rather than primary root elongation. In order to answer this question, I conducted another waterlogging experiment using the same conditions as above. At the end of the waterlogging period (day 15), the length of the primary root was measured. In addition, I counted the number of seminal roots and measured the length of the longest seminal root. For each biological replicate (2 in total), the measurements were done on roots from 4 plants. Also, the first cm of the longest seminal root (considered to be the first seminal root formed) was collected and fixed in formaldehyde and embedded in paraplast (see Section 2.1.3.7) for aerenchyma characterization. Due to time constraints, the tissue has not yet been analyzed.

As observed in FIGURE 3.35A, elongation of the primary root is severely affected upon waterlogging, with Cavalier, Dura, Golden promise, Infinity, Isa and Pilastro being more severely affected. Passport and Siberia shows a reduction in the length of the primary root in response to waterlogging, but this is not statistically significant.

The length of the seminal root is positively affected by the waterlogging treatment in all the varieties, except Infinity. For Infinity, the length of the seminal root is almost the same in waterlogged compared with control conditions. (FIGURE 3.35B). Based on FIGURE 3.35C, there seems to be an increase in the number of seminal roots in response to waterlogging in all varieties, except Golden promise. When a t-test was performed, the p-value for the differences observed in Cavalier,

Isa, Pilastro and Siberia was very close to p=0.05. Additional replicates are needed to draw conclusions.

In contrast to the primary root, the length of the seminal root is positively affected by the waterlogging in all varieties, except Infinity. It appears as if the plant was switching from 'primary root elongation' to a 'seminal root elongation' program, in response to waterlogging.

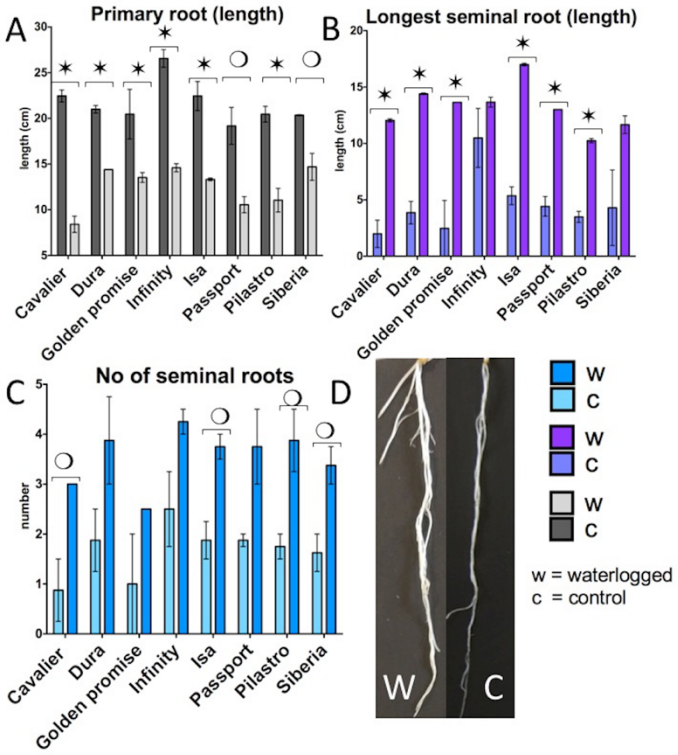

FIGURE 3.35. Overview of root architecture in control and waterlogged barley. At the end of the waterlogging treatment, at day 15, the plants were removed from pots and the root system was gently washed with tap water to remove the soil. A- Measurements of the primary root length in control and waterlogged barley; B- The length of the longest seminal root in control and waterlogged barley; C- The number of seminal roots in control and waterlogged barley; D-Control and waterlogged barley roots (Isa); Two independent experiments were performed and for each experiment 4 plants were measured. Means of length (A and B) or numbers (C) obtained from 2 independent experiments are shown. Error bars correspond to standard error of the mean. Note: for the statistical analysis if the calculated p-value is smaller than 0.05, this is indicated with a black star; an open circle indicates values for which a p-value

close to 0.05 was obtained, suggesting that the differences observed might be significant, but that additional replicates are required.

In sum, the architecture of the root system is clearly changing in response to waterlogging, with overall a reduction in the elongation of the primary root and instead am increased elongation of the seminal root. This seems to be a general mechanism (Dawood *et al*., 2014), that is observed in 7 out of 8 varieties analyzed. The energy investment in the seminal root elongation could provide some benefits. Indeed, seminal roots are able to reach faster an environment that contain more nutrients and is aerated (Dawood *et al*., 2014). In addition, in some varieties the number of seminal roots also increased in response to waterlogging, which could help to limit the negative effects of waterlogging. Based on these observations and on the known roles of roots during waterlogging (Section 1.1.2.2), varieties characterized by reduced length of primary root and increased length and number of seminal roots in waterlogged compared to control conditions, might be tolerant to waterlogging. The best varieties best on these parameters could be Cavalier, Isa, Pilastro and Siberia. This is discussed in more detail in Section 3.5.

3.4. Comparison of global gene expression changes in waterlogging sensitive and waterlogging tolerant varieties

Based on the detailed characterization, I selected (i) one variety - Pilastro - that seemed to have the expected characteristics of a tolerant variety (see Discussion) and (ii) another variety that seemed to perform less well (Passport). On purpose, I chose two 6-row varieties, (instead of a 6-row and a 2-row variety) to facilitate downstream analyses. I also included Golden Promise, as this is a 'model' variety that is used for transformation and in which we aimed at generating mutants (see Chapter 4). Based on our characterization, Golden Promise would be considered as waterlogging sensitive. Using these varieties, I monitored genome-wide gene expression changes in plants grown in control and waterlogged conditions, with the aim of comparing gene expression differences within a given variety, but also across a tolerant and a sensitive variety. Because the datasets were obtained at the very end

of my PhD, I did not have sufficient time to conduct a detailed analysis. Instead, I am presenting a basic general analysis of the different datasets.

For the transcriptomics analysis, I repeated the waterlogging treatments at the L1 stage as described above and collected the roots at day 1 after the beginning of the waterlogging treatment. For each variety and condition (control and waterlogged), 3 biological replicates were collected and sent to BGI for RNA Sequencing (RNA-seq). The initial bioinformatics analysis, including the determination of differentially expressed genes (DEGs) in waterlogged compared to control samples (for a given variety) was conducted by BGI, with the following thresholds: $|\log_2 (\text{fold change})| > 1.0$ and q-value < 0.001.

First, I determined the number of DEGs that were up- or down-regulated in each of the varieties (FIGURE 3.36). Overall, the number of DEGs is lower in Golden Promise (1105 DEGs), compared to Passport (1762 DEGs) and Pilastro (1854 DEGs). Another observation based on FIGURE 3.35 is that in Golden Promise and Passport, there are more up-regulated genes, 697 and 1055 respectively, compared to the number of down-regulated genes, 408 and 799, respectively. In contrast, in Pilastro, there are more down-regulated genes (921) compared to the number of up-regulated ones (841).

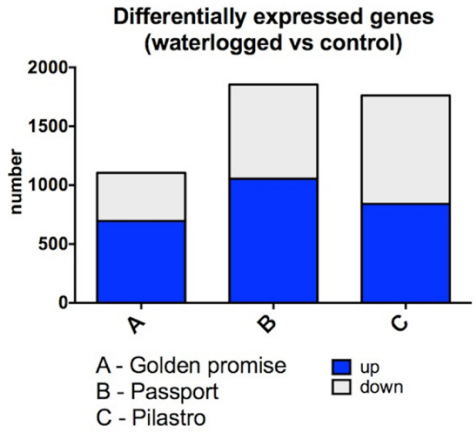

FIGURE 3.36. Differentially expressed genes in waterlogged versus control samples. The list with all the DEG in waterlogged versus control conditions was provided for Golden promise, Passport and Pilastro by BGI. The numbers of up (blue) and down-regulated (grey) genes for each variety were plotted in the above graph.

In order to analyze more in detail the differences and similarities among the 3 datasets obtained, I conducted an overlap analysis using the BioVenn software (http://www.biovenn.nl/). As indicated in FIGURE 3.37, there are 307 DEG that are common for Golden promise, Passport and Pilastro in waterlogged versus control samples. In addition, there are 390, 863 and 933 genes that respond specifically in Golden promise (yellow), Pilastro (blue) and Passport (orange), respectively. Also, a pairwise comparison suggests that some varieties tend to share more similarities in their transcriptional response to waterlogging. For example, Passport and Pilastro have an overlap of 706 DEGs, whereas Golden promise and Pilastro have in common 522 DEGs and Golden promise and Pilastro only 500 DEGs. This can be due to the fact that Passport and Pilastro are more recent and are winter barley varieties, whereas Golden Promise is an older commercial variety and is also a spring variety.

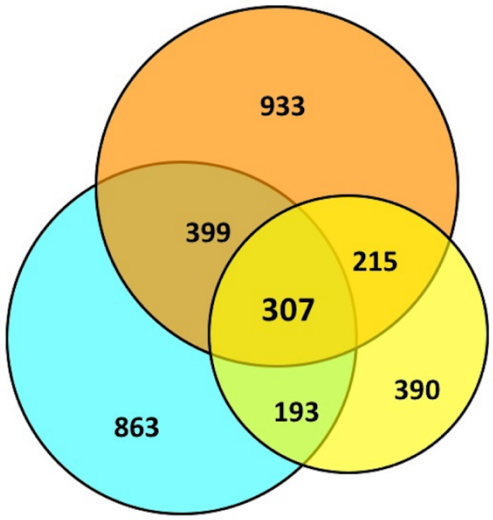

FIGURE 3.37. Overlap analysis of all DEGs in waterlogged versus control samples in Golden promise, Passport and Pilastro. Using BioVenn analysis tool, the overlap of all DEG between Golden promise (yellow), Passport (orange) and Pilastro (blue) in waterlogged versus control samples was generated.

In order to validate the results, I checked if in the 307 DEG that overlap between the 3 varieties, the hypoxia-core genes were present and up-regulated. As expected, Hv*ADH1*, Hv*HB*, Hv*PDC*, Hv*LDH*, Hv*SUS4* and genes that encode ERF transcriptional factors were part of the common 307 DEG and were all up-regulated.

This is in agreement with the previous RT-qPCR results (FIGURE 3.28) and the literature (Mustroph *et al*., 2009; Mendiondo *et al*., 2016).

Next, I used Gene Ontology (GO; pantherdb.org) analysis to identify biological processes that are over-represented in the datasets. The GO analysis was first conducted using the 307 DEGs that are common to Golden Promise, Passport and Pilastro (FIGURE 3.37.). As expected, the main GO categories that were affected in all 3 varieties were represented by cellular response to oxygen-containing compound (FIGURE 3.38., light blue), response to oxygen-containing compound (FIGURE 3.38., dark blue), cellular catabolic process (FIGURE 3.38., orange). Other GO categories common to all 3 varieties were drug metabolic process (FIGURE 3.38., yellow), response to toxic substance (FIGURE 3.38, green), small molecule metabolic process (FIGURE 3.38., pink), response to chemical (FIGURE 3.38., grey) and response to stimulus (FIGURE 3.38., purple), all of which would be expected to be affected upon waterlogging based on the literature.

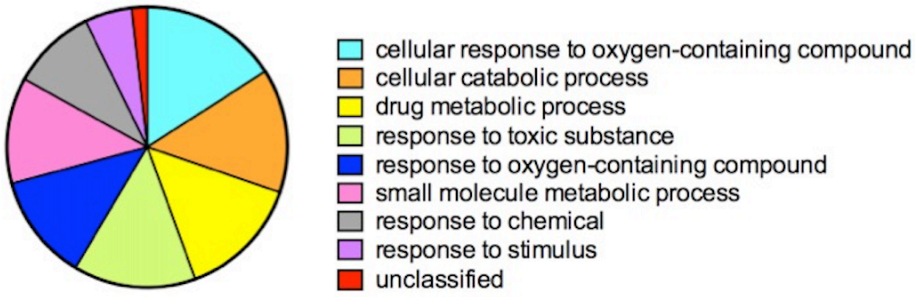

FIGURE 3.38. GO categories common to Golden promise, Passport and Pilastro. Using Pantherdb online tool, I performed the GO analysis on the 307 common DEGs between the 3 barley varieties. There are 8 GO categories affected by waterlogging.

After observing the biological processes affected by waterlogging treatment in all 3 varieties, I wanted to check what makes each variety unique in its behavior. In order to do so, I carried out a GO analysis with all the up and down-regulated genes for each variety. I observed that some GO categories are present in only one of the 3 varieties. In order to show the differences and similarities between the 3 datasets, I generated a heatmap using –log10 of the p-value for selected GO categories. The GO categories were selected based on their know role during hypoxia. As observed in FIGURE 3.39, some GO categories, such as cellular response to stimulus and

response to toxic substance are similarly affected by waterlogging in all 3 varieties, suggesting that these processes are likely characteristic for waterlogging response in general. Interestingly, the response to oxygen-containing compound category had a more strongly enriched in Pilastro (a tolerant variety based on my characterization) than in Passport (a predicted sensitive variety). Some GO categories are in fact specific to Pilastro (e.g. cellular response to nitrogen compound, sterol metabolic process, glutathione metabolic process, RNA metabolic process, nucleic acid metabolic process and non coding (nc) RNA metabolic process). However, additional analyses will be needed if this is sufficient to explain the apparent waterlogging tolerance phenotype of this variety.

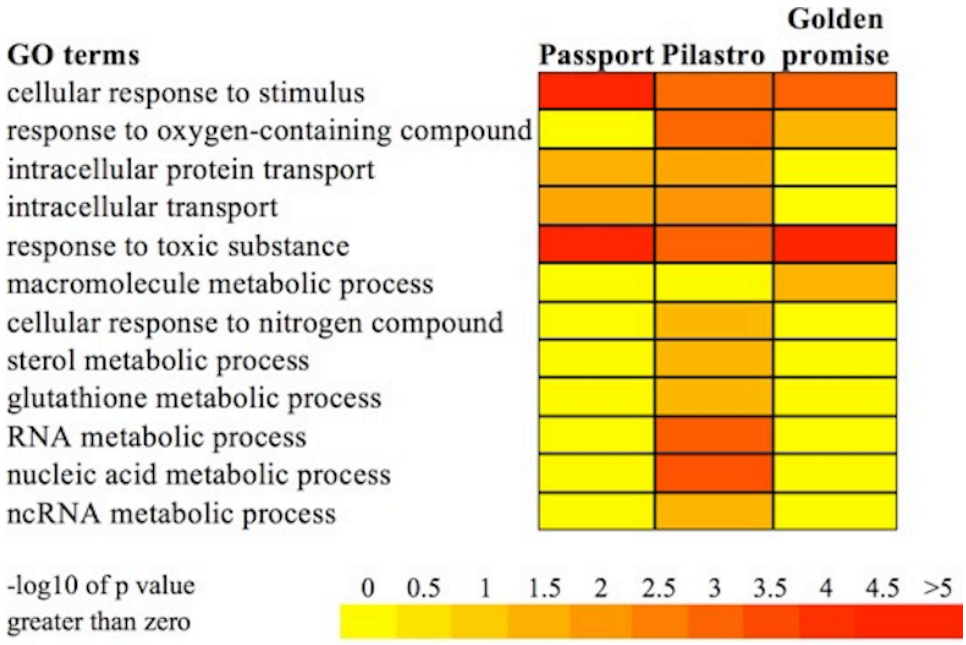

FIGURE 3.39. Heatmap of GO categories that are common to Golden promise, Passport and Pilastro in response to waterlogging. The overlap of GO categories that are present in all 3 barley varieties was generated using Pantherdb.org online tool. The p-values specific for each GO category were provided by Panterdb.org as well. I calculated –log10 of p-value and I used this to generate the heatmap, using bar.utoronto.ca online tool. The significance of their over-representation is shown as a color code from 0 (yellow; GO category not present) to 5 (red).

Further, I focused on 5 GO categories that seemed to be important for the plant response to waterlogging and were either present in all 3 varieties or specific to one

variety: response to oxygen-containing compound, intracellular protein transport, response to toxic substance, glutathione metabolic process, RNA metabolic process.

In order to see which biological processes are activated and which are repressed in response to waterlogging, I retrieved the genes specific for each GO category from Pantherdb results and I checked in the datasets how many genes were up and down-regulated. Due to time constraints, I focused on Pilastro at this stage because all GO categories were enriched among the list of DEGs for this variety (FIGURE 3.40). As expected, genes belonging to the 'response to oxygen-containing compound' category were mostly up-regulated (FIGURE 3.40). A similar observation was made for 'glutathione metabolic process', which is also epected considering the central role of glutathione in the regulation of NO and ROS signaling. Furthermore, genes associated with 'intracellular protein transport' (FIGURE 3.40) were mostly up-regulated, suggesting that in response to waterlogging, intracellular protein trafficking may be activated. Interestingly, genes associated with 'response to toxic substance' and 'RNA metabolic process' the majority of DEGs in Pilastro were down-regulated upon waterlogging. For the latter though, given the small number of DEGs, it is difficult to draw a conclusion. In fact, it is surprising that this category was identified as over-represented in the GO analysis, so that it needs to be examined more carefully in the coming months.

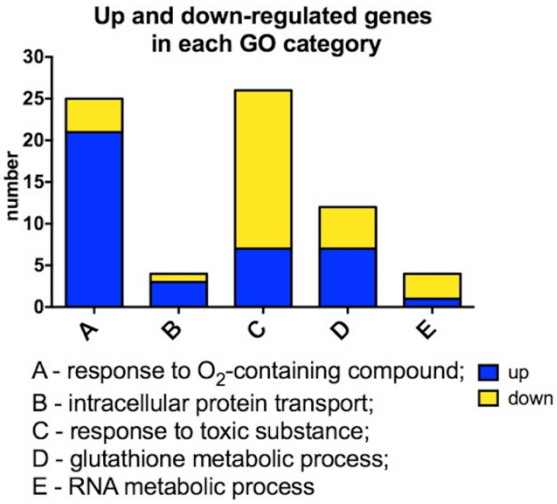

FIGURE 3.40. Number up and down-regulated genes in selected GO categories in Pilastro. Five GO categories were selected. The genes specific for each category were retrieved from Pantherdb online tool.

In conclusion, based on a limited analysis of the RNA-Seq datasets, there are clearly differences in the number of DEGs between Passport, Pilastro and Golden promise and in the nature of the processes that are regulated in the 3 varieties. However, a more detailed analysis is necessary to determine if there are differences in Pilastro, a presumed tolerant variety, that could explain its potential tolerance to waterlogging, compared to Passport and Golden Promise.

3.5 Discussion

In the course of my PhD project, I characterized the response to waterlogging of a subset of varieties from the AGOUEB collection. In doing so, I also established different approaches that we can combine to assess more accurately waterlogging tolerance in barley. However, for these results to be meaningful and genuinely allow a clear classification of barley varieties as tolerant or susceptible, it would be important to consider the different traits and criteria considered to assess their predictive potential. Because most of the replicates were completed at the very end of my PhD, I did not have sufficient time to do this in a quantitative manner. Instead, I will discuss the qualitative value of the different traits and criteria considered for the selection of waterlogging tolerant barley varieties.

- **Selection of traits that can be monitored to determine waterlogging tolerance/sensitivity in controlled conditions**

In general, for the efficiency of the selection process, it would be best if the traits considered can be scored at early stages of development, as long as they remain predictive of the later behavior of the variety (i.e. during or after the recovery period). This alone may not be a simple criterion, as it is clear that some plants may show important waterlogging-related stress symptoms immediately after the treatment and end up recovering well afterwards. This can only be assessed accurately which a much larger number of varieties assessed for all traits and following a rigorous statistical analysis for correlation. Based on the results presented, it seems that it would be best not to exclude one particular trait or parameter, but instead to integrate them to increase the selection efficiency. Furthermore, while from a biological point of view all aspects are relevant to understand how barley responds and adapts to waterlogging, from an economical/agronomical perspective yield and grain quality are clearly more important. This includes for example the number of tillers formed by a single plant. Because of their importance, they should probably be considered more carefully.

The approach that could offer the earliest assessment for waterlogging tolerance/sensitivity is the assessment of hypoxia-response gene induction. The latter provides data very quickly after the beginning of the treatment. However, it is unclear

at this stage if this has sufficient predictive value for yield at the very end of the plant's lifecycle. The second earliest trait that can be assessed are the SPAD values and photosynthetic pigments content. However, with the protocol I developed, there was not sufficient variation between waterlogged and control plants to use these measurements. As a consequence, this parameter will no longer be considered. Third, root anatomical and root structure traits can be scored. While these are destructive methods, they are quantitative. The only root trait for which there seemed to be variation between varieties was the number of seminal roots formed. It would now be interesting to conduct similar experiments with a larger number of varieties to test accurately a possible correlation between, for example, the inhibition of primary root elongation or the formation of seminal roots and yield. Finally, at a later stage of development, during the recovery period, agronomical traits can be assessed. Traits such as height and the number of tillers show some clear differences between waterlogged and control plants, and there is also some variation across the different varieties used, suggesting that this may be interesting to use in the classification of waterlogging tolerance or sensitivity.

In sum, besides the chlorophyll and SPAD measurements and some of the measurements done for root lengths, the other parameters and traits could be suitable to assess waterlogging tolerance in barley. In the coming months, I hope to use the data obtained to make cross-comparisons and see which parameters have the best predictive value. However, to do so properly would require data with a much larger number of varieties.

- **Selection of waterlogging tolerant/sensitive varieties**

Based on the data obtained, I attempted to classify varieties as either tolerant or sensitive. However, at this stage this is difficult to do, as baselines and thresholds still need to be defined. I did not have sufficient time to do so at this stage. Nevertheless, based on what is known on traits that would be expected to correlate with improved waterlogging tolerant, I attempted to classify the varieties (Table 3.1). The parameters included:

- higher expression of hypoxia-response genes (higher expression for at least 2 of the 3 genes tested was considered as being possibly linked with tolerance)

- a higher number of seminal roots in waterlogged compared to control plants (tolerance arbitrarily defined as twice as many seminal roots in waterlogged compared to control samples)

- maintenance of plant height in waterlogged compared to control plants, with more than 50% shoot elongation defect being considered as having a negative impact (i.e. sensitivity)

- higher number of tillers in waterlogged *versus* control plants

Table 3.1. Summary of the results based on the above-mentioned criteria. '-' indicates that the variety seems neither tolerant nor sensitive. 'S': variety considered as waterlogging sensitive. 'T' variety considered as waterlogging tolerant. Golden P.: Golden Promise

Variety	Gene expression	Height	Number of tillers	Number of seminal roots
Cavalier	-	-	S	T
Dura	T	-	S	S
Golden P.	S	-	T	S
Infinity	-	S	S	S
Isa	S	S	T	S
Passport	S	S	T	S
Pilastro	T	T	S	T
Siberia	T	S	T	S

Based on this simple analysis, it seems that not all traits and parameters are in agreement. Additional work, and especially more varieties, would need to be used in order to be able to define objective threshold values for each of the comparisons.

- **<u>Advantages and disadvantages of controlled waterlogging experiments compared to field experiments</u>**

The establishment of a waterlogging protocol in controlled conditions presents advantages compared to field experiments. While the latter are the best to truly assess the agronomic potential, they tend to be more variable, because crops can

be affected by different abiotic and biotic stresses within a single year. The addition of replicates over several years buffers these problems, but this takes a long time. Another problem we encountered was the difficulty to apply the stress in a homogenous manner. For example, some of the miniplots within a given replicate were waterlogged, while other were submerged. In the subsequent field trials that were conducted, the stress applied was more homogenous, as the plots were flattened and levelled slightly below the normal ground level to allow water to accumulate.

In contrast, the use of controlled conditions allowed to test specifically the effect of waterlogging on the barley plants, in the absence of other stresses. While this may not be comparable to field conditions, it would allow to study specifically the effects waterlogging stress on the different varieties tested. Another potential advantage of the controlled conditions, is that it is possible to conduct multiple replicates over a much shorter period of time, thus allowing for a faster analysis. If scoring at early developmental stages is also a good predictor of crop yield, this would constitute an additional benefit.

At this stage, with the data from only one field experiment, it is not possible to determine if (i) the field experiments are reproducible and (ii) the controlled and field experiments provide similar results.

- **Molecular mechanisms underlying waterlogging tolerance**

As part of my project, I also attempted to gain further insights into the molecular mechanisms that may contribute to tolerance or sensitivity to waterlogging. To this aim, I conducted a transcriptomics experiment with 1 presumed tolerant variety (Pilastro) and one presumed sensitive variety (Passport). Golden Promise was also included because it is a'model' variety that is more amenable to transformation. While a more detailed analysis of the results remained to be done, it appears that in the 3 varieties there are a number 'core' waterlogging response genes that are all regulated in response to the stress. Many of the expected hypoxia-response genes are present within these 'core' genes, which is a good validation for our datasets. It remains to be determined whether the gene expression changes are similar both in amplitude and directionality within this 'core' subset of DEGs.

There are also some clear differences between the 3 varieties tested. For example, the number of DEGs in response to waterlogging differs greatly, with

Golden Promise presenting fewer DEGs compared to Pilastro and Passport. In addition, among the list of DEGs in Pilastro, there are genes associated with GO categories that are not over-represented among the DEGs identified in Golden Promise or Passport. It will be interesting to analyze more in detail these particular genes to determine if these could be associated with processes that would confer an increased tolerance to Pilastro compared to Passport.

- **Conclusion**

Experiments with a larger number of varieties are needed in order to define the best parameters and traits that may be used to determine barley varieties that are either more tolerant or sensitive to waterlogging. However, it is likely that a combination of traits and parameters will be more powerful. Thresholds also need to be determined for a more objective classification.

It is also important to note that while in the last decades crop breeding has been focused on producing varieties with high yield, it is possible that this may have been done at the expense of resilience to adverse conditions in the field. Importantly too, while one may select varieties that are more tolerant to a particular stress such as waterlogging, it is also possible that this is done at the expense of tolerance to other abiotic and biotic stresses.

4. Isolation of barley mutants for Hv*ATE1*

4.1. Introduction

As indicated in Section 1.3.2, one of the aims of my PhD was not only to identify commercial varieties with improved waterlogging tolerance, but also to generate new barley germplasm that would have increased tolerance to this abiotic stress. To this aim, I focused on generating mutant plants in barley for an enzymatic component of the N-end rule pathway, the Arg-transferase (see Section 1.2.1.1).

Arginine tRNA transferases (ATEs) are conserved in eukaryotes, from yeast (Balzi *et al*., 1990) to mammals (Hu *et al*., 2005; Lee *et al*., 2005) and plants (Yoshida *et al*., 2002), but are not present in prokaryotes (Graciet *et al*., 2006). ATEs are part of the N-end rule pathway, in that they recognize secondary destabilizing residues and conjugate Arg, a primary destabilizing residue. Arg-transferases seemed to be a good candidate to improve waterlogging tolerance in barley, because they are essential to target for degradation the ERF VII transcription factors that act as master regulators of hypoxia response (see Section 1.2.1.1). In addition, in *Arabidopsis thaliana*, plants lacking Arg-transferase activity have been shown to be more tolerant to hypoxia. In the course of my PhD project, it was also shown that barley plants in which PRT6 activity was affected were also more tolerant to waterlogging (Mendiondo *et al*., 2016). Considering that PRT6 acts just downstream of the Arg-transferases, it is likely that our strategy could also result in barley germplasm with improved tolerance to waterlogging. In barley, there is only one ATE encoded in the genome, called Hv*ATE1*. The fact that there is only one gene coding for Arg-transferase may be an advantage over PRT6, of which there are 2 genes in the barley genome.

In order to isolate mutant plants for Hv*ATE1*, two strategies were used:

(i) screening an existing Targeting Induced Local Lesions in Genomes (TILLING) collection

(ii) generation of Clustered Regularly Interspaced Short Palindromic Repeats (CRISPR)/CRISPR associated protein 9 (Cas9) lines with a targeting construct for Hv*ATE1*.

4.2. Isolating Hv*ATE1* TILLING mutant alleles

In order to isolate TILLING mutants that carry mutations in Hv*ATE1*, a collaboration was established with Dr. Nils Stein, from the Leibniz Institute of Plant Genetics and Crop Plant Research (IPK, Germany). Indeed, his group has generated a TILLING collection in the Barke variety (two-row spring barley) (Gottwald *et al*., 2009; Mascher *et al*., 2014). I provided Dr. Nils Stein with a conserved region of Hv*ATE1*, in which we wished to identify TILLING mutations. His lab then used PCR-based approaches to screen the IPK TILLING collection and identify lines that carried mutations in Hv*ATE1*. This resulted in the identification of 10 different TILLING lines that should bear point mutations in Hv*ATE1*.

Based on the sequence files provided by Dr. Nils Stein, I generated alignments to determine which lines carried:

(i) a premature stop codon, which should result in an inactive enzyme (this was the preferred effect)

(ii) a point mutation in a conserved amino acid residue. The latter would be more likely to result in a loss or reduced Arg-transferase activity.

I focused my attention on lines with a missense mutation (lines number 4, 5, 6, 9 and 10). The details of these lines are presented in Table 4.1 below.

Table 4.1. Summary of the different TILLING lines isolated at the IPK. Lines I focused on are indicated in red. The position of the mutations, starting from the first base of the coding region are indicated. The reference number of the line in the IPK collection is also provided. Amino acid conservation based on alignments generated with other plant Arg-transferase protein sequences is indicated. Hom: homozygous; Het: heterozygous; Syn: synonymous; amino acid changes are indicated using single-letter amino acid abbreviations.

Number	M2 Family	Position from ATG in CDS	Mutation	Exon	State	Effect	Region is conserved
1	11684	500	G to A	yes	hom	S to N	*O. sativa*
2	4702	645	G to A	yes	hom	syn	*O. sativa*

3	13808	649	G to A	yes	het	G to R	*O. sativa*
4	4344	664	G to A	yes	hom	D to N	*O. sativa*
5	4670	725	C to T	yes	het?	P to L	*O. sativa* *S.cerevisiae*
6	6456	748	G to A	yes	het?	G to R	*M. musculus* *A. thaliana* *P. patens*
7	9761	847	C to T	yes	hom	syn	*O. sativa* *S. cerevisiae* *A. thaliana* *P. patens*
8	2460	862	G to A	yes	het?	A to T	not conserved
9	13885	1091	G to A	yes	het?	S to N	*O. sativa* *M. musculus* *A. thaliana* *P. patens*
10	10779	1199	G to A	yes	hom?	R to K	*O. sativa* *A. thaliana* *P. patens*

4.2.1. Designing dCAPS genotyping assays to isolate plants with point mutations in Hv*ATE1*

In order to isolate Hv*ATE1* mutants from TILLING lines 4, 5, 6, 9 and 10, 6-8 seeds were sown per line. Few seeds were sown because in average about 10-12 seeds for each line were. Plants were grown in John Innes No. 2, as described in Section 2.1.3.1. The plants were kept in the dark for 10 d at 4ºC before being moved to the plant room, where they were grown under long-day conditions (16 hrs light/8

hrs dark) at 15°C. Barley leaves were collected and DNA was extracted as described in Section 2.2.3.4.

In order to check the presence of the mutations in Hv*ATE1*, the TILLING lines carrying point mutations in Hv*ATE1* were genotyped using the dCAPS method, as described in section 2.1.2.4. For all TILLING lines, a first PCR was performed with primers AM103 and AM104 using genomic DNA of the line of interest as a template. This resulted in a product of ~1.2 kb that contained the region with the expected mutations. A second PCR reaction was carried out using this first product as a template and different sets of primers depending on the line being genotyped. The resulting products were then digested with different restriction enzymes to determine the presence (or absence) of the expected point mutation.

- **TILLING line 4**

For TILLING line 4, the second PCR was performed using primers AM88 and AM89, which resulted in a 225 bp PCR fragment. After digestion of the PCR fragment with *Xba*I for 2 hrs, 2 fragments were anticipated for the wild-type sequence (201 bp and 24 bp), while a 225 bp uncut fragment was expected for the mutant allele. As shown in FIGURE 4.1, a single band at ~ 225 bp was obtained for the 6 plants I genotyped, suggesting that the 6 plants were homozygous for the wild-type allele of Hv*ATE1*, or that longer digestion times would be needed for genotyping.

In order to confirm this result, I carried out a PCR reaction with primers AM103 and AM104 on genomic DNA from plants 1 and 3 as a template. I then sent the PCR product for Sanger sequencing with primer AM103. Contrary to the results obtained with the dCAPS approach, plants 1 and 3 carried the expected homozygous mutation in Hv*ATE1*. This suggest that the *Xba*I digestion did not work properly and that the protocol would need to be optimized.

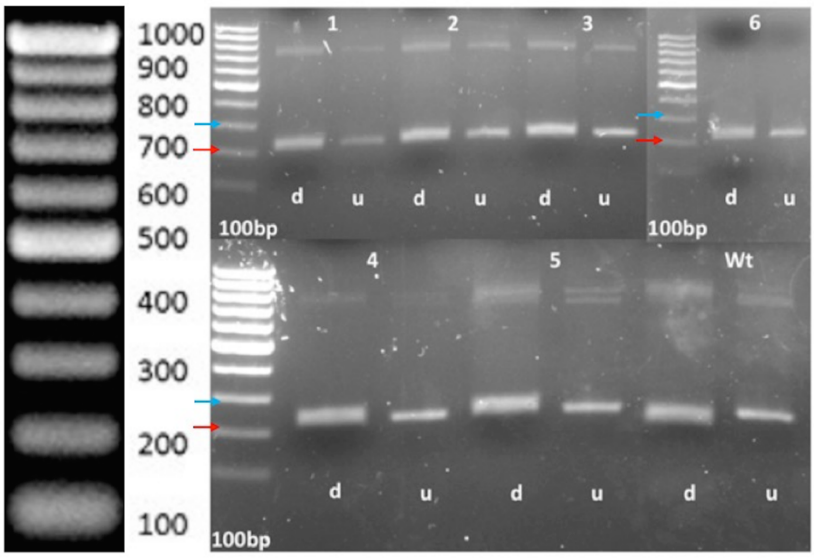

FIGURE 4.1. dCAPS genotyping of TILLING line 4. Using the dCAPS method, 6 plants from TILLING line 4 were genotyped. Genomic DNA from a wild-type Tesla plant was used as a control as seeds from wild-type Barke were not available in the lab at that time. Leaves from ~3 week-old plants were collected and the DNA was extracted. Following two sets of PCRs and *Xba*I digestion, the samples were analyzed on a 2% agarose gel. Plants from TILLING line 4 are labelled 1 to 6, while the wild type control is noted Wt. For each sample, the digested (d) and undigested (u) samples were run. The Gene ruler 100 bp ladder (left) was used as a molecular weight marker; red arrow: 200 bp; blue arrow: 300 bp.

- **TILLING line 5**

For TILLING line 5, the second PCR was performed using primers AM91 and AM92 which resulted in a product of 204 bp. After digestion of the PCR product with *Hind*III a fragment of 204 bp would indicate the presence of the wild type Hv*ATE1* sequence, whereas bands at 183 bp and 21 bp would be obtained in the presence the mutant version of Hv*ATE1*. As observed in FIGURE 4.2., even for the wild type, 2 bands were present after *Hind*III digestion, suggesting that in the Tesla variety there is a polymorphism that resulted in the presence of a *Hind*III site in the wild type. Nevertheless, samples 1, 5 and 7 seemed to have a different digestion pattern compared with samples 2, 3, 4 and 6, which are similar to the wild type. Based on this

observation, samples 1, 5 and 7 were sent for Sanger sequencing. The sequencing results demonstrated that plants 1, 5 and 7 were indeed homozygous mutants.

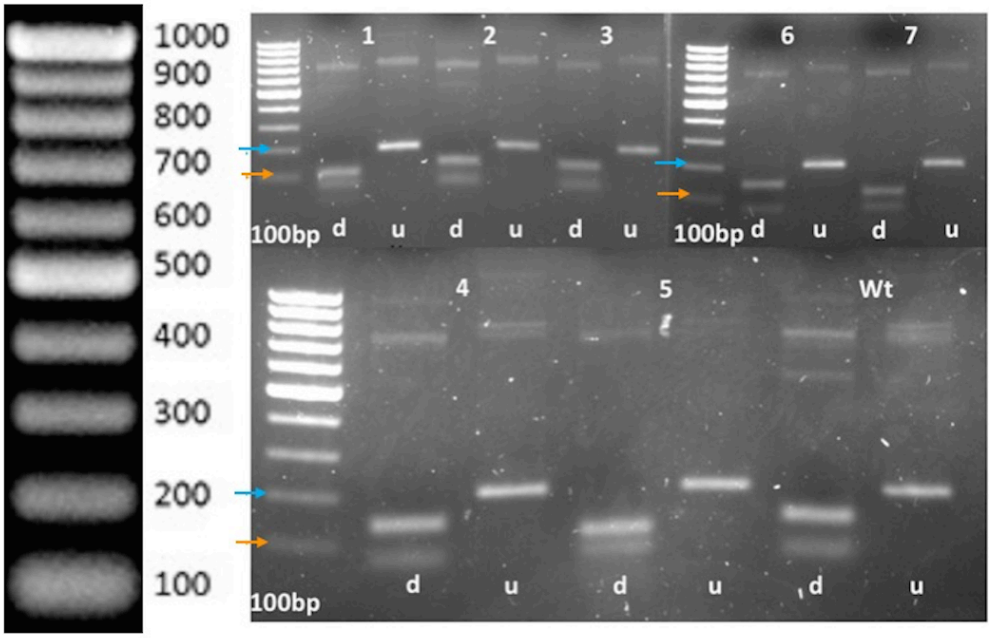

FIGURE 4.2. dCAPS genotyping on TILLING line 5. Using the dCAPS method, 7 plants from TILLING line 5 were genotyped. Genomic DNA from a wild-type Tesla plant was used as a control as seeds from wild-type Barke were not available in the lab. Leaves from ~3 week-old plants were collected and genomic DNA was extracted. Following two sets of PCRs and *Hind*III digestion, the samples were analyzed on a 2% agarose gel. Plants from TILLING line 5 are labelled 1 to 7, while the wild type control is noted Wt. For each sample, the digested (d) and undigested (u) samples were run. The Gene ruler 100 bp ladder (left) was used as a molecular weight marker; orange arrow: 100 bp; blue arrow: 200 bp;

- ## TILLING line 6

For TILLING line 6, the second PCR was performed using primers AM97 and AM98 which resulted in a PCR product of 254 bp. After digestion of the PCR product with *Psi*I, a fragment of 254 bp was expected for the wild-type allele of Hv*ATE1*, while bands at 229 bp and 25 bp were anticipated for the mutant version. As shown in FIGURE 4.3, all the samples, except number 8, gave similar results as the wild

type, with a single band at ~254 bp. For sample 8, the digested sample looked like the wild type, whereas the undigested one had more than one band. In order to check if plant 8 was indeed wild type for Hv*ATE1*, the first PCR product was sequenced using primer AM103. The sequencing results confirmed that plant 8 was wild type for Hv*ATE1*. To rule out problems with the restriction enzyme, undigested PCR products from plants 1 and 3 were sequenced, which also confirmed that they were wild type for Hv*ATE1*. Hence, none of the plants grown for TILLING line 6 carried the predicted mutation.

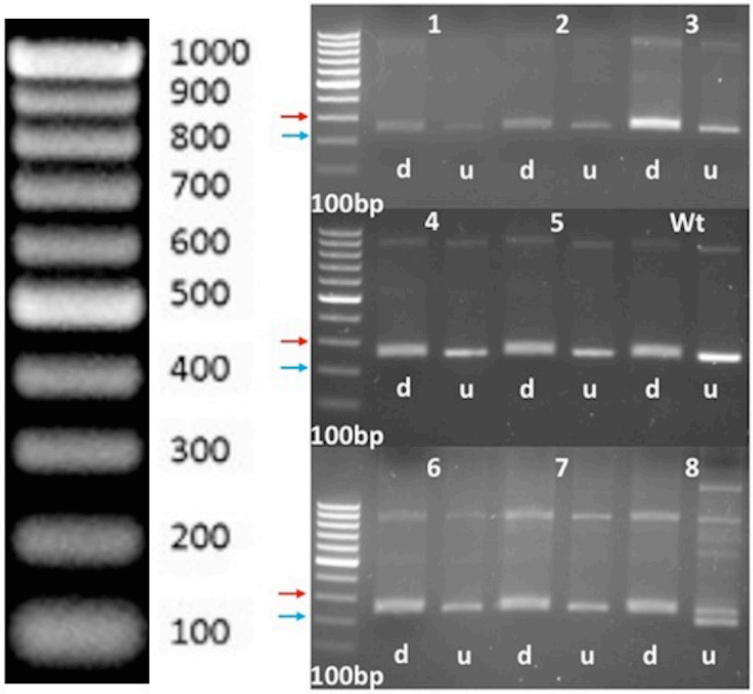

FIGURE 4.3. dCAPS genotyping on TILLING line 6. Using the dCAPS method, 8 plants from TILLING line 6 were genotyped. Genomic DNA from a wild-type Barke plant was used as a control. Following two sets of PCRs and *Psi*I digestion, the samples were analyzed on a 2% agarose gel. Plants from TILLING line 6 are labelled 1 to 8, while the wild type control is noted Wt. For each sample, the digested (d) and undigested (u) samples were run. The Gene ruler 100 bp ladder (left) was used as a molecular weight marker; blue arrow: 200 bp; red arrow: 300 bp.

- **TILLING line 9**

For TILLING line 9, primers AM99 and AM100 were used for the second PCR, which resulted in a product of 244 bp. After digestion of the PCR product with *Sac*I, a fragment of 244 bp should indicate the presence of a mutant version of Hv*ATE1*, while bands at 219 bp and 25 bp should correspond to wild-type allele of Hv*ATE1*. As shown in FIGURE 4.4, samples 1, 3, 5, 6 and 7 behaved like the wild type, with 2 fragments at ~200 bp and 400 bp, before and after digestion with *Psi*I. There was nevertheless a small size difference between the digested and undigested fragments, but not as expected. The identical profile observed for these samples and the wild type suggest that the corresponding plants are homozygous wild type. Undigested PCR for sample 1 was sent for Sanger sequencing and confirmed that the plant was homozygous wild-type for Hv*ATE1*. Samples 2 and 4 behaved differently from the wild type, with only one band after the PCR amplification. Given the fact that the lower band ~ 200 bp was around the same size in both digested and undigested samples, it is unlikely that plants 2 and 4 carry the mutation for Hv*ATE1*. A sequencing reaction would be required to confirm this.

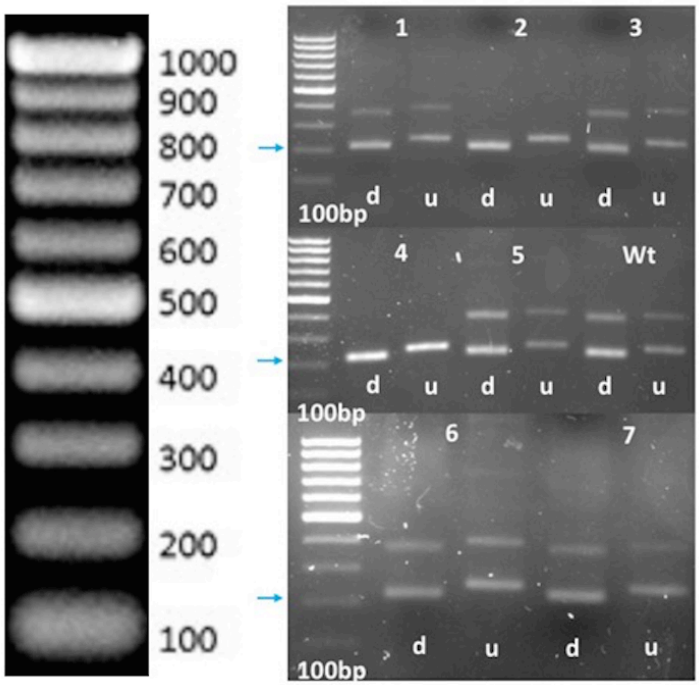

FIGURE 4.4. dCAPS genotyping on TILLING line 9. Using the dCAPS method, 7 plants from TILLING line 9 were genotyped. Genomic DNA from a Tesla plant

was used as a control as seeds from wild-type Barke were not available in the lab. Following two sets of PCRs and *Sac*I digestion, the samples were analyzed on a 2% agarose gel. Plants from TILLING line 9 are labelled 1 to 7, while the wild type control is noted Wt. For each sample, the digested (d) and undigested (u) samples were run. The Gene ruler 100 bp ladder (left) was used as a molecular weight marker; blue arrow: 200 bp.

- **TILLING line 10**

For TILLING line 10 the second PCR was performed with primers AM101 and AM102, which resulted in a product of 213 bp. After digestion of the PCR product with *Psi*I, a fragment of 213 bp would correspond to the wild type version of Hv*ATE1*. In contrast, bands at 188 bp and 25 bp are expected if the mutation in Hv*ATE1* is present. As shown in FIGURE 4.5, the PCR products from the 5 plants genotyped seem to indicate that all the plants are homozygous for the mutation in Hv*ATE1*. To verify this, the undigested PCR product for sample 2 was sequenced. The sequencing results indicated that plant 2 was in fact heterozygous for the Hv*ATE1* mutation.

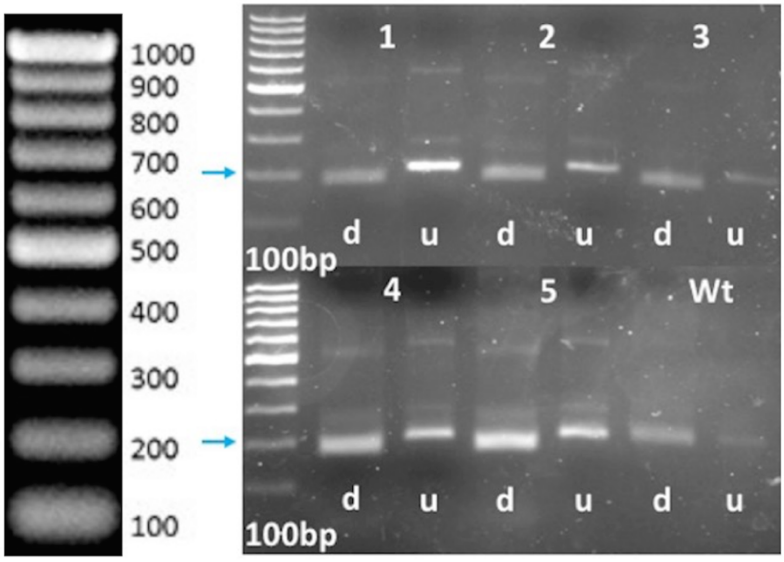

FIGURE 4.5. dCAPS genotyping on TILLING line 10. Using the dCAPS method, 5 plants from TILLING line 10 were genotyped. Genomic DNA from a wild-type Barke plant was used as a control. Following two sets of PCRs and *Psi*I digestion, the samples were analyzed on a 2% agarose gel. Plants from TILLING line 10 are labelled 1 to 5, while the wild type control is noted Wt. For each sample, the digested (d) and

undigested (u) samples were run. The Gene ruler 100 bp ladder was used as a molecular weight marker; blue arrow: 200 bp.

- **Homozygous mutants isolated**

Based on the combined dCAPS genotyping and sequencing, homozygous Hv*ATE1* mutants were found for TILLING lines 4 and 5 as indicated in Table 4.2.

Table 4.2. Summary of Hv*ate1* mutant lines isolated.

Line number	Plant number	Genotype	State
4	1	Hv*ATE1* mutant	hom
4	3	Hv*ATE1* mutant	hom
5	1	Hv*ATE1* mutant	hom
5	5	Hv*ATE1* mutant	hom
5	7	Hv*ATE1* mutant	hom
10	2	Hv*ATE1* mutant	het

4.2.2. Problems encountered

In order to clean the genetic background and remove unwanted mutations present in the TILLING lines, I planned to back-cross the different Hv*ate1* mutant plants with the wild-type Barke variety. Unfortunately none of the Hv*ate1* mutants isolated transitioned from vegetative development to flowering. As indicated in FIGURE 4.6, even after 11 months, the homozygous Hv*ate1* mutants did not produce flowers, whereas other TILLING lines that contained the wild type version of Hv*ATE1* and the parental Barke plants were able to flower.

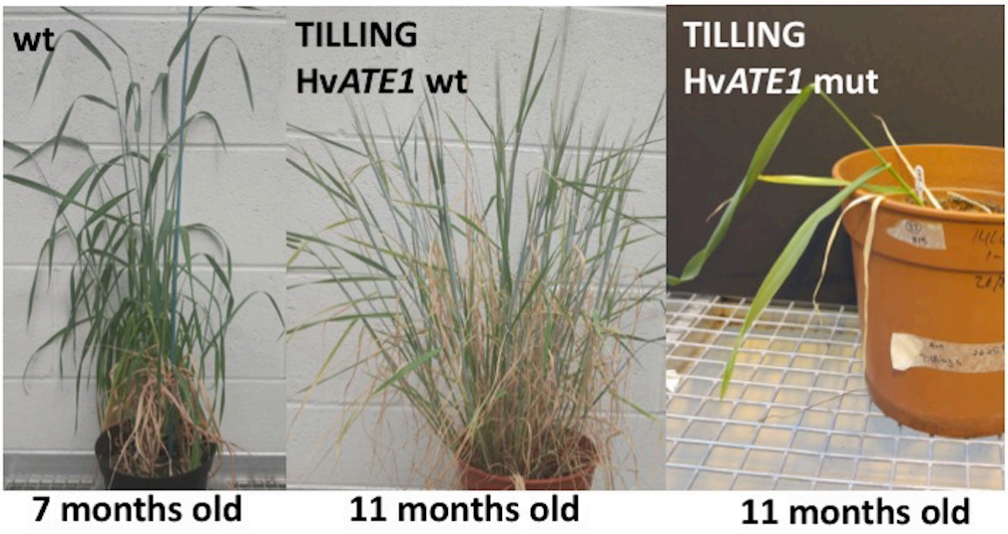

FIGURE 4.6. Pictures of wild-type and TILLING mutant plants at different stages of development. Barley plants were grown in John Innes No. 2, as described in Section 2.1.3.1. The plants were kept in the dark for 10 d at 4ºC before being moved to the plant room, where they were grown under long-day conditions (16 hrs light/8 hrs dark) at 15°C. When plant height reached 85 cm, they were transferred to the greenhouse (16 hrs light/8 hrs dark, 19°C). Plants were kept under observation. Pictures were taken when the first signs of flowering were observed (flag leaf is present and the first spikes are developing). For the wild type (labelled **wt**), pictures were taken at 7 months after germination. For the TILLING lines, plants were taken at 11 months after germination. Plant labelled 'TILLING Hv*ATE1* mut' is an isolated Hv*ATE1* mutant from line 4, whereas 'TILLING Hv*ATE1* wt' is a plant part of the TILLING collection, line 10 that contained the wild type version of Hv*ATE1*.

4.3. Generation of barley mutants for Hv*ATE1* using CRISPR/Cas9 technology

The second strategy used to generate mutant lines for Hv*ATE1* was based on the CRISPR/Cas9 system. In prokaryotes, CRISPR is involved in targeting and cleaving foreign DNA with the help of an RNA-guided endonuclease (Bhaya *et al*., 2011). In order to target and cut a specific sequence of DNA, the CRISPR/Cas9 system requires the action of 4 components: Cas9 endonuclease, 2 noncoding RNAs,

a trans-activating crRNA (tracrRNA) and a precursor crRNA (pre-crRNA). Together, the tracrRNA and pre-crRNA hybridize and form the single guide RNA (sgRNA). The sgRNA then directs the Cas9 enzyme to the target DNA sequence, resulting in double strand breaks (DSB) (Hyun *et al*., 2015). These DSBs are recognized and repaired by non-homologous end joining (Lieber *et al*., 2010). During the repair process, mutations may be introduced in the target DNA.

4.3.1. Designing *HvATE1* targeting constructs

In order to generate Hv*ATE1* mutants, 2 CRISPR/Cas9 constructs that target 2 different regions of Hv*ATE1* were generated. The first construct, called Hv*ATE1v1,* targets a sequence that is specific for *ATE1* in barley (see Section 2.2.5.7). The second construct, named Hv*ATE1v2* targets another sequence that is conserved in *ATE1* in barley and rice (see Section 2.1.4.7). It is known that in order to enhance the efficiency of CRISPR/Cas9 system, the target genomic sequence choose have to be followed by NGG, called protospacer adjacent motif (PAM) (Lawrenson *et al*., 2015). The details of the construction of the targeting constructs is provided in Section 2.1.4.7.

4.3.2. Assessing the ability of Cas9 to cut the *HvATE1* target sequences *in vitro*

In order to check that Cas9 could recognize and cut the target DNA sequences, an *in vitro* Cas9 assay was performed, as described in Section 2.2.5.6. Briefly, sgRNAs complementary to Hv*ATE1v1* and Hv*ATE1v2* were synthesized and purified (see Section 2.1.4.6). Also, a dsDNA template complementary to $HvATE1^{218\text{-}1499}$ (numbers in superscript refer to base numbers counted from the ATG in the coding sequence) was cloned in pJET1.2/blunt plasmid (Section 2.2.5.6). For the assay, this plasmid was linearized with the Dra*III* restriction enzyme. Then, the sgRNA together with the linearized pJET1.2 $HvATE1^{218\text{-}1499}$ were incubated with Cas9 (FIGURE 4.7).

Lane 1 corresponds to the linearized pJET1.2 $HvATE1^{218\text{-}1499}$ alone. The same result was obtained in lane 4 when the linearized plasmid pJET1.2 $HvATE1^{218\text{-}1499}$ and Cas9 were incubated. This indicates that the Cas9 enzyme does not cut the Hv*ATE1* sequence on its own. In lanes 5 and 6, the linearized pJET1.2 $HvATE1^{218\text{-}1499}$ and either of the 2 sgRNAs were incubated. In this case, smaller DNA fragments are

observed, which indicate the presence and size of the two sgRNAs. However, the linearized pJET1.2 *HvATE1*$^{218\text{-}1499}$ remains intact. When sgHv*ATE1v1* was incubated with the linearized pJET1.2 *HvATE1*$^{218\text{-}1499}$ and Cas9, two additional DNA fragments appeared as a result of *HvATE1*$^{218\text{-}1499}$ cleavage by Cas9 (lane 2, blue and red arrows). In addition, the sgRNA was observed at around 200 bp (yellow arrow). A similar result was obtained with sg*HvATE1v2* (lane 3).

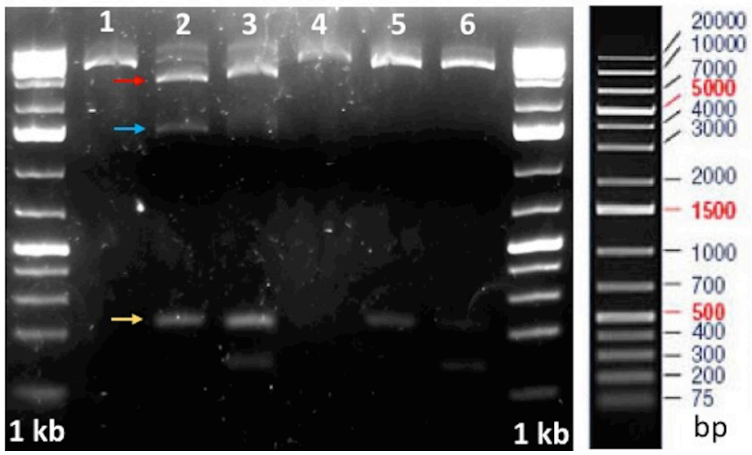

FIGURE 4.7. *In vitro* Cas9 assay to test the sgRNA sequences chosen. Each of the lanes correspond to: **1**- pJET1.2 *HvATE1*$^{218\text{-}1499}$ linearized with Dra*III*, **2**- sgHv*ATE1v1* + pJET1.2 *HvATE1*$^{218\text{-}1499}$ linearized with Dra*III* + Cas9; **3**- sgHv*ATE1v2* + pJET1.2 *HvATE1*$^{218\text{-}1499}$ linearized with Dra*III* + Cas9; **4**- pJET1.2 *HvATE1*$^{218\text{-}1499}$ linearized with Dra*III* + Cas9; **5**- pJET1.2 *HvATE1*$^{218\text{-}1499}$ linearized with Dra*III* + sgHv*ATE1v1*; **6**- pJET1.2 *HvATE1*$^{218\text{-}1499}$ linearized with Dra*III* + sgHv*ATE1v2*; Blue arrow represents the digested fragment and the yellow arrow shows the band for the sgRNA. Linearized pJET1.2 *HvATE1*$^{218\text{-}1499}$ had the expected size of 4.2 kb. The Gene Ruler 1kb Plus DNA Ladder was used as a molecular weight marker.

In conclusion, these *in vitro* Cas9 assays show that the two sgRNAs cloned are sufficient to target Cas9 to its Hv*ATE1* target sequence. In addition, Cas9 is able to cut the sequence as expected, so that *in vivo*, we would expect that the constructs cloned should be functional. I hence introduced the constructs generated into *Agrobacterium tumefaciens* strain AGL1 (Section 2.1.3), which I could use to transform barley.

4.3.3. Verifying the presence of the constructs in *A. tumefaciens*

Before proceeding with barley transformation, which is a long procedure, I checked that the *Agrobacterium* strains I obtained indeed carried the plasmids of interest. To this aim I extracted the plasmids from several *Agrobacterium* colonies and carried out PCRs to check for the presence of each of the sgRNA cassettes (FIGURE 4.8 and FIGURE 4.9).

As observed in FIGURE 4.8. and FIGURE 4.9, the *Agrobacterium* colonies carried the plasmids with the sgRNA cassettes Hv*ATE1v1*and Hv*ATE1v2*, respectively.

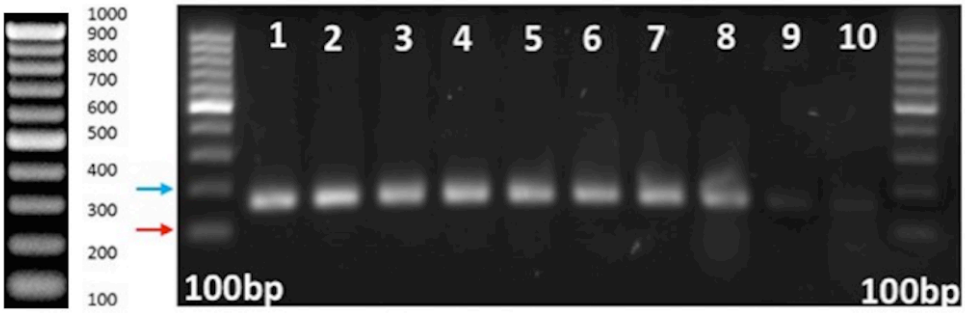

FIGURE 4.8. Hv*ATE1v1* genotyping on Level M plasmids extracted from *A. tumefaciens* AGL1. Lanes 1-7 corresponds to PCR reactions on plasmids extracted from 7 different colonies of AGL1 transformed with Hv*ATE1v1* level M construct; lane 8 is a positive control, which corresponds to a PCR reaction on the level M Hv*ATE1v1* construct used to transform *Agrobacterium*; lane 9: negative control, empty plasmid extracted from wild type AGL1; lane 10: water only control (i.e. no DNA in PCR reaction). The Gene ruler 100 bp ladder (left) was used as a molecular weight marker; red arrow: 100 bp, blue arrow: 200 bp.

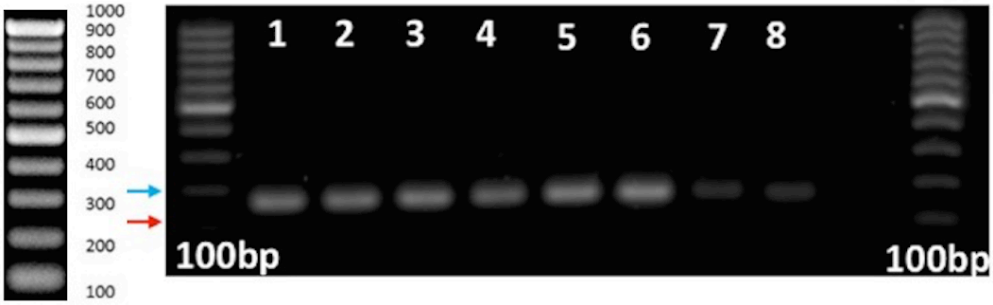

FIGURE 4.9. Hv*ATE1v2* genotyping on Level M plasmids extracted from *A. tumefaciens* AGL1. Lanes 1-5 corresponds to PCR reactions on plasmids extracted from 5 different colonies of AGL1 transformed with Hv*ATE1v2* level M construct; lane 6 is a positive control, which corresponds to a PCR reaction on the level M Hv*ATE1v2* construct used to transform *Agrobacterium*; lane 7: negative control, empty plasmid extracted from wild type AGL1; lane 8: water only control (i.e. no DNA in PCR reaction). The Gene ruler 100 bp ladder (left) was used as a molecular weight marker; red arrow: 100 bp, blue arrow: 200 bp.

I also confirmed the presence of the hygromycin-selection gene (*Hpt*) and of *Cas9* by sequencing the plasmids I isolated from *Agrobacterium*. The sequencing results confirmed the presence of both *Hpt* and *Cas9* genes in the Hv*ATE1v1* and Hv*ATE1v2* level M constructs.

4.4. Setting up the procedure for *A. tumefaciens*-mediated immature embryo transformation

A. tumefaciens-mediated transformation of immature barley embryos is a very challenging and laborious procedure. In order to set it up in the lab, I worked with Dr. Ewen Mullins and Dr. Dheeraj Rathore from Teagasc in order to learn each of the steps and then reproduce them at Maynooth University.

Briefly, *A. tumefaciens*- mediated immature embryo transformation involves the following steps (Harwood *et al*., 2009):

- Isolation of barley spikes (FIGURE 4.10A);
- Isolation and sterilization of immature barley seeds (FIGURE 4.10B);
- Isolation of intact embryos from the immature seed (FIGURE 4.10C);
- Removal of the embryonic axis from the isolated immature embryo (FIGURE 4.10D);
- Cultivation of immature embryos with removed embryonic axis on callus induction medium (CIM) prior to *Agrobacterium* inoculation (FIGURE 4.10E), for 24 hrs;

- Co-cultivation of immature embryos with *Agrobacterium* (FIGURE 4.10F) and incubation on CIM for 3 days;
- Cultivation of inoculated immature embryos on CIM with timentin for 6 weeks, used to remove the *Agrobacterium* from the plates (FIGURE 4.10G);
- Cultivation of inoculated embryos on Transition medium (FIGURE 4.10H);
- Cultivation of inoculated embryos on Regeneration medium in plates (FIGURE 4.10I and J);
- Transfer of regenerated plants on Regeneration medium, in tubes (FIGURE 4.10K), followed by transfer on soil when the plants reach the top of the tube.

As described, there are 3 different types of media used during immature embryo transformation: CIM, Regeneration media and Transition media. All 3 medias are based on Murashige and Shoog medium, but different hormones are added in respect with embryo requirements at different stages of development. For example, CIM contains synthetic forms of auxin (Harwood *et al*., 2009) that are known to be important for callus induction (Skoog and Miller, 1957). Transition medium contains a high ratio of auxin/cytokinin (Harwood *et al*., 2009) known to be involved in root and shoot regeneration (Skoog and Miller, 1957). Finally, regeneration medium does not contain any hormones but contains vitamins and nutrients required for plants to grow (Harwood *et al*., 2009).

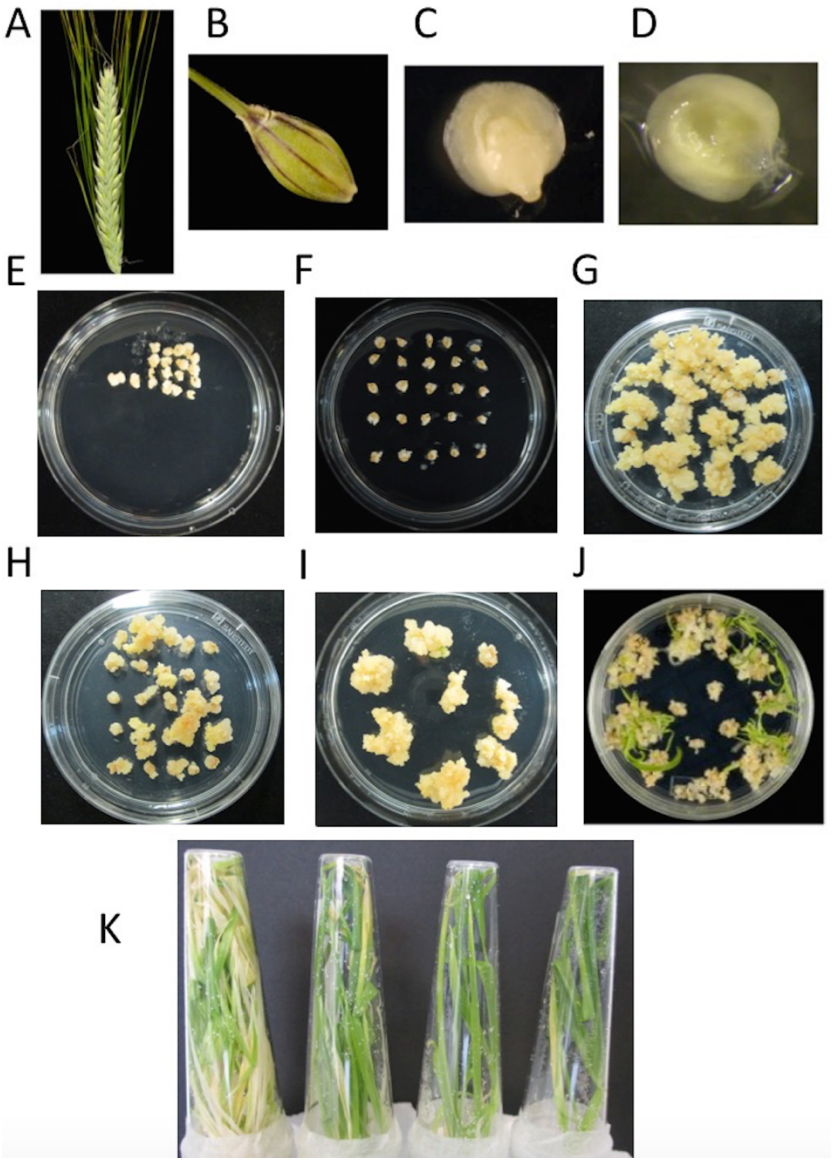

FIGURE 4.10. Overview of steps involved in immature-embryo transformation technique. A- Barley spike containing immature embryos (Harwood et al., 2009); B- Isolated immature seed (Harwood *et al*., 2009); C- Intact immature embryo isolated from immature seed (Harwood *et al*., 2009); D- Immature embryo with the embryonic axis removed (Harwood *et al*., 2009); E - Immature embryo with the embryonic axis removed cultivated on CIM before *A.tumefaciens* inoculation (this study); F - Immature embryo with the embryonic axis removed cultivated on CIM after *A.tumefaciens* inoculation (this study); G- Immature embryo, 6 weeks after co-cultivation with *A.tumefaciens*, on CIM (this study). H- Immature embryo, 8 weeks after co-cultivation with *A.tumefaciens* on Transition medium (this study); I - Immature embryo, 12 weeks after co-cultivation with *A.tumefaciens* on Regeneration medium (this study); J- Immature embryo, co-cultivated with *A.tumefaciens* on

Regeneration medium are showing signs of regeneration (green tissue) (Harwood *et al*., 2009); K – Regenerated plants in tubes provided by BRACT (John Innes Centre) (this study).

I first worked on learning how to dissect and prepare the immature embryos, as well as how to regenerate plants from callus in the absence of *A. tumefaciens* transformation. In this preliminary experiment I used the Tesla variety (instead of Golden Promise, which is typically used for transformation) because seeds were easily accessible in the lab. Seeds were sown on John Innes No. 2, and plants were grown in long-day conditions as described in Section 2.1.3.1. Immature embryos were collected when they reached 1.5-2 mm in length and sterilized as described in Section 2.1.3.2. Immature embryos were isolated as described in Section 2.1.3.3 and incubated on the CIM media without any antibiotic for 3 days at 23-24°C in the dark (FIGURE 4.11A). After 3 days, the embryos were transferred to a new CIM plate and incubated for 2 weeks at 23-24°C in the dark (FIGURE 4.11B). This was repeated twice more, so that in total, the immature embryos and associated calli were kept 6 weeks on CIM medium at 23-24°C in the dark (FIGURE 11 C and D). After 6 weeks on CIM medium, the embryos were transferred to transition medium for another 2 weeks at 24°C under low light conditions (FIGURE 11 E and F). At this stage, the calli started to produce green tissue as observed in FIGURE 4.11F, indicating that both the embryo dissection and regeneration procedure were working properly in my hands.

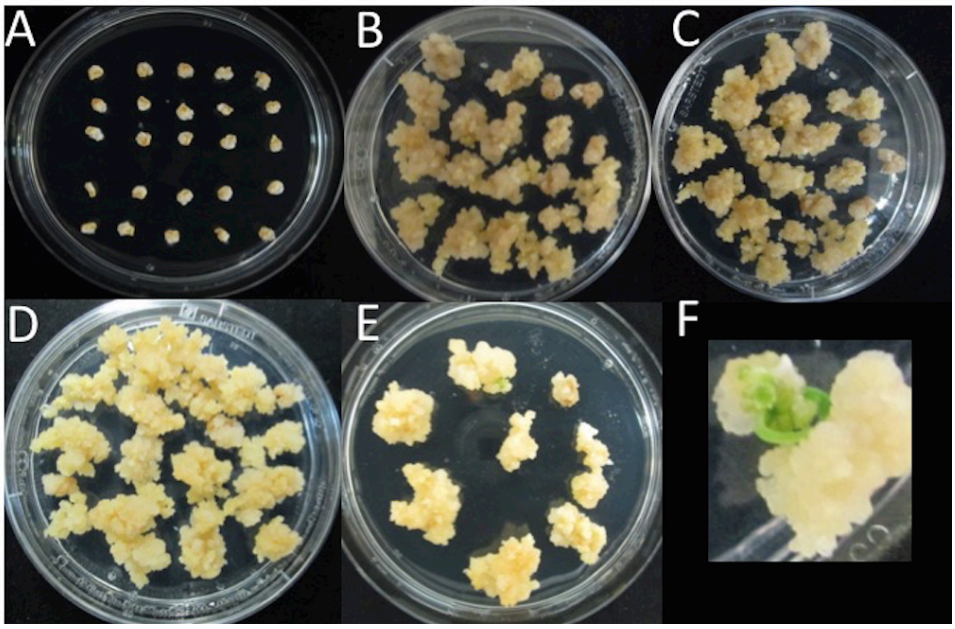

FIGURE 4.11. Immature embryo preparation and regeneration. Pictures of immature barley embryos (Tesla variety) were taken at different steps of the regeneration procedure. For one experiment, 100 immature embryos were prepared. After embryo dissection, 25 isolated embryos were placed on each CIM plate. **A.** Immature barley embryos 3 days after isolation. **B.** Immature barley embryos and associated callus after 2 weeks on CIM; **C.** Immature barley embryos and associated callus after 4 weeks on CIM; **D.** Calli after 6 weeks on CIM. **E.** Calli after 2 weeks on transition medium. **F.** Close-up on a regenerating callus.

I next used the AGL1 *Agrobacterium* strains carrying the level M constructs for Hv*ATE1v1* and Hv*ATE1v2* (FIGURES 4.8 and 4.9) to transform immature embryos of the Golden Promise variety, because this variety has increased transformation efficiency (Harwood *et al*., 2009). Seeds were sown on John Innes No. 2, and plants were grown in long-day conditions as described in Section 2.1.3.1. Immature embryos were collected when they reached 1.5-2 mm in length and sterilized as described in Section 2.1.3.2. Immature embryos were isolated as described in Section 2.1.3.3 and incubated on the CIM media without any antibiotic for 1 day at 23-24°C in the dark. The following day, the embryos were co-cultivated with *A. tumefaciens* AGL1 containing the level M plasmids. After 3 days, the embryos were transferred to a new CIM plate containing antibiotics (timentin and hygromycin), and incubated for 2 weeks at 23-24°C in the dark. Two weeks later the

embryos and the associated calli were transferred to a fresh CIM media containing timentin and hygromycin, as described in Section 2.1.3.5. This was repeated twice more. Following 6 weeks on CIM with antibiotic selection, the calli were transferred to transition medium for 2 weeks, as described in Section 2.1.3.5. After 2 weeks on transition medium for regeneration, the calli were transferred to fresh regeneration medium as described in Section 2.1.3.5. As shown in FIGURE 4.12 A and B, no green tissue was observed when plants were transferred to transition medium and the calli showed signs of necrosis, suggesting that there was a problem either with the regeneration or with the transformation. One possibility was that the hygromycin concentration used for selection of transformed calli was too high (50 mg/L), which could have a negative effect on the viability of the calli and the ability to regenerate.

To test this possibility and improve the protocol used in the lab, I carried out another set of transformations, but used a lower hygromycin concentration (25 mg/L) for half of the embryos co-cultivated with the *Agrobacterium* strains (FIGURE 4.12 C and D). The other half of the immature embryos that were co-cultivated were kept on medium without hygromycin to check the regeneration potential in the absence of selection for transformants. Callus tissue cultivated on medium containing only half of the required hygromycin concentration, looked healthy without signs of necrosis and developed green tissue, suggesting that the initial hygromycin concentration (50 mg/L) affected plant regeneration and that the second round of transformations might have worked. In the absence of hygromycin selection, the calli obtained after co-cultivation were able were greener (FIGURE 4.12 E and F), again suggesting that hygromycin selection posed a problem.

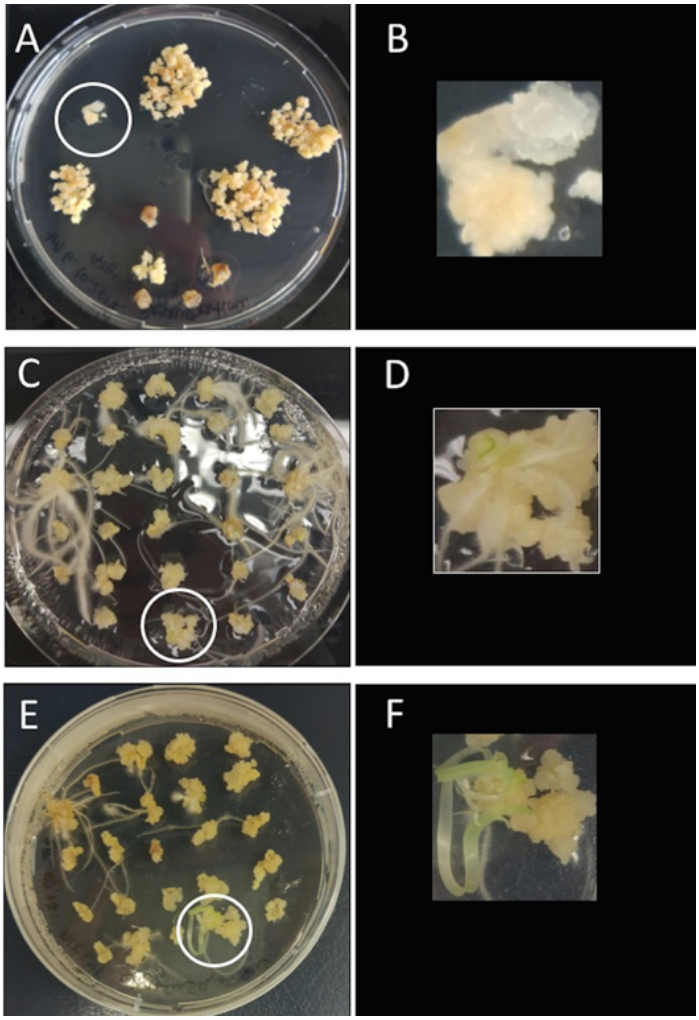

FIGURE 4.12. Golden Promise immature embryo transformation with CRISPR targeting constructs. A and B. Immature embryos on regeneration medium with 50 mg/L hygromycin (picture taken 2 months after embryo isolation). **C and D.** Immature embryos on CIM with 25 mg/L hygromycin (picture taken 2 weeks after embryo isolation). **E and F.** Immature embryos on CIM without hygromycin 2 weeks after isolation.

I next checked whether the callus that grew on medium containing only 25 mg/L of hygromycin actually carried the T-DNA coding for the level M constructs. To this aim, genomic DNA was isolated from different calli (see Section 2.1.3.6) and I carried out different sets of PCRs to verify the presence of the sgRNA cassettes (FIGURE 4.13). As a positive control for the PCR, I used the plasmids used to transform *Agrobacterium* as a template (lanes 5 and 12). The results obtained suggest

that most of the calli do not carry the sgRNA cassettes, except maybe callus 9. However, the presence of a smear made the interpretation difficult.

FIGURE 4.13. Callus genotyping for the presence of the sgRNA cassette for the Hv*ATE1v1* and Hv*ATE1v2* constructs. Lanes 1-4: calli transformed with Hv*ATE1v1*. Lane 5: positive control using to Hv*ATE1v1* level M plasmid extracted from *A. tumefaciens* AGL1 as a template. Lane 6: negative control (empty plasmid extracted from wild type *A. tumefaciens* AGL1). Lane 7: water-only control. Lanes 8-11: calli transformed with Hv*ATE1v2*. Lane 12: positive control using to Hv*ATE1v2* level M plasmid extracted from *A. tumefaciens* AGL1 as a template. Lane 13: negative control (empty plasmid extracted from wild type *A. tumefaciens* AGL1); Lane 14: water-only control. The Gene ruler 100 bp ladder (left) was used as a molecular weight marker Red arrow: 100 bp; bluer arrow: 200 bp.

Second, the presence of the *Cas9* cassette was checked by PCR (FIGURE 4.14.). As shown in FIGURE 4.14, the PCR worked with the positive control (lane 11), showing that the plasmid present in the *Agrobacterium* strain carried the *Cas9* gene. However, none of the calli appeared to contain the Cas9 gene, suggesting that they were not transformed. Another reason for the negative result, might be that only few cells in the callus contained the transgene.

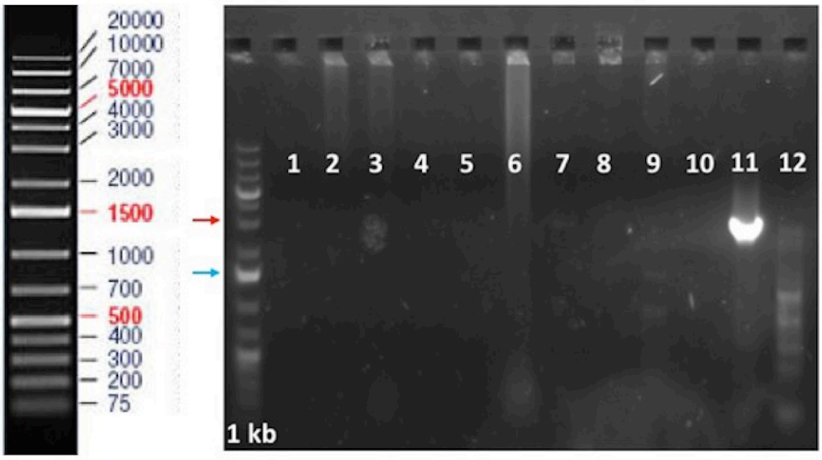

FIGURE 4.14. Callus genotyping for the presence of Cas9 cassette. Lanes 1-4: calli transformed with Hv*ATE1v1*; Lanes 5-8: calli transformed with Hv*ATE1v2;* Lane 9: genomic DNA extracted from wild type barley; Lane 10: water only control; Lane 11: positive control using to Hv*ATE1v1* level M plasmid extracted from *A. tumefaciens* AGL1 as a template; Lane 12: negative control (empty plasmid extracted from *A. tumefaciens* AGL1); blue arrow: 1.5 kb; red arrow: 3 kb. The Gene Ruler 1 kb Plus DNA Ladder was used as a molecular weight marker.

Finally, the presence of the *Hpt* gene was checked by PCR (FIGURE 4.15). As expected, the *Hpt* gene could be amplified from the plasmid extracted from *Agrobacterium* (lane 9). In addition, callus 7 seemed to also contain the *Hpt* gene, but none of the other calli appeared to be transformed.

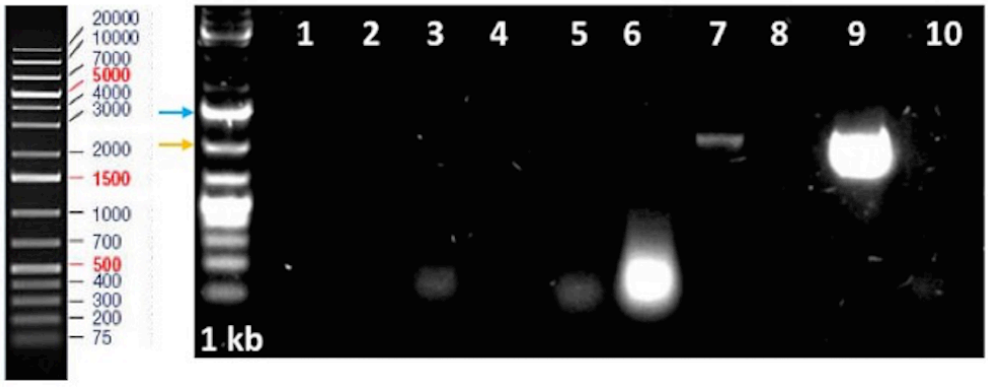

FIGURE 4.15. Callus genotyping for the presence of the *Hpt* expression cassette. Lanes 1-4: calli transformed with Hv*ATE1v1*; Lanes 5-8: calli transformed with Hv*ATE1v2*; Lane 9: positive control using to Hv*ATE1v1* level M plasmid extracted from *A. tumefaciens* AGL1 as a template; Lane 10: genomic DNA extracted from

wild type barley; blue arrow: 1.5 kb; yellow arrow: 1.0 kb. The Gene Ruler 1 kb Plus DNA Ladder was used as a molecular weight marker.

In summary, the results of the different genotyping experiments are inconclusive, in that I can detect some of the genes encoded in the T-DNA in some plants, but I could not identify a plant with all the genes. While this may be linked to the quality of the genomic and its suitability for the PCR reactions I carried out, these results strongly suggest that the transformation procedure is not working properly, and that regeneration on medium with a lower hygromycin concentration is unlikely to be suitable. It is also worth mentioning that although I kept the green calli for a long time, they never regenerated a proper shoot or root system, suggesting that regeneration is also problematic.

4.5. Discussion and conclusions

One of the aims of my PhD project was to isolate mutant barley plants for Hv*ATE1*, in order to assess their waterlogging tolerance under controlled conditions. I used two complementary approaches. The first one was based on the isolation of TILLING mutant lines in the Barke variety. One main advantage of the TILLING approach is that the resulting plants are not considered as transgenic. Although I was able to identify plants that carried mutations in Hv*ATE1*, none of the mutant lines identified, either homozygous or heterozygous, transitioned to flowering. This prevented me from (i) propagating the lines; and (ii) out-crossing the lines to the wild-type parent, which would have helped to alleviate some of the problems due to the presence of additional mutations in the genome. It is unclear at this stage whether the problems to transition to reproductive development are due to other mutations in the background or to the mutation in Hv*ATE1*. The latter is rather unlikely, considering that barley plants homozygous mutant for Hv*PRT6* can be propagated (Mendiondo *et al*., 2016)

The second approach I used to generate plants mutant for Hv*ATE1* relied on the use of the CRISPR/Cas9 system. I designed two targeting constructs and confirmed that the sgRNA sequences used could guide Cas9 to the Hv*ATE1* sequence. However, despite repeated attempts (not all attempts have been discussed above), I

was not able to optimize the immature embryo transformation procedure. To overcome this problem, the two constructs were sent to BRACT (John Innes Centre) for barley transformation. I have now 11 primary transformants for the Hv*ATE1v1* construct and 4 primary transformants for the Hv*ATE1v2* construct. I hope to characterize these in the coming months.

5. Characterization of the putative N-recognin BIG in Arabidopsis

Note that all genes in this section refer to genes in the model plant *Arabidopsis thaliana,* unless stated otherwise.

5.1. Introduction

The sets of destabilizing residues are conserved in plants and in animals, and also to some extent in yeast (Balzi *et al*., 1990; Ciechanover *et al*., 1988; Graciet *et al*., 2010). Several enzymatic components of the N-end rule pathway that are responsible for modifying tertiary and secondary destabilizing residues (see Section 1.2.1.1) have also been identified in plants, largely based on their sequence similarities with their yeast and mammalian orthologs (Garzon *et al*., 2007; Graciet *et al*., 2010). In plants, 2 N-recognins have also been identified to date. PRT1 is specific for N-terminal bulky hydrophobic residues (Phe, Trp and Tyr) (Potuschak *et al*., 1998). It appears to be plant-specific and has no ortholog in mammals or yeast. PRT6 recognizes basic N-terminal destabilizing residues such as Arg, Lys and His (Garzon *et al*., 2007), and has sequence similarities with the mammalian UBR1/2 N-recognins, and with yeast UBR1.

In mammals, one key feature of N-recognins appears to be the presence of a UBR domain, which is responsible for the binding of N-terminal basic residues. The family of UBR domain containing proteins was identified in 2005 based on the presence of a conserved UBR domain, which consists of ~ 70 amino acids zinc finger-like motif, that contain Cys and His conserved residues (Tasaki *et al*., 2005).

Several members of this family have been shown to act as N-recognins, including UBR1, UBR2, UBR4 and UBR5 (Tasaki *et al*., 2005; Tasaki *et al*., 2009; Choi *et al*., 2010; Belzil *et al*., 2014; Chitturi *et al*., 2018). UBR4 in particular is a very large protein of 600 kDa known as p600 (Nakatani *et al*., 2006) that was found initially in human central nervous system (Ohara *et al*., 1997). UBR4 plays a role in neurogenesis, neuronal signalling (Shim *et al*., 2008; Belzil *et al*., 2014) and mammalian embryogenesis, during which it contributes to vascular development in the yolk salk mainly through its role in autophagy (Tasaki *et al*., 2013). BLASTp with mouse UBR4 retrieves the Arabidopsis proteins BIG, so-called because of its

unusually large size of ~560 kDa (Gil *et al*., 2001). These sequence similarities and the presence of the UBR domain in BIG suggest that this protein could act as a potential N-recognin in plants. However, this hypothesis has not been tested to date.

5.1.1. Functional domains of the plant protein BIG

In addition to its sequence similarities with UBR4 and the conserved UBR domain, BIG also shares sequence similarities with the *Calossin*/*Pushover* protein family from *Drosophila melanogaster* (Gil *et al*., 2001). BIG contains 3 cysteine-rich domains, all of which have sequence similarities to zinc (Zn) finger domains. The first Zn finger domain corresponds to the UBR domain (Mansfield *et al*., 1994; Gil *et al*., 2001; Tasaki *et al*., 2005), the second one to a ZZ domain, which is also present in the PRT1 N-recognin (Stary *et al*., 2003) and the third Zn finger domain has sequence similarities to those found in the family of Calossin-like proteins in *Drosophila* (Gil *et al*., 2001; Altschul *et al*., 1997). The presence of at least 2 of these Zn finger domains (the UBR and ZZ domains) would be consistent with the idea that BIG could act as an E3 ligase.

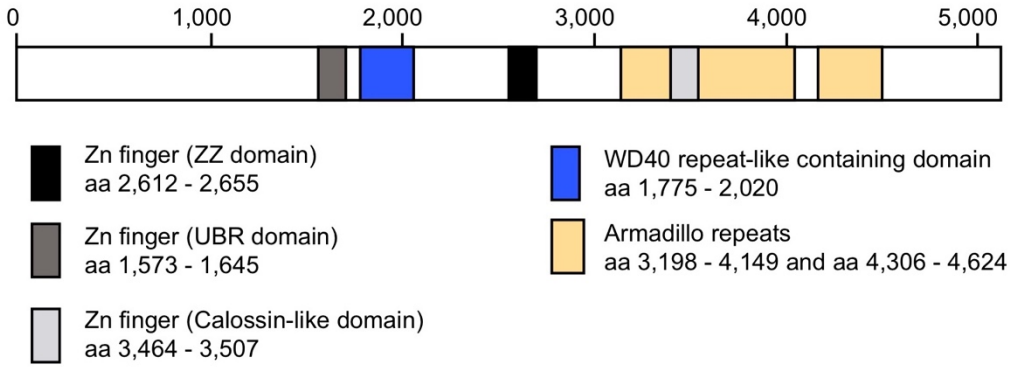

FIGURE 5.1. Predicted domains in Arabidopsis BIG. Domains indicated, as well as corresponding amino acid positions are from TAIR and (Gil *et al*., 2001).

In addition to the 3 Zn finger domains outlined above, BIG has several Armadillo (ARM) repeats domain. The latter typically fold as a superhelix that can serve as a platform to interact with other proteins. These domains are therefore most likely involved in protein-protein interactions (Tewari *et al*., 2010). Proteins with ARM repeats tend to have diverse functions, and one representative member is

Proteins with ARM repeats tend to have diverse functions (Tewari *et al*., 2010). BIG also encompasses a WD40 repeat-like domain, which is generally involved in protein-protein or protein-DNA interactions. In eukaryotes, proteins with this domain are very frequent and tend to participate to a wide range of functions including transcriptional regulation, trafficking, signal transduction and chromatin structure (Xu *et al*., 2011).

5.1.2. Known functions of BIG

Different mutant alleles of BIG have been identified in different forward genetic screens aiming at identifying genes involved in diverse processes. The involvement of BIG in a wide range of processes is not surprising, considering the presence of both ARM and WD40-like repeat domains. Based on the phenotypes observed in the different mutant alleles of *BIG* in Arabidopsis, the gene has also been referred to as *ATTENUATED SHADE AVOIDANCE1* (*ASA1*), *UMBRELLA1* (*UMB1*), *TRANSPORT INHIBITOR RESPONSE3* (*TIR3*), *CORYMBOSA1* (*CRM1*), *DARK OVER-EXPRESSION OF CAB1* (*DOC1*), *LOW-PHOSPHATE RESISTANT ROOT1* (*LPR1*) (Li *et al*., 1993; Ruegger *et al*., 1997; Kanyuka *et al*., 2003; Lopez-Bucio *et al*., 2005). These names and the associated phenotypes of the respective mutant alleles reflect the pleiotropic effect associated with a lack of *BIG* function, or changes in the function of the protein. Brief examples of phenotypic defects in the different mutant alleles include a compact rosette, fewer lateral roots, delayed flowering, increased number of secondary inflorescence and smaller seeds, shorter petioles and roots, reduced apical dominance (Ruegger *et al*., 1997; Kanyuka *et al*.,, 2003; Gil *et al*., 2001). Detailed studies also demonstrated that several of these mutant alleles of *BIG* had altered responses to a wide range of phytohormones, including auxin, abscisic acid (ABA), ethylene, cytokinin and gibberellin (GA) (Kanyuka *et al*., 2003; He *et al*., 2018). In addition, BIG has also been shown to play a role in light signalling (Terzaghi and Cashmore, 1995; Li *et al*.,1993; Gil *et al*., 2001) and in the regulation of circadian rhythms (Hearn *et al*., 2018). As mentioned above, the wide range of roles associated with BIG are not surprising considering the size of the protein and the number of different domains. A few examples of BIG roles in hormone signalling, in the regulation of plant responses to environmental stimuli and to biotic stresses are described below.

- **Roles of BIG in auxin transport**

Mutant plants for *BIG* show obvious leaf morphology defects and a loss of apical dominance, which relate to the roles of BIG in auxin transport and signalling. More specifically, the *doc*1 and *tir*3 mutant alleles of BIG are characterized by decreased auxin transport in inflorescence and in leaves (Gil *et al*., 2001; Guo *et al*., 2013). BIG is thought to regulate the protein level and the intracellular localization of PIN-FORMED1 (PIN1), an auxin efflux carrier (Gil *et al*., 2001; Guo *et al*., 2013). However, the exact molecular mechanisms of how BIG regulates polar auxin transport and how this affects a wide range of growth-related processes are not fully understood.

- **Roles of BIG in light signalling**

The *asa1* mutant allele of *BIG* was isolated in a genetic screen for mutants that supress the shade avoidance response (Kanyuka *et al*., 2003), suggesting that *BIG* regulates some aspects of light signalling. In addition, *Chlorophyll a/b-binding proteins of photosystem II* (*CAB*) genes are expressed at high levels in the light and at low levels in the dark (Terzaghi and Cashmore, 1995). The *doc1* mutant allele of *BIG* is characterized by high levels of *CAB* expression in the dark, suggesting a role of BIG as a negative regulator of *CAB* gene expression in the dark (Li *et al*.,1993; Gil *et al*., 2001). Experiments in double mutant *doc1 yucca* (*yucca* being a mutant characterized by increased auxin levels) showed that *yucca* was able to compensate the overexpression of *CAB* in the darkness specific for *doc1* (Gil *et al*., 2001). Hence, it seems that BIG acts at a crossroad between auxin and light signalling.

- **Roles of BIG in the regulation of responses to other stimuli**

Recently, it was shown that *BIG* was also involved in CO_2-dependent stomatal closure as *big* mutants were impaired in reducing the stomatal aperture in response to increased CO_2 concentrations (He *et al*., 2018). Stomata are small pores found on the leaf surface that allow water and gases to be exchanged between the plant and the environment (Kim *et al*., 2010). It was shown that stomata play an important role in plant immunity (Melotto *et al*., 2006). Pathogens can enter the leaf through stomata and in response to the pathogen attack plants tend to close their stomata (Melotto *et al*., 2006). This might affect the response of *big* mutant plants to biotic stimuli as well.

Recently it was shown that BIG regulates the rhythms as well, and contributes to the timing of biological events (Hearn *et al*., 2018). Indeed, *big* mutants are oversensitive to nicotinamide, that is known to increase the circadian period (Hearn *et al*., 2018). It was shown that BIG acts through cytosolic calcium signalling and modulation of gene expression of specific circadian rhythm regulators (Hearn *et al*., 2018).

5.1.3. Questions addressed

During my PhD, I aimed at answering several questions, all relating to a possible connection between BIG and the N-end rule pathway. This work is done in collaboration with Dr. Frederica Theodoulou and Dr. Hongtao Zhang (Rothamsted). In this thesis, I am only showing the results of experiments I have conducted myself.

- **Is BIG an N-recognin?** This question stems from (i) the sequence similarities between BIG and the mammalian N-recognin UBR4; (ii) the presence of a UBR domain, which is typically involved in recognizing and binding proteins that bear a basic N-terminal destabilizing residue; and (iii) the presence of a ZZ domain, which is also found in the plant N-recognin PRT1. To address this question, I used a set of N-end rule reporter constructs to monitor the effect of a *big* mutant background on the stability of different N-end rule reporter constructs.
- **Could BIG be the missing N-recognin for N-terminal Leu and Ile?** As mentioned in Section 1.2.1.1, PRT6 and PRT1 recognize different sets of substrates, based on the different types of N-terminal destabilizing residues. However, although N-terminal Leu and Ile are known to be destabilizing residues in plants (Graciet *et al*., 2010), the N-recognin responsible for detecting such substrates has so far remained unknown. As part of my PhD, I aimed at testing if BIG could be this missing N-recognin using the same set of N-end rule reporter constructs mentioned above.
- **Could *BIG* and *PRT6* have synergistic functions?** The latter question was asked based on observations made by a previous student in the lab (Walter, 2010). Indeed, F. Walter had generated a *big prt6-5* double mutant plant and a simple comparison of the double mutant and its 2 parental lines revealed that

the interaction may be synergistic. More specifically, the *big prt6-5* double mutant appeared to have a severely delayed flowering phenotype under short-day conditions, which was not as pronounced in each of the 2 parents. This would suggest that *BIG* and *PRT6* could act together to control developmental programs such as the transition to flowering. Another information that prompted us to study more in detail a *big prt6*-5 double mutant, was the recent finding that BIG and PRT6 proteins could potentially interact with each other (Frederica Theodoulou and Hongtao Zhang (Rothamsted), confidential communication).

5.2. Does BIG function as an N-recognin?

In order to test if BIG could act as an N-recognin, *big* mutant plants, as well as the *prt6-5* and the *big prt6-5* mutants were crossed with N-end rule reporter lines (Mesiti, 2011). These lines encoded in their genome a T-DNA that allowed expression of a GUS normalization cassette (under the control of the constitutive 35S promoter), and of the N-end rule reporter construct under the control of the ubiquitin promoter (Graciet *et al*., 2010; Worley *et al*., 1998). The N-end rule reporter constructs consist of a fusion protein between ubiquitin (Ub) and X-luciferase (X-LUC), with X being any amino acid residue (in our case: methionine (M), arginine (R), leucine (L) or phenylalanine (F)). When expressed in plants, this Ub-X-LUC fusion protein is cleaved after the last residue of Ub, thus releasing a LUC reporter protein bearing the residue X at its N-terminus. If 'X' is a destabilizing residue, this leads to low levels of LUC activity, which we can measure easily in plant extracts. Hence, to test if BIG could act as an N-recognin, I used *big* mutant plants crossed with reporters starting with Met (a canonical stabilizing residue that leads to a stable LUC protein), Arg, Leu or Phe. The latter destabilizing residues were chosen, because each of them is representative of a type of primary destabilizing residue: N-terminal Arg is typically bound by UBR-domain containing E3 ligases such as PRT6; Phe is recognized by PRT1 when made N-terminal; and the N-recognin for N-terminal Leu remains to be identified (see Section 1.2.1.1). By testing the stability of these different N-end rule reporters in a *big* mutant background and comparing the results to those obtained in wild-type plants, I could determine if BIG played a role in the N-end rule pathway.

For example, if BIG is the N-recognin for N-terminal Leu, I would expect the L-LUC reporter protein to accumulate to higher levels in a *big* mutant compared to the wild type.

In addition, because BIG and PRT6 both have the UBR domain which is essential to bind basic destabilizing N-terminal residues such as N-terminal Arg, I also generated N-end rule reporter lines in the *big prt6-5* double mutant background and in the *prt6-5* single mutant. Comparing the effects of the different mutations on the stability of the R-LUC reporter could potentially reveal partially redundant functions of BIG and PRT6 in the targeting of such substrates for N-end rule-mediated degradation. All the lines used in this study were genotyped to check that the mutations in *BIG* and/or *PRT6* were homozygous. I also checked for the presence of the Ub-X-LUC fusion based on genotyping and Basta selection. Finally, I sequenced the Ub-X-LUC reporter to ensure that the expected N-terminal residue X was present (Table 5.1.1). Unfortunately, *prt6-5* Ub-M-LUC and *big prt6-5* Ub-L-LUC did not germinate. Because of time constraints, I did not have sufficient time to complete these experiments.

Table 5.1. N-end rule reporters in *big*, *prt6-5*, *big prt6-5* and WT background. The genotype indicates the mutant background in which the N-end rule reporter was introduced. The presence of the T-DNA in *BIG* and *PRT6* was verified by PCR and homozygous plants for the T-DNAs were selected. The reporter constructs are also indicated. Note that the T-DNAs for the N-end rule reporters are segregating in the different mutant background, while they are homozygous in the wild-type. The number in subscripts correspond to the number of the wild-type lines that were used for the crosses. For the Ub-R-LUC reporter, two independent reporter lines were used, line number R9-2 and line number R6-2. Lines indicated in red did not germinate, and hence could not be characterized on time.

Genotype	Reporter
big	Ub-$L_{3\text{-}1}$-LUC
big	Ub-$M_{1\text{-}2}$-LUC
big	Ub-$R_{9\text{-}2}$-LUC
big	Ub-$R_{6\text{-}2}$-LUC
big	Ub-$F_{3\text{-}1}$-LUC

big	Ub-I_{1-1}-LUC
prt6-5	Ub-L_{3-1}-LUC
prt6-5	Ub-M_{1-2}-LUC
prt6-5	Ub-R_{9-2}-LUC
prt6-5	Ub-R_{6-2}-LUC
prt6-5	Ub-F_{3-1}-LUC
big prt6-5	Ub-L_{3-1}-LUC
big prt6-5	Ub-M_{1-2}-LUC
big prt6-5	Ub-R_{9-2}-LUC
big prt6-5	Ub-R_{6-2}-LUC
big prt6-5	Ub-F_{3-1}-LUC
WT	Ub-L_{3-1}-LUC
WT	Ub-M_{1-2}-LUC
WT	Ub-R_{9-2}-LUC
WT	Ub-R_{6-2}-LUC
WT	Ub-F_{3-1}-LUC

Because the T-DNA coding for the Ub-X-LUC reporter was still segregating in the *prt6-5*, *big* and *big prt6-5* mutant backgrounds, seedlings were grown on 0.5x MS supplemented with Basta to select for lines that carried at least one copy of the reporter construct (Section 2.2.3.1). For each reporter line, ten seedlings (10-day old) were collected, pooled and frozen in liquid nitrogen. Total proteins were extracted and LUC and GUS enzymatic assays were performed (Section 2.1.5.1). In addition, the total protein concentration in the extracts was measured using the Bradford assay. The LUC activity was calculated as luminescence/second/µg of total protein. When possible, GUS measurements were used in order to normalize the LUC activity, thus allowing us to correct for the fact that the T-DNA coding for the N-end rule reporter constructs were still segregating in the mutant backgrounds, while they were all homozygous in the parental wild-type lines. After measuring all the LUC and GUS activities, I compared the levels between the different mutant backgrounds and the wild-type. As indicated below, in some cases, the levels of GUS activity were very low, suggesting that the GUS gene that is under the control of the 35S promoter was

being silenced. This effect has been observed several times in the lab with other mutants than those used in this work. Hence, when GUS silencing occurred, I compared LUC activities without any normalization.

For the M-LUC reporter lines, the levels of LUC activity were measured in *big, big prt6-5* and wild type backgrounds (the seeds for the *prt6-5* mutant did not germinate (Table 5.1)). In agreement with the fact that N-terminal Met is a stabilizing residue, the level of M-LUC were high in all 3 genotypes (FIGURE 5.2). Unfortunately, the GUS activity levels were very low in the *big* and *big prt6-5* mutant backgrounds, so I could not normalize the data. Nevertheless, the levels of M-LUC were comparable across the 3 genotypes, implying that in the *big* and *big prt6-5* mutant backgrounds, the stability of M-LUC is not altered. This needs to be confirmed with additional biological replicate (the results below are the result of a single experiment).

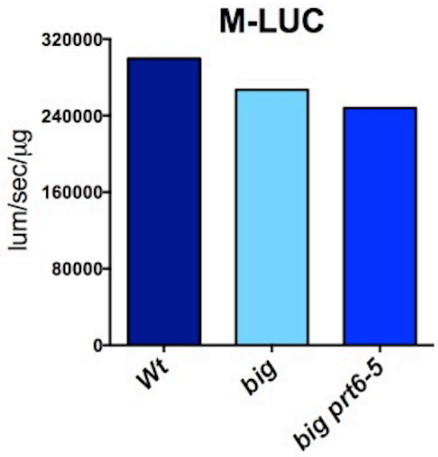

FIGURE 5.2. LUC activity in *big, prt6-5, big prt6-5* and wild type seedlings coding for the Ub-M-LUC reporter. For each genetic background, 10 seedlings (10-day old) were pooled for protein extraction and enzymatic assays. For the M-LUC reporter, the *prt6-5* mutant was not available for analysis due to germination problems. Data originates from only one biological replicate and is hence only preliminary.

I conducted the same experiments for plants expressing the F-LUC reporter construct, which is known to be targeted for degradation by the PRT1 N-recognin. With this reporter, the level of F-LUC was low in all 4 genetic backgrounds (FIGURE 5.3), with no significant differences between each of the genotypes. For this reporter, the levels of GUS activity were comparable across the 3 genotypes, so I was able to

normalize the LUC activities (FIGURE 5.3). While there are some small differences between *big*, *prt6-5* and the wild-type, they are probably not significant. Additional replicates need to be performed before any conclusions can be drawn. At this stage, though, the preliminary data suggest that neither BIG nor PRT6 are likely to play a role in regulating the stability of proteins bearing F at their N-terminus. Based on the literature, this result was to be expected with PRT6 (Garzon *et al*., 2007).

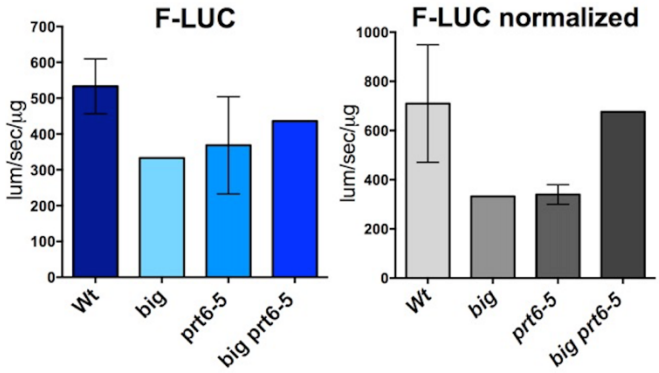

FIGURE 5.3. LUC activity in *big, prt6-5, big prt6-5* and wild type seedlings coding for the Ub-F-LUC reporter. For each genetic background, 10 seedlings (10-day old) were pooled for protein extraction and enzymatic assays. Data originates from only one biological replicate, except for the wild type and *prt6-5* backgrounds for which 2 replicates were analysed. The error bar represents the standard deviations.

As indicated above, BIG has a UBR domain, which is typically responsible for the recognition of substrates with basic N-terminal residues, such as Arg. I hence also tested if the stability of an R-LUC reporter could be affected in the *big* mutant background, as well as in *prt6-5* and *big prt6-5*. As expected based on the known specificity of PRT6 (Garzon *et al*., 2007), I found that R-LUC activity was much higher in the *prt6-5* mutant background. In contrast, it was similar in *big* mutant seedlings and in the wild type (FIGURE 5.4). To my surprise, however, in *big prt6-5* double mutant seedlings, the levels R-LUC activity were higher than those measured in a single *prt6-5* mutant (FIGURE 5.4). This suggests that in the absence of both BIG and PRT6 activities, N-end rule substrates with N-terminal Arg are much more stable than in a *prt6-5* single mutant. Hence, BIG may play a role in regulating the stability of such substrates. The effect may have been hidden in the *big* mutant background because PRT6 is still active and could indirectly rescue the lower BIG activity. I also attempted to normalize the LUC activities using the GUS normalization cassette.

Unfortunately, I could not do so in the *big prt6-5* mutant, because the GUS gene was silenced. The normalized data nevertheless confirmed that R-LUC is stabilized in a *prt6-5* mutant background, but not in a *big* single mutant (FIGURE 5.4).

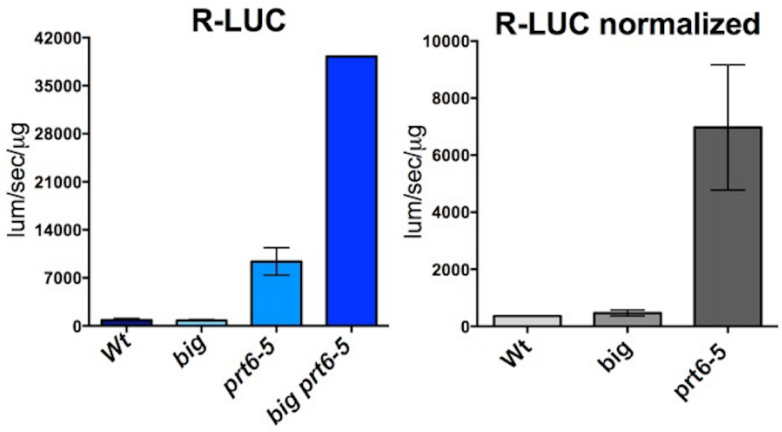

FIGURE 5.4. LUC activity in *big, prt6-5, big prt6-5* and wild type seedlings coding for the Ub-R-LUC reporter. For each genetic background, 10 seedlings (10-day old) were pooled for protein extraction and enzymatic assays. Data originates from two biological replicates, except for the *big prt6-5* background for which only one replicate was analysed. The error bars represent standard deviations.

Finally, I tested the effect of the *big* mutant on the stability of the L-LUC N-end rule reporter. Unfortunately, the *big prt6-5* double mutant expressing L-LUC reporter did not germinate, so that I could not obtain these results. As expected, the levels of L-LUC activity are low in wild type and *prt6-5* (FIGURE 5.5), confirming that (i) N-terminal Leu is a destabilizing residue (Graciet *et al*., 2010); and (ii) that PRT6 does not target substrates with N-terminal Leu for degradation (Garzon *et al*., 2007). Notably, the L-LUC activity in the *big* mutant background was slightly higher than in the wild type and in *prt6-5* mutant seedlings (FIGURE 5.5). When the data was normalized using the GUS activities, no differences between WT and *big* were observed. Note however, that the GUS activities were very variable, which needs to be further investigated before any conclusion can be drawn (FIGURE 5.5). It might be possible that BIG plays a role in degradation of proteins starting with Leu, but it is unlikely to be the main N-recognin for this residue as the level of L-LUC activity in *big* is only slightly higher than in the wild type. Additional biological replicates are required to confirm this hypothesis.

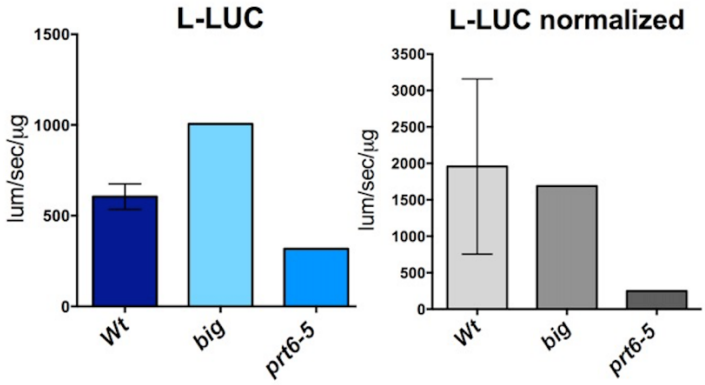

FIGURE 5.5. LUC activity in *big, prt6-5, big prt6-5* and wild type seedlings coding for the Ub-L-LUC reporter. For each genetic background, 10 seedlings (10-day old) were pooled for protein extraction and enzymatic assays. Data originates from one biological replicate, except for the wild type for which two replicates were analysed. The error bars represent the standard deviations. For L-LUC reporter the *big prt6-5* double mutant was not available for analysis due to poor germination of the seeds.

In sum, the preliminary data I have obtained at this stage suggests that BIG may contribute to the PRT6-dependent degradation of the R-LUC reporter, and hence by extension, of other substrates starting with a basic amino acid residue. However, these experiments do not provide any information as to the underlying mechanisms. Most of the data presented is also preliminary and needs to be verified by adding additional independent replicates (at least 3 for each line).

5.3. Is there a genetic interaction between *BIG* and *PRT6*?

The biochemical data I have obtained indicate that BIG and PRT6 may act together to target for degradation proteins that bear Arg at their N-terminus. In addition, data obtained by F. Walter (Walter, 2010), a previous student in the lab suggested that some phenotypes of a *big* mutant were enhanced in a *big prt6-5* double mutant background. However, a detailed characterization of the double mutant had not been performed. Here, I characterized the *big prt6-5* double mutant at different developmental stages to obtain additional information on the potential role of BIG in the N-end rule pathway.

5.3.1 Vegetative development

For the characterization of the early developmental stages of the *big*, *prt6-5*, *big prt6-5* and wild-type plants, seeds were sown on a medium containing compost, perlite and vermiculite in the following ratios 5:2:3 as described in Section 2.1.2.1. After 3 days at 4°C, the plants were transferred to short-day conditions (9 hrs light/15 hrs dark; 20°C; Section 2.1.2.1). I then checked every day for the emergence of the cotyledons and recorded the number of days it took for the cotyledons to be visible. After germination, seedlings were either kept on the germination medium mentioned above or were transferred to jiffy pots, as they are easier to handle to take pictures. As observed in FIGURE 5.6, the appearance of the cotyledons in *big*, *prt6-5* and *big prt6-5* mutant plants was delayed by about one day compared to wild-type seedlings. The difference was small but consistent across 2 biological replicates. Considering this minor delay, it seems that BIG does not play a major role in the regulation of germination and early seedling development in the growth conditions applied.

Two weeks after the cotyledons emerged, based on the picture that I have taken I compared the number of leaves and rosette size of the different genotypes and found no obvious differences (FIGURE 5.6), except that the petiole of *big* and *big prt6-5* mutant plants seemed to be shorter (red arrow) compared with *prt6-5* and wild-type (white arrow) plants. This suggests that *BIG* may play a role in petiole elongation, but more quantitative data is necessary to ascertain this possibility.

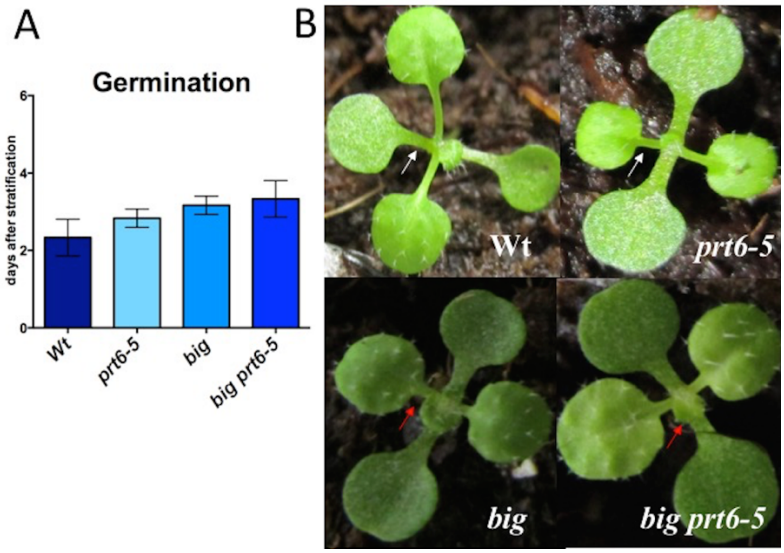

FIGURE 5.6. Cotyledon emergence time and early stages of development in *big*, *prt6-5*, *big prt6-5* and wild-type plants. A. After 3 days at 4°C, trays were transferred to short-day conditions (9 hrs light/15 hrs of dark) at 20°C. Days needed for cotyledon emergence were noted. Two biological replicates were analysed. For each biological replicate ~40 seedlings were used. The error bars represent standard deviations. **B.** At 2 weeks after germination, pictures of individual *big*, *prt6-5*, *big prt6-5* and wild type representative plants were taken. Note that the petioles of the first 2 true leaves appears to be shorter in *big* and *big prt6-5* mutants.

At 5 weeks after the emergence of the cotyledons, clear differences between the *big*, *prt6-5*, *big prt6-5* and wild-type plants were visible. Based on the picture that I have taken, the number of leaves between the 4 genotypes was not markedly different, but the size of both the leaf blades and petioles were smaller in *big* and *big prt6-5* compared with *prt6-5* and wild type. This confirms the previous observation that BIG is important for leaf and petiole development (Kanyuka *et al*., 2003). At this developmental stage, it was however difficult to see differences between *big* and *big prt6-5* double mutant (FIGURE 5.7).

FIGURE 5.7. Five-week old wild type, *prt6-5, big* and *big prt6-5* plants. After 3 days at 4°C, trays were transferred to short-day conditions (9 hrs light/15 hrs of dark) at 20°C. Seedlings were then transferred either to Jiffy pots (A) or to soil (B). Pictures of representative plants were taken 5 weeks after cotyledon emergence.

5.3.2 Reproductive development

At later stages of development, the differences between *big*, *prt6-5*, *big prt6-5* mutants and wild type plants were more pronounced. At 8 weeks after cotyledon emergence, *prt6-5* mutant plants were comparable to the wild type and had transitioned to flowering. In contrast, the *big* and *big prt6-5* mutants were still forming rosette leaves (FIGURE 5.8). Later on, at 10 weeks after cotyledon emergence, *big* and *big prt6-5* mutants started to show signs of flowering (FIGURE 5.8). Hence, these observations suggest that *BIG* plays a role in the transition from vegetative stage to flowering.

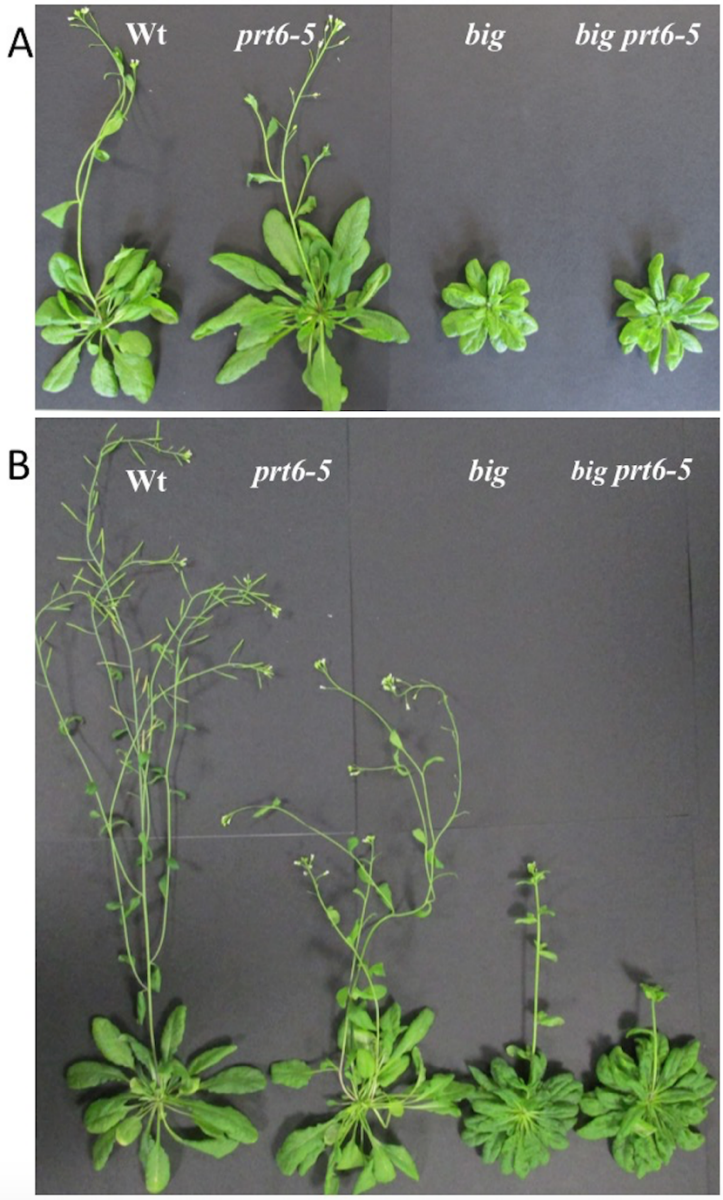

FIGURE 5.8. Characterization of 8-week old (A) and 10-week old (B) wild type, *prt6-5, big* and *big prt6-5* plants. After 3 days at 4 °C, trays were transferred to short-day growth room (9 hrs light/15 hrs of dark) at 20°C. At 8 (A) and 10 (B) weeks after cotyledon emergence, pictures were taken in order to observe the transition from vegetative stage to flowering for *big*, *prt6-5* and *big prt6-5* mutants.

In order to have a more quantitative assessment of the delay in flowering between the different genotypes, I recorded the number of days it took from cotyledon emergence until the main inflorescence started to be visible (FIGURE 5.9). The results indicate that the *big prt6-5* double mutant plants are significantly delayed compared to wild-type, and also compared to the *big* and *prt6-5* single mutants. This would suggest a synergistic interaction between *prt6-5* and *big*, as the phenotype is

much stronger than in either of the 2 parents. One potential problem with this method of scoring flowering time, though, is that with plants that have stem elongation defects, which is the case for *big* and *big prt6-5* mutant plants, the delay in flowering may simply be linked to the delay it takes for the main inflorescence to become visible due to reduced elongation. This would not correspond to a genuine delay in the transition from vegetative to reproductive development.

To overcome this potential problem, I estimated flowering time by counting the number of rosette and cauline leaves. In this case, the total number of leaves formed (number of rosette and cauline leaves) correlates with how long it takes for a plant to transition to flowering, after which, leaves are no longer initiated by the apical meristem. At 10 weeks after cotyledon emergence, the stem was removed and the number rosette and cauline leaves was counted for all 4 genotypes (FIGURE 5.9). I then analysed the differences in the total number of leaves initiated before flowering in each of the genotypes. In this analysis, the wild type and *prt6-5* formed about the same number of leaves before flowering, suggesting that they flowered around the same time. In contrast, the differences were statistically significant for the wild type versus *big* and *big prt6-5*. This confirms that both *big* and *big prt6-5* mutants have delayed flowering compared to the wild-type. Notably, the differences between *big* and *big prt6-5*, or between *prt6-5* vs *big prt6-5* were also statistically significant. These results strengthen the idea that BIG and PRT6 could act synergistically to regulate flowering time. However, these results were obtained from one biological replicate only, so additional experiments are needed to confirm this result.

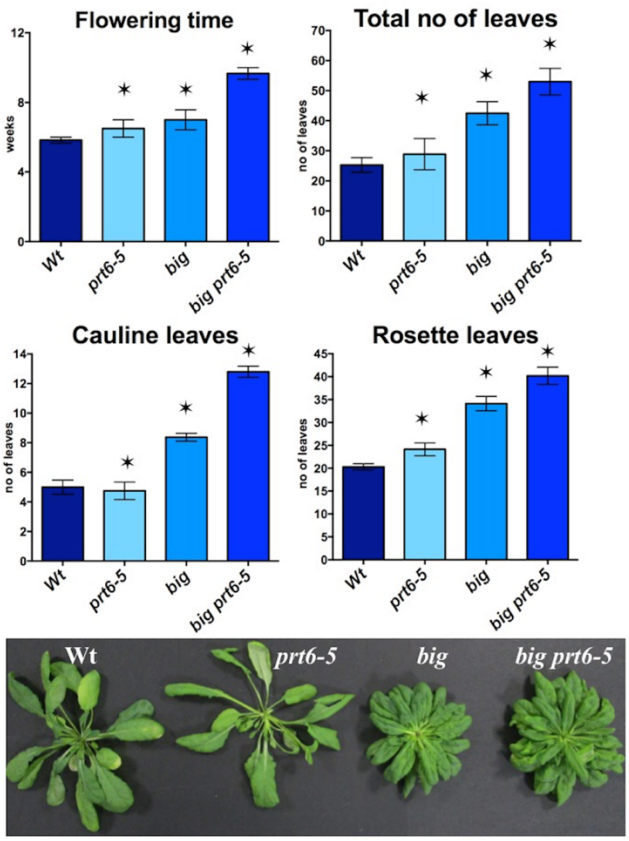

FIGURE 5.9. Determination of flowering time in *big*, *prt6-5*, *big prt6-5* and wild-type plants. After 3 days at 4 °C for stratification, plants were transferred in short-day growth room (9 hrs light/15 hrs of dark) at 20°C. Each tray contained 8 pots. For each pot, 3 plants were kept for further analysis. Flowering time was recorded for each genotype based on the number of days it took from cotyledon emergence to a visible inflorescence ('flowering time'). For each genotype ~15 plants were scored. In addition, for each genotype, rosette and cauline leaves were counted. Due to problems with the germination of *big prt6-5* and a low seed stock, for the leaf numbers, 5 plants were used for *big prt6-5*, 8 plants for *big* and *prt6-5*, and 10 plants for the wild type. The error bars represent standard deviations. Only one biological replicate was analysed. Statistical significance for the differences observed between *big* vs *big prt6-5* and *prt6-5* vs *big prt6-5* were calculated at $p<0.05$ and are labelled with a star.

Based on the phenotypic characterization, it seems that *BIG* plays a role in the transition from vegetative development to flowering, and in the absence of *BIG*, the

transition is delayed. Also, it is likely that there is a synergistic interaction between *BIG* and *PRT6* in the control of flowering time.

5.5 Discussion

The use N-end rule reporter lines indicates that N-end rule reporter constructs with N-terminal Arg are more stable in a *big prt6-5* mutant background compared to a *prt6-5* single mutant. This was unexpected because so far, PRT6 was thought to be the only N-recognin having the ability to target proteins with N-terminal basic destabilizing residues in plants. The data I have obtained needs to be confirmed with additional replicates. Notably, though, the phenotypic characterization of a *big prt6-5* mutant also suggests that *BIG* and *PRT6* may act synergistically to regulate flowering time. This genetic interaction strengthens the idea of a functional connection between *BIG* and *PRT6*.

It is unclear at this stage how BIG and PRT6 could cooperate to destabilize proteins that start with the primary destabilizing residue Arg. One possibility is that BIG acts as a true N-recognin and binds N-terminal Arg residues via its UBR domain, similarly to PRT6 and mammalian UBR4, the putative BIG ortholog. It is surprising in this case that a *big* single mutant is not affected for the degradation of R-LUC. However, that could simply due to the fact that PRT6 plays a more dominant role in seedlings for the degradation of this reporter, so that the effects of a *big* mutant are masked. Another possibility is that BIG and PRT6 act together on R-LUC reporters, but that BIG's role is not dependent on its UBR domain. It would hence be interesting to test if the synergistic effect of *big* and *prt6* could be rescued by re-introducing full-length *BIG* or a truncated version of *BIG* in which the UBR domain is deleted. Unfortunately, the large size of the *BIG* coding region makes such experiments extremely challenging.

Regarding the synergistic interactions between *big* and *prt6-5* in the regulation of flowering time, it is difficult to point to a particular pathway that may be regulated by both genes in a synergistic manner. It is known that GA signalling is important to mediate the transition to flowering in short day conditions (Xu *et al*., 1997). It was shown that mutations in *BIG* negatively affect plant response to exogenous GA (Desgagne-Penix *et al*., 2015). Auxin is required for GA20-oxidation (Desgagne-Penix *et al*., 2015), a limiting step in GA biosynthesis (Coles *et al*., 1999; Huang *et al*., 1998). It might be possible that the crosstalk between auxin and gibberellin is

affected in *big* mutants and this could contribute to delayed flowering. Interestingly, it was previously shown that the shorter stem and leaf morphology defects of *ate1 ate2* double mutant plants could be rescued by GA treatment. Because *prt6-5* plants show similar phenotypes and PRT6 acts downstream of the Arg-transferasess, one could speculate that there could also be a link between *PRT6* and GA signalling. Additional experiments are needed to test if there is a synergistic role between *PRT6* and *BIG* in GA signalling (e.g. GA signalling mutants such as DELLA genes, that encodes for GA repressors (Sun *et al*., 2008)). This could be addressed using a genetic interaction analysis with mutant affected for GA synthesis and GA levels. The expression of GA response genes could also be monitored in the different mutant backgrounds (i.e. *big*, *prt6-5* and *big prt6-5*).

The other mutant phenotype I observed in *big* and *big prt6-5* mutants was a short petiole, which suggests that *BIG* could play many roles in plant growth at different stages of development. At early stages of plant development is could play a positive role in petiole and leaf growth. The latter effect could be due to defects in auxin concentrations and transport (Guo *et al*., 2013), which have been previously described for a *big* mutant.

One important result obtained with the mammalian ortholog of BIG - UBR4 - is that this protein is also involved in autophagy (Tasaki *et al*., 2013). Hence one key question that also needs to be addressed is whether BIG also acts through the autophagy pathway in plants.

6. Discussion and future work

The main aim of my PhD project was to identify commercial winter barley varieties that are tolerant to waterlogging. This information may be particularly relevant in the context global climate change in Ireland, as well as in other areas of the Northern hemisphere, because rainfall is forecasted to increase in these regions, especially during the winter. While field experiments are more appropriate to assess crop performance, the first preliminary results I obtained in waterlogging field experiments highlighted a number of issues. One of the main problems I encountered was the difficulty in applying the waterlogging stress in a homogenous and consistent manner for a prolonged period of time across different plots. Due to this limitation, it was very difficult to select sensitive and tolerant varieties. In addition, in the field, a range of both biotic and abiotic factors were combined, which increased the variability of the results and the difficulties in assessing the sensitivity or tolerance to waterlogging.

To overcome these limitations, I focused on establishing a reliable waterlogging protocol in controlled conditions. This protocol was also developed to allow for the rapid screening of a large number of varieties that could be analysed in a shorter period of time compared to field experiments. The results I have obtained with this protocol allowed me to identify parameters that could be monitored in order to assess the response of different barley cultivars. Early-stage parameters or responses showed changes and differences among varieties during the waterlogging treatment or within days after the onset of waterlogging. These include (i) the induction of hypoxia-core genes (Hv*ADH1*, Hv*HB* and Hv*PDC1*) at 24 hours after the beginning of waterlogging; and (ii) changes in the root architecture at 15 days after the onset waterlogging. In contrast, late-stage parameters appeared to be relevant during the recovery period (typically at 6 weeks after the end of waterlogging treatment), including height, number of tillers, chlorosis and necrosis.

Because it takes up to 8 weeks (2 weeks of waterlogging and 6 weeks of recovery) to observe changes in parameters that are directly linked to yield (e.g number of tillers), in order to increase the efficiency of the selection process, it would be ideal to find parameters that are affected at an early stage and that are good indicators of the waterlogging tolerance and subsequent yield. For this strategy to work reliably, baselines and thresholds also need to be clearly defined, which would

require a larger number of varieties to assess the different parameters. In addition, using the protocol I developed, it would be important to perform statistical analyses to determine (i) if there is a correlation between early-stage and late-stage parameters; and (ii) which early-stage parameters are the best predictors for waterlogging tolerance and yield performance. This will be a priority in the future.

To complement the phenotypic and molecular characterization of the different barley cultivars in response to waterlogging under controlled conditions, I also conducted transcriptomics experiments to gain insights into pathways or genes that may be differentially regulated among a presumed tolerant variety (Pilastro) and a presumed sensitive variety (Passport). I also included a 'model' variety that is used for transformation, Golden promise. Due to the fact that this experiment was performed in the last months of my PhD, only a general analysis was conducted on the RNA-Seq datasets. Nevertheless, it appears that in the 3 varieties used, there are some 'core' waterlogging response genes that are regulated in response to the stress. Most of the hypoxia-response genes are present within these 'core' genes, which serves as a validation for our datasets. In the future, it will be important to determine if the gene expression changes are similar both in amplitude and directionality within this 'core' subset of DEGs. Notably, there were also differences between the 3 varieties tested. For example, the number of DEGs in response to waterlogging differs greatly, with Golden Promise presenting fewer DEGs compared to Pilastro and Passport. In addition, among the list of DEGs in Pilastro, there were genes associated with GO categories that are not over-represented among the DEGs identified in Golden Promise or Passport. Future work will focus on analyzing more in detail these particular sets of genes to determine if they could be associated with processes that would confer an increased waterlogging tolerance to Pilastro compared to Passport. In addition, as the RNA-Seq analysis was performed using plants that were waterlogged for 24 hours, this approach may allow the identification of new early-stage parameters that can be used further to identify tolerant varieties.

Another part of my PhD project focused on isolating barley plants that were affected for the activity of the Arg-transferase Hv*ATE1*, and to characterize their response to waterlogging. The first approach I used to generate Hv*ATE1* mutant plants was based on the isolation of TILLING mutant lines in the Barke variety. As mentioned before, one main advantage of the TILLING approach is that the resulting plants are not considered as transgenic. Although I was able to identify plants that

carried mutations in Hv*ATE1*, none of the mutant lines identified, either homozygous or heterozygous, transitioned to flowering. The problem encountered prevented me from propagating the lines and out-crossing them to the wild-type parent. It is unclear at this stage whether the problems to transition to reproductive development were due to other mutations in the background or to the mutation in Hv*ATE1*. The latter is rather unlikely, considering that barley plants homozygous mutant for Hv*PRT6*, the E3 ligase that acts downstream of the Arg-transferase, can be propagated (Mendiondo *et al*., 2016). The second approach I used to generate plants mutant for Hv*ATE1* relied on the use of the CRISPR/Cas9 system. I designed two targeting constructs and confirmed that the sgRNA sequences used could guide Cas9 to the Hv*ATE1* sequence. However, despite repeated attempts (not all attempts have been discussed above), I was not able to optimize the immature embryo transformation procedure. To overcome this problem, the two constructs were sent to BRACT (John Innes Centre) for barley transformation. Eleven primary transformants for the Hv*ATE1v1* construct and 4 primary transformants for the Hv*ATE1v2* construct have been isolated, and will be further characterized in the future.

As indicated above, the N-end rule pathway is a central regulator of plant responses to waterlogging. Although much progress has been made in recent years and many of its enzymatic components in plants have been identified, several questions remain unanswered. For example, the genome of plants, including *Arabidopsis*, code for additional proteins that contain the UBR domain, which is involved in binding proteins that have a basic N-terminal residue (Tasaki *et al*., 2005). One of the proteins, named BIG, has sequence similarities with mouse UBR4, a known N-recognin (Tasaki *et al*., 2005). During my PhD, I focused on answering several questions relevant to our understanding of BIG. One of the main questions was: is BIG an N-recognin in plants? To answer this question, I used a set of N-end rule reporter constructs to monitor the effect of a *big* mutant background on the stability of different N-end rule reporter proteins. The preliminary results obtained so far indicate that N-end rule reporter constructs with N-terminal Arg are more stable in a *big prt6-5* mutant background compared to a *prt6-5* single mutant, suggesting that both BIG and PRT6 may be involved in recognizing N-terminal basic residues. This was unexpected, because so far, PRT6 was thought to be the only N-recognin with the ability to target proteins with N-terminal basic destabilizing residues in plants. The data I have obtained needs to be confirmed with additional replicates. It

is also known that N-terminal Leu and Ile are destabilizing residues in plants (Graciet *et al*., 2010), but the N-recognin responsible for their detection is not known. During my PhD, I also aimed at testing if BIG could be the N-recognin specific for N-terminal Leu, using the same set of N-end rule reporter constructs mentioned above. Based on the results obtained so far, BIG seems to have a minor effect on the stability of proteins bearing Leu at their N-terminus, but it is unlikely to be the main N-recognin involved in this process. The data I have obtained also needs to be confirmed with additional replicates.

It remains unknown how BIG and PRT6 could cooperate to destabilize proteins that start with the primary destabilizing residue Arg. One possibility is that BIG acts as a true N-recognin and binds N-terminal Arg residues *via* its UBR domain, similarly to PRT6 and mammalian UBR4, the putative BIG ortholog. It is surprising in this case that a *big* single mutant is not affected for the degradation of R-LUC. However, that could simply due to the fact that PRT6 plays a more dominant role in seedlings for the degradation of this reporter, so that the effects of a *big* mutant may be masked. Another possibility is that BIG and PRT6 act together on R-LUC reporters, but that BIG's role is not dependent on its UBR domain. In order to assess the role of BIG and of its different domains in regulating the stability of proteins bearing Arg at their N-terminus, it would be interesting to transform *big* mutant plants with transgenes containing different versions of *BIG*, that contain different domains, and to assess the N-end rule reporter stability in each of the transformed lines. Unfortunately, the large size of the *BIG* coding region makes such experiments extremely challenging. It is also possible that BIG and PRT6 form a complex together, although this needs to be verified and examined carefully.

Another question that I aimed at answering during my PhD was 'could *BIG* and *PRT6* have synergistic or overlapping functions?'. Indeed, previous work carried out in the lab (Walter, 2010) indicated that there may be a synergistic interaction between *BIG* and *PRT6*. To verify this, I performed a more detailed phenotypic comparison of *big*, *prt6-5*, *big prt6-5* and wild-type plants. At early stages of development, I observed that *big* and *big prt6-5* mutants had shorter petioles compared to *prt6-5* and wild-type plants, suggesting that *BIG* could play a positive role in petiole and leaf growth. The leaf growth phenotype could be due to defects in auxin concentration and transport (Guo *et al*., 2013), which have been previously described for a *big* mutant. At later stages of development, I observed that *big prt6-5*

double mutant plants appeared to have a delayed flowering phenotype under short-day conditions, which was not as pronounced in each of the 2 parents. This would suggest that *BIG* and *PRT6* could act together to control the transition to flowering. This genetic interaction strengthens the idea of a functional connection between *BIG* and *PRT6*, at least in the context of some developmental processes. It is however difficult to point to a particular pathway that may be regulated by both genes in a synergistic manner. Due to the fact that BIG is such a large protein and that different *big* alleles are affected for their sensitivity to a wide range of hormones, it is difficult to conclude if one specific hormone signalling pathway is involved in this process or if multiple hormone signalling pathways result in the delayed flowering phenotype of the *big prt6-5* double mutant. For example, GA signalling is important to mediate the transition to flowering in short-day conditions (Xu *et al*., 1997). Plants with mutations in *BIG* have reduced sensitivity to exogenous GA (Desgagne-Penix *et al*., 2015). It is known that auxin is required for GA20-oxidation (Desgagne-Penix *et al*., 2015), a limiting step in GA biosynthesis (Coles *et al*., 1999; Huang *et al*., 1998). Hence, it may be possible that the delays in flowering could be due to the crosstalk between auxin and GA being affected in *big* mutants. Notably, it was shown that the stem and leaf morphology defects of *ate1 ate2* double mutant plants could be rescued by GA treatment (Graciet *et al*., 2009). Since PRT6 acts downstream of the Arg-transferases, there may also be a link between *PRT6* and GA signalling, which could contribute to the synergistic interaction between *big* and *prt6-5*. Additional experiments are needed to test if there is a synergistic role between *PRT6* and *BIG* in the context of GA signalling. This could be addressed by monitoring the response of *prt6-5*, *big* and *big prt6-5* mutant plants to exogenous GA treatment (e.g. by monitoring the expression of specific GA-regulated genes). Another interesting trait worth assessing in *big prt6-5* compared to *big* and *prt6-5* would be the response to waterlogging and hypoxia. Indeed, the data obtained with the N-end rule reporter constructs suggest that a *big prt6-5* double mutant accumulates to a much higher level proteins that start with an Arg. This would be the case for the ERF-VII transcription factors that act as master regulators of hypoxia and waterlogging response. It is therefore possible that these transcription factors accumulate to higher levels in the *big prt6-5* double mutant compared to the *prt6-5* single mutant (Gibbs *et al*., 2011), thus possibly conferring a higher level of tolerance to waterlogging.

7. References

Abiko, T., and Obara, M. (2014). Enhancement of porosity and aerenchyma formation in nitrogen-deficient rice roots. Plant Sci 215-216, 76-83.

Altschul, S.F., Madden, T.L., Schäffer, A.A., Zhang, J., Zhang, Z., Miller, W. and Lipman, D.J., 1997. Gapped BLAST and PSI-BLAST: a new generation of protein database search programs. Nucleic acids research, 25, 3389-02.

Armstrong, J.J., RE.; Armstrong, W. (2006). Rhizome phyllosphere oxygenation in Phragmites and other species in relation to redox potential, convective gas flow, submergence and aeration pathways. New Phytol. 172, 719-731.

Armstrong, W. (1979). Aeration in higher plants. Adv. Bot. Res 7, 225-232.

Armstrong, W.a.D., M. (2002). Root growth and metabolism under oxygen deficiency. Plant Roots: The Hidden Half, 729-761.

Arora, K., Panda, K.K., Mittal, S., Mallikarjuna, M.G., Rao, A.R., Dash, P.K. and Thirunavukkarasu, N., 2017. RNAseq revealed the important gene pathways controlling adaptive mechanisms under waterlogged stress in maize. Scientific reports, 7, 10950.

Ashikari, M., Sasaki, A., Ueguchi-Tanaka, M., Itoh, H., Nishimura, A., Datta, S., Ishiyama, K., Saito, T., Kobayashi, M., Khush, G.S. and Kitano, H., 2002. Loss-of-function of a rice gibberellin biosynthetic gene, GA20 oxidase (GA20ox-2), led to the rice 'green revolution'. Breeding Science, 52, 143-50.

Aurisano, N.B., A.; Reggiani, R. (1995). Involvement of calcium and calmodulin in protein and amino acid metabolism in rice roots under anoxia. Plant Cell Physiol. 36, 1525-1529.

Bachmair, A., and Varshavsky, A. (1989). The degradation signal in a short-lived protein. Cell 56, 1019-1032.

Bachmair, A., Becker, F., and Schell, J. (1993). Use of a reporter transgene to generate arabidopsis mutants in ubiquitin-dependent protein degradation. Proc Natl Acad Sci U S A 90, 418-421.

Bachmair, A., Finley, D., and Varshavsky, A. (1986). In vivo half-life of a protein is a function of its amino-terminal residue. Science 234, 179-186.

Bailey-Serres, J., and Voesenek, L.A. (2008). Flooding stress: acclimations and genetic diversity. Annu Rev Plant Biol 59, 313-339.

Bailey-Serres, J., and Voesenek, L.A. (2010). Life in the balance: a signaling network controlling survival of flooding. Curr Opin Plant Biol 13, 489-494.

Bailey-Serres, J., Fukao, T., Gibbs, D.J., Holdsworth, M.J., Lee, S.C., Licausi, F., Perata, P., Voesenek, L.A., and van Dongen, J.T. (2012). Making sense of low oxygen sensing. Trends Plant Sci 17, 129-138.

Baker, R.T. and Varshavsky, A., 1995. Yeast N-terminal Amidase A NEW ENZYME AND COMPONENT OF THE N-END RULE PATHWAY. Journal of Biological Chemistry, 270, 12065-74.

Balzi, E., Choder, M., Chen, W.N., Varshavsky, A., and Goffeau, A. (1990). Cloning and functional analysis of the arginyl-tRNA-protein transferase gene ATE1 of Saccharomyces cerevisiae. J Biol Chem 265, 7464-7471.

Banti, V., Giuntoli, B., Gonzali, S., Loreti, E., Magneschi, L., Novi, G., Paparelli, E., Parlanti, S., Pucciariello, C., Santaniello, A., et al. (2013). Low oxygen response mechanisms in green organisms. Int J Mol Sci 14, 4734-4761.

Beligni, M.V., Fath, A., Bethke, P.C., Lamattina, L., and Jones, R.L. (2002). Nitric oxide acts as an antioxidant and delays programmed cell death in barley aleurone layers. Plant Physiol 129, 1642-1650.

Belzil, C., Asada, N., Ishiguro, K.I., Nakaya, T., Parsons, K., Pendolino, V., Neumayer, G., Mapelli, M., Nakatani, Y., Sanada, K. and Nguyen, M.D., 2014. p600 regulates spindle orientation in apical neural progenitors and contributes to neurogenesis in the developing neocortex. Biology open, 3, 475-85.

Besson-Bard, A., Pugin, A., and Wendehenne, D. (2008). New insights into nitric oxide signaling in plants. Annu Rev Plant Biol 59, 21-39.

Bhaya, D., Davison, M. and Barrangou, R., 2011. CRISPR-Cas systems in bacteria and archaea: versatile small RNAs for adaptive defense and regulation. Annual review of genetics, 45, 273-97.

Bouranis, D.L., Chorianopoulou, S.N., Siyiannis, V.F., Protonotarios, V.E., and Hawkesford, M.J. (2003). Aerenchyma formation in roots of maize during sulphate starvation. Planta 217, 382-391.

Bradshaw, R.A., Brickey, W.W., and Walker, K.W. (1998). N-terminal processing: the methionine aminopeptidase and N alpha-acetyl transferase families. Trends Biochem Sci 23, 263-267.

Branco-Price, C., Kaiser, K.A., Jang, C.J., Larive, C.K., and Bailey-Serres, J. (2008). Selective mRNA translation coordinates energetic and metabolic adjustments to cellular oxygen deprivation and reoxygenation in Arabidopsis thaliana. Plant J 56, 743-755.

Bui, L.T., Giuntoli, B., Kosmacz, M., Parlanti, S., and Licausi, F. (2015). Constitutively expressed ERF-VII transcription factors redundantly activate the core anaerobic response in Arabidopsis thaliana. Plant Sci 236, 37-43.

Callis, J., Carpenter, T., Sun, CW., Vierstra RD. (1995). Structure and evolution of

genes encoding polyubiquitin and ubiquitin-like proteins in *Arabidopsis thaliana* ecotype Columbia. Genetics 139, 921–939.

Ciechanover, A., Elias, S., Heller, H. & Hershko, A. (1982). "Covalent affinity" purification of ubiquitin activating enzyme. J. Biol. Chem. 257**,** 2537–2542.

Chitturi, J., Hung, W., Rahman, A.M.A., Wu, M., Lim, M.A., Calarco, J., Baran, R., Huang, X., Dennis, J.W. and Zhen, M., 2018. The UBR-1 ubiquitin ligase regulates glutamate metabolism to generate coordinated motor pattern in Caenorhabditis elegans. PLoS genetics, 14, 1007303.

Choi, W.S., Jeong, B.C., Joo, Y.J., Lee, M.R., Kim, J., Eck, M.J. and Song, H.K., 2010. Structural basis for the recognition of N-end rule substrates by the UBR box of ubiquitin ligases. Nature structural & molecular biology, 17, 1175.

Christianson, J.A., Llewellyn, D.J., Dennis, E.S., and Wilson, I.W. (2010). Global gene expression responses to waterlogging in roots and leaves of cotton (Gossypium hirsutum L.). Plant Cell Physiol 51, 21-37.

Christopher, M.E., and Good, A.G. (1996). Characterization of Hypoxically Inducible Lactate Dehydrogenase in Maize. Plant Physiol 112, 1015-1022.

Chung, H.F., RJ. (1999). Arabidopsis alcohol dehydrogenase expression in both shoots and roots is conditioned by root growth environment. . Plant Physiol 121, 429-436.

Ciechanover, A.F., S.; Ganoth, D.; Elias, S.; Hershko, A.; Arfin, S. (1988). Purification and Characterization of Arginyl-tRNA-Protein Transferase from Rabbit Reticulocytes. The Journal of Biological Chemistry 263, 11155-11167.

Colmer, T.D. (2003). Aerenchyma and an inducible barrier to radial oxygen loss facilitate root aeration in upland, paddy and deep-water rice (Oryza sativa L.). Ann Bot 91 Spec No, 301-309.

Colmer, T.D.a.V., L.A.C.J. (2009). Flooding Tolerance: Suites of Plant Traits in Variable Environments. Functional Plant Biology, 665-681.

Conrad, R., and Klose, M. (1999). Anaerobic conversion of carbon dioxide to methane, acetate and propionate on washed rice roots. FEMS Microbiol Ecol 30, 147-155.

Crane, B.R., Arvai, A.S., Ghosh, D.K., Wu, C., Getzoff, E.D., Stuehr, D.J. and Tainer, J.A., 1998. Structure of nitric oxide synthase oxygenase dimer with pterin and substrate. Science, 279, 2121-26.

Dawood, T., Rieu, I., Wolters-Arts, M., Derksen, E.B., Mariani, C., and Visser, E.J. (2014). Rapid flooding-induced adventitious root development from preformed primordia in Solanum dulcamara. AoB Plants 6.

De Marchi, R., Sorel, M., Mooney, B., Fudal, I., Goslin, K., Kwaśniewska, K., Ryan, P.T., Pfalz, M., Kroymann, J., Pollmann, S. and Feechan, A., 2016. The N-end rule pathway regulates pathogen responses in plants. Scientific reports, 6, 26020.

de San Celedonio, R.P., Abeledo, L.G., Brihet, J.M. and Miralles, D.J., 2016. Waterlogging affects leaf and tillering dynamics in wheat and barley. Journal of Agronomy and Crop Science, 202, 409-420.

De Simone, O., Haase, K., Muller, E., Junk, W.J., Hartmann, K., Schreiber, L., and Schmidt, W. (2003). Apoplasmic barriers and oxygen transport properties of hypodermal cell walls in roots from four amazonian tree species. Plant Physiol 132, 206-217.

de Sousa, C.S., L. (2003). Alanine metabolism and alanine amino-transferase activity in soybean (Glycine max) during hypoxia of the root system and subsequent return to normoxia. Environ Exp Bot 50, 1-8.

Desgagné-Penix, I., Eakanunkul, S., Coles, J.P., Phillips, A.L., Hedden, P. and Sponsel, V.M., 2005. The auxin transport inhibitor response 3 (tir3) allele of BIG and auxin transport inhibitors affect the gibberellin status of Arabidopsis. The Plant Journal, 41, 231-42.

Desikan, R., Griffiths, R., Hancock, J., and Neill, S. (2002). A new role for an old enzyme: nitrate reductase-mediated nitric oxide generation is required for abscisic acid-induced stomatal closure in Arabidopsis thaliana. Proc Natl Acad Sci USA 99, 16314-16318.

Ditzel, M., Wilson, R., Tenev, T., Zachariou, A., Paul, A., Deas, E., and Meier, P. (2003). Degradation of DIAP1 by the N-end rule pathway is essential for regulating apoptosis. Nat Cell Biol 5, 467-473.

Dolferus, R., Osterman, J.C., Peacock, W.J., and Dennis, E.S. (1997). Cloning of the Arabidopsis and rice formaldehyde dehydrogenase genes: implications for the origin of plant ADH enzymes. Genetics 146, 1131-1141.

Dolferus, R.W., M.; Carroll, R.R.; Miyashita, R.Y.; Ismond, K.K.; Good, A. (2008). Functional analysis of lactate dehydrogenase during hypoxic stress in Arabidopsis. . Funct. Plant Biol. 35, 131-140.

Dordas, C.H., BB.; Igamberdiev, AU.; Manac'h, N.; Rivoal, J.; Hill, RD. (2003). Expression of a stress-induced hemoglobin affects NO levels produced by alfalfa root cultures under hypoxic stress. . Plant Journal 35, 763-770.

Drew, M.C., Saglio, P.H., and Pradet, A. (1985). Larger adenylate energy charge and ATP/ADP ratios in aerenchymatous roots of Zea mays in anaerobic media as a consequence of improved internal oxygen transport. Planta 165, 51-58.

Drew, M.H., CJ.; Morgan, PW. (2000). Programmed cell death and aerenchyma formation in roots. Trends in Plant Science 5, 123-127.

Edwards, K., Johnstone, C. and Thompson, C., 1991. A simple and rapid method for the preparation of plant genomic DNA for PCR analysis. Nucleic acids research, 19, 1349.

Ellis, M.H.D., E.S.; Peacock, W.J. (1999). Arabidopsis roots and shoots have different mechanisms for hypoxic stress tolerance. Plant Physiol. 119, 57-64.

Enstone, D.E.P., C. A.; and Ma, F. (2003). Root endodermis and exodermis: structure, function, and responses to the environment. J. Plant Growth Regul. 21, 335-351.

Evans, D.E. (2003). Aerenchyma formation. New Phytol 161, 35-49.

Felle, H.H. (2005). pH regulation in anoxic plants. Ann Bot 96, 519-532.

Ferdous, J., Li, Y., Reid, N., Langridge, P., Shi, B.J. and Tricker, P.J., 2015. Identification of reference genes for quantitative expression analysis of MicroRNAs and mRNAs in barley under various stress conditions. PLoS One, 10, 0118503.

Formation using laser microdissection and microarray analyses. New Phytol 190, 351-368.

Fukao, T., Xu, K., Ronald, P.C., and Bailey-Serres, J. (2006). A variable cluster of ethylene response factor-like genes regulates metabolic and developmental acclimation responses to submergence in rice. Plant Cell 18, 2021-2034.

Fukao, T.H., T.; Bailey-Serres, J. (2009). Evolutionary analysis of the Sub1 gene cluster that confers submergence tolerance to domesticated rice. Ann Bot 103, 143-150.

Garthwaite, A.J., Armstrong, W., and Colmer, T.D. (2008). Assessment of O2 diffusivity across the barrier to radial O2 loss in adventitious roots of Hordeum marinum. New Phytol 179, 405-416.

Garzon, M., Eifler, K., Faust, A., Scheel, H., Hofmann, K., Koncz, C., Yephremov, A., and Bachmair, A. (2007). PRT6/At5g02310 encodes an Arabidopsis ubiquitin ligase of the N-end rule pathway with arginine specificity and is not the CER3 locus. FEBS Lett 581, 3189-3196.

Geigenberger, P.F., AR.; Gibon, Y.; Christ, M.; Stitt, M. (2000). Metabolic activity decreases as an adaptive response to low internal oxygen in growing potato tubers. . Biol Chem 381, 723-740.

Gibbs, D.J., Lee, S.C., Isa, N.M., Gramuglia, S., Fukao, T., Bassel, G.W., Correia, C.S., Corbineau, F., Theodoulou, F.L., Bailey-Serres, J., et al. (2011). Homeostatic response to hypoxia is regulated by the N-end rule pathway in plants. Nature 479, 415-418.

Gibbs, D.J., Md Isa, N., Movahedi, M., Lozano-Juste, J., Mendiondo, G.M., Berckhan, S., Marin-de la Rosa, N., Vicente Conde, J., Sousa Correia, C., Pearce, S.P., et al. (2014). Nitric oxide sensing in plants is mediated by proteolytic control of group VII ERF transcription factors. Mol Cell 53, 369-379.

Gibbs, D.J., Tedds, H.M., Labandera, A.M., Bailey, M., White, M.D., Hartman, S., Sprigg, C., Mogg, S.L., Osborne, R., Dambire, C., et al. (2018). Oxygen-dependent proteolysis regulates the stability of angiosperm polycomb repressive complex 2 subunit VERNALIZATION 2. Nat Commun 9, 5438.

Gietz, D., St Jean, A., Woods, R.A. and Schiestl, R.H., 1992. Improved method for high efficiency transformation of intact yeast cells. Nucleic acids research, 20, 1425.

Gil, P., Dewey, E., Friml, J., Zhao, Y., Snowden, K.C., Putterill, J., Palme, K., Estelle, M., and Chory, J. (2001). BIG: a calossin-like protein required for polar auxin transport in Arabidopsis. Genes Dev 15, 1985-1997.

Glaser, P., F. Kunst, M. Arnaud, M.-P. Coudart, W. Gonzales, M.-F. Hullo,M. Ionescu, B. Lubochinsky, L. Marcelino, I. Moszer, E. Presecan, M.Santana, E. Schneider, J. Schweizer, A. Vertes, G. Rapoport, and A.Danchin (1993). Bacillus subtilis genome project: cloning and sequencing of the 97 kilobase region from 325° to 333°. Mol. Microbiol. 10, 371-384.

Gonda, D.K., Bachmair, A., Wünning, I., Tobias, J.W., Lane, W.S. and Varshavsky, A., 1989. Universality and structure of the N-end rule. Journal of Biological Chemistry, 264, 16700-12.

Graciet, E., Hu, R.G., Piatkov, K., Rhee, J.H., Schwarz, E.M. and Varshavsky, A., 2006. Aminoacyl-transferases and the N-end rule pathway of prokaryotic/eukaryotic specificity in a human pathogen. Proceedings of the National Academy of Sciences, 103, 3078-3083.

Graciet, E., Mesiti, F., and Wellmer, F. (2010). Structure and evolutionary conservation of the plant N-end rule pathway. Plant J 61, 741-751.

Graciet, E., Walter, F., O'Maoileidigh, D.S., Pollmann, S., Meyerowitz, E.M., Varshavsky, A., and Wellmer, F. (2009). The N-end rule pathway controls multiple functions during Arabidopsis shoot and leaf development. Proc Natl Acad Sci U S A 106, 13618-13623.

Grigoryev, S., Stewart, A.E., Kwon, Y.T., Arfin, S.M., Bradshaw, R.A., Jenkins, N.A., Copeland, N.G. and Varshavsky, A., 1996. A mouse amidase specific for N-terminal asparagine the gene, the enzyme, and their function in the N-end rule pathway. Journal of Biological Chemistry, 271, 28521-32.

Gupta, K.J., Zabalza, A., and van Dongen, J.T. (2009). Regulation of respiration when the oxygen availability changes. Physiol Plant 137, 383-391.

Hanna, J.F., D. (2007). A proteasome for all occasions. FEBS Lett 581, 2854-2861.

Harwood, W.A., Bartlett, J.G., Alves, S.C., Perry, M., Smedley, M.A., Leyl, N. and Snape, J.W., 2009. Barley transformation using Agrobacterium-mediated techniques. In Transgenic Wheat, Barley and Oats, 137-47. Humana Press.

Hattori, Y., Nagai, K., Furukawa, S., Song, X.J., Kawano, R., Sakakibara, H., Wu, J., Matsumoto, T., Yoshimura, A., Kitano, H., et al. (2009). The ethylene response factors SNORKEL1 and SNORKEL2 allow rice to adapt to deep water. Nature 460, 1026-1030.

He, C., Finlayson, S.A., Drew, M.C., Jordan, W.R., and Morgan, P.W. (1996). Ethylene Biosynthesis during Aerenchyma Formation in Roots of Maize Subjected to Mechanical Impedance and Hypoxia. Plant Physiol 112, 1679-1685.

He, C.J., Drew, M.C., and Morgan, P.W. (1994). Induction of Enzymes Associated with Lysigenous Aerenchyma Formation in Roots of Zea mays during Hypoxia or Nitrogen Starvation. Plant Physiol 105, 861-865.

He, J., Zhang, R.X., Peng, K., Tagliavia, C., Li, S., Xue, S., Liu, A., Hu, H., Zhang, J., Hubbard, K.E. and Held, K., 2018. The BIG protein distinguishes the process of CO2-induced stomatal closure from the inhibition of stomatal opening by CO2. New Phytologist, 218, 232-41.

Hearn, T.J.M.R., M.C.; Abdul-Awal, S.M.; Wimalasekera, R.; Stanton, C.R.; Haydon, M.J.; Theodoulou, F.L.; Hannah, M.A.; Webb, A.A.R (2018). BIG Regulates Dynamic Adjustment of Circadian Period in Arabidopsis thaliana. Plant Physiol 178, 358-371.

Hebelstrup, K.H.S., J.K.; Simpson, C.; Schjoerring, J.K.; Mandon, J.; Cristescu, S.M.; Harren, F.J.M.; Christiansen, M.W.; Mur, L.A.J.; Igamberdiev, A.U. (2014). An assessment of the biotechnological use of hemoglobin modulation in cereals. Physiologia Plantarum 150, 593-503.

Hebelstrup, K.H.v.Z., M.; Mandon, J.; Voesenek, L.A.C.J.; Harren, F.J.M.; Cristescu, S.M.; Moller, I.M.; Mur, L.A.J. (2012). Haemoglobin modulates NO emission and hyponasty under hypoxia-related stress in Arabidopsis thaliana. Journal of Experimental Botany 63, 5581-5591.

Hershko, A., Ciechanover A., Varshavsky A. (2000) Ubiquitin-mediated protein degradation: The early days. Nature Medicine 6, 1073–1081.

Hershko, A., Heller, H., Elias, S. & Ciechanover, A. (1983). Components of ubiquitin-protein ligase system: resolution, affinitypurification and role in protein break-down. J. Biol. Chem. 258, 8206–8214.

Hill, J., Donald, K.A., Griffiths, D.E. and Donald, G., 1991. DMSO-enhanced whole cell yeast transformation. Nucleic acids research, 19, 5791.

Hoffman, N.E., Bent, A.F., and Hanson, A.D. (1986). Induction of lactate dehydrogenase isozymes by oxygen deficit in barley root tissue. Plant Physiol 82, 658-663.

Holman, T.J., P.D.; Russell, L.; Medhurst, A.; Tomas, S.U.; Talloji, P.; Marques, J; Schmuts, H.; Tung, S-A.; Taylor, I.; Footit, S.; Bachmair, A.; Theodoulou, F.L.; Holdsworth, M.J. (2009). The N-end rule pathway promotes seed germination and establishment through removal of ABA sensitivity in Arabidopsis. Proc Natl Acad Sci U S A 106, 4549-4554.

Hondred, D.H., AD. (1990). Hypoxically inducible barley lactate dehydrogenase: cDNA cloning and molecular analysis. Proc Natl Acad Sci U S A 87, 7300-7304.

Hong, Y.F., Ho, T.H.D., Wu, C.F., Ho, S.L., Yeh, R.H., Lu, C.A., Chen, P.W., Yu, L.C., Chao, A. and Yu, S.M., 2012. Convergent starvation signals and hormone crosstalk in regulating nutrient mobilization upon germination in cereals. The Plant Cell, 24, 2857-73.

Hose, E., Clarkson, D.T., Steudle, E., Schreiber, L., and Hartung, W. (2001). The exodermis: a variable apoplastic barrier. J Exp Bot 52, 2245-2264.

Hu, R.G., Sheng, J., Qi, X., Xu, Z., Takahashi, T.T., and Varshavsky, A. (2005). The N-end rule pathway as a nitric oxide sensor controlling the levels of multiple regulators. Nature 437, 981-986.

Huang, S., Elliott, R.C., Liu, P.S., Koduri, R.K., Blair, L.C., Bryan, K.M., Ghosh-Dastidar, P., Einarson, B. and Kendall, R.L., 1987. Specificity of cotranslational amino-terminal processing of proteins in yeast. Biochemistry, 26, 8242-46.

Huang, S., Elliott, R.C., Liu, P.S., Koduri, R.K., Weickmann, J.L., Lee, J.H., Blair, L.C., Ghosh-Dastidar, P., Bradshaw, R.A., Bryan, K.M., et al. (1987). Specificity of cotranslational amino-terminal processing of proteins in yeast. Biochemistry 26, 8242-8246.

Huang, S., Raman, A.S., Ream, J.E., Fujiwara, H., Cerny, R.E. and Brown, S.M., 1998. Overexpression of 20-oxidase confers a gibberellin-overproduction phenotype in Arabidopsis. Plant physiology, 118, 773-81.

Huang, X., Shabala, S., Shabala, L., Rengel, Z., Wu, X., Zhang, G. and Zhou, M., 2015. Linking waterlogging tolerance with Mn2+ toxicity: a case study for barley. Plant Biology, 17, 26-33.

Hunt, P.W., Klok, E.J., Trevaskis, B., Watts, R.A., Ellis, M.H., Peacock, W.J., and Dennis, E.S. (2002). Increased level of hemoglobin 1 enhances survival of hypoxic stress and promotes early growth in Arabidopsis thaliana. Proc Natl Acad Sci U S A 99, 17197-17202.

Hyun, Y., Kim, J., Cho, S.W., Choi, Y., Kim, J.S. and Coupland, G., 2015. Site-directed mutagenesis in Arabidopsis thaliana using dividing tissue-targeted RGEN of the CRISPR/Cas system to generate heritable null alleles. Planta, 241, 271-84.

Igamberdiev, A.B., K.; Manac'h-Little, N.; Stoimenova, M.; Hill, RD. (2005). The haemoglobin/nitric oxide cycle: involvement in flooding stress and effects on hormone signalling. Annals of Botany 96, 557-564.

Ismond, K.P., Dolferus, R., de Pauw, M., Dennis, E.S., and Good, A.G. (2003). Enhanced low oxygen survival in Arabidopsis through increased metabolic flux in the fermentative pathway. Plant Physiol 132, 1292-1302.

Ito, H., Fukuda, Y.A.S.U.K.I., Murata, K. and Kimura, A., 1983. Transformation of intact yeast cells treated with alkali cations. Journal of bacteriology, 153, 163-68.

Ivanova, A., Law, S.R., Narsai, R., Duncan, O., Lee, J.H., Zhang, B., Van Aken, O., Radomiljac, J.D., van der Merwe, M., Yi, K., et al. (2014). A Functional Antagonistic Relationship between Auxin and Mitochondrial Retrograde Signaling Regulates Alternative Oxidase1a Expression in Arabidopsis. Plant Physiol 165, 1233-1254.

James, P., Halladay, J. and Craig, E.A., 1996. Genomic libraries and a host strain designed for highly efficient two-hybrid selection in yeast. Genetics, 144, 1425-36.

Janská, A., Hodek, J., Svoboda, P., Zámečník, J., Prášil, I.T., Vlasáková, E., Milella, L. and Ovesná, J., 2013. The choice of reference gene set for assessing gene expression in barley (Hordeum vulgare L.) under low temperature and drought stress. Molecular genetics and genomics, 288, 639-49

Jeremy, P., Croker, S.J., García-Lepe, R., Lewis, M.J. and Hedden, P., 1999. Modification of gibberellin production and plant development in Arabidopsis by sense and antisense expression of gibberellin 20-oxidase genes. The Plant Journal, 17, 547-56.

Johnson, J.C., JB.; Drew, MC. (1994). Hypoxic induction of anoxia tolerance in roots of Adh1 null Zea mays L. Plant Physiol 105, 61-67.

Joshi, R., and Kumar, P. (2012). Lysigenous aerenchyma formation involves non-apoptotic programmed cell death in rice (Oryza sativa L.) roots. Physiol Mol Biol Plants 18, 1-9.

Jung, J., Won, S.Y., Suh, S.C., Kim, H., Wing, R., Jeong, Y., Hwang, I., and Kim, M. (2007). The barley ERF-type transcription factor HvRAF confers enhanced pathogen resistance and salt tolerance in Arabidopsis. Planta 225, 575-588.

Kaneko, M., Itoh, H., Inukai, Y., Sakamoto, T., Ueguchi-Tanaka, M., Ashikari, M. and Matsuoka, M., 2003. Where do gibberellin biosynthesis and gibberellin signaling occur in rice plants?. The Plant Journal, 35, 104-15

Kanyuka, K., Praekelt, U., Franklin, K.A., Billingham, O.E., Hooley, R., Whitelam, G.C., and Halliday, K.J. (2003). Mutations in the huge Arabidopsis gene BIG affect a range of hormone and light responses. Plant J 35, 57-70.

Kennedy, R.A., Rumpho, M.E., and Fox, T.C. (1992). Anaerobic metabolism in plants. Plant Physiol 100, 1-6.

Kim, T.H., Böhmer, M., Hu, H., Nishimura, N. and Schroeder, J.I., 2010. Guard cell signal transduction network: advances in understanding abscisic acid, CO2, and Ca2+ signaling. Annual review of plant biology, 61, 561-91.

Knipfer, T. and Fricke, W., 2014. Root aquaporins. In Root Engineering (269-96). Springer, Berlin, Heidelberg.

Kolattukudy, P.E. (2001). Polyesters in higher plants. Adv Biochem Eng Biotechnol 71, 1-49.

Kotula, L., and Steudle, E. (2009). Measurements of oxygen permeability coefficients of rice (Oryza sativa L.) roots using a new perfusion technique. J Exp Bot 60, 567-580.

Kursteiner, O.D., I.; Kuhlemeier, C. (2003). The Pyruvate decarboxylase1 Gene of Arabidopsis Is Required during Anoxia But Not Other Environmental Stresses. Plant Physiol 132, 968-978.

Kwon, Y.T., Balogh, S.A., Davydov, I.V., Kashina, A.S., Yoon, J.K., Xie, Y., Gaur, A., Hyde, L., Denenberg, V.H. and Varshavsky, A., 2000. Altered activity, social behavior, and spatial memory in mice lacking the NTAN1p amidase and the asparagine branch of the N-end rule pathway. Molecular and cellular biology, 20, 4135-48.

Kwon, Y.T., Kashina, A.S., Davydov, I.V., Hu, R.G., An, J.Y., Seo, J.W., Du, F. and Varshavsky, A., 2002. An essential role of N-terminal arginylation in cardiovascular development. Science, 297, 96-99.

Laan, P.B., M.J.; Lythe, S.; Armstrong, W.; Blom, C.W.P.M. (1989). Root Morphology and Aerenchyma Formation as Indicators of the Flood-Tolerance of

Laanbroek, H.J. (2010). Methane emission from natural wetlands: interplay between emergent macrophytes and soil microbial processes. A mini-review. Ann Bot 105, 141-153.

Lawrenson, T., Shorinola, O., Stacey, N., Li, C., Ostergaard, L., Patron, N., Uauy, C., and Harwood, W. (2015). Induction of targeted, heritable mutations in barley and Brassica oleracea using RNA-guided Cas9 nuclease. Genome Biol 16, 258.

Lee, S.C., Mustroph, A., Sasidharan, R., Vashisht, D., Pedersen, O., Oosumi, T., Voesenek, L.A., and Bailey-Serres, J. (2011). Molecular characterization of the submergence response of the Arabidopsis thaliana ecotype Columbia. New Phytol 190, 457-471.

Li, H.M., Altschmied, L. and Chory, J., 1994. Arabidopsis mutants define downstream branches in the phototransduction pathway. Genes & development, 8, 339-49.

Licausi, F. (2011). Regulation of the molecular response to oxygen limitations in plants. New Phytol 190, 550-555.

Licausi, F., Kosmacz, M., Weits, D.A., Giuntoli, B., Giorgi, F.M., Voesenek, L.A., Perata, P., and van Dongen, J.T. (2011). Oxygen sensing in plants is mediated by an N-end rule pathway for protein destabilization. Nature 479, 419-422.

Licausi, F., van Dongen, J.T., Giuntoli, B., Novi, G., Santaniello, A., Geigenberger, P., and Perata, P. (2010). HRE1 and HRE2, two hypoxia-inducible ethylene response factors, affect anaerobic responses in Arabidopsis thaliana. Plant J 62, 302-315.

Licausi, F.P., P. (2009). Low oxygen signaling and tolerance in plants. . Adv. Bot. Res. 50, 139-198.

Lieber, M.R., 2010. The mechanism of double-strand DNA break repair by the nonhomologous DNA end-joining pathway. Annual review of biochemistry, 79, 181-11.

López-Bucio, J., Hernández-Abreu, E., Sánchez-Calderón, L., Pérez-Torres, A., Rampey, R.A., Bartel, B. and Herrera-Estrella, L., 2005. An auxin transport independent pathway is involved in phosphate stress-induced root architectural alterations in Arabidopsis. Identification of BIG as a mediator of auxin in pericycle cell activation. Plant physiology, 137, 681-91.

Loreti, E., Poggi, A., Novi, G., Alpi, A., and Perata, P. (2005). A genome-wide analysis of the effects of sucrose on gene expression in Arabidopsis seedlings under anoxia. Plant Physiol 137, 1130-1138.

Lozano-Juste, J., and Leon, J. (2010). Enhanced abscisic acid-mediated responses in nia1nia2noa1-2 triple mutant impaired in NIA/NR- and AtNOA1-dependent nitric oxide biosynthesis in Arabidopsis. Plant Physiol 152, 891-903.

Magneschi, L., and Perata, P. (2009). Rice germination and seedling growth in the absence of oxygen. Ann Bot 103, 181-196.

Mansfield, E., Hersperger, E., Biggs, J. and Shearn, A., 1994. Genetic and molecular analysis of hyperplastic discs, a gene whose product is required for regulation of cell proliferation in Drosophila melanogaster imaginal discs and germ cells. Developmental biology, 165, 507-26.

Mascher, M., Jost, M., Kuon, J.E., Himmelbach, A., Aßfalg, A., Beier, S., Scholz, U., Graner, A. and Stein, N., 2014. Mapping-by-sequencing accelerates forward genetics in barley. Genome biology, 15, R78.

Matsumura, H.T., T.; Takeda, G.; Uchimiya, H. (1998). Adh1 is transcriptionally active but its translational product is reduced in a rad mutant of rice (Oryza sativa L.), which is vulnerable to submergence stress. Theor Appl Genet 97, 1197-1103.

Matsumura, H.T., T.; Yoshida, KT.; Takeda, G. (1995). A rice mutant lacking alcohol dehydrogenase. Breed Sci 45, 365-367.

Matthews, P.R.M.-B.W., Peter M., Waterhouse Sarah, Thornton Sarah J., Fieg Frank Gubler, John V. Jacobsen (2001). Marker gene elimination from transgenic barley, using co-transformation with adjacent `twin T-DNAs' on a standard Agrobacterium transformation vector. Molecular Breeding 7, 195-102.

Melotto, M., Underwood, W., Koczan, J., Nomura, K. and He, S.Y., 2006. Plant stomata function in innate immunity against bacterial invasion. Cell, 126, 969-80.

Mendiondo, G.M., Gibbs, D.J., Szurman-Zubrzycka, M., Korn, A., Marquez, J., Szarejko, I., Maluszynski, M., King, J., Axcell, B., Smart, K., et al. (2016). Enhanced waterlogging tolerance in barley by manipulation of expression of the N-end rule pathway E3 ligase PROTEOLYSIS6. Plant Biotechnol J 14, 40-50.

Mesiti, F. (2011). The N-end rule pathway in Arabidopsis: characterization of N-recognins. (Trinity College Dublin).

Mithran, M., Paparelli, E., Novi, G., Perata, P., and Loreti, E. (2014). Analysis of the role of the pyruvate decarboxylase gene family in Arabidopsis thaliana under low-oxygen conditions. Plant Biol (Stuttg) 16, 28-34.

Mommer, L., and Visser, E.J. (2005). Underwater photosynthesis in flooded terrestrial plants: a matter of leaf plasticity. Ann Bot 96, 581-589.

Mühlenbock, P., Plaszczyca, M., Plaszczyca, M., Mellerowicz, E. and Karpinski, S., 2007. Lysigenous aerenchyma formation in Arabidopsis is controlled by LESION SIMULATING DISEASE1. The Plant Cell, 19, 3819-30.

Mustroph, A., and Bailey-Serres, J. (2010). The Arabidopsis translatome cell-specific mRNA atlas: Mining suberin and cutin lipid monomer biosynthesis genes as an example for data application. Plant Signal Behav 5, 320-324.

Mustroph, A., Zanetti, M.E., Jang, C.J., Holtan, H.E., Repetti, P.P., Galbraith, D.W., Girke, T., and Bailey-Serres, J. (2009). Profiling translatomes of discrete cell populations resolves altered cellular priorities during hypoxia in Arabidopsis. Proc Natl Acad Sci U S A 106, 18843-18848.

Nakano, T., Suzuki, K., Fujimura, T., and Shinshi, H. (2006). Genome-wide analysis of the ERF gene family in Arabidopsis and rice. Plant Physiol 140, 411-432.

Nakatani, Y., Konishi, H., Vassilev, A., Kurooka, H., Ishiguro, K., Sawada, J.I., Ikura, T., Korsmeyer, S.J., Qin, J. and Herlitz, A.M., 2005. p600, a unique protein required for membrane morphogenesis and cell survival. Proceedings of the National Academy of Sciences, 102, 15093-98.

Nanjo, Y., Maruyama, K., Yasue, H., Yamaguchi-Shinozaki, K., Shinozaki, K., and Komatsu, S. (2011). Transcriptional responses to flooding stress in roots including hypocotyl of soybean seedlings. Plant Mol Biol 77, 129-144.

Narsai, R., Howell, K.A., Carroll, A., Ivanova, A., Millar, A.H., and Whelan, J. (2009). Defining core metabolic and transcriptomic responses to oxygen availability in rice embryos and young seedlings. Plant Physiol 151, 306-322.

Neill, S.J., Desikan, R., Clarke, A., and Hancock, J.T. (2002a). Nitric oxide is a novel component of abscisic acid signaling in stomatal guard cells. Plant Physiol 128, 13-16.

Neill, S.J., Desikan, R., Clarke, A., Hurst, R.D., and Hancock, J.T. (2002b). Hydrogen peroxide and nitric oxide as signalling molecules in plants. J Exp Bot 53, 1237-1247.

Ohara, O., Nagase, T., Ishikawa, K.I., Nakajima, D., Ohira, M., Seki, N. and Nomura, N., 1997. Construction and characterization of human brain cDNA libraries suitable for analysis of cDNA clones encoding relatively large proteins. DNA Research, 4, 53-59.

Osnato, M.S., M.S.; Wang, Y.; Meynard, D.; Curiale, S.; Guiderdoni, E.; Liu, Y.; Horner, D.S.; Ouwerkerk, P.B.F.; Pozzi, C.; Muller, K.J.; Salamini, F.; Rossini, L. (2010). Cross Talk between the KNOX and Ethylene Pathways Is Mediated by Intron-Binding Transcription Factors in Barley. Plant Physiol 154, 1616-1632.

Pedroso, M.C., Magalhaes, J.R., and Durzan, D. (2000). Nitric oxide induces cell death in Taxus cells. Plant Sci 157, 173-180.

Perata, P.V., LA. (2007). Submergence tolerance in rice requires Sub1A, an ethylene-response-factor-like gene. Trends Plant Sci 12, 43-46.

Pickart, CM., Fushman, D. (2004). Polyubiquitin chains: polymeric protein signals. Current Opinion in Chemical Biology 8, 610–616.

Ploschuk, R.A.M., D.J.; Colmer, T.D., Ploschuk, E.L., Striker G.G. (2018). Waterlogging of Winter Crops at Early and Late Stages: Impacts on Leaf Physiology, Growth and Yield. Front Plant Sci 9, 1-15.

Poolman, M.G., Miguet, L., Sweetlove, L.J. and Fell, D.A., 2009. A genome-scale metabolic model of Arabidopsis and some of its properties. Plant physiology, 151, 1570-81.

Potuschak, T., Stary, S., Schlogelhofer, P., Becker, F., Nejinskaia, V., and Bachmair, A. (1998). PRT1 of Arabidopsis thaliana encodes a component of the plant N-end rule pathway. Proc Natl Acad Sci U S A 95, 7904-7908.

Qi, X., Li, Q., Ma, X., Qian, C., Wang, H., Ren, N., Shen, C., Huang, S., Xu, X., Xu, Q., et al. (2018). Waterlogging-induced adventitious root formation in cucumber is regulated by ethylene and auxin through reactive oxygen species signalling. Plant Cell Environ.

Rajhi, I.Y., T.; Takahashi, H.; Nishiuchi, S.; Shiono, K.; Watanabe, R.; Mliki, A.; Nagamura, Y.; Tsutsumi, N.; Nishizawa, N.K.; Nakazono, M. (2011). Identification of genes expressed in maize root cortical cells during lysigenous aerenchyma

Raskin, I. and Kende, H., 1984. Role of gibberellin in the growth response of submerged deep water rice. Plant Physiology, 76, 947-50.

Ren, B., Zhang, J., Li, X., Fan, X., Dong, S., Liu, P. and Zhao, B., 2014. Effects of waterlogging on the yield and growth of summer maize under field conditions. Canadian Journal of plant science, 94, 23-31.

Ricard, B.C., I.; Raymond, P.; Saglio, P.H.; Saint-Ges, V.; Pradet, A. (1994). Plant metabolism under hypoxia and anoxia. Plant Physiol. Biochem. 32, 1-10.

Ricoult, C., Echeverria, L.O., Cliquet, J.B., and Limami, A.M. (2006). Characterization of alanine aminotransferase (AlaAT) multigene family and hypoxic response in young seedlings of the model legume Medicago truncatula. J Exp Bot 57, 3079-3089.

Rivoal, J., and Hanson, A.D. (1994). Metabolic Control of Anaerobic Glycolysis (Overexpression of Lactate Dehydrogenase in Transgenic Tomato Roots Supports the Davies-Roberts Hypothesis and Points to a Critical Role for Lactate Secretion. Plant Physiol 106, 1179-1185.

Rivoal, J., Ricard, B., and Pradet, A. (1991). Lactate Dehydrogenase in Oryza sativa L. Seedlings and Roots: Identification and Partial Characterization. Plant Physiol 95, 682-686.

Roberts, J.C., J.; Jardetsky, O.; Walbot, V.; Freeling, M. (1984). Cytoplasmic acidosis as a determinant of flooding intolerance in plants. Proc Natl Acad Sci U S A 81, 6029-6033.

Rocha, M., Licausi, F., Araujo, W.L., Nunes-Nesi, A., Sodek, L., Fernie, A.R., and van Dongen, J.T. (2010a). Glycolysis and the tricarboxylic acid cycle are linked by alanine aminotransferase during hypoxia induced by waterlogging of Lotus japonicus. Plant Physiol 152, 1501-1513.

Rocha, M., Sodek, L., Licausi, F., Hameed, M.W., Dornelas, M.C., and van Dongen, J.T. (2010b). Analysis of alanine aminotransferase in various organs of soybean (Glycine max) and in dependence of different nitrogen fertilisers during hypoxic stress. Amino Acids 39, 1043-1053.

Rockel, P., Strube, F., Rockel, A., Wildt, J., and Kaiser, W.M. (2002). Regulation of nitric oxide (NO) production by plant nitrate reductase in vivo and in vitro. J Exp Bot 53, 103-110.

Ruegger, M., Dewey, E., Hobbie, L., Brown, D., Bernasconi, P., Turner, J., Muday, G. and Estelle, M., 1997. Reduced naphthylphthalamic acid binding in the tir3 mutant of Arabidopsis is associated with a reduction in polar auxin transport and diverse morphological defects. The Plant Cell, 9, 745-57.

Sadanandom, A., Bailey, M., Ewan, R., Lee, J., Nelis, S. (2012). The ubiquitin-proteasome system: central modifier of plant signalling. New Phytologist 196, 13-28.

Sasidharan, R., and Voesenek, L.A. (2013). Lowland rice: high-end submergence tolerance. New Phytol 197, 1029-1031.

Sasidharan, R., Bailey-Serres, J., Ashikari, M., Atwell, B.J., Colmer, T.D., Fagerstedt, K., Fukao, T., Geigenberger, P., Hebelstrup, K.H., Hill, R.D., et al. (2017). Community recommendations on terminology and procedures used in flooding and low oxygen stress research. New Phytol 214, 1403-1407.

Sasidharan, R., Mustroph, A., Boonman, A., Akman, M., Ammerlaan, A.M., Breit, T., Schranz, M.E., Voesenek, L.A., and van Tienderen, P.H. (2013). Root transcript profiling of two Rorippa species reveals gene clusters associated with extreme submergence tolerance. Plant Physiol 163, 1277-1292.

Sauter, M. (2013). Root responses to flooding. Curr Opin Plant Biol 16, 282-286.

Schreiber, L. (2010). Transport barriers made of cutin, suberin and associated waxes. Trends Plant Sci 15, 546-553.

Seago, J.L., Jr., Marsh, L.C., Stevens, K.J., Soukup, A., Votrubova, O., and Enstone, D.E. (2005). A re-examination of the root cortex in wetland flowering plants with respect to aerenchyma. Ann Bot 96, 565-579.

Setter, T.L.a.W., I. (2003). Review of prospects for germplasm improvement for waterlogging tolerance in wheat, barley and oats. Plant Soil 253, 1-34.

Shim, S.Y., Wang, J., Asada, N., Neumayer, G., Tran, H.C., Ishiguro, K.I., Sanada, K., Nakatani, Y. and Nguyen, M.D., 2008. Protein 600 is a microtubule/endoplasmic reticulum-associated protein in CNS neurons. Journal of Neuroscience, 28, 3604-14.

Shiono, K., Ogawa, S., Yamazaki, S., Isoda, H., Fujimura, T., Nakazono, M., and Colmer, T.D. (2011). Contrasting dynamics of radial O2-loss barrier induction and aerenchyma formation in rice roots of two lengths. Ann Bot 107, 89-99.

Shiono, K.T., H.; Colmer, T.D.; Nakazono, M. (2008). Role of ethylene in acclimations to promote oxygen transport in roots of plants in waterlogged soils. Plant Sci 175, 52-58.

Skoog, F. and Miller, C.O., 1957. Chemical regulation of growth and organ formation in plant tissues cultured. In Vitro, Symp. Soc. Exp. Biol (No. 11).

Soukup, A., Armstrong, W., Schreiber, L., Franke, R., and Votrubova, O. (2007). Apoplastic barriers to radial oxygen loss and solute penetration: a chemical and functional comparison of the exodermis of two wetland species, Phragmites australis and Glyceria maxima. New Phytol 173, 264-278.

Stary, S., Yin, X.J., Potuschak, T., Schlögelhofer, P., Nizhynska, V. and Bachmair, A., 2003. PRT1 of Arabidopsis is a ubiquitin protein ligase of the plant N-end rule pathway with specificity for aromatic amino-terminal residues. Plant physiology, 133, 1360-66.

Stary, S., Yin, X.J., Potuschak, T., Schlogelhofer, P., Nizhynska, V., and Bachmair, A. (2003). PRT1 of Arabidopsis is a ubiquitin protein ligase of the plant N-end rule pathway with specificity for aromatic amino-terminal residues. Plant Physiol 133, 1360-1366.

Steffens, B. and Rasmussen, A., 2016. The physiology of adventitious roots. Plant Physiology, 170, 603-17.

Steffens, B., Geske, T., and Sauter, M. (2011). Aerenchyma formation in the rice stem and its promotion by H2O2. New Phytol 190, 369-378.

Steffens, B., Kovalev, A., Gorb, S.N., and Sauter, M. (2012). Emerging roots alter epidermal cell fate through mechanical and reactive oxygen species signaling. Plant Cell 24, 3296-3306.

Steuer, R., Nesi, A.N., Fernie, A.R., Gross, T., Blasius, B. and Selbig, J., 2007. From structure to dynamics of metabolic pathways: application to the plant mitochondrial TCA cycle. Bioinformatics, 23, 1378-85.

Sumanta, N.H., C.I.; Nishika, J.; Suprakash, E.; (2014). Spectrophotometric Analysis of Chlorophylls and Carotenoids from Commonly Grown Fern Species by Using Various Extracting Solvents. Research Journal of Chemical Sciences 4, 63-69.

Suzuki, T., and Varshavsky, A. (1999). Degradation signals in the lysine-asparagine sequence space. EMBO J 18, 6017-6026.

Sweetlove, L.J., Beard, K.F., Nunes-Nesi, A., Fernie, A.R. and Ratcliffe, R.G., 2010. Not just a circle: flux modes in the plant TCA cycle. Trends in plant science, 15, 462-70.

Tamang, B.G., Magliozzi, J.O., Maroof, M.A., and Fukao, T. (2014). Physiological and transcriptomic characterization of submergence and reoxygenation responses in soybean seedlings. Plant Cell Environ 37, 2350-2365.

Tasaki, T., Kim, S.T., Zakrzewska, A., Lee, B.E., Kang, M.J., Yoo, Y.D., Cha-Molstad, H.J., Hwang, J., Soung, N.K., Sung, K.S. and Kim, S.H., 2013. UBR box N-recognin-4 (UBR4), an N-recognin of the N-end rule pathway, and its role in yolk

sac vascular development and autophagy. Proceedings of the National Academy of Sciences, 110, 3800-05.

Tasaki, T., Mulder, L.C., Iwamatsu, A., Lee, M.J., Davydov, I.V., Varshavsky, A., Muesing, M., and Kwon, Y.T. (2005). A family of mammalian E3 ubiquitin ligases that contain the UBR box motif and recognize N-degrons. Mol Cell Biol 25, 7120-7136.

Tasaki, T., Zakrzewska, A., Dudgeon, D.D., Jiang, Y., Lazo, J.S. and Kwon, Y.T., 2009. The substrate recognition domains of the N-end rule pathway. Journal of Biological Chemistry, 284, 1884-95.

Terzaghi, W.B. and Cashmore, A.R., 1995. Light-regulated transcription. Annual review of plant biology, 46, 445-74.

Tewari, R.B., E.; Bunting, K.A.; Coates, J.C. (2010). Armadillo-repeat protein functions: questions for little creatures. Trends in Cell Biology 20, 470-481.

Thiel, J., Rolletschek, H., Friedel, S., Lunn, J.E., Nguyen, T.H., Feil, R., Tschiersch, H., Muller, M., and Borisjuk, L. (2011). Seed-specific elevation of non-symbiotic hemoglobin AtHb1: beneficial effects and underlying molecular networks in Arabidopsis thaliana. BMC Plant Biol 11, 48.

Thomas, A.L., Guerreiro, S.M., and Sodek, L. (2005). Aerenchyma formation and recovery from hypoxia of the flooded root system of nodulated soybean. Ann Bot 96, 1191-1198.

Trevisan, S.M., A.; Begheldo, M.; Nonis, A.; Enna, M.; Vaccaro, S.; Caporale, G.; Ruperti, B.; Quaggiotti, S. (2011). Transcriptome analysis reveals coordinated spatiotemporal regulation of hemoglobin and nitrate reductase in response to nitrate in maize roots. New Phytologist 192, 338-352.

van Veen, H.M., A.; Barding, G.A.; Vergeer-van Ejik, M.; Welschen-Evertman, R.A.M.; Pedersen, Ole.; Visser, E.J.W.; Larive, C.K.; Pierik, R.; Bailey-Serres, J.; Voesenek, L.A.C.J.; Saidharan, R; (2013). Two Rumex Species from Contrasting Hydrological Niches Regulate Flooding Tolerance through Distinct Mechanisms. Plant Cell 25, 4691-4607.

Varshavsky, A. (1996). The N-end rule: functions, mysteries, uses. Proc Natl Acad Sci U S A 93, 12142-12149.

Varshavsky, A. (2005). Regulated protein degradation. Trends Biochem Sci 30, 283-286.

Varshavsky A. (2006). The early history of the ubiquitin field. Protein Science, 15, 647–654.

Varshavsky, A., 2011. The N-end rule pathway and regulation by proteolysis. Protein science, 20, 1298-45.

Vashisht, D., Hesselink, A., Pierik, R., Ammerlaan, J.M., Bailey-Serres, J., Visser, E.J., Pedersen, O., van Zanten, M., Vreugdenhil, D., Jamar, D.C., et al. (2011). Natural variation of submergence tolerance among Arabidopsis thaliana accessions. New Phytol 190, 299-310.

Vervuren, P.J.A. (2003). Extreme flooding events on the rhine and the survival and distribution of riparian plant species. Journal of Ecology 91, 135-146.

Vervuren, P.J.A.B., S. M. J. H. and Blom, C. W. P. M. (1999). Light acclimation, CO2 response and longterm capacity of underwater photosynthesis in three terestrial plant species. . Plant, Cell and Environ 22, 959-968.

Vicente, J., Mendiondo, G.M., Pauwels, J., Pastor, V., Izquierdo, Y., Naumann, C., Movahedi, M., Rooney, D., Gibbs, D.J., Smart, K., et al. (2019). Distinct branches of the N-end rule pathway modulate the plant immune response. New Phytol 221, 988-1000.

Visser, E.J., and Pierik, R. (2007). Inhibition of root elongation by ethylene in wetland and non-wetland plant species and the impact of longitudinal ventilation. Plant Cell Environ 30, 31-38.

Visser, E.V., LACJ. (2005). Acclimation to soil flooding – sensing and signal-transduction. Plant and Soil 254, 197-114.

Voesenek, L.A., and Bailey-Serres, J. (2015). Flood adaptive traits and processes: an overview. New Phytol 206, 57-73.

Voesenek, L.A.C.J.R., J. H. G. M.; Peeters, A. J. M.; van de Steeg, H. M. and de Kroon H. (2004). Plant Hormones Regulate Fast Shoot Elongation under Water: From Genes to Communities. Ecology 85, 16-27.

Voesenek, L.C., TD.; Pierik, R.; Millenaar, FF.; Peeters, AJ. (2006). How plants cope with complete submergence. New Phytol 170, 213-226.

Walter, F. (2010). Identification and characterization of N-recognins in Arabidopsis. (Trinity College Dublin).

Wang, H., Piatkov, K.I., Brower, C.S. and Varshavsky, A., 2009. Glutamine-specific N-terminal amidase, a component of the N-end rule pathway. Molecular cell, 34, 686-95.

Wang, X., Deng, Z., Zhang, W., Meng, Z., Chang, X. and Lv, M., 2017. Effect of waterlogging duration at different growth stages on the growth, yield and quality of cotton. PloS one, 12, 0169029.

Watanabe, K.N., S.; Kulichikhin, K.; Nakazono, M. (2013). Does suberin accumulation in plant roots contribute to waterlogging tolerance? Front Plant Sci 4, 1-7.

Weits, D.A., Giuntoli, B., Kosmacz, M., Parlanti, S., Hubberten, H.M., Riegler, H., Hoefgen, R., Perata, P., van Dongen, J.T., and Licausi, F. (2014). Plant cysteine oxidases control the oxygen-dependent branch of the N-end-rule pathway. Nat Commun 5, 3425.

White, M.D.K., M.; Hopkinson, R.J.; Weits, D.A.; Mueller, C.; Naumann, C.; O'Neill, R.; Wickens, J.; Yang, J.; Brooks-Bartlett, C.; Garman, E.F.; Grossmann, T.N.; Dissmeyer, N and Flashman, E. (2017). Plant cysteine oxidases are dioxygenases thatdirectly enable arginyl transferase-catalysedarginylation of N-end rule targets. Nat Commun 8, 1-9.

Wilkinson, J.Q.C., N.M. (1993). Identification and characterisation of a chlorate-resistant mutant of Arabidopsis thaliana with mutations in both nitrate reductase structural genes NIA1 and NIA2. Molecular and General Genetics 239, 289-297.

Worley, C.K.L., R.; and Callis, J. (1998). Engineering in vivo instability of firefly luciferase and Escherichia coli b-glucuroni- dase in higher plants using recognition elements from the ubiquitin pathway. . Plant. Mol. Biol. 37, 337-347.

Xu, C.M., J. (2011). Structure and function of WD40 domain proteins. Protein and Cell 2, 202-214.

Xu, K., Xu, X., Fukao, T., Canlas, P., Maghirang-Rodriguez, R., Heuer, S., Ismail, A.M., Bailey-Serres, J., Ronald, P.C., and Mackill, D.J. (2006). Sub1A is an ethylene-response-factor-like gene that confers submergence tolerance to rice. Nature 442, 705-708.

Xu, K., Mackill, D. J. (1996). A major locus for submergence tolerance mapped on rice chromosome 9. Mol. Breed. 2, 219-224.

Xu, X., Sharma, R., Tondelli, A., Russell, J., Comadran, J., Schnaithmann, F., Pillen, K., Kilian, B., Cattivelli, L., Thomas, W.T.B., et al. (2018). Genome-Wide Association Analysis of Grain Yield-Associated Traits in a Pan-European Barley Cultivar Collection. Plant Genome 11.

Xu, Y.L., Gage, D.A. and Zeevaart, J.A., 1997. Gibberellins and Stem Growth in Arabidopsis thaliana (Effects of Photoperiod on Expression of the GA4 and GA5 Loci). Plant physiology, 114, 1471-76.

Yamasaki, H., and Sakihama, Y. (2000). Simultaneous production of nitric oxide and peroxynitrite by plant nitrate reductase: in vitro evidence for the NR-dependent formation of active nitrogen species. FEBS Lett 468, 89-92.

Yamauchi, T., Watanabe, K., Fukazawa, A., Mori, H., Abe, F., Kawaguchi, K., Oyanagi, A., and Nakazono, M. (2014). Ethylene and reactive oxygen species are involved in root aerenchyma formation and adaptation of wheat seedlings to oxygen-deficient conditions. J Exp Bot 65, 261-273.

Yavas, I., Unay, A., and Aydin, M. (2012). The waterlogging tolerance of wheat varieties in western of Turkey. ScientificWorldJournal 2012, 529128.

Yoshida, S.I., M.; Callis, J.; Nishida, I.; Watanabe, A. (2002). A delayed leaf senescence mutant is defective in arginyl-tRNA:protein arginyltransferase, a component of the N-end rule pathway in Arabidopsis. The Plant Journal 32, 129-137.

Zeng, F., Shabala, L., Zhou, M., Zhang, G., and Shabala, S. (2013). Barley responses to combined waterlogging and salinity stress: separating effects of oxygen deprivation and elemental toxicity. Front Plant Sci 4, 313.

Zhang, X., Zhou, G.; Shabala, S.; Koutoulis, A.; Shabala, L.; Johnson, P.; Li, C.; Zhou, M. (2016). Identification of aerenchyma formation-related QTL in barley that can be effective in breeding for waterlogging tolerance. Theor Appl Genet 129, 1167-1177.

Zottini, M., Formentin, E., Scattolin, M., Carimi, F., Lo Schiavo, F., and Terzi, M. (2002). Nitric oxide affects plant mitochondrial functionality in vivo. FEBS Lett 515, 75-78.

Websites:

www.biovenn.nl

www.cereals.ahdb.orh.uk

http://eu.idtdna.com

www.plantensembl.org

http://www.biovenn.nl

www.pantherdb.org

Appendices

Appendix **1**

Buffers used in this work

Name	Composition
CTAB	100 mM Tris HCl (pH8.0), 20 mM EDTA, 1.4 M NaCl, 2% (w/v) cetyltrimethyl ammonium bromide Facultative 1% polyvinyl pyrrolidone 40, 000
Edward's extraction buffer	200 mM Tris-HCl pH7.5-8.0, 250 mM NaCl, 25 mM EDTA, 0.5% (w/v) SDS
LB	1% (w/v) tryptone, 0.5% (w/v) yeast extract, 1% (w/v) NaCl
LB agar	1% (w/v) tryptone, 0.5% (w/v) yeast extract, 1% (w/v) NaCl, 4.5% (w/v) agar
SOB	2% (w/v) tryptone, 0.5% (w/v) yeast extract, 0.05% (w/v) NaCl, 10 mM $MgSO_4$, 10 mM $MgCl_2$
TB buffer	10 mM PIPES/KOH pH6.7, 15 mM $CaCl_2$, 250 mM KCl, 55 mM $MnCl_2$
YPD	1 % yeast extract, 2 % peptone, 2% dextrose;
YPD agar	1 % yeast extract, 2 % peptone, 2% dextrose, 20 g/L agar;
SC	1.3 g/L dropout powder; 1.7 g/L yeast nitrogen base without amino acids or ammonium sulphate; 5 g/L $(NH_4)_2SO_4$; 20 g/L dextrose;
SC agar	1.3 g/L dropout powder; 1.7 g/L yeast nitrogen base without amino acids or ammonium sulphate; 5 g/L $(NH_4)_2SO_4$; 20 g/L dextrose, 20 g/L agar;
TE/LiAc	100 mM LiAc, TE 10mM/ 1mM
TE/LiAc/PEG	TE 10mM/ 1mM, 100 mM LiAc
CIM	4.3 g/L MS plant base (Duchefa M0221), 30g/L maltose, 1 g/L casein hydrolysate, 350 mg/L myo-inositol, 690 mg/L proline, 1.0 mg/L thiamine HCl, 2.5 mg/L Dicamba (Sigma-Aldrich D5417), 3.5 g/L Phytagel. The media is adjusted to pH 5.8 with NaOH.

Transition Media	2.7 g/L MS modified plant salt base (without NH_4NO_3) (Duchefa M0238), 20 g/L maltose, 165 mg/L NH_4NO_3; 750 mg/L glutamine, 100 mg/L myo-inositol, 0.4 mg/L thiamine HCl, 2.5 mg/L 2,4-dichlorophenoxy acetic acid (2,4-D; Duchefa), 0.1 mg/L 6-benzylamnopurine (BAP; Duchefa), 3.5 g/L Phytagel. The pH is adjusted to 5.8
Regeneration Media	2.7 g/L MS modified plant salt base (without NH_4NO_3) (Duchefa M0238), 20 g/L maltose, 165 mg/L NH_4NO_3; 750 mg/L glutamine, 100 mg/L myo-inositol, 0.4 mg/L thiamine HCl, 3.5 g/L Phytagel. The pH is adjusted to 5.8
10x LUC buffer	200 mM tricine, pH 7.8, 10.7 mM $Mg(CO_3)_4Mg(OH)_2$ $5H_2O$, 26.7 mM $MgSO_4$; 1mM ethylene-diamine-tetra-acetic-acid (EDTA); 333 mM dithiothreitol (DTT); 5.3 mM adenosine triphosphate (ATP);
1x LUC buffer	prepared using 10 x LUC buffer and 270 M luciferine and 470 M coenzyme A are added fresh in the buffer;
2x GUS buffer	100 mM NaPi pH7.0, 20 mM EDTA pH8.0, 0.2% sodium dodecyl sulphate (SDS), 0.2 % Triton 100x;
1x GUS buffer	prepared using 2x GUS buffer and 10 mM ß-mercaptoethanol; 1mM phenylmethane sulfonyl fluoride (PMSF), 1mM 4-MUG;
MS agar	4.4 g/L MS, 30 g/L sucrose, 8g/L agar. The media is adjusted to pH 5.
SOC	0.5 % yeast extract, 2% tryptone, 10mM NaCl, 2.5 mM KCl, 10 mM $MgCl_2$, 10 mM $MgSO_4$; 20 mM glucose.